LBL-2015
c.2

THE USE OF AROMATIC RESIDUES TO PROBE THE IRON-SULFUR CLUSTERS OF CLOSTRIDIUM ACIDI-URICI AND CLOSTRIDIUM PASTEURIANUM FERREDOXINS

RECEIVED
LAWRENCE
RADIATION LABORATORY

JUL 20 1973

LIBRARY AND
DOCUMENTS SECTION

Elliot L. Packer
(Ph. D. Thesis)

DONNER LABORATORY

June 1973

Prepared for the U.S. Atomic Energy Commission
under Contract W-7405-ENG-48

TWO-WEEK LOAN COPY

This is a Library Circulating Copy which may be borrowed for two weeks. For a personal retention copy, call Tech. Info. Division, Ext. 5545

LAWRENCE BERKELEY LABORATORY
UNIVERSITY OF CALIFORNIA
BERKELEY

LBL-2015
c.2

DISCLAIMER

This document was prepared as an account of work sponsored by the United States Government. While this document is believed to contain correct information, neither the United States Government nor any agency thereof, nor the Regents of the University of California, nor any of their employees, makes any warranty, express or implied, or assumes any legal responsibility for the accuracy, completeness, or usefulness of any information, apparatus, product, or process disclosed, or represents that its use would not infringe privately owned rights. Reference herein to any specific commercial product, process, or service by its trade name, trademark, manufacturer, or otherwise, does not necessarily constitute or imply its endorsement, recommendation, or favoring by the United States Government or any agency thereof, or the Regents of the University of California. The views and opinions of authors expressed herein do not necessarily state or reflect those of the United States Government or any agency thereof or the Regents of the University of California.

The Use of Aromatic Residues to Probe the Iron-Sulfur Clusters of *Clostridium acidi-urici* and *Clostridium pasteurianum* Ferredoxins.

ABSTRACT

Elliot L. Packer

The published x-ray structure of oxidized *Peptococcus aerogenes* ferredoxin, a clostridial-type ferredoxin, reveals that: (i) its iron and inorganic sulfur atoms are arranged into two cube-like iron-sulfur (Fe-S) clusters in which each iron atom is coordinated to a cysteinyl sulfur atom; and (ii) its two aromatic amino acid residues, that are in conserved positions in all sequenced clostridial-type ferredoxins are physically close to each Fe-S cluster.

With ^{13}C-NMR and ^{1}H-NMR techniques, the work reported here independently demonstrates that in oxidized and reduced *C. acidi-urici* and *C. pasteurianum* ferredoxins: (A) the aromatic residues and certain aliphatic residues are physically close to Fe-S clusters and may form weak chemical bonds with the Fe-S clusters; (B) the electron spin is delocalized over (or is rapidly exchanged with) all the Fe atoms in both Fe-S clusters; (C) each Fe-S cluster is accessible to a reducing electron; (D) the midpoint redox potentials of each Fe-S cluster, in each protein, differ by $\leq$ 10 mV; and (E) the midpoint redox potential of each protein differs by 47 ± 10 mV.

Conclusions A, B, and C are based on the following observations. For both aromatic residues the 2', 6'- and 1'- ring carbon resonances in the oxidized protein and all of the ring carbon resonances in the reduced protein are significantly shifted relative to the corresponding resonances of model polypeptides. (The magnitude of

the shift is larger in the reduced protein). Unpaired electron spins of the Fe-S clusters are expected to shift the resonances of nuclei that are physically close to the Fe-S clusters. This assumes that the electron spins are thermally unpaired in the oxidized protein and that the reducing electron is associated with the Fe atoms of the clusters. (The latter assumption was confirmed by showing that the ESR resonances of reduced C. acidi-urici and C. pasteurianum [^{57}Fe] ferredoxins were broader than the resonances of the corresponding [^{56}Fe] ferredoxins).

In the oxidized and reduced ferredoxins the magnitude of the ring proton resonance shifts was 5-10 times smaller than that of the ring carbon shifts of the corresponding (bonded) carbon atoms, and the proton and carbon resonance shift pattern was symmetric about the 1', 4'-ring carbon axis. The large carbon:proton shift ratio and symmetrical shift pattern is characteristic of shifts produced by orbital overlap and suggests that a weak bond may form between the aromatic residues and the Fe-S clusters.

Large carbon:proton shift ratios exist for tentatively assigned δ-carbon and δ-proton resonances of most of the isoleucyl residues and the α-carbon and α-proton resonances of at least three other carbon atoms. The δ-carbon atoms of most of the isoleucyl residues may form weak chemical bonds with the Fe-S clusters. The above mentioned α-carbon resonances appear in a group of 7 or 8 significantly shifted resonances and shift as a group upon reduction. This suggests that the reducing electron (spin) is distributed over all the iron atoms and if these resonances do not correspond to the 8 cysteinyl residues, then these carbon atoms may also form weak

chemical bonds.

Conclusions D and E are based on the fact that: (i) the ring carbon shifts of the tyrosyl and phenylalanyl residues can be distinguished in C. pasteurianum and C. acidi-urici [Phe^2]-ferredoxin (a modified ferredoxin in which one tyrosyl residue has been replaced by a phenylalanyl residue); (ii) the aromatic residue shift parameters of the reduced protein is different from that of the oxidized protein; and (iii) the magnitude of the ring carbon shifts is proportional to the degree of protein reduction and Fe-S cluster reduction within each protein.

In partially (methyl viologen) reduced ferredoxin the shifts are proportional to the degree of protein reduction because the reducing electron is rapidly exchanging between the oxidized and reduced forms of the protein. The relative midpoint redox potential of each protein can be calculated from the ^{13}C-NMR spectrum of an equilibrium mixture of C. acidi-urici and C. pasteurianum ferredoxins because the protein midpoint redox potential is proportional to the degree of protein reduction. Similarly one can calculate the relative Fe-S cluster midpoint redox potentials within each protein.

ACKNOWLEDGEMENTS

I wish to thank Drs. Jesse C. Rabinowitz, Alan J. Bearden, Douglas T. Browne, Himan Sternlicht, and Seiji Ogawa for their valuable advice, insight, enthusiastic support and encouragement. Dr. Rabinowitz provided the biochemical facilities at the Biochemistry Department of the University of California, Berkeley. Dr. Bearden performed the ESR experiments at the Donner Laboratories of the Lawrence Berkeley Laboratory. Drs. Sternlicht and Ogawa performed the ^{13}C- and ^{1}H-NMR experiments, respectively, at Bell Laboratories, Murray Hill, N.J.

Special thanks are also due to Dr. Eglis T. Lode for providing valuable advice and C. acidi-urici [Phe^2]-ferredoxin, James Brodrick for providing C. pasteurianum ferredoxin, Drs. William B. Sweeney, R. Malkin, C.-S. Chen, Alex B. Champion and Claire C. Davison, all of the University of California, for valuable advice, Dr. Jack Cohen of the NIH, Bethesda, Md. for providing [3',5'-$^2H_2$]tyrosine, Drs. W. D. Phillips of du Pont de Nemours and Co., Wilmington, Del., and L. H. Jensen of the University of Washington for unpublished data, Dr. R. G. Shulman of Bell Laboratories for valuable information, Dr. W. Blumberg of Bell Laboratories for

performing ESR measurements, and Dr. E. Meier and J. Consolo of Stanford University for performing the fluorine analysis.

I am especially grateful to the Beinstein family for their generous hospitality in New Jersey.

TABLE OF CONTENTS

PART I. GENERAL INTRODUCTION 1

Role of aromatic residues 3

Direct observation of aromatic residues in clostridial-type ferredoxins with ^{13}C-NMR techniques 5

Direct observation of aliphatic residues in clostridial-type ferredoxins with ^{13}C-NMR techniques 5

Direct observation of aromatic residues in clostridial-type ferredoxins with ^{1}H-NMR techniques 6

Direct observation of aliphatic residues in clostridial-type ferredoxins with ^{1}H-NMR techniques 6

Use of ESR to probe the Fe-S cluster 7

Use of other physical methods to probe the Fe-S cluster 8

Unique features of NMR 8

Outline of experiments 9

PART II. GENERAL METHODS AND MATERIALS 17

Section 1. Growth of bacteria 17

Section 2. Sample preparation 19

Preparation of ferredoxin 19

Preparation of apoferredoxin 22

Reconstitution of ferredoxin from apoferredoxin 23

Preparation of cell protein 24

Preparation of samples for amino acid analysis 25

Preparation of samples for NMR 25

Preparation of samples for ESR 26

Section 3. Instrumentation 27

ESR Instrumentation 27

NMR Instrumentation 27

PART III. RESULTS 31

Section 1. Incorporation of modified tyrosine into

Clostridium acidi-urici ferredoxin 31

Experiment 1. Incorporation of [^{14}C]tyrosine into

Clostridium acidi-urici ferredoxin 31

[^{14}C]amino acid incorporation into growing

C. acidi-urici cells 35

Effect of [^{12}C]tyrosine carrier concentration on

[^{14}C]tyrosine incorporation 36

Effect of yeast extract concentration on [U-^{14}C]tyrosine incorporation 37

Purification of ferredoxin obtained from C. acidi-urici grown in the presence of [U-^{14}C]tyrosine . . . 38

Regulation of amino acid synthesis 38

Experiment 2. Incorporation of [3′, 5′-^{2}H$_2$]tyrosine into

Clostridium acidi-urici ferredoxin 65

^{1}H-NMR studies 69

ESR studies 71

Appendix A. Calculating the line width of the ESR

g = 2 resonance of C. acidi-urici normal and [[3', 5'-$^2H_2$] Tyr]-ferredoxin 82

Experiment 3. Incorporation of 3-fluorotyrosine into Clostridium acidi-urici protein 84

Section 2. ESR Experiments 95

Experiment 4. Association of the reducing electron with the iron atoms of the Fe-S clusters in clostridial-type ferredoxins 95

Experiment 5. Tentative assignment of the g = 2 ESR resonance to a tyrosyl radical electron in oxidized Clostridium acidi-urici and Clostridium pasteurianum ferredoxins 108

Section 3. ^{1}H-NMR Experiments 117

Experiment 6a. Conformational changes in oxidized Clostridium acidi-urici native and [Phe^2]-ferredoxin and Clostridium pasteurianum ferredoxin 117

Changes in protein conformation 118

Effect of H_2O and D_2O 118

Effect of temperature 120

Effect of ionic strength 120

Comparison of ferredoxins 121

Experiment 6b. Slowly exchangeable protons of Clostridium acidi-urici ferredoxin 150

Oxidized ferredoxin 152

Reduced ferredoxin 152

Rapidly exchangeable protons 158

Central water molecule 158

Section 4. ^{13}C-NMR Experiments 179

Experiment 7a. ^{13}C-NMR of the aromatic residues of *Clostridium acidi-urici* ferredoxin 179

Assignment of ring carbon resonances 181

Oxidized ferredoxin 181

Reduced ferredoxin 183

Similar magnetic environments 183

Symmetry about the 1', 4'-ring carbon axis 184

Two state hypothesis 188

Paramagnetic shifts 189

Ring carbon resonance shifts 190

Weak chemical bond 191

Possible shift mechanisms 191

Experiment 7b. The possible formation of a weak chemical bond between the aromatic residues and the Fe-S clusters of clostridial-type ferredoxins 219

^{13}C-NMR of the aromatic residues 221

Oxidized ferredoxin 221

Reduced ferredoxin 224

^{1}H-NMR of the aromatic residues 227

Oxidized ferredoxin 227

Reduced ferredoxin 228

Magnetic and electronic properties of the Fe-S clusters 230

Formation of a weak bond 231

Tyrosyl radical 232

Accessibility of the reducing electron 233

Experiment 7c. The redox potential of each Fe-S cluster of Clostridium acidi-urici and Clostridium pasteurianum ferredoxins 265

Degree of reduction 269

Midpoint redox potential 269

Distinguishable reduction sites 273

Interaction between Fe-S clusters 273

pH-independent midpoint redox potential 274

Protein conformation changes upon reduction 279

Protein conformation changes with pH. 279

Amino acid sequence homology 281

Appendix B. Redox potential measurements 294

Consequences of neglecting (O-R) and (R-O) 295

Consequences of considering (O-R) and (R-O) 297

Appendix C. Midpoint redox potentials of distinguishable Fe-S clusters 300

Experiment 8. The possible formation of a weak chemical bond between the aliphatic residues and the Fe-S clusters of clostridial-type ferredoxins 317

Reconstructed ^{13}C-NMR spectra 319

Cysteinyl β-carbon resonances 324

Cysteinyl α-carbon resonances 324

Isoleucyl δ -carbon resonances 326

Other aliphatic carbon resonances 326

PART IV. GENERAL DISCUSSION 357
Distinguishable Fe-S clusters 357
Aromatic residues 358
Symmetric shifts 358
Shift mechanisms 358
Possible functional role of aromatic residues 360
Electron transfer 360
Model compounds 361
The role of aromatic residues in other electron-carrier proteins 362
Aliphatic residues 364
Cysteinyl carbon resonances 364
Unassigned carbon resonances 365
Slowly exchangeable proton resonances 366
Conformational changes 366
Prospectus 367

PART I. GENERAL INTRODUCTION

The name "ferredoxin" was coined by D. L. Wharton of the Dupont Company and was first applied to the "iron-redox protein" obtained from Clostridium pasteurianum (89). Since then, this name has been applied (115) to a number of iron-sulfur proteins that:

(i) contain equal amounts of non-heme iron and inorganic sulfur atoms;

(ii) are electron carriers of low redox potentials ($E^{0\prime}$ = -240 to -490 mV, referenced to the H_2 electrode, pH 7);

(iii) have temperature-sensitive ESR resonances centered around g = 1.94 in the reduced state; and

(iv) have characteristic absorption spectra in the 260-600 nm region, the reduced form having a lower absorption than the oxidized forms.

Clostridial-type ferredoxins are defined as those which have eight iron and eight inorganic sulfur atoms, low molecular weight (~ 6,000 daltons), and low redox potential (~ -400 mV). X-ray studies (121) of Peptococcus aerogenes ferredoxin, a clostridial-type ferredoxin, show that the eight iron and eight inorganic sulfur atoms are arranged into two "cube-like" iron-sulfur (Fe-S) clusters (Fig. 1), which form two interpenetrating tetrahedra with a cysteinyl sulfur atom coordinated to each iron atom.

Clostridial-type ferredoxin (Fd) can function as an electron carrier in the phosphoroclastic reaction (23):

$$\text{Pyrivate} + Fd_{ox} + CoA \xrightarrow[\text{genase}]{\text{Pyruvic dehydro-}} \text{acetyl CoA} + Fd_{red} + CO_2$$

which transfers electrons to hydrogenase or nitrogenase. The ferredoxins function on the "hydrogen side" of NAD and NADP, and the transfer of electrons from pyruvate to H_2 gas is coupled to the synthesis of ATP, which (among other things) is essential for the fermentation of carbon sources (23). The role of ferredoxin in fermentative metabolism is summarized in Fig. 2.

Clostridial-type ferredoxins (that have been examined to date) contain only two aromatic residues, usually either phenylalanyl or tyrosyl or both (Fig. 3), and these occur in conserved positions (129). The only exception to the above is C. tartarivorum ferredoxin, which contains a histidyl and tyrosyl residue in the conserved aromatic positions, and a histidyl residue in a non-conserved position. The clostridial-type ferredoxins from P. aerogenes and C. acidi-urici have two tyrosyl residues, and C. pasteurianum ferredoxin has one tyrosyl and one phenylalanyl residue. X-ray studies of oxidized P. aerogenes ferredoxin show that its two aromatic residues, Tyr^2 and Tyr^{28}, are each close to a single "cube-like" Fe-S cluster (Fig. 1). (These clusters are designated II and I, respectively (2), and the superscript refers to the amino acid residue sequence position, starting at the N-terminal residue. Amino acid position 30 in C. acidi-urici and C. pasteurianum ferredoxin is homologous to position 28 (129) in P. aerogenes ferredoxin.)

Since other clostridial-type ferredoxins have amino acid sequences homologous to that of P. aerogenes ferredoxin (129), all clostridial-type ferredoxins are assumed to contain two "cube-like" Fe-S clusters and to have similar three-dimensional structures, in which the aromatic residues at positions 2 and 30 are physically close to Fe-S clusters II and I respectively.

ROLE OF AROMATIC RESIDUES:

The aromatic residues in clostridial ferredoxin may have a structural or functional role or both. The structural role could be: (i) to provide a hydrophobic environment for each Fe-S cluster, thus protecting it from oxygen or solvent; or (ii) to stabilize the structure of the Fe-S cluster by the formation of a weak chemical bond between the aromatic rings and the iron and sulfur atoms, where the special orientation of the aromatic residues could be stabilized by a type of van der Waals interaction between the clusters and the potentially polarizable tyrosyl rings: or (iii) both. The following facts are consistent with the hypothesis that the tyrosyl residues can provide a hydrophobic environment for the Fe-S cluster: (i) Elimination of two amino acids by Edman degradation from the N-terminal end of C. acidi-urici apoferredoxin and subsequent reconstitution produces an extremely unstable protein (76). The same is true when Tyr^2 is substituted for smaller amino acid residues. But the stability of the reconstituted protein generally increases with the size of the substituted amino acid (77). A bulky side chain can substitute for an aromatic ring. For example, one of these derivatives, C. acidi-urici [Leu^2] -ferredoxin, which has a leucyl residue in position 2 instead of a tyrosyl residue (77), is biologically active and stable (though less stable than native C. acidi-urici ferredoxin); (ii) Chromatium ferredoxin, a ferredoxin which has an amino acid sequence homologous to that of other clostridial-type ferredoxins but with a larger molecular weight, also has a leucyl residue in position 2 instead of a tyrosyl residue.

The amino acid sequences of both Chromatium and C. acidi-urici ferredoxins are homologous for the first 41 amino acids (N- to C-terminal, Fig. 3), and thus contain a tyrosyl residue at position 30. Since all sequenced clostridial ferredoxins contain an aromatic residue in a conserved position 30, the functional role of the aromatic residues cannot be ruled out at present.

In order to elucidate the structural and functional roles of aromatic residues in clostridial-type ferredoxins, C. acidi-urici and C. pasteurianum ferredoxins were chosen for study, because their amino acid sequences are known. The NMR technique was used because it allows one to probe the physical environment of the aromatic ring nuclei, since each nucleus of the ring has a characteristic resonance absorption frequency. This technique could also be used to probe the physical environment of aliphatic nuclei. The focus of this thesis, however, is on the aromatic residues of clostridial-type ferredoxins because aromatic residues have been implicated in electron transfer reactions of other electron carrier proteins (127) and protein model compounds (31).

Interpretation of the NMR spectra of aromatic residues is facilitated by comparing the NMR spectra of C. acidi-urici ferredoxins that contain modified aromatic residues with those of the native ferredoxin. Thus it was necessary to determine the feasibility of exclusively incorporating normal tyrosine and modified tyrosine undiluted by cell metabolism, into this ferredoxin (Experiments 1, 2, and 3).

DIRECT OBSERVATION OF AROMATIC RESIDUES IN CLOSTRIDIAL-TYPE FERREDOXINS WITH ^{13}C-NMR TECHNIQUES:

Ring carbon resonances are separated from the resonances of aliphatic and carbonyl carbons in ^{13}C-NMR spectra of proteins and can thus be readily assigned. Ring carbon resonances can be resolved in ^{13}C-NMR spectra of clostridial-type ferredoxins that contain ^{13}C in natural abundance (~ 1%), but this requires high ($\geq$ 10 mM) protein concentrations and the use of a sensitive ^{13}C-NMR Fourier transform spectrometer. Carbon resonances of protein amino acid residues, unlike proton resonances, are not very sensitive to changes in protein conformation and are rarely shifted ~ 1-2 ppm from the corresponding carbon resonance positions of free amino acids (53). Carbon resonances can be perturbed, however, by nearby paramagnetic electrons, and the effect of oxidation and reduction of ferredoxin upon the tyrosyl ring carbons can be monitored and correlated with that of the tyrosyl ring protons by double resonance decoupling techniques (128). Since the aromatic rings should each be close to one Fe-S cluster (65) in clostridial-type ferredoxins, one can use the aromatic residues to probe the magnetic environment of each cluster in the oxidized and reduced protein. The fact that the aromatic residues can be used as probes is independent of whether they have structural or functional roles in electron transport.

DIRECT OBSERVATION OF ALIPHATIC RESIDUES IN CLOSTRIDIAL-TYPE FERREDOXINS WITH ^{13}C-NMR TECHNIQUES:

Any aliphatic amino acid that is close enough to an identifiable Fe-S cluster and that exhibits a shift in its carbon resonances due to this cluster could also be used as a probe. In order to assign the resonances

of such aliphatic amino acids, however, one needs to label the clostridial-type ferredoxin selectively with a 10-15% enriched [^{13}C] amino acid. The aliphatic carbon resonances of each amino acid residue overlap and are not easy to assign in natural ^{13}C abundance. Labeling could be accomplished by growing the bacterium in the presence of a labeled amino acid so that it may be incorporated specifically without dilution into the cell ferredoxin.

DIRECT OBSERVATION OF AROMATIC RESIDUES IN CLOSTRIDIAL-TYPE FERREDOXINS WITH ^{1}H-NMR TECHNIQUES:

^{1}H-NMR techniques by themselves cannot be used to observe isotopically unlabeled aromatic residues in clostridial-type ferredoxin, because the ring-proton resonances occur in a region which contains other shifted resonances. The ring proton resonances (unlike those of the carbon nuclei) do not shift significantly in the oxidized or reduced C. acidi-urici and C. pasteurianum ferredoxins (see Experiments 7 and 8), thus ^{1}H-NMR studies of the aromatic residues of clostridial ferredoxins alone would not have revealed that the aromatic residues are close to and magnetically perturbed by the Fe-S clusters.

DIRECT OBSERVATION OF ALIPHATIC RESIDUES IN CLOSTRIDIAL-TYPE FERREDOXINS WITH ^{1}H-NMR TECHNIQUES:

Phillips and his coworkers (106) have made ^{1}H-NMR studies of oxidized and reduced C. acidi-urici and C. pasteurianum ferredoxins. They have observed at least sixteen proton resonances that are significantly shifted from the normal proton resonances of free amino acids. These shifted resonances cannot be assigned at present, but, because of the magnitude of their shifts, they are tentatively assigned (110, 111) to the β-protons of the eight cysteinyl residues of these ferredoxins.

(β-protons are protons covalently bound to β-carbon atoms.) Even with this tentative assignment, none of the shifted proton resonances can be used to probe the Fe-S clusters, because (assuming their β-proton assignment is correct) the cysteinyl residues cannot be distinguished from one another.

Some of the shifted proton resonances could be due to very slowly exchangeable protons, if these protons are closely packed around the Fe-S clusters. This hypothesis can be tested by reconstituting C. acidi-urici ferredoxin in D_2O (Experiment 6b).

USE OF ESR TO PROBE THE Fe-S CLUSTER:

g = 1.94 RESONANCES:

ESR studies of reduced C. pasteurianum (94, 100) and C. acidi-urici (95) ferredoxin suggest that there are two kinds of ESR resonances produced by these proteins. In C. pasteurianum ferredoxin, initially a pattern with $g_{\parallel} = 2.06$, $g_{\perp} = 1.94$ is observed, but, as more dithionite is added, this pattern continues to grow and narrower resonances appear nearer g = 2. This is consistent with the fact that clostridial ferredoxins contain two types of Fe-S clusters, each accepting one electron.

g = 2 RESONANCE:

A tyrosyl radical may be responsible for the g = 2 resonance observed in certain oxidized clostridial-type ferredoxins (96, 100). This can be tested by comparing the ESR spectra of oxidized ferredoxins that do not contain tyrosyl residues with those that do (Experiment 4).

USE OF OTHER PHYSICAL METHODS TO PROBE THE Fe-S CLUSTERS:

Mössbauer spectroscopic studies of oxidized clostridial ferredoxin were performed by Phillips, Bloomstrom and coworkers (15) and by Bearden (10). This method can distinguish between oxidation and spin states of iron, but not between Fe-S clusters.

Optical spectroscopy of clostridial ferredoxins cannot distinguish between Fe-S clusters, since the disappearance of the absorption maximum at A_{390} with reduction represents the sum of reduced chromophores.

X-ray crystallography has determined the physical environment of each Fe-S cluster of crystalline, oxidized P. aerogenes ferredoxin. Knowledge of the x-ray structure of reduced P. aerogenes ferredoxin would also be especially useful. The x-ray structure, however, only provides "anatomical" information, while other techniques, such as NMR, can provide "physiological" information. The x-ray techniques study the static properties of crystalline protein, while NMR studies dynamic properties of the protein in solution. Both approaches are complementary and essential to the understanding of ferredoxin structure and function.

UNIQUE FEATURES OF NMR:

The NMR technique, can determine: (i) if the reducing electron is localized or distributed over all the iron atoms (Experiment 8); (ii) if one Fe-S cluster is easier to reduce than the other (Experiment 7c); (iii) if there is interaction between Fe-S clusters, i.e., if reducing one cluster makes the other easier or more difficult to reduce; and (iv) if the electron is transferred between proteins and between Fe-S clusters.

Hopefully, this information will help us learn about how the electron is transferred in and out of the protein, and about what determines the different redox optentials for different Fe-S proteins that have similar Fe-S clusters. NMR and ESR techniques can thus provide information that is very useful to the biochemist.

OUTLINE OF EXPERIMENTS:

In order to use the aromatic residues to probe the Fe-S clusters of clostridial-type ferredoxins by NMR and ESR techniques it was necessary to demonstrate: (i) that modified aromatic residues could be incorporated into ferredoxin (Experiments 1, 2 and 3); (ii) that the reducing electron is associated with the Fe-S clusters (Experiment 4); and (iii) that the aromatic residues are close to the Fe-S clusters (Experiments 5, 7a, 7b).

If the aromatic residues are close enough to the Fe-S clusters to be magnetically perturbed by their electron spins, these residues could be used to probe the Fe-S clusters of the oxidized and reduced ferredoxins. The perturbed aromatic residues could be used to determine, for example, the relative midpoint redox potential of each Fe-S cluster in C. acidi-urici and C. pasteurianum ferredoxins (Experiment 7c).

The aliphatic nuclei of these ferredoxins were also studied by ^{1}H-NMR (Experiment 6) and ^{13}C-NMR (Experiment 8) techniques, to determine if aliphatic amino acid residues which are also close to the Fe-S clusters are magnetically perturbed by the unpaired spins in the Fe-S clusters.

In Experiment 6 one can monitor, with ^{1}H-NMR techniques, small changes in the conformation of the aliphatic amino acid residues directly bonded to the Fe-S clusters in clostridial-type ferredoxins by

altering the ferredoxin solvent to contain either D_2O or H_2O or NaCl or no NaCl. These solvent changes can affect protein conformation. ^{1}H-NMR of such oxidized and reduced clostridial ferredoxins could help us determine if differences in ferredoxin redox potentials are due to differences in protein conformation about each Fe-S cluster within and between clostridial-type ferredoxins.

Fig. 1. Approximate three-dimensional structure of P. aerogenes ferredoxin. Drawing from reference (65). Numbers next to open circles (cysteinyl sulfur atoms) refer to cysteinyl residue positions. Closed and open circles in the Fe-S clusters refer to the iron and inorganic sulfur atoms, respectively.

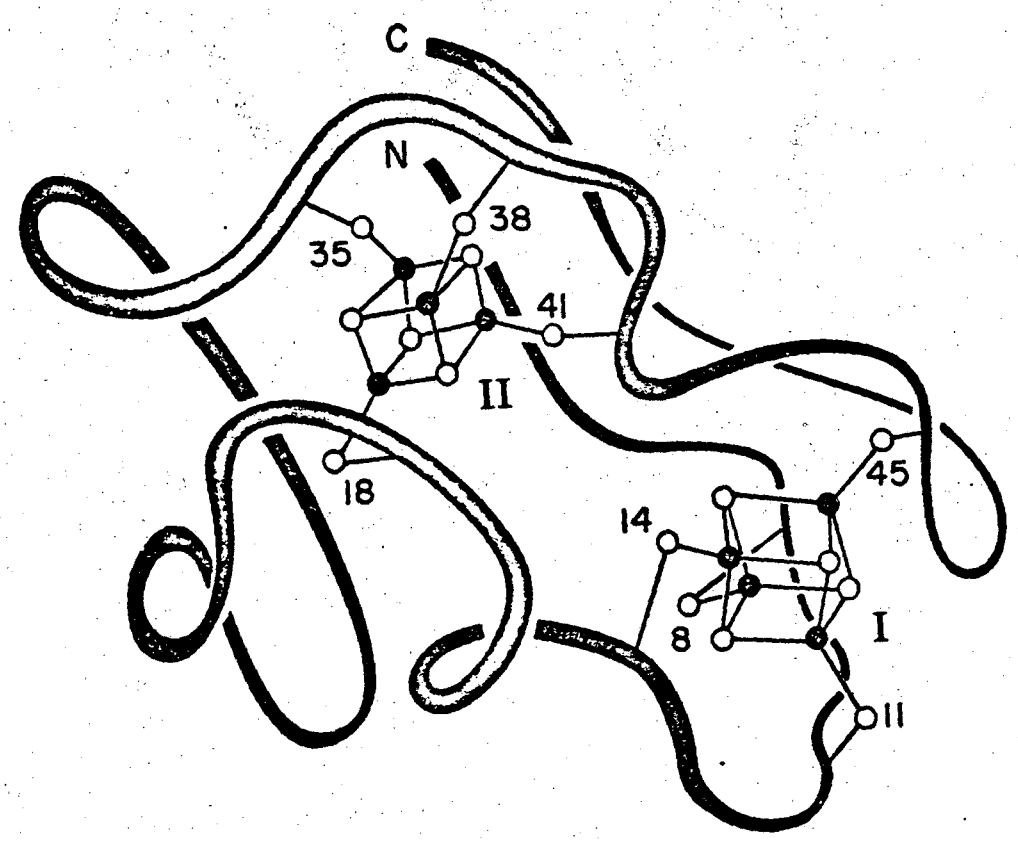
C
N
38
35
41
II
18
45
14
8
I
11

Fig. 2. Role of ferredoxin in fermentation metabolism. Taken from reference 23.

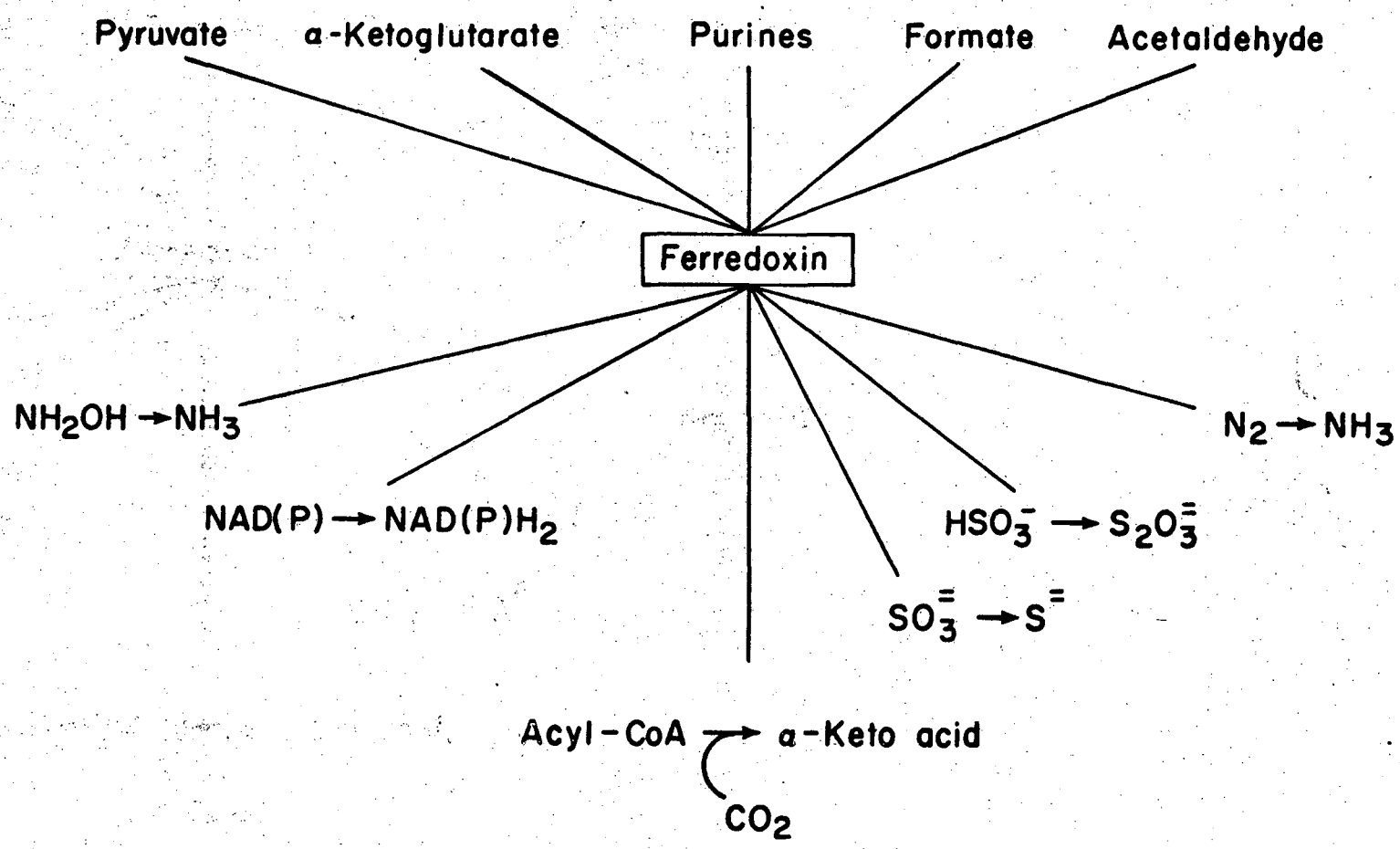
Pyruvate
α-Ketoglutarate
Purines
Formate
Acetaldehyde
Ferredoxin
$NH_2OH \rightarrow NH_3$
$NAD(P) \rightarrow NAD(P)H_2$
$HSO_3^- \rightarrow S_2O_3^=$
$SO_3^= \rightarrow S^=$
$N_2 \rightarrow NH_3$
Acyl-CoA → α-Keto acid
CO_2

Fig.3. A comparison of the primary structures of the ferredoxins sequenced to date. D. G., M. A., C. B., C. P., C. A., C. T., and C. D., represent Desulfovibrio gigas (incomplete sequence), Micrococcus (Peptococcus) aerogenes, Clostridium butyricum, Clostridium pasteurianum, Clostridium acidi-urici, Clostridium tartarivorum and Chromatium D. ferredoxins, respectively. Taken from references 132, 165, 13, 130, 117, 129, and 84 respectively. Figure from reference 75.

```
        1          4    5                 10                15                20                25
D.G.          Pro-Ile-Gln-Val-Asp-Asn-Cys-Met-Ala-Cys-Gln-Ala-Cys-Ile-Asn-Glu-Cys-Pro-Val-Asp-Val-

M.A.    Ala-Tyr-Val-Ile-  -Asn-Asp-Ser-Cys-Ile-Ala-Cys-Gly-Ala-Cys-Lys-Pro-Glu-Cys-Pro-Val-Asn-   -Ile-Gln-Gln-Gly-   -Ser-
C.B.    Ala-Phe-Val-Ile-  -Asn-Asp-Ser-Cys-Val-Ser-Cys-Gly-Ala-Cys-Ala-Gly-Glu-Cys-Pro-Val-Ser-Ala-Ile-Thr-Gln-Gly-Asp-Thr-
C.P.    Ala-Tyr-Lys-Ile-  -Ala-Glu-Ser-Cys-Val-Ser-Cys-Gly-Ala-Cys-Ala-Ser-Glu-Cys-Pro-Val-Asn-Ala-Ile-Ser-Gln-Gly-Asp-Ser-
C.A.    Ala-Tyr-Val-Ile-  -Asn-Asp-Ala-Cys-Ile-Ser-Cys-Gly-Ala-Cys-Asp-Pro-Glu-Cys-Pro-Val-Asp-Ala-Ile-Ser-Gln-Gly-Asp-Ser-
C.T.    Ala-His-Ile-Ile-  -Thr-Asp-Glu-Cys-Ile-Ser-Cys-Gly-Ala-Cys-Ala-Ala-Glu-Cys-Pro-Val-Glu-Ala-Ile-His-Glu-Gly-Thr-Gly-

C.D.    Ala-Leu-Met-Ile-  -Thr-Asp-Gln-Cys-Ile-Asn-Cys-Asn-Val-Cys-Gln-Pro-Glu-Cys-Pro-Asn-Gly-Ala-Ile-Ser-Gln-Gly-Asp-Glu-

        30                35                40                45                50                55
M.A.    Ile-Tyr-Ala-Ile-Asp-Ala-Asp-Ser-Cys-Ile-Asp-Cys-Gly-Ser-Cys-Ala-Ser-Val-Cys-Pro-Val-Gly-Ala-Pro-Asn-Pro-Glu-Asp-COOH
C.B.    Gln-Phe-Val-Ile-Asp-Ala-Asp-Thr-Cys-Ile-Asp-Cys-Gly-Asn-Cys-Ala-Asn-Val-Cys-Pro-Val-Gly-Ala-Pro-Asn-Gln-Glu-COOH
C.P.    Ile-Phe-Val-Ile-Asp-Ala-Asp-Thr-Cys-Ile-Asp-Cys-Gly-Asn-Cys-Ala-Asn-Val-Cys-Pro-Val-Gly-Ala-Pro-Val-Gln-Glu-COOH
C.A.    Arg-Tyr-Val-Ile-Asp-Ala-Asp-Thr-Cys-Ile-Asp-Cys-Gly-Ala-Cys-Ala-Gly-Val-Cys-Pro-Val-Asp-Ala-Pro-Val-Gln-Ala-COOH
C.T.    Lys-Tyr-Gln-Val-Asp-Ala-Asp-Thr-Cys-Ile-Asp-Cys-Gly-Ala-Cys-Gln-Ala-Val-Cys-Pro-Thr-Gly-Ala-Val-Lys-Ala-Glu-COOH

C.D.    Thr-Tyr-Val-Ile-Glu-Pro-Ser-Leu-Cys-Thr-Glu-Cys-Val Asp-Cys-Val-Glu-Val-Cys-Pro-Ile-Lys-Asp-Pro-Ser-His-Glu-Glu-Thr-
                                                            Gly Val
                                                         His     Cys
                                                        Tyr       Gln
                                                         Glu     Ser
                                                            Thr
```

PART II. GENERAL METHODS AND MATERIALS

Section 1. Growth of bacteria

Clostridium acidi-urici

C. acidi-urici was grown and growth was measured by a previously described method (115), except that the growth medium contained little or no yeast extract. Yeast extract contains significant quantities of amino acids (Table 1), and the concentration of yeast extract normally used in *C. acidi-urici* growth medium would dilute the amino acid label. *C. acidi-urici* does not require yeast extract for growth (8), but the presence of yeast extract increases cell yield. The concentration of yeast extract that gave the largest cell yield and the smallest dilution of amino acid label was approximately 0.004% (25 times less than normally used). Yeast extract was sterilized by millipore filtration before adding aseptically to the growth medium.

Clostridium pasteurianum

C. pasteurianum was grown according to methods described elsewhere (115).

Clostridium butyricum

C. butyricum was grown according to methods described elsewhere (9).

Table 1. Concentration of amino acids in Difco yeast extract (1 mg/ml)[a].

Amino Acid	[nM/ml]
aspartate	114.0
threonine	134.6
serine	201.7
glutamate	358.0
citrulline	22.3[b]
proline	55.9
glycine	130.3
alanine	340.8
1/2 cystine	14.9
valine	204.3
methionine	36.6
isoleucine	133.0
leucine	200.3
tyrosine	18.2
phenylalanine	101.6

a. This was determined by Dr. A. B. Champion (27) using a Beckman amino acid analyzer.
b. Value was based on the assumption that 10 umoles of citrulline has a color value of 0.58.

Section 2. Sample Preparation

PREPARATION OF FERREDOXIN:

C. acidi-urici FERREDOXIN:

The purification procedure used is a modification by A. B. Champion (28) of a previously described method (115). 100 g. of frozen wet cells of *C. acidi-urici* were thawed overnight at 4°C and suspended in 0.15 M Tris-Cl, pH 7.4, to a final volume of 300 ml. 40 μl. of a 5 mg/ml solution of DN'ase (Worthington, RN'ase-free) was added to facilitate suspension and reduce the viscosity of the mixture. 60 ml. aliquots were sonicated for 9-12 minutes in a Raytheon sonic oscillator, 10 kHz, model DF101. The sonicate was centrifuged at 30,000 × G for 30 minutes, and the supernatant (crude extract) collected.

The crude extract was applied to a 2×40 cm DEAE-cellulose (Carl Schleicher and Schuell Co.) column, which had been equilibrated with 10 column volumes of H_2O. The column was washed with pressure with 1.3 l. of 0.15 M Tris-Cl, pH 7.4, and then with 1.3 l. of 0.05 M Tris-Cl, pH 7.4, plus 0.16 M NaCl. The ferredoxin was eluted with a linear salt gradient of 500 ml. of 0.05 M Tris-Cl, pH 7.4, plus 0.16 M NaCl and 500 ml. of 0.05 M Tris-Cl, pH 7.4, plus 0.50 M NaCl. Ten ml. fractions were collected and the appropriate fractions analyzed for A_{390} (ferredoxin) and A_{280} (total protein).

The pooled ferredoxin peak was diluted two-fold with H_2O and applied to a 2.5×8 cm. DEAE-cellulose column which had been equilibrated with 10 column volumes of H_2O. The column was washed with 200 ml. of 0.05 M Tris-Cl, pH 7.4, plus 0.23 M NaCl. The ferredoxin was eluted with a small volume of 0.15 M Tris-Cl plus 0.38 M NaCl.

The ferredoxin from the second DEAE-cellulose column was concentrated by addition of solid ammonium sulfate to make the solution 90% saturated. The pH was adjusted to 7.5 with concentrated ammonium hydroxide, the solution stirred for 30-40 minutes at 4°C, and then centrifuged at 30,000×G for 20 minutes. The pellet containing the ferredoxin was dissolved in 1-2 ml. of 0.075 M Tris-Cl, pH 7.4, and applied to a 2.5×90 cm Sephadex G-75 column which had been equilibrated with 1 l. of 0.075 M Tris-Cl, pH 7.4. The ferredoxin was eluted with the equilibration buffer, five ml. fractions were collected, and the appropriate fractions analyzed for A_{390} and A_{280}.

The fractions containing the ferredoxin were pooled and solid ammonium sulfate was added in small portions over a 15 minute period to make the solution 80% saturated. The pH was adjusted to 7.5 and the solution stirred for 30-40 minutes at 4°C. The solution was centrifuged at 30,000×G for 20 minutes, and the pellet containing the ferredoxin dissolved in 80 to 10 ml. of 0.15 M Tris-Cl, pH 7.4, and stored in a Thunberg tube under vacuum at 4°C.

C. butyricum FERREDOXIN:

Preparation was the same as that for C. acidi-urici with the following exceptions.

64.8 g. of C. butyricum (strain 2981A from Dr. C. S. Cummins of the Virginia Polytechnic Institute, Blacksburg, Va., which sould be equivalent to ATCC 6014) was suspended in 100 ml. 0.1 N Tris-Cl buffer, pH 7.4.

The ferredoxin was washed on the second DEAE column (2.5×8 cm) with 40 ml. 0.05 M Tris buffer, pH 7.4, plus 0.19 M NaCl. It was

eluted with 100 ml. 0.15 M Tris-Cl buffer, pH 7.4, plus 0.23 N NaCl.

Pooled ferredoxin fractions from the second DEAE cellulose column were brought to 95% of saturation with ammonium sulfate. C. butyricum does not readily crystallize with even 100% saturated ammonium sulfate. Any coprecipitated ferredoxin in the precipitate of the 95% of saturation ammonium solution was purified by passing it through a Sephadex G-75 column. The pooled ferredoxin fractions (A_{390}/A_{280} = 0.82) were added to the supernate (mother liquor) of the 95% of saturation ammonium sulfate solution. This was added to an ammonium sulfate-DEAE cellulose column (third DEAE cellulose column).

The third DEAE cellulose column (1.5×8.0 cm), that had been equilibrated with H_2O, was now equilibrated with 75% of saturation ammonium sulfate solution. The mother liquors, of all the ammonium sulfate ferredoxin crystallization attempts, were added to this column, the ferredoxin stuck to the column and it was eluted off the 0.38 M NaCl plus 0.05 M Tris-Cl, pH 7.4. This concentrated the ferredoxin 10-fold.

The pooled fractions were further concentrated in a Thunberg tube by careful evacuation of H_2O with a lyophilizer to about half of the original volume. The final concentration of ferredoxin was 2.26 mg/ml, or a total of 4.52 mg. of ferredoxin per 64 g. of wet cells.

C. pasteurianum FERREDOXIN:

C. pasteurianum ferredoxin was prepared by James Brodrick by previously described methods (115).

C. cylindrosporum FERREDOXIN:

Preparation of C. cylindrosporum ferredoxin was the same as for C. acidi-urici ferredoxin with the following exceptions.

Cells were suspended in 0.12 M Tris-Cl buffer, pH 7.4.

The first DEAE cellulose column was washed with 1.3 liter 0.012 M Tris-Cl buffer, pH 7.4, and then with 1.3 liter 0.12 M NaCl plus 0.05 M Tris-Cl buffer (pH 7.4). The ferredoxin was eluted with a linear salt gradient of 500 ml of 0.12 M NaCl plus 0.05 M Tris-Cl, pH 7.4, and 500 ml of 0.5 M NaCl plus 0.05 M Tris-Cl, pH 7.4.

The ferredoxin in the second DEAE cellulose column (2.5×8 cm) was washed with 50 ml 0.19 M NaCl plus 0.05 M Tris-Cl buffer, pH 7.4.

C. cylindrosporum ferredoxin was crystallized from the G-75 column with ammonium sulfate brought to 95% of saturation.

PREPARATION OF APOFERREDOXIN:

This preparation is based on a previously described procedure (59) with the following modifications. C. acidi-urici ferredoxin, 14 mg in 11 ml of 0.015 M Tris-Cl, pH 7.4, was made 4% in trichloroacetic acid with a 15% trichloroacetic acid solution. This mixture was allowed to stand for 1 hour at 0°C. Evolution of H_2S gas was noted throughout this period, and the brown color of ferredoxin was completely bleached at the end of this period. The white suspension was centrifuged at 33,000× G for 10 minutes and the supernatant solution was discarded. The precipitate was washed with 3 ml. of 0.023 M formic acid and allowed to stand for 30 minutes at 0°C and centrifuged. The washing was repeated once. The precipitate was finally taken up in 4 ml of 0.1 M Tris-HCl, pH 9.0, and the insoluble material was removed by centrifugation.

RECONSTITUTION OF FERREDOXIN FROM APOFERREDOXIN:

Apoferredoxin was reconstituted by previously published methods (59) with the following modifications.

To 0.5 ml of 0.5 M Tris-Cl (pH 8.3 at 25°C) that had been flushed with N_2 for 5 minutes, 0.48 g recrystallized urea (to make 8 M urea) and H_2O were added to bring the volume to 2.0 ml. This solution was bubbled with N_2 for 5-10 minutes, and 21 mg dithiothreitol (to make 0.07 M dithiothreitol) was added. 0.5 ml of this solution was added to 2 mg of apoferredoxin, which was flushed with N_2 for 2-3 minutes and incubated at 37° for 1 hour.

Recrystallized urea was prepared by dissolving commercial urea (J. T. Baker, Chemical Co.) in a minimal volume of hot acidic absolute ethanol, to which were added 1-2 drops concentrated HCl. This was allowed to stand at room temperature. The resultant crystals were filtered by Whatman No. 1 filter paper in a Buchner funnel, washed with cold ethanol, and dried in a desiccator over P_2O_5 overnight.

First 0.1 ml of 0.1 M $Na_2S \cdot 9H_2O$ and then 0.1 ml of 0.1 M $FeSO_4(NH_4)_2SO_4$ were added to the ferredoxin solution. This was mixed and 3.0 ml of a solution of 0.1 M Tris-Cl, pH 7.4, plus 0.035 M dithiothreitol (that had been previously flushed with N_2) was quickly added. This mixture was incubated and flushed with N_2 at room temperature for 15 minutes. Then it was cooled on ice and applied to a 1.0×8.0 cm DEAE cellulose column that had been equilibrated in the cold with 0.15 M Tris-Cl, pH 7.4. The ferredoxin was washed with 20 ml 0.23 M NaCl plus 0.005 M Tris-Cl, pH 7.4, and eluted with 10-20 ml 0.58 M NaCl plus 0.005 M Tris-Cl, pH 7.4.

Larger quantities of apoferredoxin were reconstituted by scaling up the quantities. When apoferredoxin was reconstituted in D_2O all reagents that could be lyophilized were, and were then redissolved in D_2O. Those reagents which could not be lyophilized (such as DEAE cellulose) were equilibrated with D_2O (Biorad Laboratories 99.84% pure).

PREPARATION OF CELL PROTEIN:

Two methods were used in the preparation of cell protein. In the first method (146), cells grown in 2 l. flasks were centrifuged at 30,000 × G for 1 hour and suspended in cold 5% trichloroacetic acid (TCA) to precipitate protein. The TCA suspension was centrifuged at 30,000 × G for twenty minutes after standing for 1 hour. The supernate solution was discarded and the pellet washed with cold 5% TCA. This suspension was then incubated for 15 minutes at 90°C to solubilize nucleic acid components, and then centrifuged for 20 minutes at 30,000 × G. The supernate solution was discarded and the pellet was dissolved in 1 M Tris-Cl base. This alkaline solution was dialized against H_2O for 48 hours, and the desalted protein solution was then lyophilized and stored in a vacuum desiccator.

In the second method, the pass-through of the first DEAE cellulose column (see Preparation of Ferredoxin) was brought to 95% of saturation by $(NH_4)_2SO_4$. This was dialyzed three times against six liters of H_2O for 24 hours, lyophilized, and stored in a vacuum desiccator. (The DEAE cellulose column presumably removed most of the nucleic acid components).

PREPARATION OF SAMPLES FOR AMINO ACID ANALYSIS:

Apoferredoxin prepared from ferredoxin (59) was hydrolyzed with 6 N HCl in a vacuum for 24 hours at 110°. The hydrolysate was evaporated to dryness at 37°, resuspended in 250 μl amino acid analyzer buffer A (Na citrate 0.2 M, boric acid 0.001 M, thiodiglycol 0.25%, pH 3.2), centrifuged, and the supernate solution applied to an amino acid analyzer column that was connected directly to a fraction collector. With ^{14}C-ferredoxin the radioactivity of 0.4 ml of the 1.5 ml fractions was determined, and the elution pattern was compared with that of a standard set 0.33 μCi of [^{14}C] amino acids which had been previously analyzed on the same analyzer.

PREPARATION OF SAMPLES FOR NMR:

Partially reduced ferredoxin was prepared at 4°C by dissolving 30 mg of ferredoxin in 2 ml of 20 mM Zn-reduced methyl viologen, 0.07 M KD_2PO_4-K_2DPO_4, pD 7.0 (pH 7.4). C. acidi-urici ferredoxin was only partially reduced by this procedure. More completely reduced ferredoxin was obtained by first washing the ferredoxin pellet with 20 ml of 20 mM reduced methyl viologen in 80% saturated $(ND_4)_2SO_4$. The methyl viologen was reduced by passing it anaerobically through a column of powdered Zn that had been cleaned with 0.1 N HCl (133) and washed with 0.2 M KD_2PO_4-K_2DPO_4 buffer, pD 7.0. The bottom of the column was fitted with a sintered glass disk, and the methyl viologen was added to the ferredoxin with a syringe. This procedure was used to insure that no Zn particles entered the methyl viologen solutions. Reduced methyl viologen cannot be stored in Zn because methyl viologen will accept two electrons with an excessive amount of Zn and become

doubly reduced. The doubly reduced form of methyl viologen is very insoluble in H_2O and does not react with ferredoxin. When the doubly reduced form of methyl viologen precipitates out of solution, the electrode potential of the solution increases because the electrode potential is a function of the concentration ratio:

$$\frac{[\text{singly reduced methyl viologen}]}{[\text{oxidized methyl viologen}]}$$

Partially reduced ferredoxin free of $(ND_4)_2SO_4$ was prepared by adding reduced methyl viologen to a dialyzed ferredoxin preparation previously deaerated and concentrated by careful evacuation in a Thunberg tube modified to contain a septum cap. ESR and ^{1}H-NMR measurements of reduced and reoxidized C. acidi-urici ferredoxin show that methyl viologen reduction does not detectably denature this ferredoxin (96).

PREPARATION OF SAMPLES FOR ESR:

OXIDIZED FERREDOXIN:

0.4 ml of 5 mg/ml ferredoxin in 0.15 M Tris-Cl buffer, pH 7.4, in a 4 mm quartz ESR tube was slowly immersed in a liquid N_2 bath. Frozen samples were quickly placed into the ESR cavity, which had been precooled by liquid He. After the ESR measurement, the frozen samples were quickly immersed into H_2O at room temperature. When thawed, an aliquot of the ferredoxin sample was diluted with 0.15 M Tris-Cl buffer, pH 7.0, and the ratio of A_{390}/A_{280} was determined.

REDUCED FERREDOXIN:

10 ml 0.2M methyl viologen, deaerated by repeated evacuation and flushing with Ar, was added by a syringe (previously flushed with Ar) to 5-10 mg of 20 mesh Zn pellets in a Thunberg tube, modified as described above. Aliquots of this Zn-reduced methyl viologen were added to aliquots of

ferredoxin which had been previously deaerated by repeated evacuation and flushing with Ar in an ESR tube, which had been modified into a Thunberg tube with a septum cap, to make a total volume of 0.4 ml.

For dithionite-reduced ferredoxin, 2-5 M excess of 0.15 M Tris-Cl buffered (pH 7.4) $Na_2S_2O_4$ was added to aliquots of deaerated ferredoxin.

Section 3. Instrumentation

ESR INSTRUMENTATION (80)

ESR spectra were obtained at X-band using a JEOL ME-1X ESR spectrometer operating at 1.4 mW and a frequency of 9.10 GHz. Samples in standard quartz tubes (3 mm inside diameter × 4 mm outside diameter) were cooled to 25° K by a stream of boiling ^{4}He gas passing through a quartz dewar assembly placed in the cylindrical-mode ESR cavity. The temperature of the sample was monitored by a carbon-resistance thermometer placed 10 mm upstream from the sample position; its readings were compared with those of a similar carbon-resistance thermometer used as a substitution probe in place of the sample tube. Temperatures with carbon-resistance thermometers were determined by interpolation between resistance values at the boiling temperatures of ^{4}He and N_2. First-derivative ESR spectra were obtained using 100 kHz modulation of the magnetic field; 8-15 spectra were "signal-averaged" by using a small digital computer (PDP-8/L with AX08 analog-to-digital converter), and the resultant averaged spectrum was plotted on a X-Y recorder.

NMR INSTRUMENTATION

The ^{13}C-NMR measurements were done at 23.4 KGauss with a Varian XL-100 spectrometer interfaced to a Nicolet 1080 computer, and modified

for Fourier transform (FT) operation (123). Signal accumulation in the FT mode is generally much more efficient than in the continuous wave mode, and a significant gain in signal to noise relative to the continuous wave mode is possible (45, 11). A 12 mm probe insert coil was used to maximize sensitivity, and a Wilmad cylindrical capillary macrocell was used to contain the sample to minimize sample volume. (The macrocells require approximately 0.7 cc of material). The protons were decoupled from the carbons with either coherent or noise-modulated radio frequency (rf) radiation at ca. 100.06 MHz. The magnetic field was locked to the first lower sideband resonance of the deuterium in the solvent D_2O, which occurs at 15.400950 MHz in the XL-100 spectrometer used. A repetitive series of ca. 25.167 MHz rf pulses of 60 μsec duration and 300 V peak to peak (p-p) were used to rotate the ^{13}C magnetization 90° from its equilibrium position along the external magnetic field. In the ferredoxin study the free induction decay signal produced after each rf pulse was sampled at a 20 KHz rate after a delay of 800 μsec measured from the rise of the rf pulse. The free induction decays were accumulated in either 4096 or 8192 channels of the Nicolet computer, filtered by multiplying the decay function by a suitable exponential, Fourier transforming the result using 8192 channels and then phase corrected to obtain absorption mode spectra extending 10 KHz in theory with ca. 2.5 Hz maximal resolution. The crystal filters of the Varian receiver, however, limited the extent of the spectra of 7.5 KHz.

A delay time, τ_D, of 800 μsecs was introduced to eliminate or reduce transients introduced by the rf pulse and subsequent gating. The appearance of the ferredoxin spectra were sensitive to these transients

because of; (i) the large number of accumulation required ($\geq$ 100,000) to obtain a reasonable signal to noise ratio, and (ii) the difficult experienced in balancing the probe because of the high ionic strength of the protein solution. This balancing difficulty resulted in increased rf leakage and a relatively large transient. The free induction signal obtained after a sampling delay, τ_D, is mathematically equivalent to multiplying the free induction signal obtained without any sampling delay by a function f(t) that is 0 in the time interval $0 < t < \tau_D$ and 1 for $t > \tau_D$. The FT of the delayed free induction decay is therefore identical to the function obtained by convoluting the FT of the non-delayed free induction decay signal with $F(\omega)$, the FT of the f(t) function. $F(\omega)$ is of the form where ω denotes frequency in Rad Sec^{-1}. The consequence of this convolution is twofold: (i) residual transients manifest themselves in a sinusoidal-like base line oscillation which extends across the entire spectrum. As τ_D is increased the frequency of this base line oscillation increases but the amplitude decreases. (The baseline oscillations in the figures below, while esthetically disturbing, did not significantly interfere with measurements of the intensity or frequency of the aromatic resonances.); (ii) Any intense resonances present in the spectra acquire oscillating tails which can interfere or obscure weaker resonances.

A further consequence of a long delay τ_D is to cause selective intensity changes whereby broad lines with transverse relaxation times comparable to τ_D are diminished relative to narrow line resonances which are unaffected. In our study this causes an intensity decrease in the broad aliphatic region of the spectra. The relatively narrow aromatic resonances are unaffected.

The distortions that result from a delay time, τ_D, can be reduced through cosmetic software, appropriate apodization of the f(t) function so that it does not rise rapidly, and improved gating so that τ_D can be decreased.

High-resolution proton NMR spectra were obtained on a Varian 220-MHz (HR 220) spectrometer. A standard Varian variable temperature control unit was used. The temperature in the sample zone was determined from the chemical shifts of the resonances of an ethylene glycol sample. In the temperature range 7° - 35°C, the regulation is better than ± 1° over the period of time required for any of the experiments described in this thesis. Signal-to-noise ratios were improved by employing a Fabritek 1062 computer of average transients. An rf field of 1 milligauss was used with a sweep rate of 20 Hz sec^{-1}.

PART III. RESULTS

Section 1. Incorporation of modified tyrosine into *Clostridium acidi-urici* ferredoxin

Experiment 1.
Incorporation of [^{14}C] tyrosine into *Clostridium acidi-urici* ferredoxin

SUMMARY:

[U-^{14}C] Tyrosine is incorporated into growing *C. acidi-urici*, and the only [^{14}C] amino acid present in ferredoxin purified from *C. acidi-urici* grown in the presence of [^{14}C] tyrosine is [^{14}C] tyrosine. The experiments that demonstrated this result were:

(i) uptake of [U-^{14}C] tyrosine, in the presence and absence of [^{12}C] carrier tyrosine. This was determined by measuring the radioactivity of cells and trichloroacetic acid-precipitable material as a function of time;

(ii) purification of [^{14}C] ferredoxing from two liter cultures grown in [U-^{14}C] tyrosine;

(iii) preparation of [^{14}C] apoferredoxin for amino acid hydrolysis;

(iv) amino acid analysis of the acid hydrolysate of [^{14}C] ferredoxin. Ninhydrin analysis was performed by the amino acid analyzer to provide further proof of the purity of ferredoxin. The effluent of the amino acid analyzer column was collected in fractions. The

presence of radioactivity in these fractions was then determined after standardization of the column with a known mixture of [^{14}C] amino acids. The amino acid hydrolysate of ferredoxin isolated from cells grown in the presence of [^{14}C] tyrosine, exhibited one radioactive peak, which was identified as tyrosine.

INTRODUCTION:

Isotopically labeled tyrosine is very expensive to prepare and it is necessary to know the concentration that is most efficiently incorporated into cell protein. If too little is added to the growing culture, there may not be enough to induce a permease (if it exists), or, if there is enough to induce a permease, it may not saturate the cells, and the labeled tyrosine will be diluted by [^{12}C] tyrosine produced by cell metabolism. If too much tyrosine is added, not all of it may be incorporated, since the final cell density is limited by the solubility of its carbon source, uric acid.

The purpose of the first series of experiments was to determine:

(i) if [^{14}C] tyrosine and [^{14}C] alanine are incorporated into growing C. acidi-urici. Incorporation of these amino acids has not been previously demonstrated. [^{14}C] Serine incorporation into C. acidi-urici protein has been demonstrated by Dr. A. B. Champion (28), and its incorporation was used as a control.

(ii) the minimum tyrosine concentration that induces a permease, and the concentration of tyrosine that saturates the system. In this experiment incorporation into TCA precipitable material was used to measure the extent of [^{14}C] tyrosine incorporation into protein to see if the increase in incorporation was a function of cell growth.

(iii) the effect of yeast extract on the efficient incorporation of [^{14}C] tyrosine into protein. The growth medium normally includes 0.1% yeast extract, which contains 1.8×10^{-2} mM tyrosine, which is about four times greater than the concentration of new tyrosine produced by one generation of cells; medium with 0.01% yeast extract will not significantly dilute any [^{14}C] tyrosine in cell protein after four generations, but it may increase cell yield.

METHODS AND MATERIALS:

[^{14}C] AMINO ACID INCORPORATION INTO GROWING *C. acidi-urici* CELLS:

Log phase *C. acidi-urici* grown on uric acid medium (115) with no yeast extract were transferred to serum-capped test tubes containing either [U-^{14}C] tyrosine, [U-^{14}C] serine, or [U-^{14}C] alanine (Amersham/Searle Corporation), and were incubated at 37° C. for various times. These test tubes had been flushed with N_2 and pre-incubated at 37° C. for 5 minutes before inoculating them with cells. The complete incubation mixture (1 ml) contained 5×10^7 cells, 5 ml NaCl, 1 mM carrier [^{12}C] amino acid, and either 1 μCi [U-^{14}C) tyrosine, [U-^{14}C) serine, or [U-^{14}C] alanine (2.44, 6.25, and 8.55 μM, respectively).

At different incubation times 2 ml of cold 0.15 M Tris-Cl buffer (pH 7.0) were introduced into each tube. The contents of these tubes were filtered with 0.45 μ millipore filters, which were then washed with 6 ml of the same buffer. The washed filters were transferred into 10 ml Bray's solution (21) for scintillation counting.

EFFECT OF [^{12}C] TYROSINE CARRIER CONCENTRATION ON [^{14}C] TYROSINE INCORPORATION:

Cells were grown as above, except that the 5 mM NaCl was removed from the incubation medium, which now contained 5×10^{7} cells, 1 mg. yeast extract (1.8×10^{-2} mM tyrosine), 1 μCi [^{14}C] tyrosine (2.5 μM) and 0, 0.1 mM, and 1.0 mM [^{12}C] tyrosine, all in 1 ml.

Uric acid concentration and cell density were monitored by measuring 1/100 dilution of culture at A_{290} and 0.5 ml culture plus 0.5 ml 0.9% NaCl at A_{660}, respectively (29). One ml of incubation mixture was filtered and washed with Tris-Cl as above. This represented the cell fraction (pool plus protein). The protein fraction was prepared by adding to another 1 ml sample of incubation mixture 0.1 ml of 50% TCA at various times, to precipitate protein. This sample has then incubated at 90° for 10 minutes, cooled 20 minutes in an ice bath and millipore-filtered and washed with 7 ml cold 5% TCA. This step removed nucleic acids (146). The millipore filter containing TCA-precipitable material was put into Bray's solution for scintillation counting.

EFFECT OF YEAST EXTRACT CONCENTRATION ON [U^{14}C] TYROSINE INCORPORATION:

Cells were grown as above, except that the incubation mixture (33 ml) contained 1.5×10^{9} cells (suspended in 30 ml growth medium without yeast extract), 0.5 μCi (1.25 μm) [^{14}C] tyrosine, and 0, 3, and 30 mg yeast extract, in serum-capped bottles. At various times 1 ml of incubation mixture was millipored and washed with cold 0.15 M Tris-Cl buffer to measure total incorporation into cells, 1 ml was made 5% with respect to TCA with 0.1 ml 50% cold TCA and treated as

described above, 5 ml was made 5% TCA with 0.5 ml 50% TCA and saved for protein determination by the Lowry method (147). 5-10 μl were placed on a Pretroff-Hauser cell counter to measure cell number, and the remaining 27 ml was centrifuged at 30,000 × G. The supernate solution was dried in glass scintillation vials to determine how much [U-^{14}C] tyrosine was not incorporated into the cells. This latter measurement is only qualitative, because of the quenching effect of the residue of salts from 30 ml of growth medium. A better method used in subsequent experiments, involves testing 0.4 ml of a millipored filtrate for unincorporated radioactivity.

PURIFICATION OF FERREDOXIN OBTAINED FROM C. acidi-urici GROWN IN THE PRESENCE OF [U-^{14}C] TYROSINE:

C. acidi-urici was grown in 2 liters of growth medium (see General Methods) containing 50 μCi [^{14}C] cells were added to 33 g (wet weight) of unlabeled cells. Ferredoxin was purified by a procedure (115), modified by Champion (28).

RESULTS AND DISCUSSION:

[^{14}C] AMINO ACID INCORPORATION INTO GROWING C. acidi-urici CELLS:

[U-^{14}C] tyrosine, [U-^{14}C] alanine, and [U-^{14}C] serine were individually incorporated into growing C. acidi-urici (Figs. 4, 5, and 6 respectively). The "expected" incorporation of [^{14}C] amino acids is calculated as follows. Roberts et al. (118) derive a theoretical quantity of radioactive product per cell mass:

$$\frac{X^*}{Q} = \frac{X_0}{Q_0} (1 - e^{-at})$$

where X^* = quantity of ^{14}C amino acid in cells at time t (hours). This quantity is corrected for the dilution due to [^{12}C] amino acid carrier.

X_0 = quantity of [^{14}C] amino acid at t = 0.

Q = mass of cells at time t.

Q_0 = mass of cells at time t = 0.

a = specific rate of incorporation.

If the specific rate of incorporation, a, is proportional to the specific growth rate of the cells, then the incorporation of [^{14}C] amino acid is a function of cell growth.

The observed concentration of incorporated [^{14}C] amino acids deviated slightly from the expected concentration and it is not due to the dilution produced by [^{12}C] tyrosine carrier, since the dilution was taken into account in the calculations.

EFFECT OF [^{12}C] TYROSINE CARRIER CONCENTRATION ON [^{14}C] TYROSINE INCORPORATION:

The total incorporation of [U-^{14}C] tyrosine (μmole/ml) was diluted by [^{12}C] tyrosine carrier but the specific incorporation (μmole/ml/g cells) is essentially constant (Fig. 8) after the initial burst of incorporation, i.e., the total [^{14}C] tyrosine incorporation increases with the increase in cell mass, and incorporation is thus a function of cell growth.

EFFECT OF YEAST EXTRACT CONCENTRATION ON [U-^{14}C] TYROSINE INCORPORATION:

Reduction of the yeast extract concentration in the growth medium increases the total amount of [U-^{14}C] tyrosine incorporated into C. acidi-urici protein (Fig. 9).

The leveling off of [U-^{14}C] tyrosine incorporation when there is no or 0.01% yeast extract present (Fig. 9) may be because there is not enough [^{14}C] tyrosine in the incubation medium to account for the tyrosine content of newly synthesized protein from one generation of cells. In fact, the concentration of [^{14}C] tyrosine in the incubation mixture is at least 100 times less than the tyrosine content of 40 μg dry weight (one generation/ml) of cells. This assumes a tyrosine content of 4×10^{-3} μmoles/ml/generation, if tyrosine is 2% of the cell's dry weight (29).

The tyrosine concentration that induces a hypothetical permease was not determined; it is at least 3.7×10^{-8} M since there is incorporation with that much [U-^{14}C] tyrosine in the medium with no yeast extract (Fig. 9). The tyrosine concentration that gives maximum incorporation is at least 1.8×10^{-6} M. This is because the observed maximum [^{14}C] tyrosine specific activity (Table 2) essentially agrees with the quantities calculated for various input concentrations of [[^{12}C] tyrosine + [^{14}C] tyrosine] > 1.8×10^{-5} M.

The 1.8×10^{-6} M tyrosine concentration that begins to give maximum tyrosine incorporation is consistent with the observation by Chen (29) that the concentration of amino acid that produces one half the maximum rate of its incorporation is 10^{-5} M.

PURIFICATION OF FERREDOXIN OBTAINED FROM C. acidi-urici GROWN IN THE PRESENCE OF [U-^{14}C] TYROSINE:

The purification procedure and results are summarized in Table 3 and Figs. 10 and 11. One radioactive peak, 50 times greater than background radioactivity, was observed (Fig. 12), and its position corresponded to that of a [^{14}C] tyrosine standard (Fig. 13, Table 4). The radioactivity in this peak accounted for 70% of the radioactivity of the labeled ferredoxin. This is a reasonable yield, considering the losses that can occur on preparation and transfer of small volumes of apoferredoxin and its hydrolysate.

Amino acid analysis of the [^{14}C] ferredoxin hydrolysate revealed that, as with [^{12}C] ferredoxin, no methionine, leucine, phenylalanine, histidine, or lysine are present in this protein. The amino acids that are present in the [^{14}C] ferredoxin hydrolysate occur in the same molar quantities found (61) in [^{12}C] ferredoxin (Table 5).

The UV and visible absorption spectra of C. acidi-urici [^{14}C] ferredoxin are identical to those of C. acidi-urici [^{12}C] ferredoxin.

REGULATION OF AMINO ACID SYNTHESIS:

The fact that [^{14}C] tyrosine was incorporated undiluted into C. acidi-urici ferredoxin demonstrates the existence of some regulatory mechanism for the synthesis of tyrosine in C. acidi-urici. Regulation may involve induction of a permease and repression of tyrosine synthesizing enzymes analogous to regulation mechansims demonstrated for other bacteria (3, 14, 22, 90, 91, 92).

[^{14}C] Serine incorporation has been demonstrated by Champion (27), and was used as a control for the previously-undemonstated [^{14}C] alanine and [^{14}C] tyrosine incorporation. Chen (29) has shown by the use of [1-^{14}C] glycine and [2-^{14}C] glycine that both glycine carbon atoms are incorporated into all the amino acids of C. acidi-urici protein. Thus, glycine is metabolized. Presumably alanine and serine are also metabolized by C. acidi-urici. The metabolic pathway proposed by Champion (28) for the utilization of glycine in C. acidi-urici shows that glycine produces serine via Serine hydroxymethyltransferase. Presumably acetate (which should be produced by serine after at least four enzymatic steps (28)) produces alanine by a transamination reaction (29). The labeling pattern of protein from C. acidi-urici grown individually on [U-^{14}C] alanine and [U-^{14}C] serine was not tested, however.

[^{14}C] Tyrosine, if it is incorporated, is usually not metabolized by bacterial cells (14), but instead goes directly into proteins (90). Tyrosine incorporation and the fate of labeled tyrosine have not been previously studied in C. acidi-urici. In Escherichia coli [1-^{14}C] glucose and [2-^{14}C] glucose contribute radioactivity to protein tyrosine (135), but [^{14}C] alanine and [^{14}C] serine do not contribute radioactivity to tyrosine in E. coli (135). Chen (29) found that ^{14}C of [1-^{14}C] glycine and [2-^{14}C] glycine is found in the tyrosine of C. acidi-urici protein. The [^{14}C] tyrosine specific activity observed (29) was three and four times that of the [^{14}C] serine found in the protein from cells grown in the presence of [1-^{14}C] glycine and [2-^{14}C]

glycine respectively. From this labeling pattern one cannot determine how tyrosine is synthesized in C. acidi-urici except that the relative specific activity observed by Chen is consistent with the pathway for tyrosine synthesis observed for E. coli (135). (In E. coli one mole of erythrose-4-phosphate and two moles phosphoenolpyruvate react and eventually form one mole of tyrosine and one mole of phenylalanine, and Chen finds that [^{14}C] tyrosine and [^{14}C] phenylalanine have essentially equal relative specific activities when C. acidi-urici is grown in the presence of [^{14}C] glycine. Presumably in C. acidi-urici the ^{14}C would enter phosphoenolpyruvate and erythrose-4-phosphate from [^{14}C] acetate produced by the [^{14}C] glycine.) If the E. coli tyrosine synthetic pathwya occurred in C. acidi-urici, then one would expect that tyrosine synthesis would be regulated as it is in E. coli (135).

Fig. 4. Kinetics of incorporation of [^{14}C] tyrosine into *C. acidi-urici* grown in the presence of 1 μM [^{12}C] tyrosine carrier, 5 mM NaCl, and no yeast extract.
(——) = expected (see text). (- - -) = observed × 10.

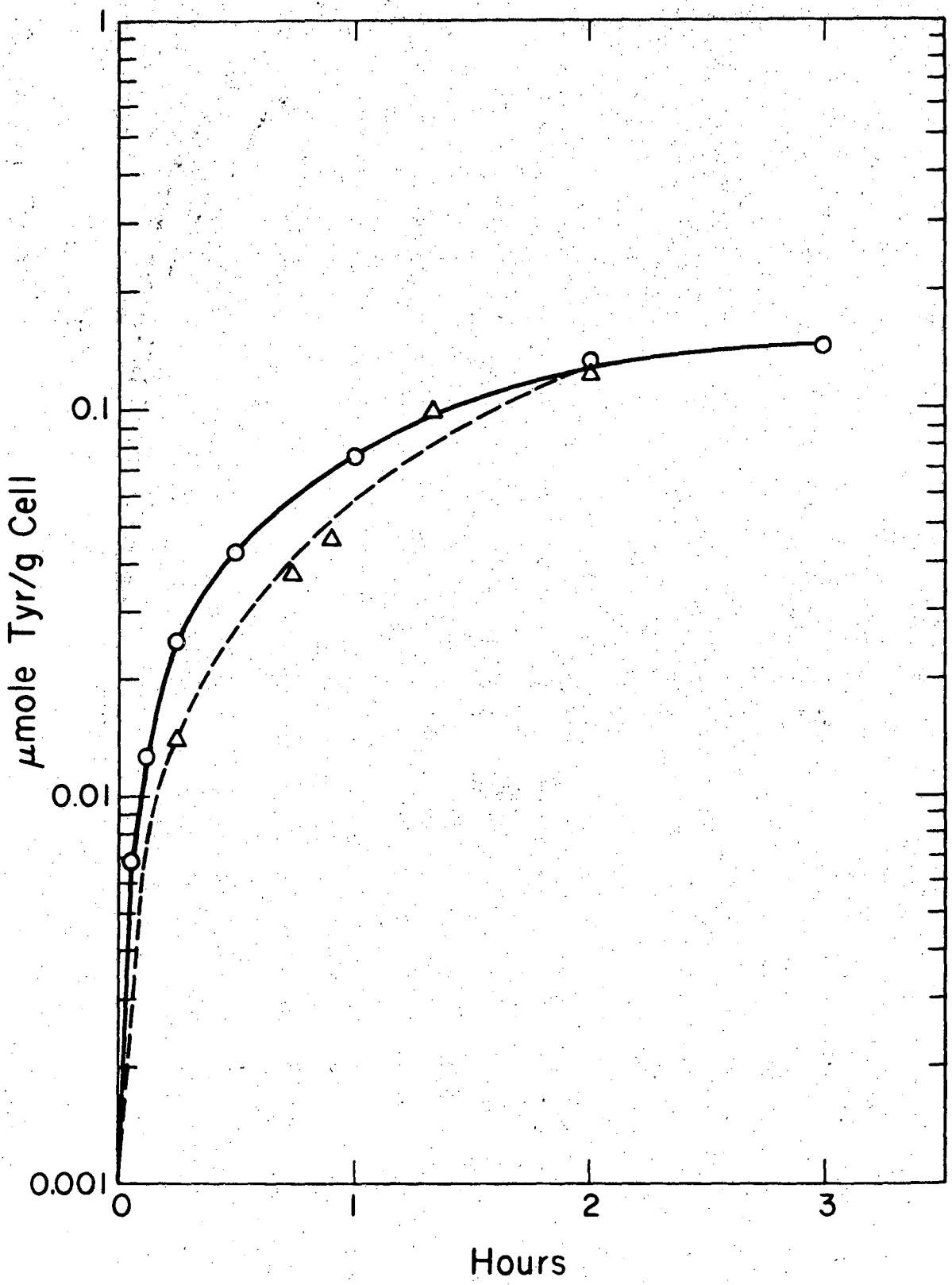
1
0.1
0.01
0.001
μmole Tyr/g Cell
0
1
2
3
Hours

Fig. 5. Kinetics of incorporation of [^{14}C] alanine into C. acidi-urici grown in the presence of 1 μM [^{12}C] alanine carrier, 5 mM NaCl, and no yeast extract.

(——) = expected (see text). (- - -) = observed.

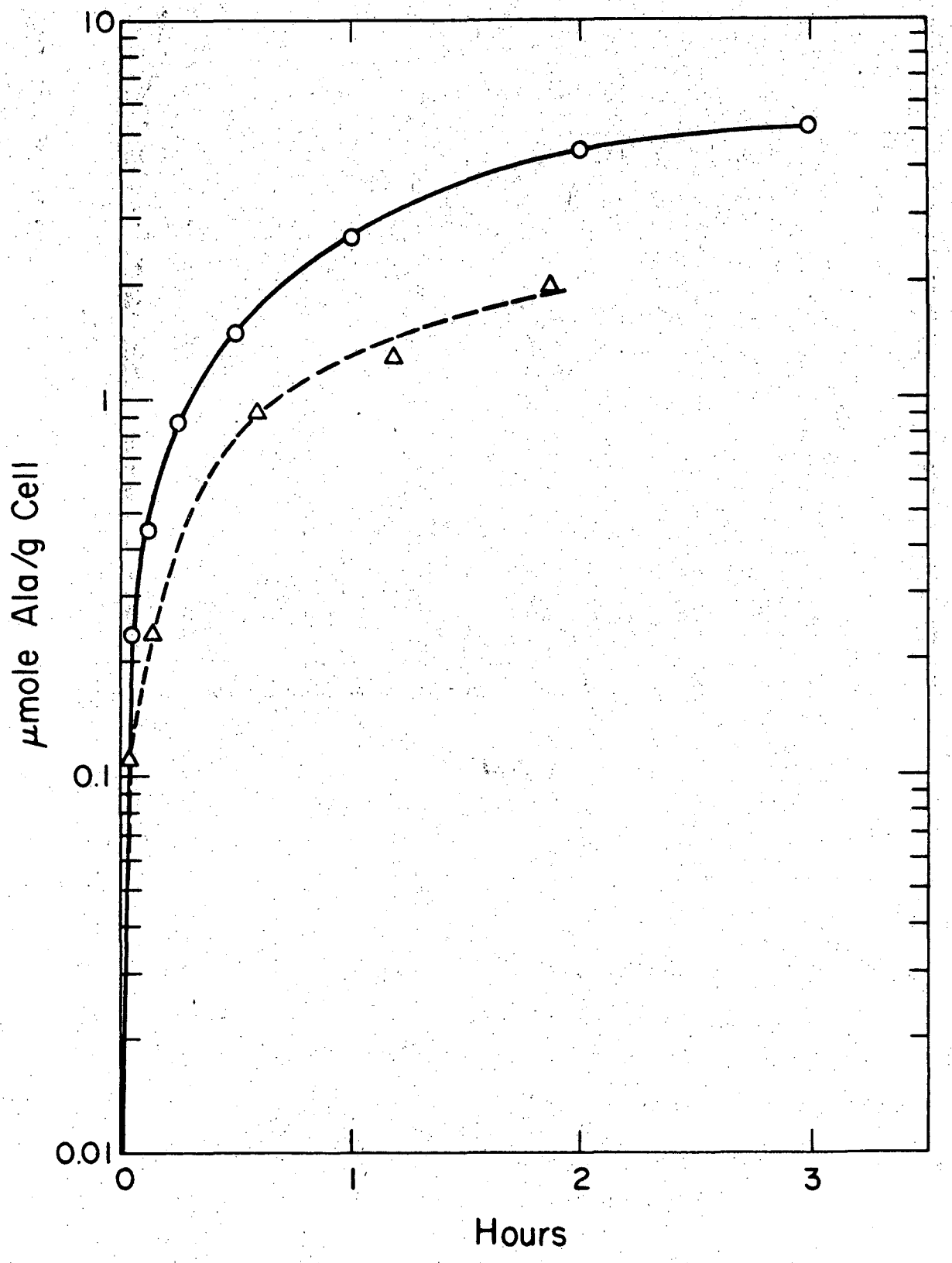
10
1
0.1
0.01
μmole Ala/g Cell
0
1
2
3
Hours

Fig. 6. Kinetics of incorporation of [^{14}C] serine into *C. acidi-urici* grown in the presence of 1 μM [^{12}C] serine carrier, 5 mM NaCl, and no yeast extract. (——) = expected (see text). (- - -) = observed.

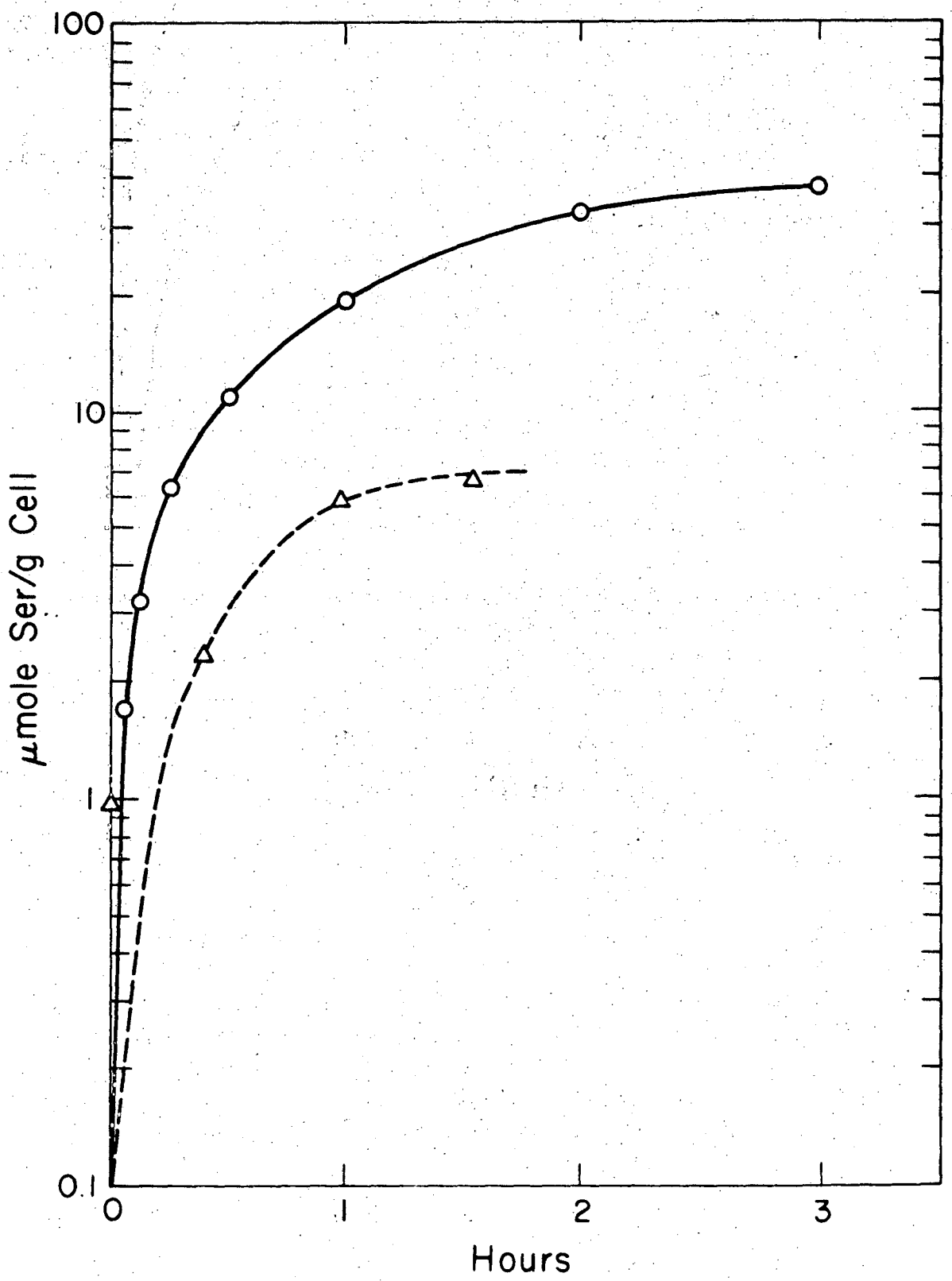
100
10
1
0.1
μmole Ser/g Cell
0
1
2
3
Hours

Fig. 7. Rate of incorporation of serine (△), alanine (□), and tyrosine (O). Conditions as in Figures 6, 5, and 4, respectively.

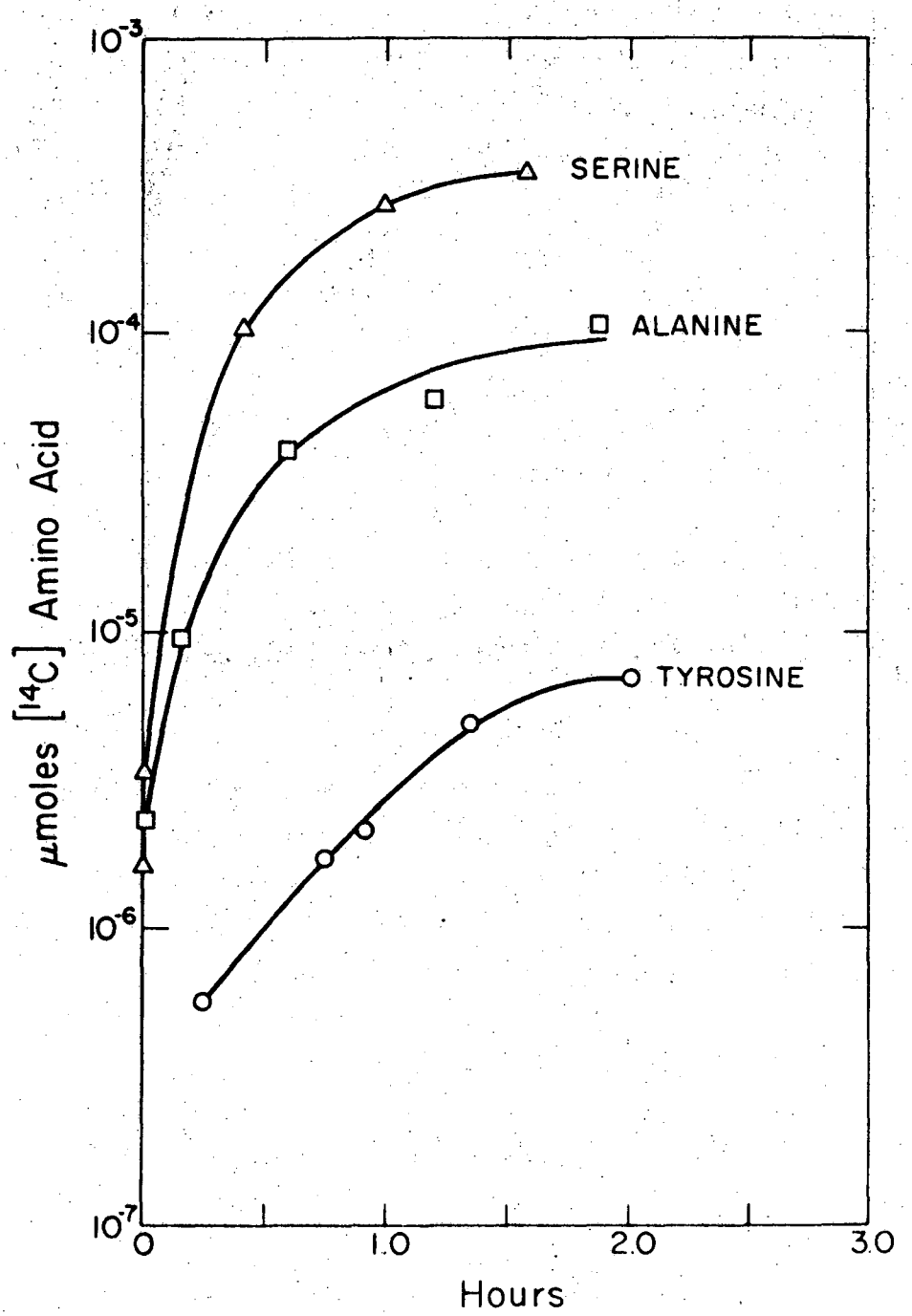
10^{-3}
10^{-4}
10^{-5}
10^{-6}
10^{-7}
μmoles [^{14}C] Amino Acid
SERINE
ALANINE
TYROSINE
0
1.0
2.0
3.0
Hours

Fig. 8. Specific rate of incorporation of 2.5 μM [^{14}C] tyrosine as a function of [^{12}C] tyrosine carrier concentration (—O—) = μmoles [^{14}C] Tyr/ml/g cells (pool + proteins) (--●--) = μmoles [^{14}C] Tyr/ml/g cells (TCA precipitable protein).

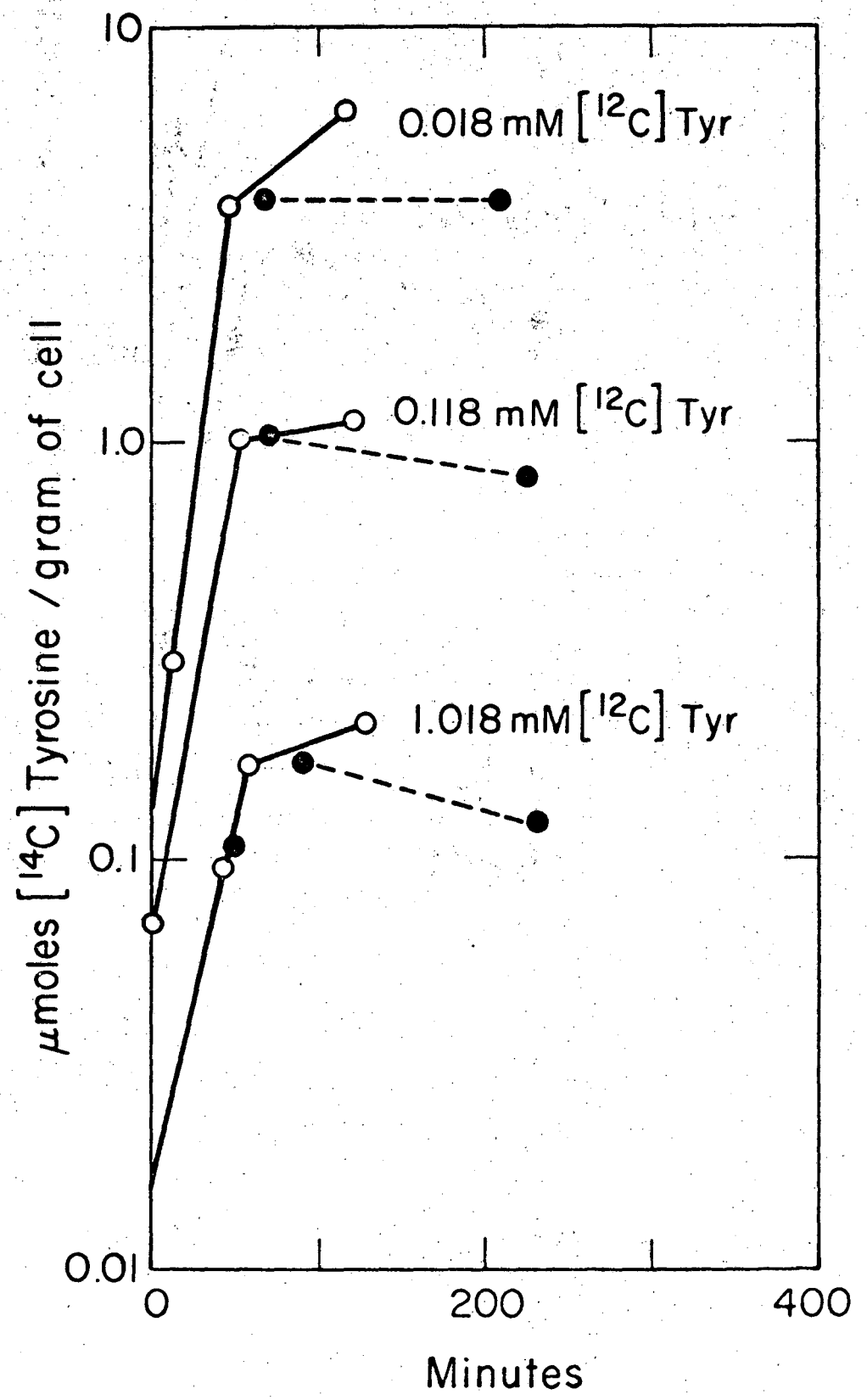
10
1.0
0.1
0.01
0
200
400
Minutes
μmoles [14C] Tyrosine / gram of cell
0.018 mM [12C] Tyr
0.118 mM [12C] Tyr
1.018 mM [12C] Tyr

Fig. 9. Specific rate of incorporation of 2.5 μM [^{14}C] tyrosine as a function of yeast extract (YE) concentration.

(- - -) = Cell density (A_{660})

(——) = μmoles [^{14}C] Tyr/g dry weight cells/ml

O, △, □ = Pool + protein

●, ▲, ■ = TCA precipitable protein

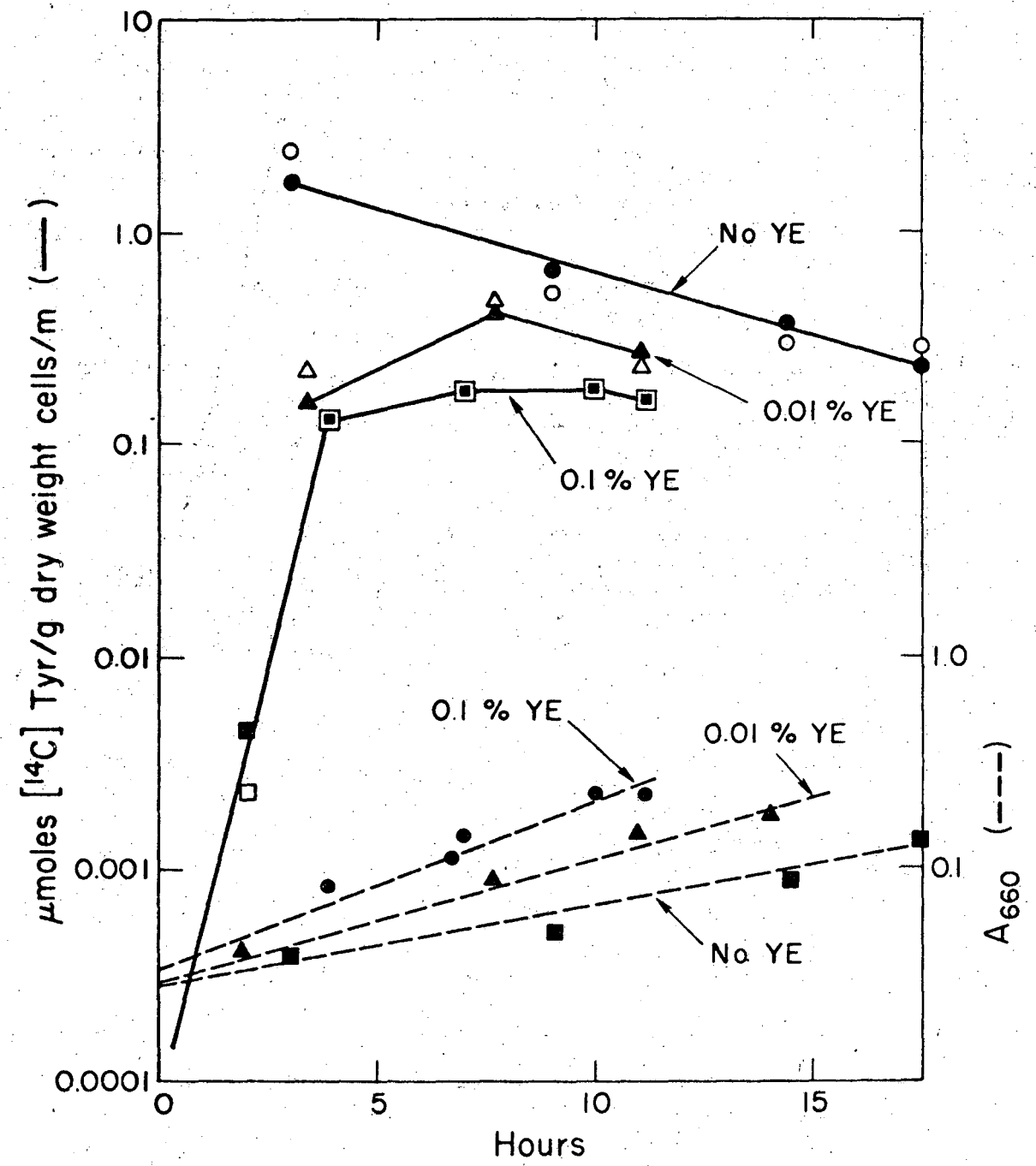
10
1.0
0.1
0.01
0.001
0.0001
0
5
10
15
Hours
μmoles [14C] Tyr/g dry weight cells/m (——)
A660 (- - -)
No YE
0.01 % YE
0.1 % YE
0.1 % YE
0.01 % YE
No YE

Fig. 10. Elution pattern of [^{14}C] ferredoxin preparation for DEAE cellulose column no. 1.

●—● = cpm/0.4 ml

○—○ = A_{280}

△—△ = A_{390}

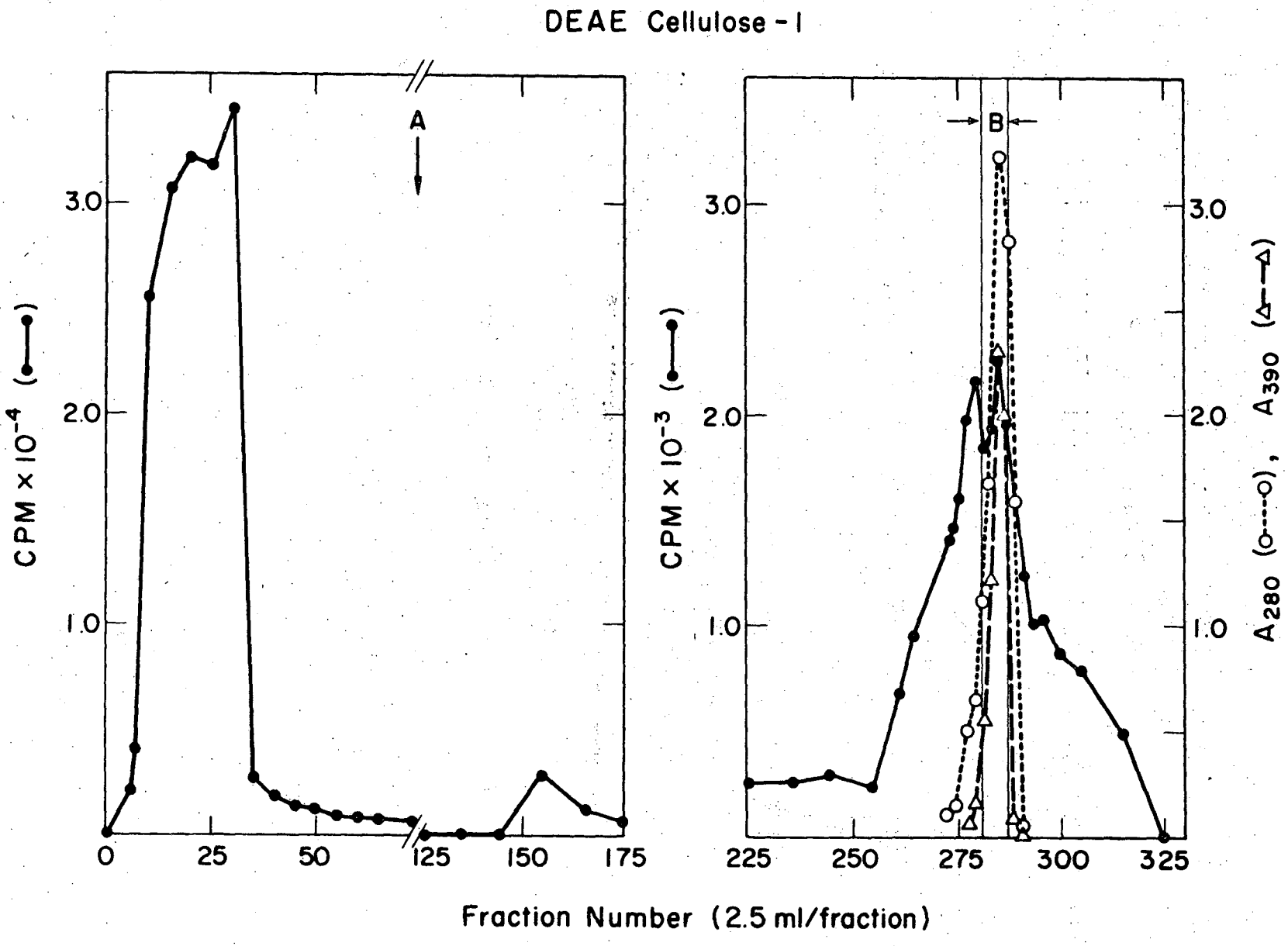
DEAE Cellulose - I
A
B
CPM × 10^-4 (●—●)
CPM × 10^-3 (●—●)
A280 (○----○), A390 (△—△)
3.0
2.0
1.0
0
25
50
125
150
175
225
250
275
300
325
Fraction Number (2.5 ml/fraction)

Fig. 11. Elution pattern of [^{14}C] ferredoxin preparation for DEAE cellulose column No. 2 and Sephadex G-75 column

●—● = cpm/0.4 ml

○—○ = A_{280}

△—△ = A_{390}.

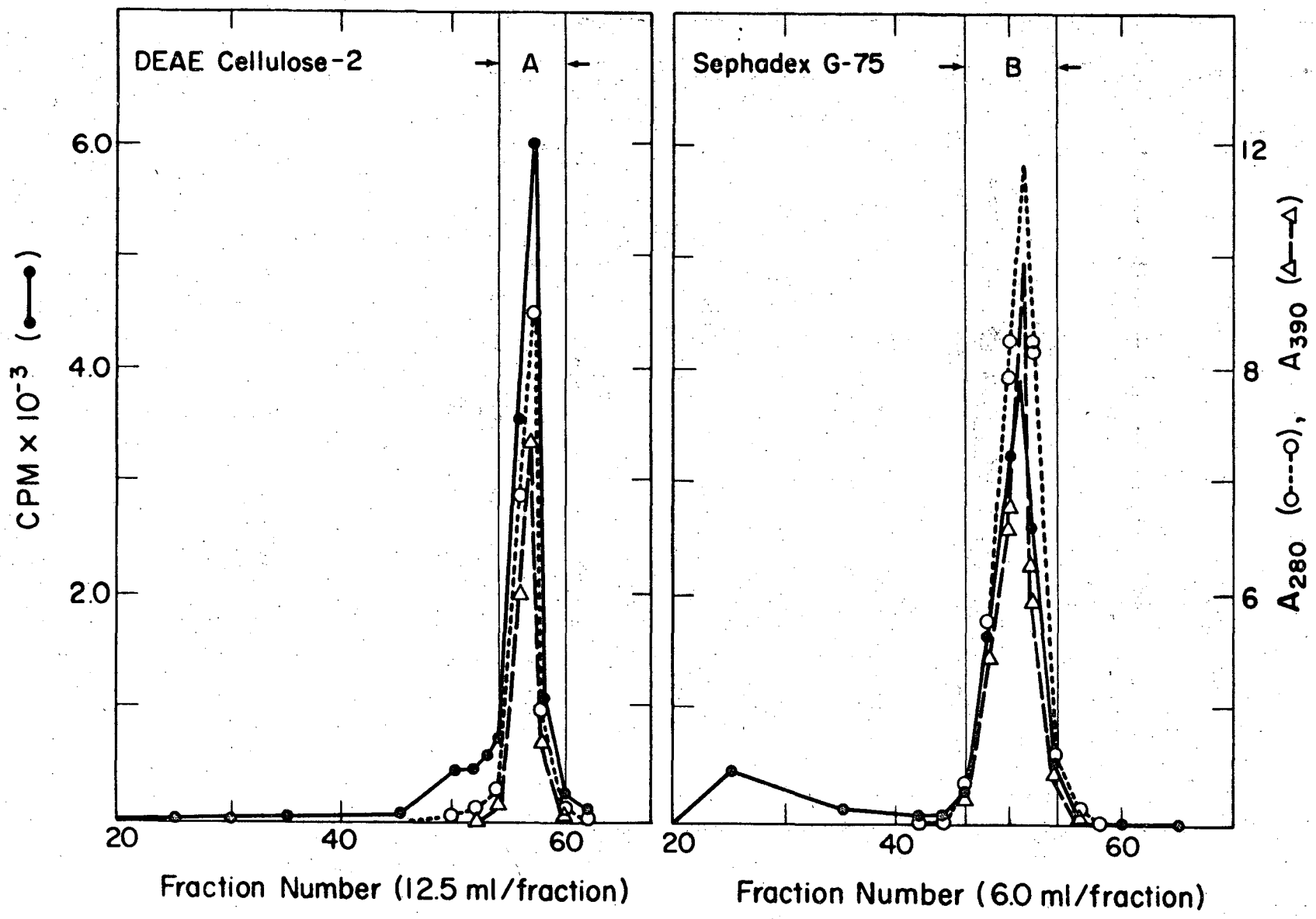
DEAE Cellulose-2
A
Sephadex G-75
B
CPM × 10⁻³ (●—●)
6.0
4.0
2.0
12
8
6
A280 (○---○), A390 (△—△)
20
40
60
Fraction Number (12.5 ml/fraction)
Fraction Number (6.0 ml/fraction)

Fig. 12. Single [^{14}C] tyrosine elution peak from hydrolysate of [^{14}C] ferredoxin. In the [^{14}C] amino acid standard mixture (Fig. 13), [^{14}C] tyrosine elutes at 2.5 ml/fraction × 83 fractions = 207 ml. In the [^{14}C] ferredoxin hydrolysate, the single [^{14}C] peak elutes at 1.35 ml/fraction × 152 fractions = 205 ml.

Yield: (%) [^{14}C] tyrosine

$$= \frac{\text{total cpm/ml [}^{14}\text{C] tyrosine}}{\text{total cpm/ml [}^{14}\text{C] apoferredoxin}} \times 100$$

$$= \text{peak height (cpm/ml)} \times 1/2 \text{ peak width (fractions)} \times \frac{\text{vol/fraction}}{\text{cpm/ml apoferredoxin}}$$

$$= \frac{525 \text{ cpm/ml} \times (3.8) \times (1.35)}{3950}$$

$$\approx 70\%$$

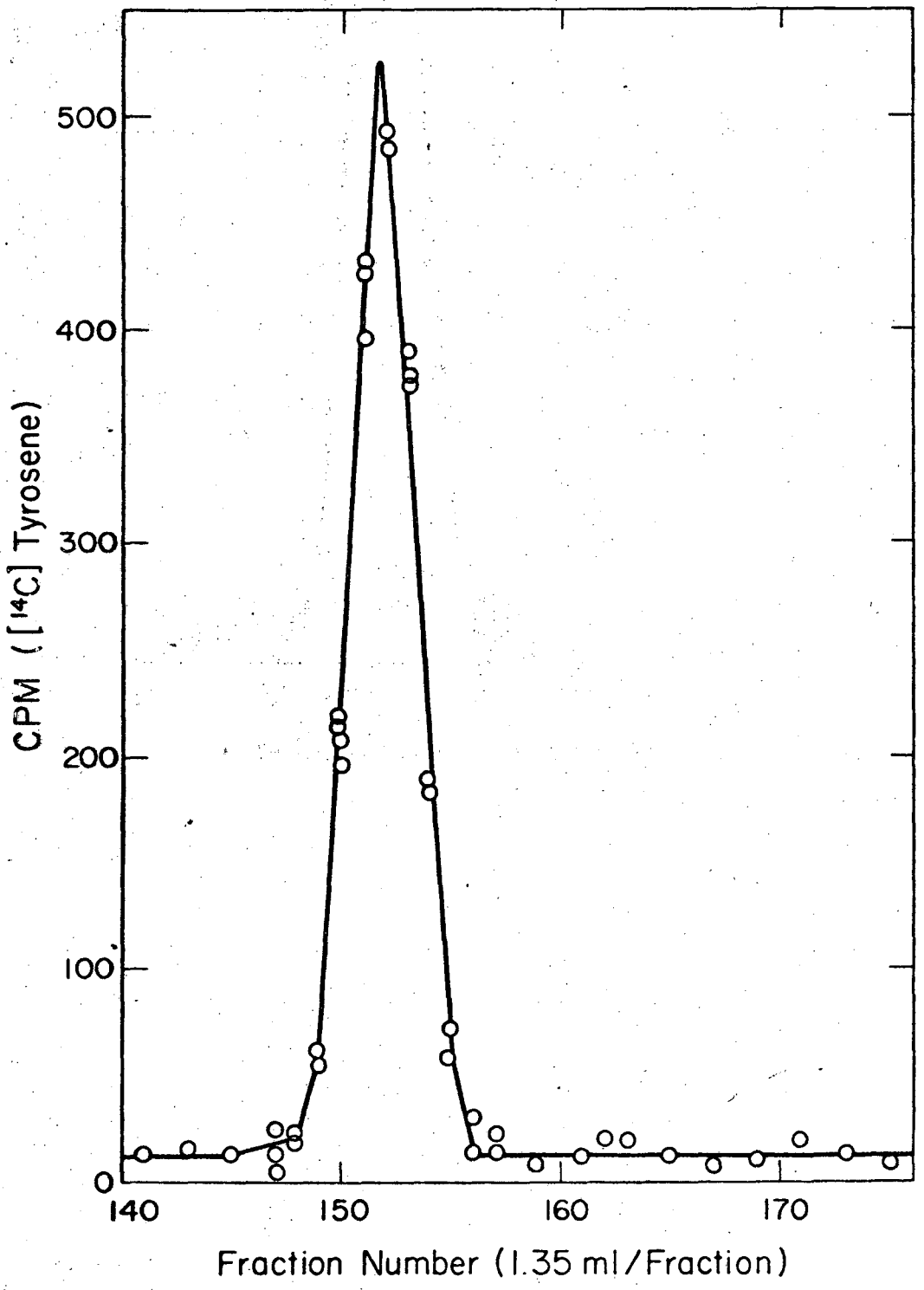
500
400
300
200
100
0
CPM ([14C] Tyrosene)
140
150
160
170
Fraction Number (1.35 ml/Fraction)

Fig. 13. Elution pattern of [^{14}C] amino acid standards (see Table 4).

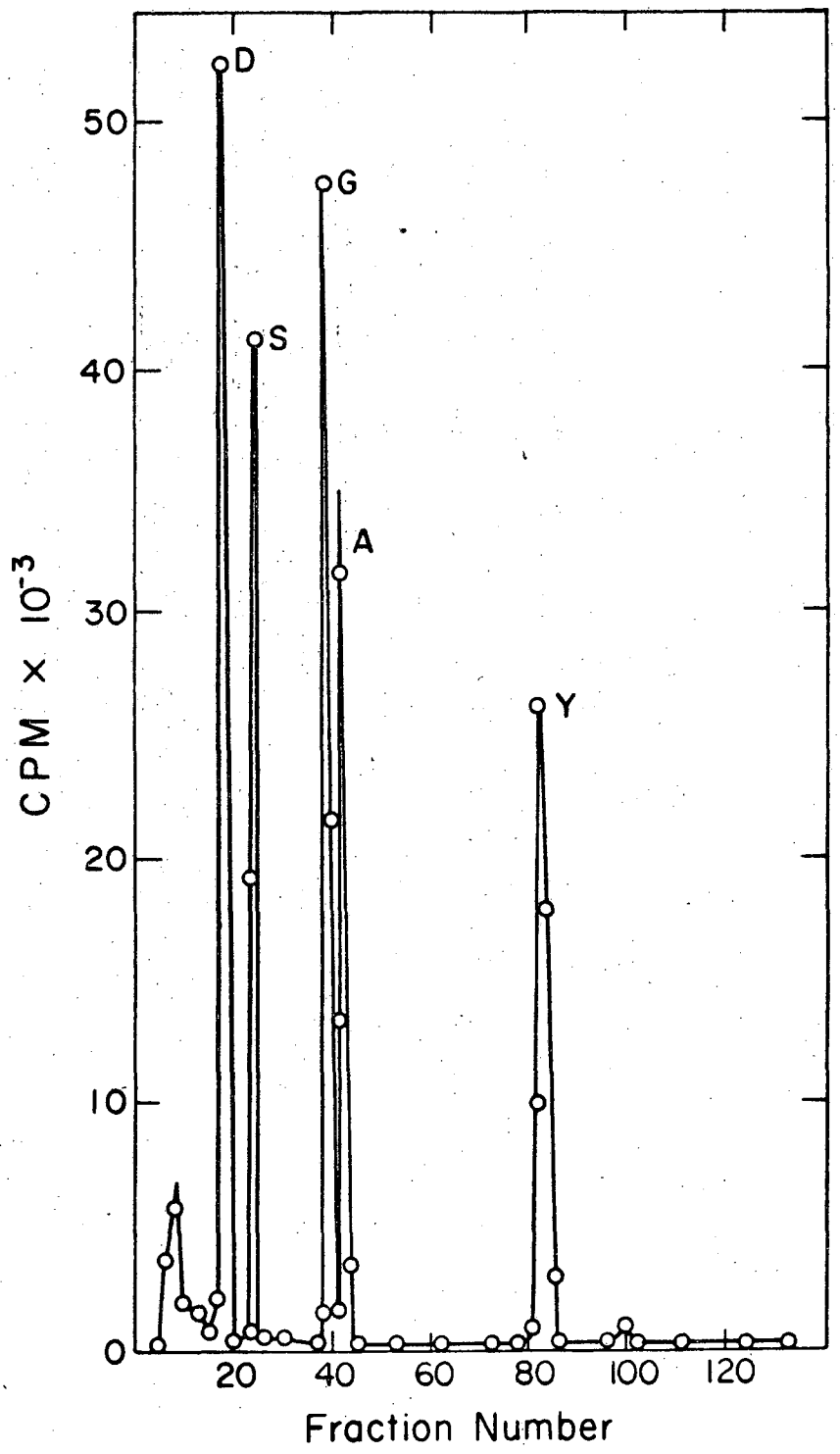
D
G
S
A
Y
50
40
30
20
10
0
CPM × 10⁻³
20
40
60
80
100
120
Fraction Number

Table 2. Effect of [^{12}C]tyrosine carrier concentration on maximum specific activity.

[[^{12}C]Tyr] μmoles/ml	Input [[^{14}C]Tyr] μmoles/ml x 10^3	Input Total [[^{12}C]Tyr] + [[^{14}C]Tyr] μmoles/ml	Ratio [[^{12}C]Tyr] / [[^{14}C]Tyr]	Maximum Specific Activity[a] [[^{14}C]Tyr]/g newly synthesized cells[b] Observed[c] Cells[b]	Observed[c] Protein[d]	Expected[e] Cells
0.018	2.44	0.02	7.36	4.0	4.0	13.6
0.118	2.44	0.12	48.3	1.05	1.05	2.07
0.0018	0.037	0.0018[f]	48.7	0.16	0.16	2.06
1.018	2.44	1.02	427.0	0.17	0.16	0.24
0.018	0.037	0.018	487.0	0.22	0.16	0.21

a. When specific activity is relatively constant (Fig. 8).

b. ~ 4 x 10^{-5} g newly synthesized cells/ml, including pool plus protein.

c. Based on experiments described in Fig. 8. Total newly synthesized cells was about 4 x 10^{-5} mg/ml.

d. TCA-precipitable material.

e. (100 μmoles Tyr needed/g newly synthesized cells/ml)/([[^{12}C]Tyr]/[[^{14}C]Tyr]).

f. This total tyrosine input is less than half of the total tyrosine produced by 4 x 10^{-5} g/ml newly synthesized cells.

Table 3. Purification of [^{14}C]ferredoxin (Fd) from *C. acidi-urici*.

Fraction	Vol. (ml)	[^{14}C]Tyr (μmoles x 10^4)	Fd[a] (mg)	Fd/[^{14}C]Tyr (μmoles x 10^4)	$\frac{A_{390}}{A_{280}}$
extract[b]	300	500.0	-[c]	-[c]	0.041
DEAE-cellulose-1[d]	100	8.3	24.4	0.47	0.72
DEAE-cellulose-2[e]	31	4.2	27.5	1.05	0.70
Sephadex G-75[f]	24	2.7	24.0	1.33	0.74
Crystals[g]	8	1.5	22.0	2.36	0.81

a. Based on $\epsilon_{ferredoxin} = 3.06 \times 10^4$ (115) for A_{390}.

b. From 35 g wet cells.

c. A_{390} of this fraction will overestimate ferredoxin concentration.

d. 2 x 40 cm. column eluted with 0.16 M - 0.05 M NaCl gradient in 0.05 M Tris-Cl (pH 7.4).

e. 2.5 x 8 cm. column eluted with 0.38 M NaCl in 0.15 M Tris-Cl (pH 7.4).

f. 2.5 x 90 cm. column eluted with 0.075 M Tris-Cl (pH 7.4).

g. Crystallized twice by solid $(NH_4)_2SO_4$ added to make a solution 67.5% saturated.

Table 4. [^{14}C]Amino acid standards used on amino acid analyzer.

Amino acid (Fig. 13)	Reciprocal specific activity (μmole/uCi x 10^9)	Input on analyzer column (nmole)	Elution time for ninhydrin analysis (min.)	Elution peak[a] (fraction number)	
				Expect[b]	Observe
Asp (D)	6.5	1.95	45	15 ± 2	19
Ser (S)	6.26	3.12	59	23 ± 2	25
Gly (G)	8.62	2.58	90	38 ± 2	39
Ala (A)	1.79	5.35	97	41 ± 2	42
Tyr (Y)	2.40	0.78	173	76 ± 2	83

a. 2.5 ml fractions, 2 minutes/fraction.

b. Elution time of each amino acid into a fraction collector is ~10 minutes less than the ninhydrin amino acid analysis elution times of each amino acid.

Table 5. Amino acid analysis of C. acidi-urici ferredoxin.(moles amino acid/mole ferredoxin).

Amino acid	[^{14}C]ferredoxin	[^{12}C]ferredoxin (61)	Expected
Asp	8.37	7.87	8
Thr	0.97	0.99	1
Ser	2.82	2.65	3
Glu	4.00	4.13	4
Pro	3.99	3.89	4
Gly	4.25	3.78	4
Ala	9.39	8.37	9
Cys	6.78	6.86	8
Val	5.38	5.22	6
Met	0.00	0.00	0
Ile	4.24	4.43	5
Leu	0.00	0.00	0
Tyr	1.68	1.78	2
Phe	0.00	0.00	0
His	0.00	0.00	0
Lys	0.00	0.00	0
Arg	0.93	0.93	1

Experiment 2
Incorporation of [3', 5'-$^2H_2$] tyrosine into *Clostridium acidi-urici* ferredoxin

SUMMARY:

[3', 5'-$^2H_2$] Tyrosine is incorporated into ferredoxin purified from *C. acidi-urici* grown in the presence of [3', 5'-$^2H_2$]tyrosine. Evidence supporting this conclusion was obtained by comparing the ^{1}H-NMR spectra of *C. acidi-urici* [[3', 5'-$^2H_2$] Tyr]-ferredoxin with that of unlabeled normal *C. acidi-urici* ferredoxin.

INTRODUCTION:

The specific activity of [^{14}C]tyrosine recovered from the hydrolyzed [^{14}C]ferredoxin was 70% of the specific activity of the protein (See experiment 1). It was considered possible that no dilution had occurred, and that the small amount of dilution observed reflected experimental artifacts. A more direct method to prove that no dilution of label occurred would be desirable.

If [3', 5'-$^2H_2$]tyrosine could be incorporated into *C. acidi-urici* ferredoxin, comparison of the ^{1}H-NMR spectrum of the aromatic region of *C. acidi-urici* [[3', 5'-$^2H_2$] Tyr]-ferredoxin with that of unlabeled normal *C. acidi-urici* ferredoxin would reveal how much [3', 5'-$^2H_2$]-tyrosine label had been incorporated into ferredoxin. This comparison would also facilitate assignment of the 3', 5'-tyrosyl ring proton resonances in *C. acidi-urici* ferredoxin.

METHODS AND MATERIALS:

[3', 5'-$^2H_2$] Tyrosine was obtained as a gift from Jack S. Cohen of the NIH, Bethesda, Md. [3', 5'-$^2H_2$] tyrosine is prepared by refluxing L-tyrosine in 2 N DCl. Thus, it is essential to dissolve high concentrations of [3', 5'-$^2H_2$] tyrosine in DCl (30).

Cells were grown first in 7.5 liter cultures (containing 0.37 mM [3', 5'-$^2H_2$] tyrosine and 0.0012% yeast extract. One gram of [3', 5'-$^2H_2$]-tyrosine was added to 15 liter carboy cultures in 10 ml of 6 N DCl. The pH of the culture was readjusted to pH 7.4 with 10 N KOH.

Fifteen liter carboys were inoculated with 1.5 liters from the 7.5 liter culture. Yeast extract and [3', 5'-$^2H_2$] tyrosine were added to the 15 liter carboys to a final concentration of 0.0012% yeast extract and 0.37 mM [3', 5'-$^2H_2$] tyrosine.

The first batch of cells (30 g wet weight) was obtained from four of these carboys by centrifugation with a Sorval continuous centrifuge. The fifth carboy was used to inoculate five other carboys (a 3 liter inoculum/carboy), and these carboys (with no added yeast extract) had a final concentration of 0.54 mM [3', 5'-$^2H_2$] tyrosine. Four of the five carboys from the second batch produced 24.25 g wet cells.

[[3', 5'-$^2H_2$] Tyr]-ferredoxin was purified as described under General Methods and Materials. The yield was ~ 1 mg/g wet cells. The optical spectra and amino acid analysis of [[3', 5'-$^2H_2$] Tyr]-ferredoxin were indistinguishable from those of C. acidi-urici ferredoxin grown without [3', 5'-$^2H_2$] tyrosine.

^{1}H-NMR METHOD:

0.15 ml of a 5-10 mg/ml sample of ferredoxin is put between the "poles" of a superconducting electromagnet and the temperature of the sample and probe is usually maintained at 15° C. This temperature can be varied if needed. A constant magnetic field is applied, and this causes the protons in the sample (since they have a spin) to be aligned parallel and antiparallel to the magnetic field. The parallel orientation has the lowest energy, and the spins precess with a characteristic frequency about the applied magnetic field. A variable frequency is applied to the sample. The resonance condition* occurs if a particular nuclear spin absorbs energy and reverses its direction with respect to the magnetic field. This process is analogous to the ESR method (See Experiments 4 and 5). The difference between the ESR and NMR methods is that the magnetic field is varied and the applied frequency is kept constant for ESR spectrometers and the reverse is true for NMR spectrometers. Also the lowest energy for an electron is the antiparallel orientation, and the reverse is true for nuclei. The applied frequency at the resonant condition is constant for a bare proton, but the frequency required for the resonance condition will vary with each

---

*The energy absorbed is (112):

$$E = h\nu = g_n \beta_n H$$

where h = Planck's constant
ν = frequency (the oscillating field)
g_n = g value of a particular nucleus
β_n = nuclear magneton, a constant
H = effective magnetic field

kind of proton in a protein. The different kinds of protons include, for example, α-, β-, δ- and ring-protons for different amino acids. This is because each kind proton in a protein has a slightly different magnetic environment depending on the atom it is bonded to and its neighboring atoms.

For example, the ring-proton resonances are near the electric currents of the ring which produce a "deshielding" magnetic field. Thus one needs to apply a lower frequency to achieve the resonant condition of ring protons. The ring protons, for this reason are characteristically at lower fields than the aliphatic protons.

The ring proton resonances of the two tyrosyl residues in the ^{1}H-NMR spectrum (Fig. 14, Fig. 15B) in C. acidi-urici apoferredoxin occur at 6.66 and 6.93 ppm from the reference proton resonance of sodium 2,2-dimethyl-2-silapentane-5-sulfonate (DSS). The aliphatic protons occur at resonance frequencies upfield of the sharp HDO resonance at 4.84 ppm. Many of the overlapping aliphatic resonances in the ^{1}H-NMR spectrum (Fig. 14) of C. acidi-urici apoferredoxin can be assigned by reconstructing the spectrum with the known resonances of the free amino acids (119). The intensity of each resonance is proportional to the number of protons it represents and thus a fairly good approximation of the ^{1}H-NMR spectrum of the apoprotein can be obtained when the amino acid composition is known (86). In the native protein, the proton resonances cannot be readily assigned because the positions of proton resonances are extremely sensitive to protein conformation.

RESULTS AND DISCUSSION:

Since a 10% inoculum is needed to grow C. acidi-urici in these experiments, it was necessary to inoculate cells that had already incorporated [3', 5' -$^2H_2$] tyrosine intotheir protein. The first and second batches of carboy-grown cells were exposed to 0.37 mM and 0.54 mM [3', 5' -$^2H_2$]-tyrosine, respectively, and this should have been more than enough to insure total incorporation of [3', 5' -$^2H_2$] tyrosine into cell protein.

^{1}H-NMR STUDIES:

^{1}H-NMR of oxidized (Fig. 16B) and reduced (Fig. 17B) C. acidi-urici [[3', 5' -$^2H_2$] Tyr] -ferredoxin shows that essentially complete incorporation of [3', 5' -$^2H_2$] tyrosine was achieved. Because an area corresponding to four protons was missing from the ring proton region of the ^{1}H-NMR spectrum of [[3', 5' -$^2H_2$] Tyr] -ferredoxin (Fig. 16B, 17B) when this was compared with the ^{1}H-NMR spectrum of C. acidi-urici normal ferredoxin (Fig. 16A, 17A).

ASSIGNMENT OF RESONANCES: The 3', 5' - and 2', 6'-tyrosyl ring proton resonances in the free amino acids are 6.90 and 7.19 ppm from DSS respectively (119), but it is not uncommon for these resonances to shift ±0.3 ppm when amino acids occur in polypeptides (86). Thus, in the ^{1}H-NMR spectrum of the aromatic region of C. acidi-urici apoferredoxin (Fig. 15B) the resonances at 6.66 and 6.93 ppm that are observed are assigned to the 3', 5'- and 2', 6'-tyrosyl ring protons respectively.

3', 5'-tyrosyl ring proton assignment:

The resonances at 6.39 and 6.57 ppm in the oxidized holoferredoxin (Fig. 15A) are tentatively assigned to the 3', 5'-ring protons of both tyrosyl residues. This assignment is supported by a comparison of the spectrum of [[3', 5'-$^2H_2$] Tyr]-ferredoxin (Fig. 16B) with that of normal ferrodoxin (Fig. 15A, 16A). Subtraction of the ^{1}H-NMR spectrum of the aromatic region of the [[3', 5'-$^2H_2$] Tyr]-ferredoxin (Fig. 16B) from that of the unenriched normal ferredoxin (Fig. 16A) leaves a narrow doublet with peaks at 6.57 and 6.39 ppm (Fig. 16C). This narrow doublet has an area corresponding to four proton resonances. The broad doublet that is observed in the region of the 3', 5'-ring protons in the [[3', 5'-$^2H_2$] Tyr]-ferredoxin spectrum (Fig. 16B) has peaks at 6.65 and 6.32 ppm, and may correspond to the α-protons of the cysteinyl residues (See Experiment 8).

The 3', 5'-ring proton assignment is confirmed when one compares the spectrum of reduced [[3', 5'-$^2H_2$] Tyr]-ferredoxin (Fig. 17B) with that of reduced normal ferredoxin (Fig. 17A). In Fig. 17, the normal and [[3', 5'-$^2H_2$] Tyr]-ferredoxins were reduced to the same degree (See Experiment 7b). The 3', 5'-tyrosyl resonances are completely missing from the 3', 5'-proton resonance region in the H-NMR spectrum (Fig. 17B) of reduced [[3', 5'-$^2H_2$] Tyr]-ferredoxin, and there are no other resonances remaining in this region.

2', 6'-tyrosyl ring proton assignment:

In the ^{1}H-NMR spectrum of the aromatic region of oxidized

C. acidi-urici ferredoxin (Fig. 15, 16) there are two resonances downfield from the 3', 5'-ring proton resonances. They occur at 7.32 and 7.07 ppm and are tentatively assigned to the 2', 6'-ring protons of both tyrosyl residues (See Experiment 6a), since the peaks are within 0.13 and 0.38 ppm (respectively) of the 2', 6'-tyrosyl proton position (6.94 ppm) of C. acidi-urici apoferredoxin. Subsequent experiments (See Experiments 7a, 7b) confirm that there are 2', 6'-tyrosyl ring proton resonances.

The UV visible optical spectra and the ^{1}H-NMR spectrum (excluding the aromatic region) of C. acidi-urici [[3', 5'-$^{2}H_2$] Tyr]-ferredoxin were indistinguishable from those of normal C. acidi-urici ferredoxin.

ESR STUDIES:

The ESR spectrum of the dithionite-reduced C. acidi-urici [[3', 5'-$^{2}H_2$] Tyr]-ferredoxin was the same as that of normal C. acidi-urici ferredoxin. The g = 2 signal that is present in oxidized normal C. acidi-urici ferredoxin was 5-7 gauss broader than the corresponding g = 2 signal in [[3', 5'-$^{2}H_2$] Tyr]-ferredoxin (See Experiment 4 and Appendix A). This measurement of the enriched and normal oxidized ferredoxin was made under the same conditions with fresh samples that had been exhaustively dialyzed against D_2O in KD_2PO_4-K_2DPO_4 buffer, pD 7.0. The measurements were made by Dr. W. Blumberg of Bell Telephone Laboratories, Inc.

Fig. 14. ^{1}H-NMR of oxidized C. acidi-urici holoferredoxin (20 mg/ml) and apoferredoxin (80 mg/ml) in 0.2 M KD_2PO_4-K_2DPO_4. (A): Tyrosyl ring proton resonances in holoferredoxin; (B): Holoferredoxin (15° C) pD 7.0; (C): Apoferredoxin (20° C), pD 7.8, plus 0.1 M Na_2S.

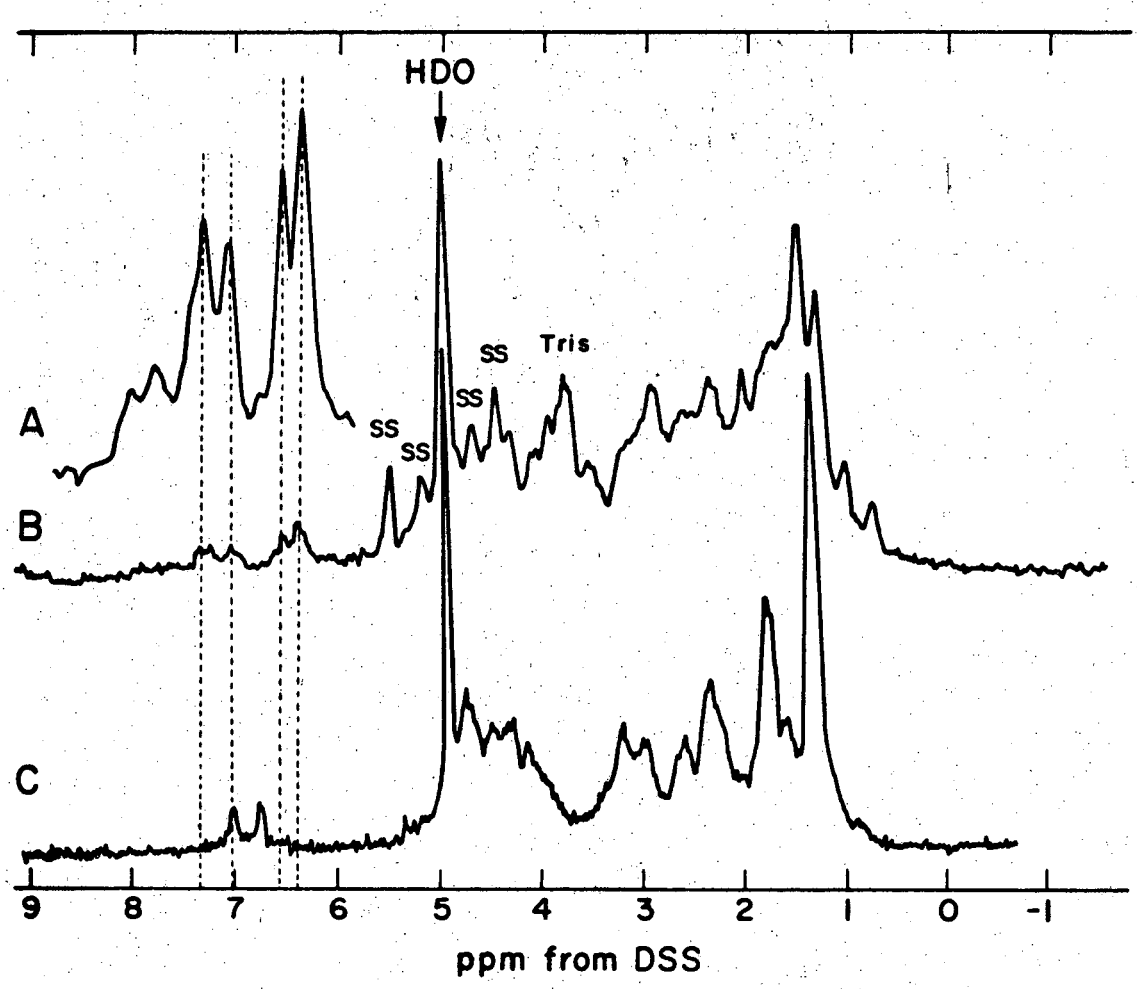
HDO
SS
SS
SS
SS
Tris
A
B
C
9
8
7
6
5
4
3
2
1
0
-1
ppm from DSS

Fig. 15. ^{1}H-NMR (15° C) of the aromatic region of C. acidi-urici ferredoxin (A): oxidized protein (20 mg/ml) dissolved in 0.2 M K_2DPO_4-KD_2PO_4 buffer, pD 7.0; (B): Apoferredoxin (80 mg/ml) dissolved in 0.1 M Na_2S and 0.2 M K_2DPO_4-KD_2PO_4 buffer, pD 7.8. There are no resonances between 6.66 and 4.84 ppm from DSS, nor below 6.93 ppm, in this spectrum (B). (See Figure 14).

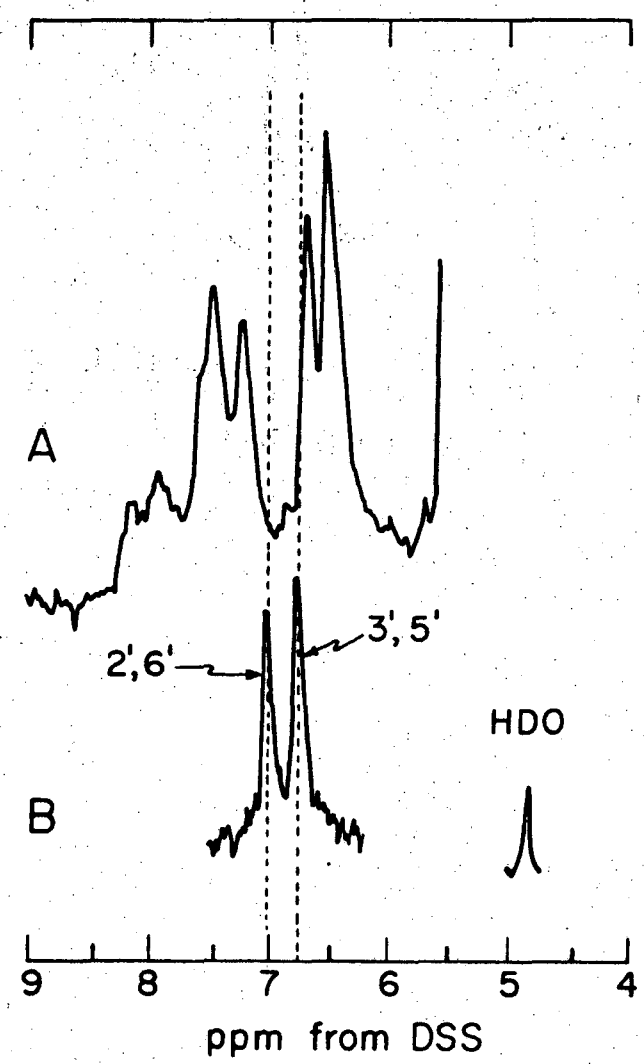
A
B
2',6'
3',5'
HDO
9
8
7
6
5
4
ppm from DSS

Fig. 16. ^{1}H-NMR (15° C.) of the aromatic region of oxidized C. acidiurici ferredoxin. (A): Normal ferredoxin prepared as described in Fig. 15A; (B): [[3', 5'-$^{2}H_2$] Tyr]-ferredoxin, prepared as described in Fig. 15A.

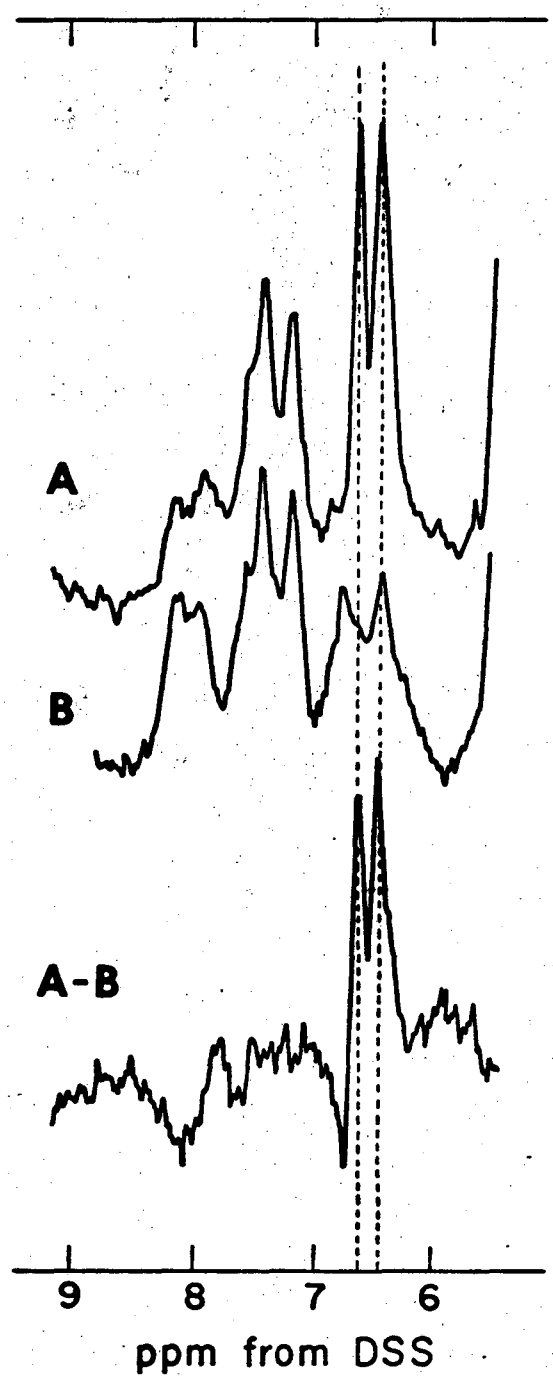
A
B
A-B
9
8
7
6
ppm from DSS

Fig. 17. ^{1}H-NMR (15° C.) of the aromatic region of reduced C. acidiurici ferredoxin. (A): Normal ferredoxin prepared as described in Fig. 15A except that it was reduced by 0.2 M Zn-reduced methyl viologen (see General Methods). The degree of reduction was ~18.5% (See Experiment 7b); (B): [[3', 5'-$^{2}H_2$] Tyr]-ferredoxin prepared as described in Fig. 17B, and 4A.

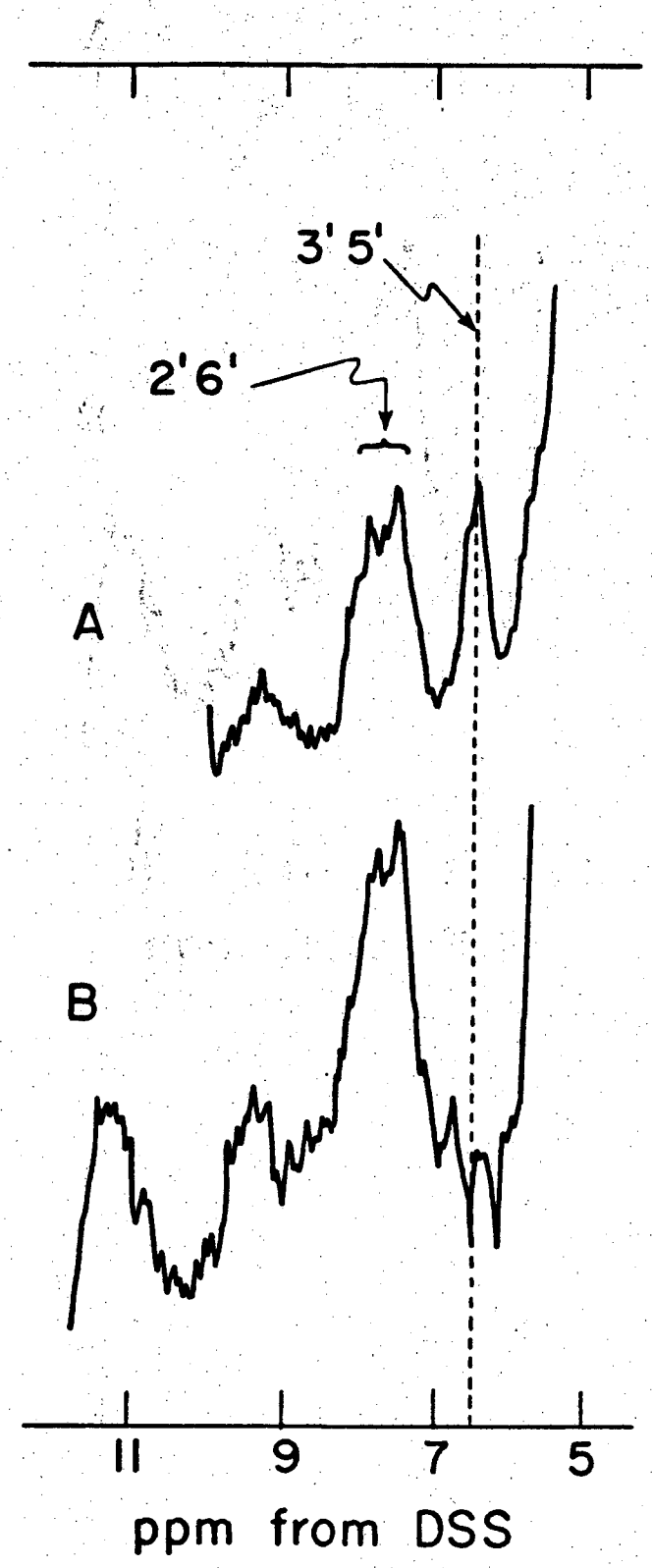
3' 5'
2' 6'
A
B
11
9
7
5
ppm from DSS

Fig. 18. ESR spectra (1.4° K.) of C. acidi-urici ferredoxin (A): Normal ferredoxin (3.2 mg/ml) in 0.7 ml of 0.15 M Tris-Cl (H_2O) buffer, pH 7.4; (B): [[3', 5'-$^2H_2$] Tyr]-ferredoxin (4.6 mg/ml) in 0.7 ml 0.15 M Tris-Cl (H_2O) buffer, pH 7.4.

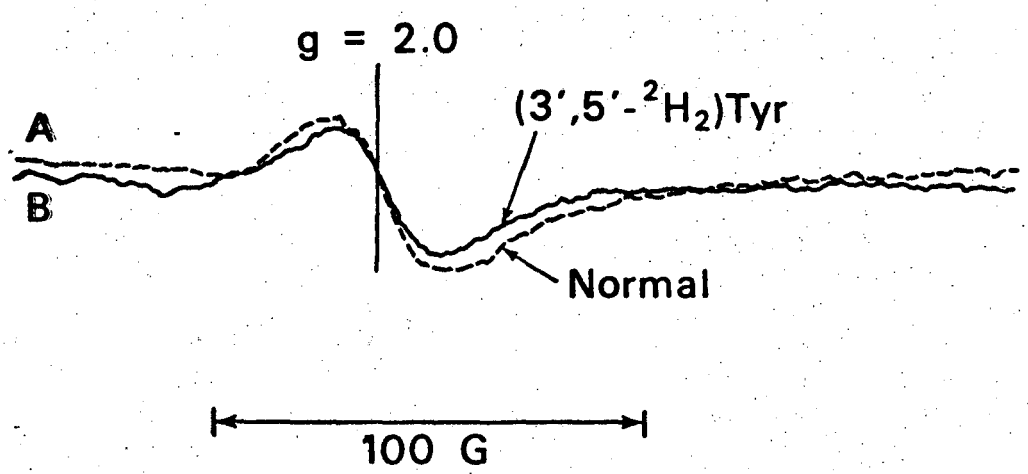
g = 2.0
A
B
(3',5'-$^2H_2$)Tyr
Normal
100 G

Appendix A. Calculating the line width of the ESR g = 2 resonance of <u>Clostridium acidi-urici</u> normal and $\left[[3', 5'-{}^2H_2]\ \text{Tyr}\right]$-ferredoxin.

The hyperfine tensor, a, describes the magnetic interaction between the magnetic moment of the nucleus with spin within the free radical. The proton has spin = 1/2 and the deutron has spin = 1, but the hyperfine constant of the deutron is 0.153 times that of the proton (113).

In aromatic hydrocarbons, the hyperfine splitting constant, a_i, due to one proton of a C-H group is 28 gause $\times$ the electron density, ρ_i. Since $\rho_i = 1/6$, $a_i = 4.7$ gauss the overall hyperfine splitting is thus 28 gauss since $\sum_{i=6} \rho_i = 1$.

This is also approximately true for a tyrosyl radical. If we chose for example the monosubstituted 4-methyl-phenoxy radical (48) as a model compound:

$a_{2'} = a_{6'} = 1.45$ gauss

$a_{3'} = a_{5'} = 6.0$ gauss

$a_{H(CH_3)} = 11.95$ gauss

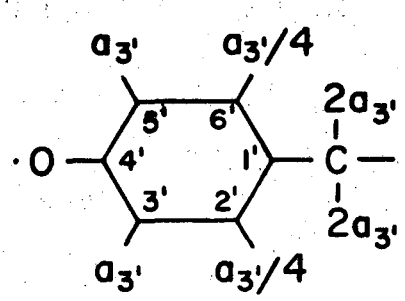

The sum of these constants is 26.9 gauss. To see if the line width observed for unenriched ferredoxin (28.5 gauss) and $\left[[3', 5'-{}^2H_2]\ \text{Tyr}\right]$-ferredoxin (22.1 gauss) is consistent with the hypothesis that the g = 2 signal is due to a tyrosyl radical we write the following relations for the unenriched (u) and enriched (e) tyrosyl radicals.

unenriched ferredoxin:

$$2\left(a_{H(CH_3)}\right) + \left(\frac{a_{2'}}{4} + \frac{a_{6'}}{4}\right) + (a_{3'} + a_{5'}) = 4a_{3'(u)} + \frac{2a_{3'(u)}}{4} + 2a_{3'(u)} = (28.5 \pm 0.5)\ \text{gauss}$$

$$a_{3'(u)} = (4.4 \pm 0.1) \text{ gauss}$$

$\left[[3', 5'\text{-}^2H_2]\ \text{Tyr}\right]$-ferredoxin:

$$4a_{3'(e)} + \frac{2a_{3'(e)}}{4} + 2(0.153)a_{3'(e)} + \frac{2a_{3'(e)}}{4} = (22.1 \pm 0.5) \text{ gauss}$$

$$a_{3'(e)} = (4.6 \pm 0.1) \text{ gauss}$$

Thus the 5-7 gauss difference between the enriched and unenriched normal ferredoxin is consistent with the hypothesis that the g = 2 resonance is produced by a tyrosyl radical in oxidized C. acidi-urici ferredoxin.

Experiment 3.

Incorporation of 3-fluorotyrosine into *Clostridium acidi-urici* protein

SUMMARY:

C. acidi-urici grown in the presence of 3-fluorotyrosine were not normal; they had no flagella and produced extremely long filaments, some as long as 200 microns. However, 3-fluorotyrosine was incorporated into *C. acidi-urici* protein. This was demonstrated by fluorine analysis of the cell protein extracted from *C. acidi-urici* grown in the presence of 3-fluorotyrosine.

INTRODUCTION:

As will be shown in Section 4, the ring carbon resonances of oxidized and reduced *C. acidi-urici* ferredoxin were significantly shifted from their positions in free amino acids. One way to determine the basis for these shifts is to do NMR studies of *C. acidi-urici* [[3' - $^{19}F_1$] Tyr] - ferredoxin. In Experiment 2 we have demonstrated that [3', 5' - $^{2}H_2$] tyrosine can be totally incorporated into *C. acidi-urici* ferredoxin by growing *C. acidi-urici* in the presence of [3', 5' - $^{2}H_2$] tyrosine. In view of these results, *C. acidi-urici* was grown in the presence of [3' - $^{19}F_1$] tyrosine to obtain [[3' - $^{19}F_1$] Tyr] -ferredoxin.

METHODS AND MATERIALS:

Two batches of 3-fluoro-DL-tyrosine were purchased from Cyclo Chemical Corporation. The first batch (lot #R5981) was the hemihydrate and was colored. The second batch (lot #032070) was not the hemihydrate and was not colored.

Cells were grown in 2 liter cultures (See General Methods) with or without 0.004% yeast extract and with either $\sim 7\times10^{-4}$M[3-$^{19}F_1$] DL-tyrosine

or DL-tyrosine. This concentration of tyrosine is > 10 times the amount that will produce a maximum rate of L-tyrosine incorporation (See Experiment 1).

Cells growing with yeast extract plus 3-fluoro-DL-tyrosine lysed after reaching stationary phase. Cells grown with 3-fluoro-DL-tyrosine did not lyse when grown without yeast extract. Thus the 3-fluorotyrosine cells grown in the absence of yeast extract were used to inoculate a 15 liter carboy containing 7×10^{-4}M 3-fluoro-DL-tyrosine. (2 g. 3-fluoro-DL-tyrosine were added to each carboy in 20 ml 2 N NaOH. This raised the pH of the carboy culture, which then was readjusted with HCl.) 1.2 liters of this carboy culture were used to inoculate twelve carboy cultures containing the same ingredients.

Cell protein that was to be analyzed for fluorine was prepared according to protein preparation method 1 (See General Methods and Materials). Cell protein from the carboy cultures that were to be analyzed for fluorine was obtained from the pass-through of the first DEAE cellulose column and was additionally purified by subjecting it to protein preparation method 1.

RESULTS AND DISCUSSION:

C. acidi-urici grown in the presence of 3-fluoro-DL-tyrosine were abnormal. Many cells produced long filaments, some as long as 100-200 cell lengths (Plate 1).

Sagers and coworkers (131) report that C. acidi-urici cells which are normally 2.5-4 μ in length, produce 500 μ filaments when grown at elevated (42°C) temperatures. Filament formation in bacteria may also be induced by radiation (1), variation of pressure (145) and temperature

(58, 79), the presence of antibiotics and other metabolic inhibitors (62) and the deficiency of essential growth factors (41, 54, 139). Electron micrographs (Plate 2) reveal that the abnormal cells also lacked flagella. Cells isolated from medium with and without DL-tyrosine were normal (Plate 2).

Cells grown in 3-fluoro-DL-tyrosine tended to lyse more than those grown with or without DL-tyrosine when the uric acid in the growth medium was exhausted.

Cells grown in 3-fluorotyrosine did incorporate 3-fluorotyrosine. Different samples of the cell protein contained between 0.05 to 0.19% fluorine (by weight) (Table 5a). Amino acid analysis of these proteins shows that C. acidi-urici protein contains 3.15% tyrosine by weight. (This is consistent with Chen's measurement (29) of 3.2% tyrosine for C. acidi-urici protein.) Since 3-fluorotyrosine contains 9.15% fluorine by weight, the total 3-fluorotyrosine incorporation into C. acidi-urici protein is:

$$\frac{(\%\ \text{fluorine observed in protein}) \times (100)}{(\%\ \text{fluorine in 3-fluorotyrosine}) \times (\%\ \text{tyrosine in protein})}$$

17 to 67% incorporation is observed for different protein samples (Table 5a). The 17% is calculated from protein that had been extracted from the pass-through of the first DEAE cellulose column when purifying the ferredoxin. It is thus believed to be the most accurate figure. Nevertheless the best estimate of fluorine incorporation will be obtained when the ferredoxin isolated from these 3-fluorotyrosine-grown cells is analyzed. This will be done when the ^{19}F-NMR studies of these samples are completed.

Plate 1. Light micrograph (480x, methylene blue stain) of *C. acidi-urici*. Top: grown in the presence of 3-fluoro-DL-tyrosine. Bottom: grown in the presence of DL-tyrosine (see text). (|——|) = 100 μ.

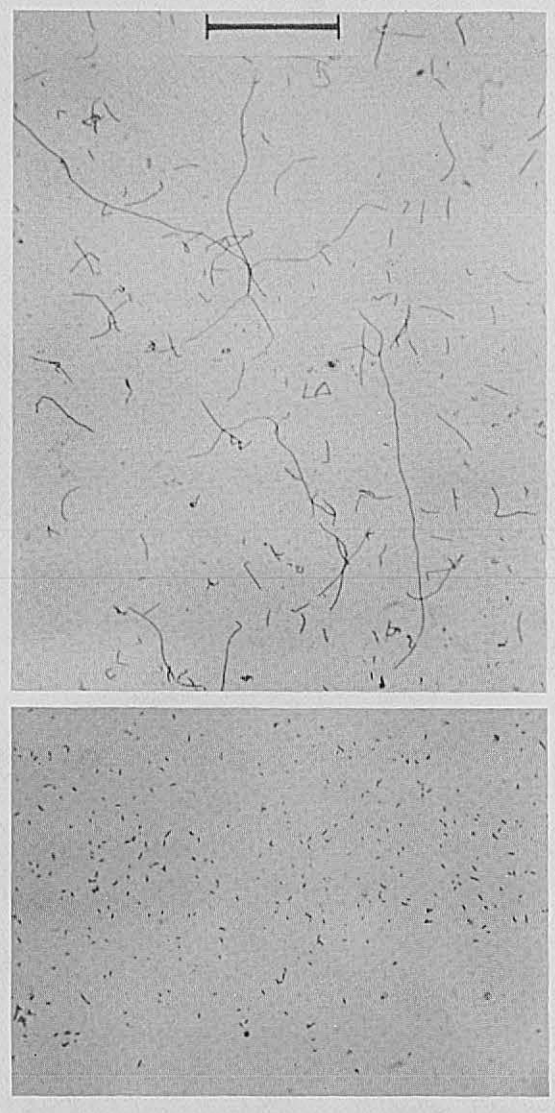

XBB 736-3684

Plate 2. Electron micrograph of C. acidi-urici grown in the presence of 3-fluoro-DL-tyrosine. Insert shows C. acidi-urici grown in the presence of DL-tyrosine. (Both at 8,000x, uranyl acetate negative stain.)

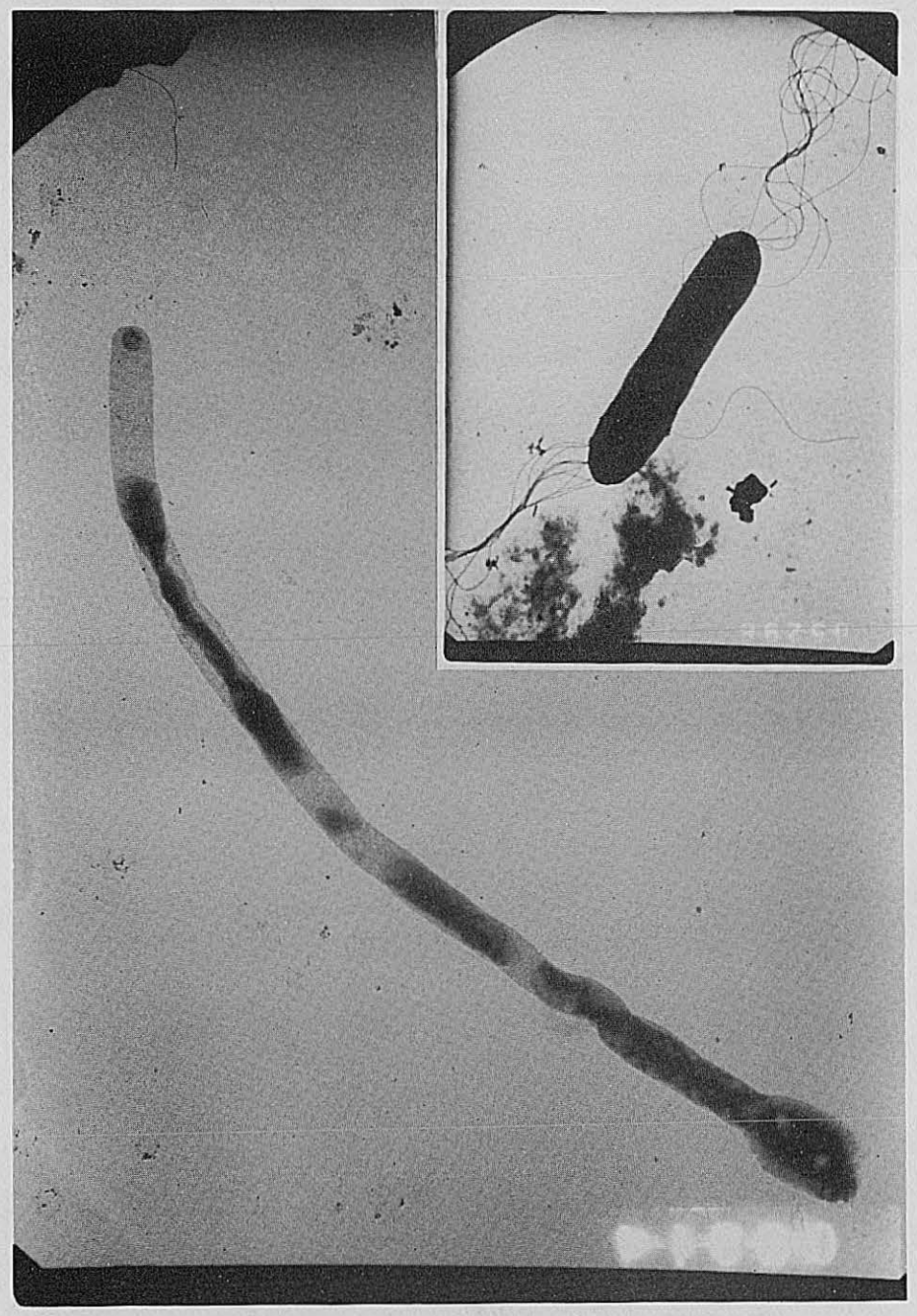

XBB 736-3685

Plate 3. Electron micrograph (12,000x, uranyl acetate negative stain) of C. acidi-urici grown in the presence of 3-fluoro-DL-tyrosine.

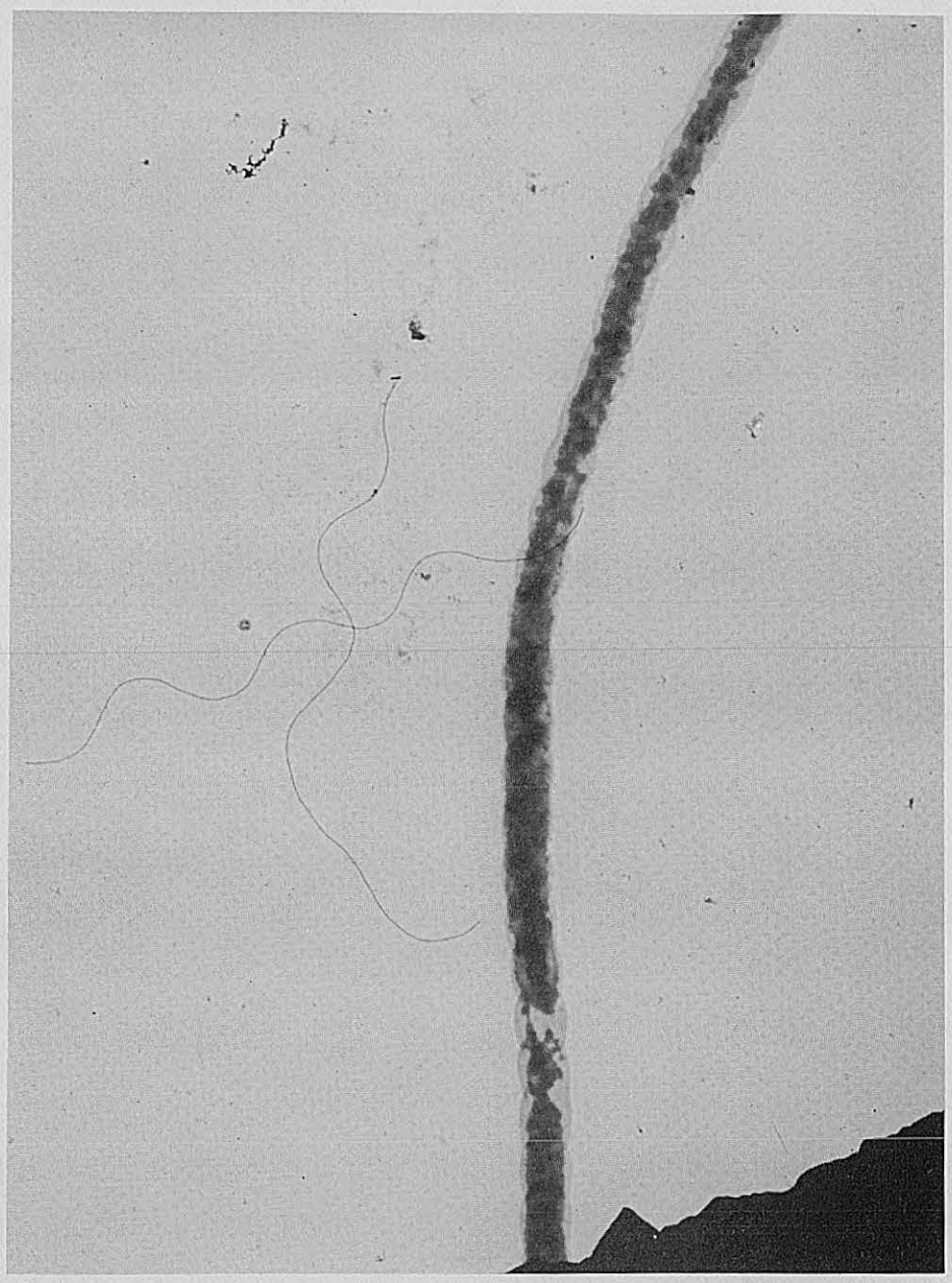

XBB 736-3686

Table 5a. Incorporation of fluorine into protein[a] of C. acidi-urici grown in the presence of 3-fluoro-DL-tyrosine.

Culture	Fraction[b]	Volume of culture (l)	DL tyrosine in culture (mM)	3-fluoro-DL-tyrosine in culture (mM)	Fluorine[c] in protein (Weight %)	3-fluoro tyrosine incorporation[d] (%)
C	Soluble	1.70	0.7	0	<0.01	-
E-1[e]	Soluble	9.25	0	0.33	0.19	67
	Insoluble				0.17	67
E-2[e]	Soluble				0.17	60
F[f]	Soluble	1.70	0	0.5	0.12	43
	Insoluble					
J[g]	Soluble	17.0	0	0.8	0.05	17

a. Protein from cultures C, E, and F was obtained by adding solid TCA to cold cultures containing cells to make the culture medium 5% TCA. The TCA precipitate was centrifuged, washed three times with 5% TCA, incubated at 90° C for 15-20 minutes, centrifuged, and washed with TCA three more times. The precipitate was dissolved in 1 M Tris-Cl and dialyzed against large volumes of H_2O.

b. "Soluble" and "insoluble" fractions are the two phases obtained after dialysis against H_2O.

c. Fluorine was determined by an Orion fluorine-sensitive electrode (88).

Notes to Table 5a continued.

d. % incorporation is:

$$\frac{\text{\% fluorine observed in protein} \times 100}{\text{\% fluorine in 3-fluoro-tyrosine} \times \text{\% tyrosine in protein}}$$

The percent tyrosine (by weight) is 3.15%, from amino acid analysis.

e. Culture E had lysed prior to preparation of protein.

f. Part of culture F was used to inoculate culture J.

g. Protein from culture J was obtained from the pass-through of the first DEAE cellulose column of the ferredoxin purification procedure. This pass-through was precipitated with ammonium sulfate at 95% of saturation. The precipitate was centrifuged, redissolved in H_2O, dialyzed against H_2O, and precipitated with TCA. The TCA precipitate was then treated as above with culture C, E, and F.

Section 2. ESR Experiments

Experiment 4.

Association of the reducing electron with the iron atoms of the Fe-S clusters in clostridial-type ferredoxins

SUMMARY:

The reducing electron was shown to be associated with the iron atoms of the Fe-S clusters in C. acidi-urici and C. pasteurianum ferredoxin because the ESR resonances of dithionite-reduced C. acidi-urici and C. pasteurianum [^{57}Fe] ferredoxins were ~ 11 gauss broader than the corresponding resonances of [^{56}Fe] ferredoxins.

The g = 2 resonance in oxidized C. acidi-urici [^{57}Fe] ferredoxin was also broadened, suggesting that the electron spin responsible for the g = 2 resonance may be near an Fe atom as well. This interpretation is clouded by the fact that the intensity of the g = 2 resonance of oxidized [^{57}Fe] ferredoxin was > 10 times less than that of the g = 2 resonance of [^{56}Fe] ferredoxin at 1.4°K. We have no explanation for this difference in intensity.

INTRODUCTION:

Since the aromatic residues are close to the Fe-S clusters in clostridial-type ferredoxins and the ring carbon resonances are shifted significantly from their positions in free amino acids (see Section 4), it is important to know whether these shifts are caused by paramagnetic electrons in the Fe-S clusters.

The reduced iron-sulfur proteins are characterized by a group of ESR resonances centered about g = 1.94. The ^{56}Fe and ^{32}S atoms present in normal ferredoxins do not have a nuclear spin, and thus do not interact with the spin of an unpaired electron. ^{57}Fe or ^{33}S does

have a nuclear spin and will interact with the spin of an unpaired electron, if this electron is in an Fe or S orbital, to produce a broadened resonance (24). This interaction produces a hyperfine splitting in the ESR resonance which may be observed as line broadening. In order to determine if the reducing electron was associated with the iron and sulfur atoms of the iron-sulfur proteins, several investigators (12, 66, 99) have performed ESR studies of plant-type (2 Fe, 2 S) [^{57}Fe] -ferredoxins and [^{33}S] ferredoxins, and observed that the reduced [^{57}Fe]ferredoxins and [^{33}S] ferredoxins exhibit broadened ESR resonances centered around g = 1.94.

Clostridial-type ferredoxins also produce ESR resonances centered about g = 1.94, but no one has published analogous ESR studies with reduced clostridial-type [^{57}Fe] ferredoxins. Thus, to determine whether the reducing electron is associated with the iron atoms of the clostridial-type ferredoxins, ^{57}Fe was incorporated into C. acidi-urici and C. pasteurianum ferredoxins.

Oxidized clostridial-type ferredoxins, unlike oxidized plant-type ferredoxins, also exhibit a single resonance at g = 2 if the clostridial ferredoxin constains at least one tyrosyl residue (see Experiment 5). If the g = 2 resonance is produced by a tyrosyl radical, as suggested by Experiment 2, then the ^{57}Fe should not broaden the g = 2 resonance unless the unpaired electron in the tyrosyl radical is also in an Fe orbital.

METHODS AND MATERIALS:

C. acidi-urici and C. pasteurianum [^{57}Fe] ferredoxin and [^{56}Fe] ferredoxin were prepared from C. acidi-urici and C. pasteurianum apoferredoxin by previously published methods (see General Methods

and Materials), with the following modifications.

The $FeSO_4(NH_4)_2SO_4$ used in the reconstitution was made from ^{57}Fe (obtained from Oak Ridge National Laboratory) and ^{56}Fe (J. T. Baker Chemical Company) by adding 11 mg Fe metal to 2 ml hot 0.36 N H_2SO_4, then adding 1.5 ml of 0.74 M NH_4OH until precipitate first appears at pH 3.5. This method is a modification of published procedures (148, 149).

ESR METHOD:

A 4 mm (ID) quartz tube containing 0.4 ml of a ferredoxin sample is quickly frozen in liquid N_2 and placed in a cavity between the poles of an electromagnet. The temperature of the cavity is reduced to ~ 25° K (or lower) with cooled ^4He gas. ESR resonances are more easily detected at lower temperatures because the number of spins that absorb energy follow a Boltzmann distribution. The magnetic field is varied while the frequency of applied microwave radiation is kept constant. The electron spins are oriented parallel and antiparallel to the magnetic field, and the antiparallel orientation has the lowest energy. The electron spins precess about the applied magnetic field with a characteristic frequency, and this characteristic frequency is called the resonance frequency of the electron, because when one externally applies radiation of this frequency the electron spins will absorb energy and be aligned parallel to the applied magnetic field. For an isolated spin 1/2 system, the energy, E, of the transition which occurs is given by the expression:

$$E = h\nu = g\beta H$$

where ν = the oscillating field

H = the magnetic field

g = "g value," which varies depending upon the type of ligand the electron spin is in.

β = Bohr magneton of the electron, a constant

h = Planck's constant

One can vary the magnetic field and keep the oscillating field constant in order to find a resonance condition. This technique is normally done in ESR experiments for instrumental reasons.

The g value of an unpaired electron spin is g = 2.0023. Free radicals normally exhibit a resonance near this g value at room temperature. Oxidized clostridial-type ferredoxins exhibit a g value close to g = 2.0023; the width of the g = 2 resonance is ~28 Gauss (see Appendix A), but it is not detectable above 40°K. Oxidized plant-type ferredoxins do not exhibit any ESR resonances (12).

ESR resonances of reduced clostridial-type and plant-type ferredoxins usually exhibit at least three g values, for example, in C. pasteurianum ferredoxin they are $g_z = 2.03$, $g_y = 1.94$, and $g_x = 1.86$ (100), and these represent the parameters which describe the orientation of an electron spin in a rhombic environment (24). Electron g values can vary with the kind of element, the oxidation state of the element, and the kind of ligand.

As one varies the magnetic field in ESR spectrometers the absorption of energy at the resonance condition is not displayed as an absorption line, as the NMR spectrometers, but as the first derivative of the absorption. Thus for a single resonance the g value is measured as the point of inflection of the derivative plot. The width of the electron resonance is the peak to peak (trough) distance of the derivative spectrum and can depend on many factors (see Discussion).

RESULTS:

g = 1.94 RESONANCE:

ESR spectra of dithionite-reduced C. acidi-urici [^{56}Fe] ferredoxin and [^{57}Fe] ferredoxin (Fig. 19) and of C. pasteurianum [^{56}Fe] ferredoxin and [^{57}Fe]ferredoxin (Fig. 20) show that ESR resonances of the [^{57}Fe] ferredoxins are broader than those of the [^{56}Fe] ferredoxins. ^{57}Fe should broaden the electron resonance by about 19 gauss (80, 99), and we observe that reduced [^{57}Fe] ferredoxin resonances are 11-15 gauss broader than the reduced [^{56}Fe] ferredoxin resonances. This degree of broadening is also consistent with the amount of broadening observed in reduced plant-type [^{57}Fe] ferredoxins (80, 99).

g = 2 RESONANCE:

The g = 2 resonances of oxidized reconstituted and native C. acidi-urici and C. pasteurianum [^{56}Fe] ferredoxins were detected and have comparable intensities. The g = 2 resonances were not detectable in oxidized reconstituted C. acidi-urici and C. pasteurianum [^{57}Fe]ferredoxins at > 1.4°K. (Fig. 21). The g = 2 resonance in the oxidized [^{57}Fe] ferredoxins was much less intense than that of oxidized [^{56}Fe] ferredoxins at 1.4°K. This attenuated signal was also broader by ~5 gauss.

DISCUSSION:

g = 1.94 RESONANCES:

The reducing electron can now be associated with the Fe atoms of clostridial-type ferredoxins, as it has been associated with the Fe and S atoms of 2 Fe, 2 S plant-type ferredoxins, because the g = 1.94 resonances of reduced clostridial-type [^{57}Fe] ferredoxins were broader than the corresponding resonances in reduced clostridial-type [^{56}Fe] ferredoxins.

g=2 RESONANCE:

It is unknown why the g = 2 resonance of oxidized reconstituted C. acidi-urici and C. pasteurianum [^{57}Fe] ferredoxins is much less intense than that of the corresponding [^{56}Fe] ferredoxins. Both reconstituted [^{57}Fe] ferredoxins and [^{56}Fe] ferredoxins were prepared under identical conditions on the same day. The fact that the less intense g = 2 resonances of [^{57}Fe] ferredoxins are broader than those of [^{56}Fe] ferredoxins suggests that the unpaired electron(s) in oxidized ferredoxin are also close to the iron atoms of ferredoxin. This interpretation is not the only possible one, since the [^{57}Fe] ferredoxin g = 2 resonance is much less intense than the [^{56}Fe] ferredoxin resonance. The [^{57}Fe] ferredoxin resonance could be more relaxed and may be broadened by some other mechanism(6). For example, ESR resonances can be broadened by: (i) the interaction of the electron spin with a nuclear (e. g., a proton) spin or other electron spins; (ii) the interaction of the electron spin with surrounding diamagnetic molecules or both; and (iii) increased temperature or anything that affects the vibrational, rotational and translational motion of these species or affects electron exchange between them. These interactions can increase the ESR line width (and hence lower its intensity) by decreasing the lifetime of a spin state that can absorb energy at the resonance frequency. This "lifetime broadening" is a consequence of the Heisenberg uncertainty principle which requires that when the lifetime of an excited state, Δt, is small, the uncertainty in the energy of transition, ΔE, (where $E = h\nu$) becomes large and less defined.

TYROSYL RADICAL:

The assignment of the g = 2 resonance has not been determined. We have some incomplete evidence (see Experiment 5) that the g = 2 resonance may be an artifact due to a tyrosyl radical produced by freezing clostridial-type ferredoxins which contain at least one tyrosyl residue. If a tyrosyl radical is formed at low temperatures then the tyrosyl radical electron also has to be close to the Fe atoms.

Fig. 19. ESR (20° K.) spectra of dithionite-reduced C. acidi-urici ferredoxin. (A): [^{57}Fe] ferredoxin. (B): [^{56}Fe] ferredoxin.

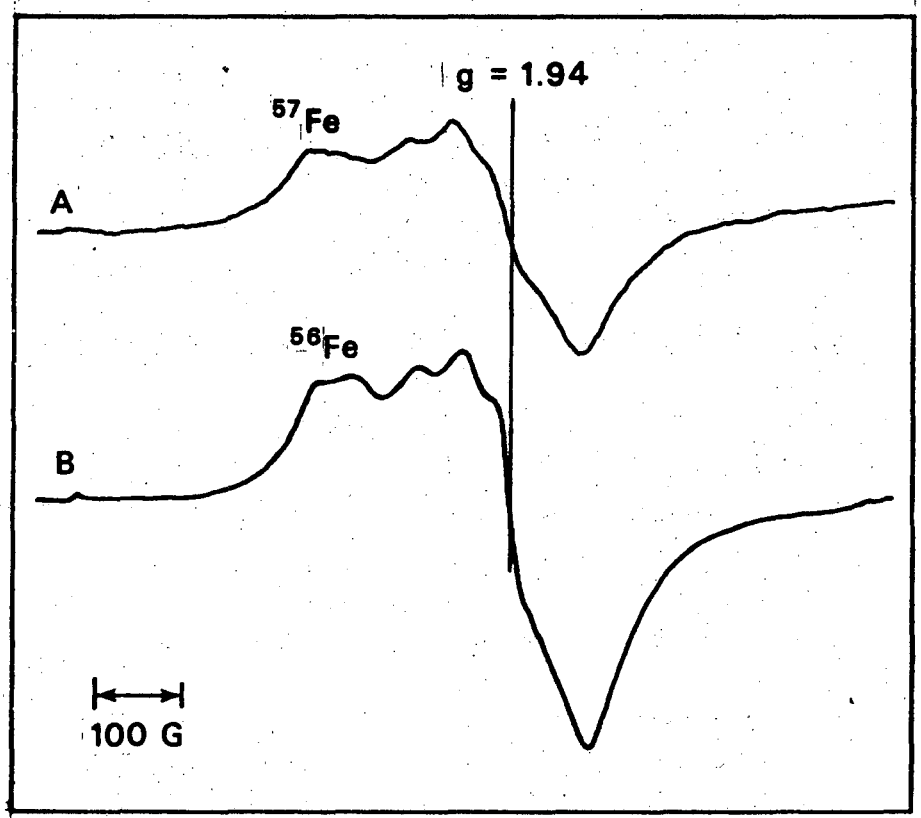
g = 1.94
57Fe
A
56Fe
B
100 G

Fig. 20. ESR (20° K.) spectra of dithionite-reduced *C. pasteurianum* ferredoxin. (A): [^{57}Fe] ferredoxin. (B): [^{56}Fe] ferredoxin.

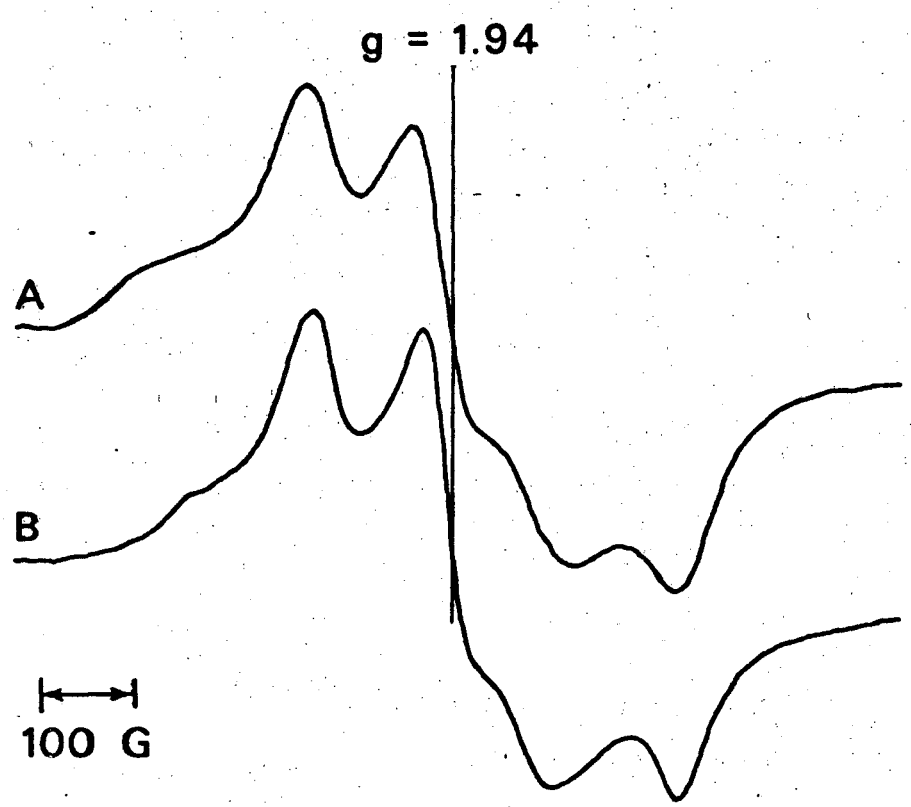
g = 1.94
A
B
100 G

Fig. 21. ESR (20° K) spectra of oxidized C. pasteurianum and C. acidi-urici ferredoxins. (A): Reconstituted C. pasteurianum [^{56}Fe] ferredoxin, 25° K. (B): C. acidi-urici [^{56}Fe] ferredoxin, 25°K. (C): Reconstituted C. pasteurianum [^{57}Fe] ferredoxin, 10°K.

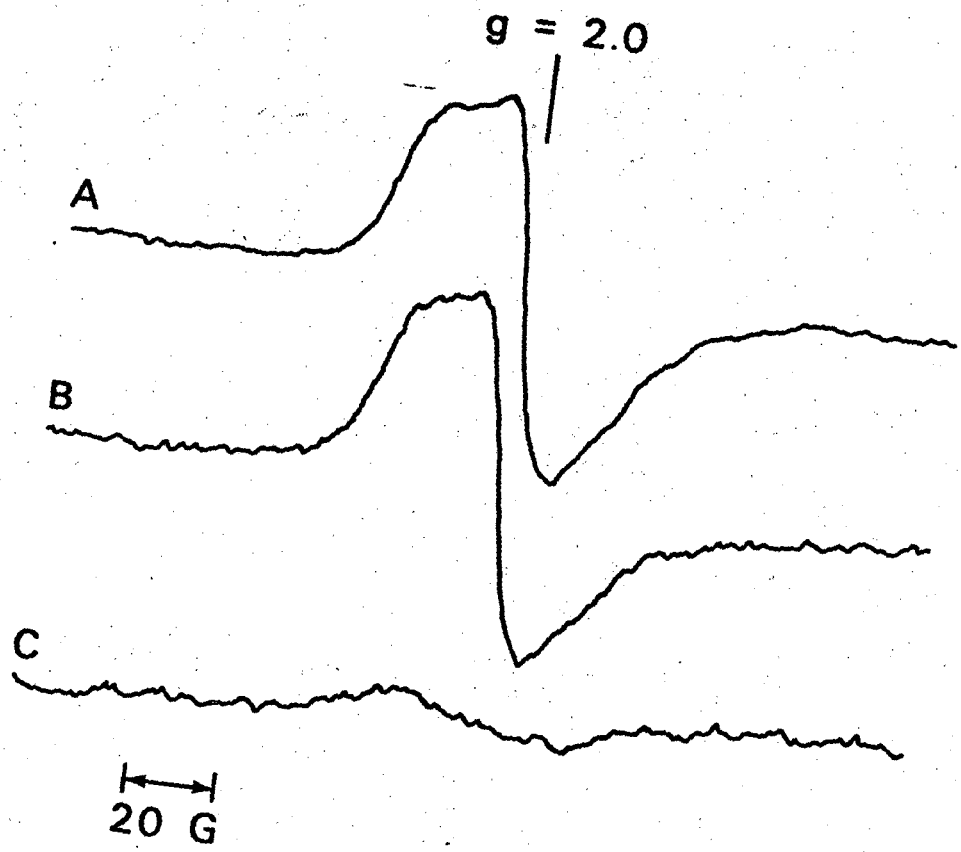
g = 2.0
A
B
C
20 G

Experiment 5.

Tentative assignment of the g = 2 ESR resonance to a tyrosyl radical electron in oxidized *Clostridium acidi-urici* and *Clostridium pasteurianum* ferrdoxins

SUMMARY:

The g = 2 ESR resonance is seen in ESR spectra of oxidized *C. acidi-urici* and *C. pasteurianum* ferredoxins below 40° K, and these ferredoxins contain at least one tyrosyl residue. No g = 2 resonance is seen in ESR spectra of oxidized *C. butyricum* and *C. cylindrosporum* ferredoxins below 40° K, and the two aromatic residues in *C. butyricum* and *C. cylindrosporum* ferredoxins are phenylalanyl residues. Thus, the g = 2 resonance is tentatively assigned to a tyrosyl radical electron in *C. acidi-urici* and *C. pasteurianum* ferredoxin.

The ESR spectra of reduced *C. butyricum* and *C. cylindrosporum* ferredoxins, however, are similar to those of reduced *C. acidi-urici* and *C. pasteurianum* ferredoxins in that they exhibit ESR resonances centered around g = 1.94.

INTRODUCTION:

Blumberg and Peisach (17) have proposed that the g = 1.94 resonance of reduced iron-sulfur proteins can be explained by an ion containing an even number of d electrons in the diamagnetic state bonded to a free radical species, such as Fe^{2+} and a reduced radical species. This hypothesis is no longer tenable, but it is of interest to know if clostridial ferredoxins contain a radical moiety because the g = 2 resonance in oxidized *C. acidi-urici* and *C. pasteurianum* ferredoxin is like a free radical resonance. Since tyrosyl rings under certain conditions can form free radicals (141, 142), one would like to know if the g = 2 resonance is due to the tyrosyl residues in these ferredoxins.

If the g = 2 resonance is present in oxidized clostridial ferredoxins which contain no tyrosyl residues, then the g = 2 resonance is probably not due to a tyrosyl radical. If the g = 2 resonance is absent, it suggests, but does not prove, that the g = 2 resonance is due to a tyrosyl radical.

METHODS AND MATERIALS:

The amino acid composition of C. butyricum and C. cylindrosporum ferredoxins was determined by methods described in the General Methods and Materials section, by Dr. A. B. Champion and the author.

RESULTS AND DISCUSSION:

The amino acid composition of the C. butyricum and C. cylindrosporum ferredoxins used for the ESR studies was consistent with the amino acid composition previously reported (13, 28). No tyrosyl residues were present in either ferredoxin and this fact is confirmed by the absence of a peak at 280 nm in the UV spectrum of C. butyricum ferredoxin (Fig. 22) (Ferredoxins which contain at least one tyrosyl residue exhibit a peak at 280 nm (78)).

No g = 2 resonance was seen in ESR spectra of oxidized C. butyricum and C. cylindrosporum ferredoxin at 1.4°K. Dithionite reduction of these ferredoxins, however, produced normal reduced ferredoxin ESR resonances centered around g = 1.94 (Figs. 23 and 24). This negative evidence suggests that the g = 2 resonance is produced by a tyrosyl radical.

The formation of a tyrosyl radical may be an artifact produced by freezing, since clostridial ferredoxins which contain tyrosyl residues do not produce tyrosyl radicals at room temperature. (See Experiments 6b, 7a, 7b). Until one demonstrates that the number of spins that produces the g = 2 resonance is reduced by one-half, in derivatives of C. acidi-urici ferredoxin, in which one of the tyrosyl residues is replaced by other aromatic or aliphatic residues, one cannot yet prove unequivocally that the g = 2 resonance is due to a tyrosyl radical. The only positive evidence that suggests that the g = 2 resonance is due to a tyrosyl radical is the fact that this resonance was narrowed by 5-7 gauss in oxidized C. acidi-urici [[3', 5' -$^2H_2$] Tyr] -ferredoxin (Experiment 2).

One can conclude, however, that a tyrosyl radical does not produce the resonances centered about g = 1.94 in reduced ferredoxin because these resonances are present in reduced C. butyricum and C. cylindrosporum ferredoxins, and these ferredoxins do not contain tyrosyl residues.

Fig. 22. UV and visible spectrum of C. butyricum ferredoxin.

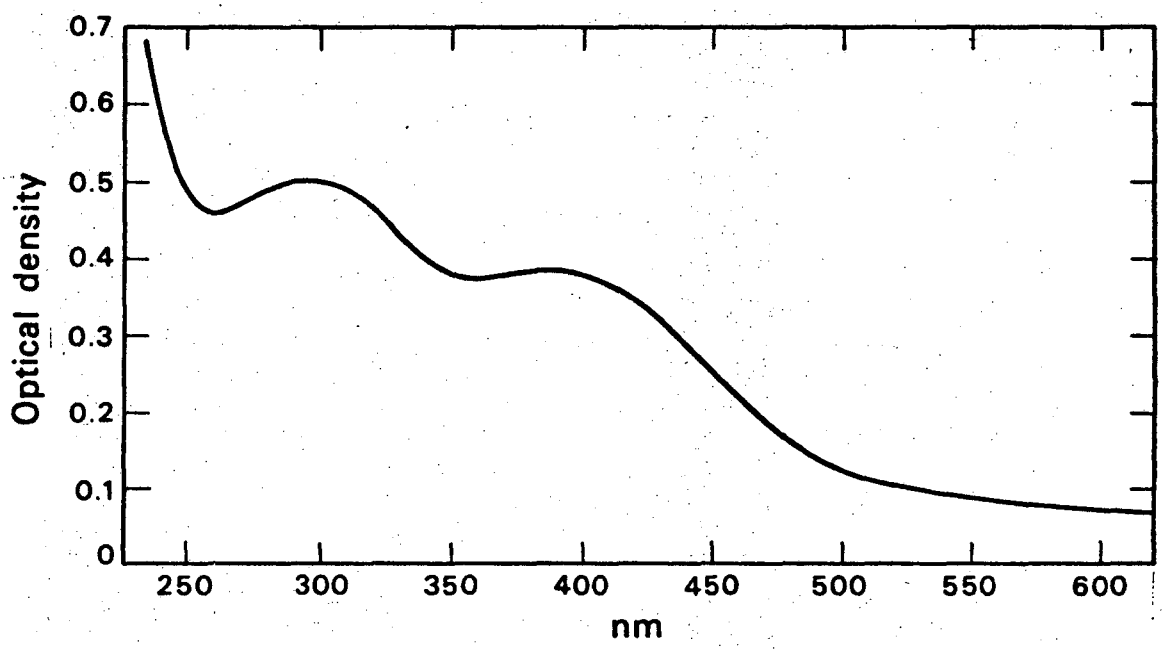
0.7
0.6
0.5
0.4
0.3
0.2
0.1
0
Optical density
250
300
350
400
450
500
550
600
nm

Fig. 23. ESR (25° K) of oxidized and reduced C. butyricum ferredoxin.

(A) Reduced ferredoxin (0.86 mg/ml) + ~ 100 nmoles $Na_2S_2O_4$.

(B) Oxidized ferredoxin (0.86 mg/ml).

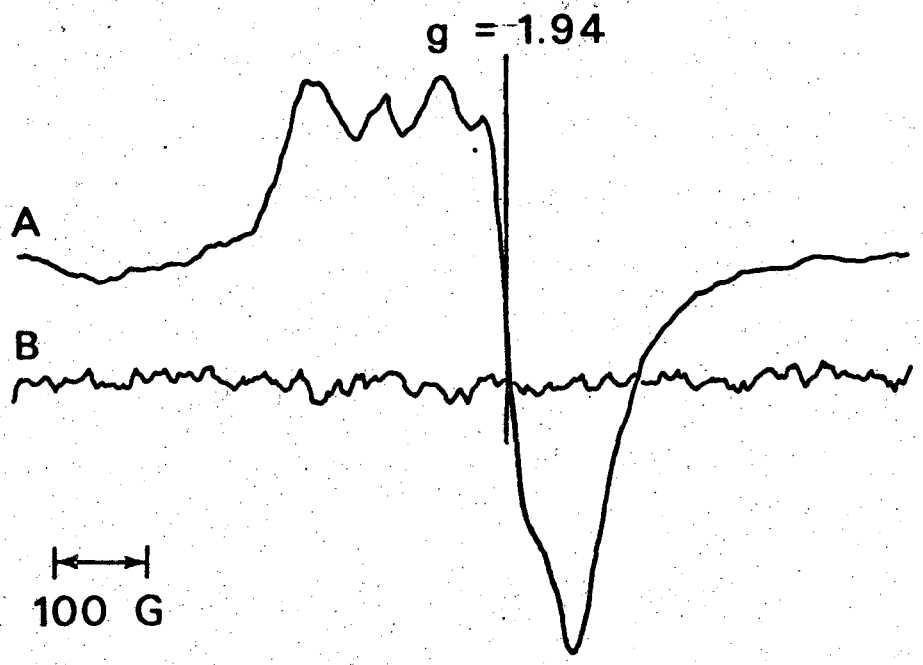
g = 1.94
A
B
100 G

Fig. 24. ESR (25° K) of reduced C. cylindrosporum ferredoxin (0.59 mg/ml). Reduced with ~ 100 n moles $Na_2S_2)_4$.

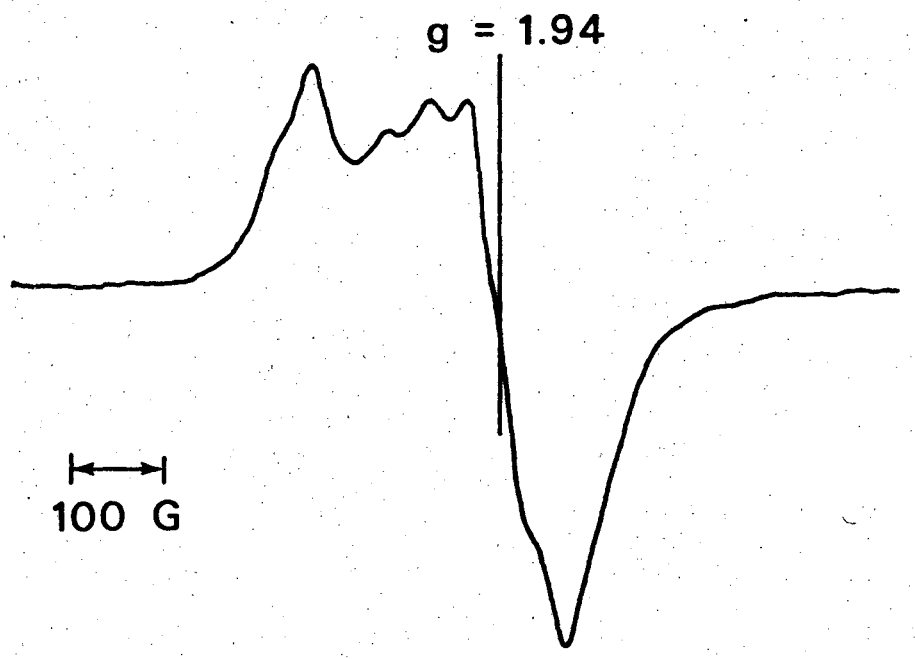
g = 1.94
100 G

Section 3. ^{1}H-NMR Experiments

Experiement 6a.

Conformational changes in oxidized *Clostridium acidi-urici* native and [Phe^2] -ferredoxin and *Clostridium pasteurianum* ferredoxin.

SUMMARY:

The pattern of the downfield-shifted resonances in the ^{1}H-NMR spectrum of oxidized *C. acidi-urici* native ferredoxin is essentially identical to that of oxidized *C. acidi-urici* [Phe^2] -ferredoxin, but is significantly different from that of oxidized *C. pasteurianum* ferredoxin. This pattern of downfield-shifted proton resonances is altered when *C. acidi-urici* ferredoxin is dissolved in buffered 0.58 M NaCl or buffered H_2O when compared with ferredoxin dissolved in buffered D_2O. We attribute the different shift patterns to small conformational differences within each protein.

INTRODUCTION:

C. acidi-urici and *C. pasteurianum* ferredoxin have different amino acid sequences, but 40 of the 55 amino acids are homologous (Fig. 3 General Introduction). If one assumes that the x-ray structures of these proteins are similar to that of *P. aerogenes* ferredoxin, eleven of the twelve amino acid residues conserved in evolution may be closely packed around the Fe-S clusters. Five of the sixteen amino acid residues directly bonded to cysteinyl residues in *C. acidi-urici* and *C. pasteurianum* ferredoxins are not homologous, and these non-homologous amino acid residues could cause the cysteinyl residues to have a slightly different conformation about the Fe-S clusters in each protein.

Phillips and coworkers have demonstrated that the resonance positions of the downfield-shifted proton resonances of oxidized C. acidi-urici (111) and C. pasteurianum ferredoxin (110) are very sensitive to temperature, and assigned these shifted resonances to the β-protons of the eight cysteinyl residues of the proteins. Their assignment is based on: (i) the magnitude and temperature dependence of these shifts in the oxidized and reduced proteins (106); and (ii) the fact that the downfield-shifted resonances correspond to at least sixteen protons. The magnitudes of the contact shifts would depend upon the dihedral angle θ (Fig. 25) about the C—S bond axis (105).

The resonances of other protons, not bonded to cysteinyl residues, could also be shifted if they were close enough to the Fe-S clusters (See Experiment 8), and these shifts would also depend on the orientation of the proton to the Fe-S cluster.

METHODS AND MATERIALS:

C. acidi-urici apoferredoxin was reconstituted in D_2O to eliminate all exchangeable protons. C. acidi-urici [Phe^2] -ferredoxin prepared according to procedures described in Experiment 7b, has a phenylalanyl residue in position 2 instead of a tyrosyl residue.

RESULTS:

CHANGES IN PROTEIN CONFORMATION:

EFFECT OF H_2O AND D_2O: The pattern of downfield-shifted resonances in the ^{1}H-NMR spectrum of oxidized C. acidi-urici ferredoxin dissolved in H_2O is different from that of C. acidi-urici ferredoxin dissolved in D_2O (Tables 6, 7, 8 and Figs. 26, 28, 29). This isotope effect is reversible and is observed at three different temperatures

(Fig. 29). For example, peaks I and II are each shifted ~ 0.2 ppm further downfield in H_2O than the corresponding peaks are in D_2O, at any given temperature.

The most plausible explanation for this isotope effect is that the protein has a different conformation in D_2O with deuterium hydrogen-bonds than it does in H_2O with proton hydrogen-bonds. The kinds of hydrogen-bonds which may be affected by the substitution of (rapidly exchangeable) deuterium atoms for protons could be internal or external hydrogen-bonds or both.

Internal H-bonds:

At least three internal hydrogen-bonds have been proposed (2) for *P. aerogenes* ferredoxin (Fig. 30), and if these hydrogen bonds also exist in *C. acidi-urici* ferredoxin they could bind amino acid residues 1 and 39, 3 and 52, and 3 and 53. Since the deuterium hydrogen-bond is weaker than the proton hydrogen bond, deuterium bonds could produce a different protein conformation around the Fe-S cluster and thus affect the magnitudes of the magnetic shifts.

External H-bonds:

Changes in the strength of external hydrogen bonds could also produce protein conformational changes. The external H-bonds that may be affected by deuterium substitution include: (i) hydrogen bonds between the surface of the protein and the solvent shell; (ii) hydrogen bonds within the solvent shell; and (iii) the hydrogen bonds that affect the water structure within the protein. Changes in protein surface conformation can affect the internal protein conformation (20).

EFFECT OF TEMPERATURE: The magnitude of the shifts of the downfield-shifted resonances of oxidized C. acidi-urici ferredoxin (111) oxidized C. pasteurianum ferredoxin (110), other iron sulfur porteins such as oxidized plant-type ferredoxins (109), and reduced Chromatium high potential ion protein (107) increase with temperature. These shifts are called magnetic shifts because the magnitude and temperature dependence of these shifts is larger than one expects for chemical shifts, i.e., shifts due to the changes in protein conformation with temperature. Proton resonances experience downfield chemical shifts if the nuclei are deshielded by the magnetic field produced by electron currents of neighboring atoms. Magnetic shifts on the other hand are caused by the magnetic moment of unpaired electron spins.

Magnetic shifts, however, usually decrease with increasing temperature (Curie behavior) (105) and in reduced C. acidi-urici ferredoxin eight of the sixteen shifted proton resonances follow this behavior (111). This has led Phillips and coworkers (106) to hypothesize that in the oxidized ferredoxins (and reduced Chromatium high potential iron protein), the iron atoms are antiferromagnetically coupled, and the net observed shifts are due to thermal unpairing of electron spins in the iron and sulfur atoms. (Increased shifts would occur with increasing temperature because more spin states are occupied at higher temperatures (110)).

EFFECT OF IONIC STRENGTH: The pattern of downfield-shifted proton resonances of the ^{1}H-NMR spectrum (Fig. 31 and Table 9) of oxidized C. acidi-urici ferredoxin dissolved in buffered 0.58 M NaCl (Fig. 31B) is different from that of ferredoxin dissolved in buffered D_2O (Fig. 31A). This effect is reversible when one removes NaCl by

dialysis against KD_2PO_4-K_2DPO_4 (pD 7.0) buffer. This fact suggests that 0.58 M NaCl changes the conformation of the protons close to the Fe-S clusters.

Salts usually change the conformation of proteins by decreasing the electrostatic repulsion between changed groups in the protein (137). The fact that NaCl can cause the resonances of protons close to the Fe-S clusters to shift suggests that NaCl is altering the conformation of the protein by neutralizing changes on the protein surface or within the protein, or both. It is unknown how such a gross perturbation of protein structure can affect the proton conformations of amino acids inside the protein, but if NaCl decreases electrostatic repulsion of charges within the protein, then the protein is a relatively open structure. This is consistent with the X-ray structure of P. aerogenes ferredoxin, and the recent report of Phillips (104) that in some iron-sulfur proteins, when H_2O, rather than D_2O is used as a solvent, additional contact-shifted resonances are observed. He attributes these additional resonances to rapidly exchangeable protons.

COMPARISON OF FERREDOXINS:

The pattern of the downfield shifted resonances of the ^{1}H-NMR spectrum of oxidized C. acidi-urici native ferredoxin (Fig. 32B) is identical to that of C. acidi-urici [Phe^2]-ferredoxin (Fig. 32A). As expected they differ only in the aromatic region (Table 10). This suggests that the substitution of a phenylalanyl residue for a tyrosyl residue in position 2 does not change the oxidized protein conformation around the Fe-S clusters. The pattern of aliphatic resonances in ^{1}H-NMR spectra (Fig. 33) and ^{13}C-NMR spectra (Experiment 8) of both proteins is also identical.

The pattern of the downfield-shifted resonances of ^{1}H-NMR spectra of oxidized C. acidi-urici native ferredoxin (Fig. 32A) and C. acidi-urici [Phe^{2}] -ferredoxin Figs. 23B and 34B) is different from that of oxidized C. pasteurianum ferredoxin (Fig. 34A, Table 11). If we assume that the conformation of C. acidi-urici and C. pasteurianum ferredoxins are different, the downfield-shifted resonance shift patterns can be a sensitive indicator of protein conformational change around the Fe-S cluster. Thus, ^{1}H-NMR of the downfield-shifted proton region could be used to determine if changes in protein conformation occur around the Fe-S clusters when one chemically modifies ferredoxins.

Fig. 25. Dihedral angles θ_1 and θ_2 about the β-carbon and sulfur atoms of a cysteinyl residue in clostridial-type ferredoxins.

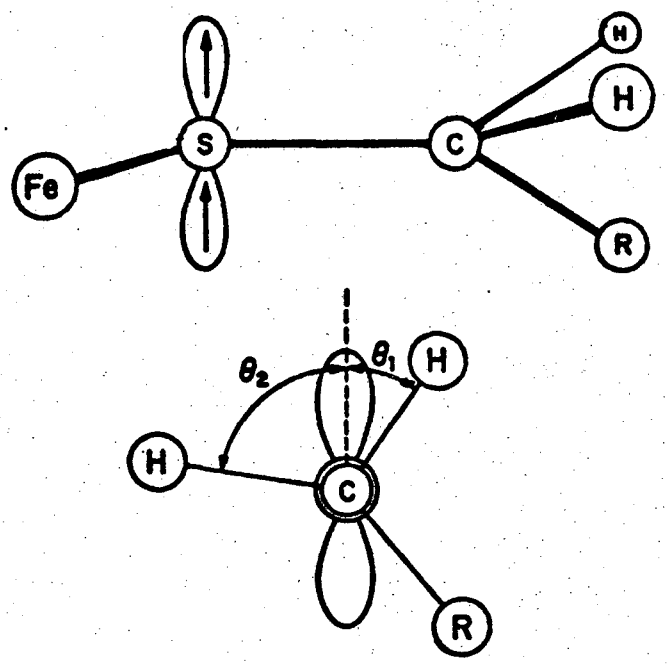
Fe
S
C
H
H
R
θ_2
θ_1
H
H
C
R

Fig. 26. ^{1}H-NMR (4°C) of oxidized C. acidi-urici ferredoxin (30 mg/ml) ferredoxin is dissolved in H_2O (A) and D_2O (B). (A): 0.2 M KH_2PO_4-K_2HPO_4 buffer, pH 7.4; (B): 0.2 M KD_2PO_4-K_2DPO_4 buffer, pH 7.0.

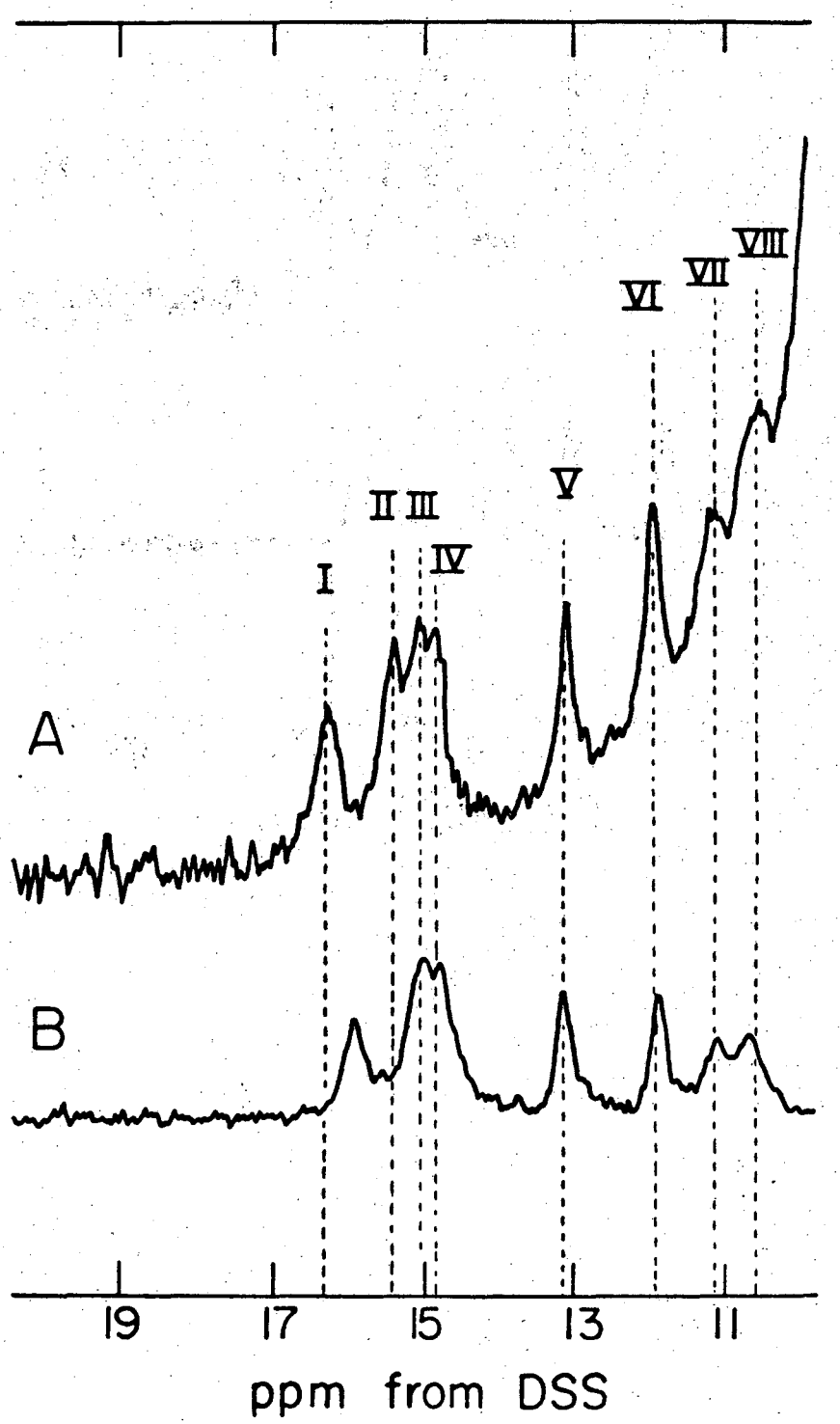
I
II
III
IV
V
VI
VII
VIII
A
B
19
17
15
13
11
ppm from DSS

Fig. 28. ^{1}H-NMR (15° C) of oxidized C. acidi-urici ferredoxin in H_2O (A) and D_2O (B). Conditions same as described in Fig. 26.

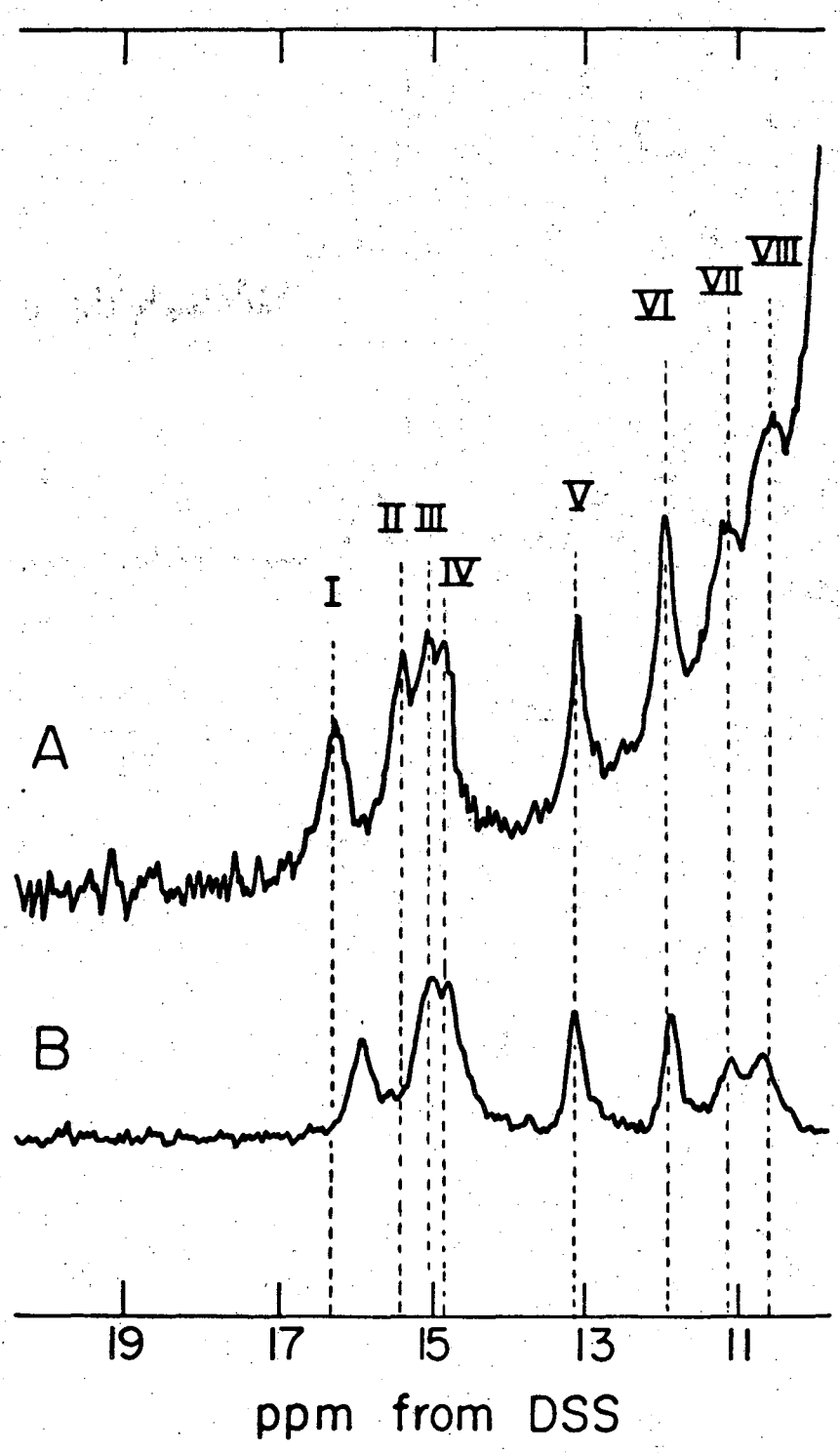
I
II
III
IV
V
VI
VII
VIII
A
B
19
17
15
13
11
ppm from DSS

Fig. 29. ^{1}H-NMR of downfield-shifted proton resonances (Tables 6, 7, 8) in oxidized C. acidi-urici ferredoxin in H_2O and D_2O as a function of temperature. Primed peak numbers I through VII refer to ferredoxin in H_2O, and unprimed peak numbers refer to ferredoxin in D_2O.

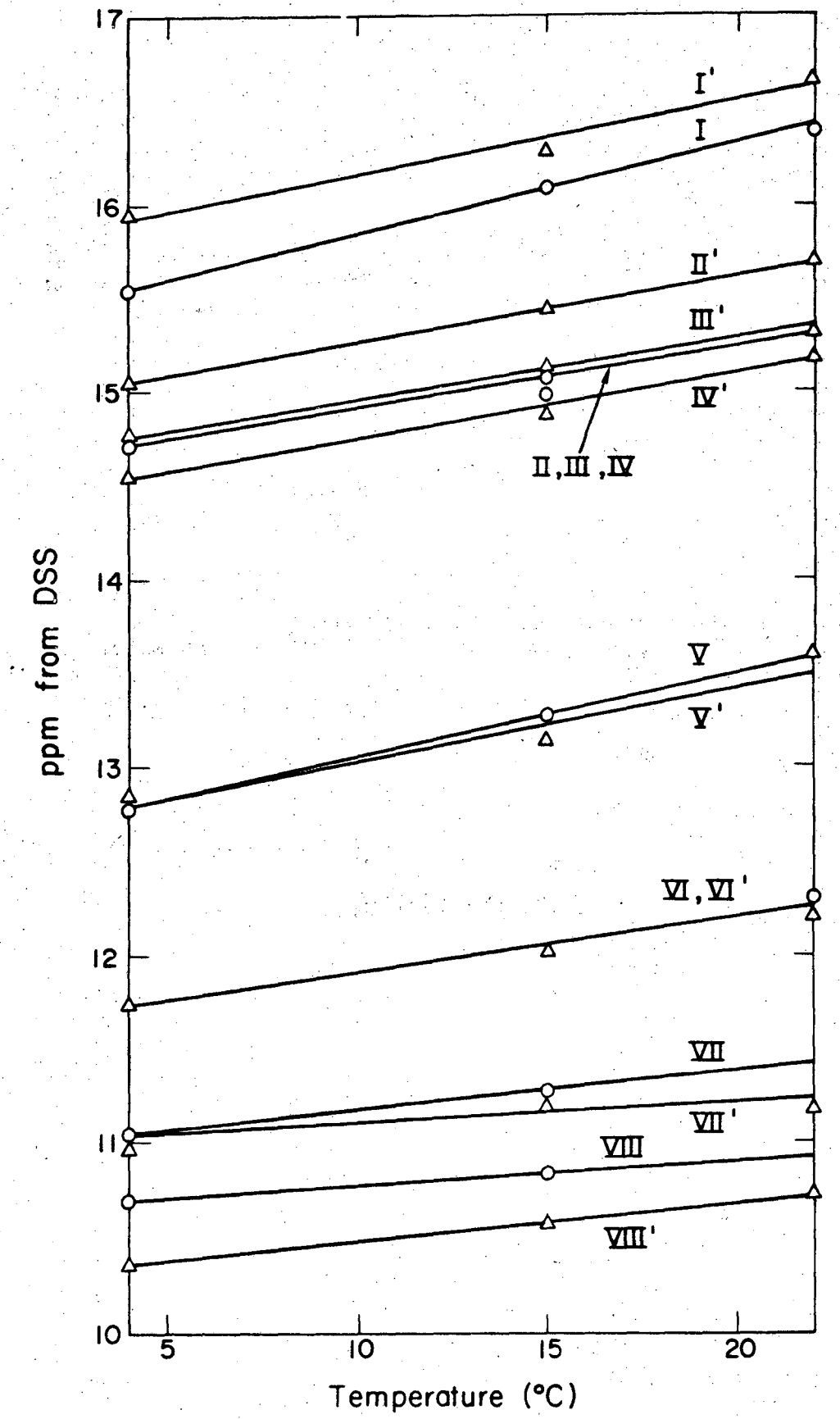
17
16
15
14
13
12
11
10
ppm from DSS
5
10
15
20
Temperature (°C)
I'
I
II'
III'
IV'
II,III,IV
V
V'
VI,VI'
VII
VII'
VIII
VIII'

Fig. 30. Three-dimensional structure of the peptide backbone of *P. aerogenes* ferredoxin (2) showing hydrogen bonding at amino acid residues 1 and 37, 3 and 51, and 3 and 50. (For *C. acidi-urici* ferredoxin add two to the residue number for residues succeeding *P. aerogenes* ferredoxin residue 21.)

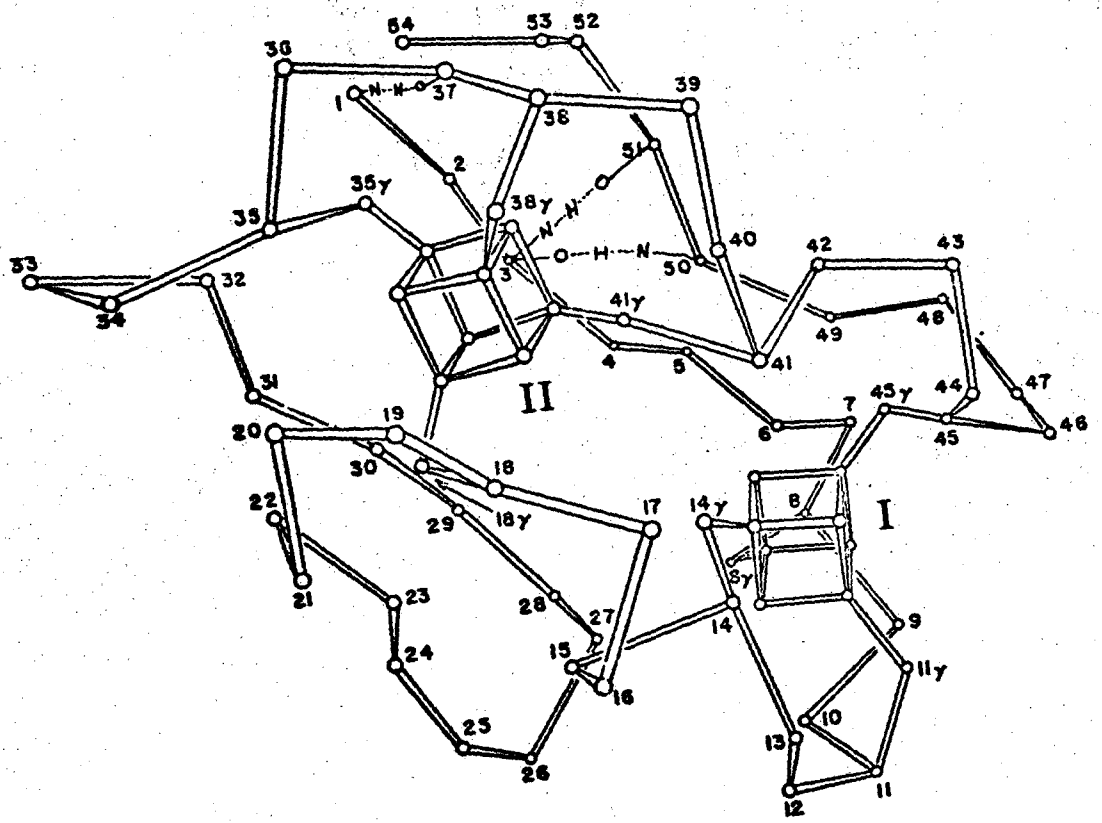
54
53
52
36
37
39
1
38
51
2
35γ
38γ
35
40
42
43
33
32
3
50
34
41γ
49
48
4
5
41
31
II
7
45γ
44
47
19
6
45
46
20
30
18
22
17
14γ
8
I
29
18γ
8γ
21
23
28
27
14
9
24
15
11γ
16
10
25
13
26
11
12

Fig. 31. ^{1}H-NMR (15° C) of oxidized C. acidi-urici ferredoxin in the presence (A) and absence (B) of NaCl. (30 mg/ml ferredoxin is dissolved in 0.2 M KD_2PO_4-K_2DPO_4 buffer, pD 7.0).

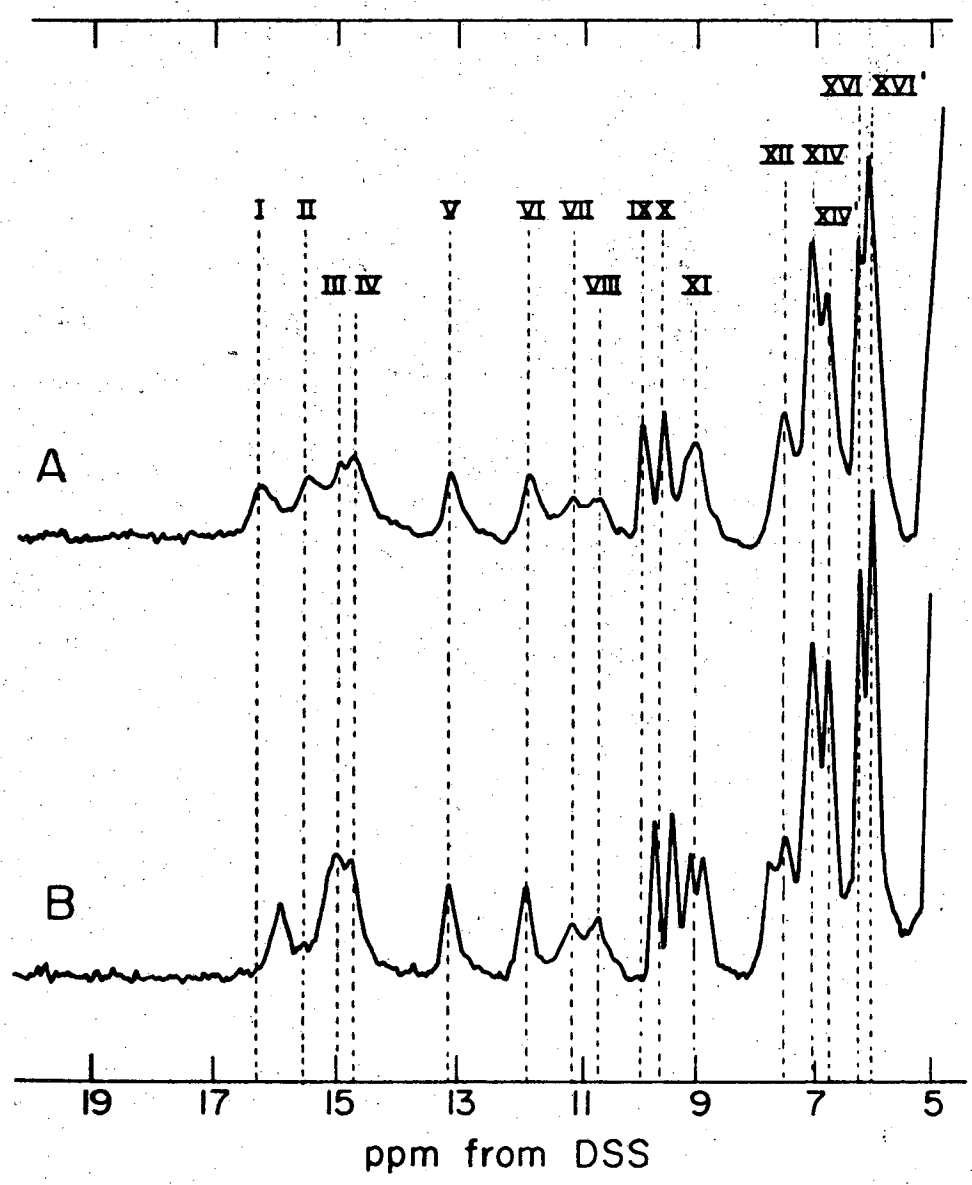
I
II
III
IV
V
VI
VII
VIII
IX
X
XI
XII
XIV
XIV'
XVI
XVI'
A
B
19
17
15
13
11
9
7
5
ppm from DSS

Fig. 32. ^{1}H-NMR (15° C) of C. acidi-urici [Phe^{2}]-ferredoxin (A) and C. acidi-urici native ferredoxin (B). Conditions are the same as in Fig. 28B.

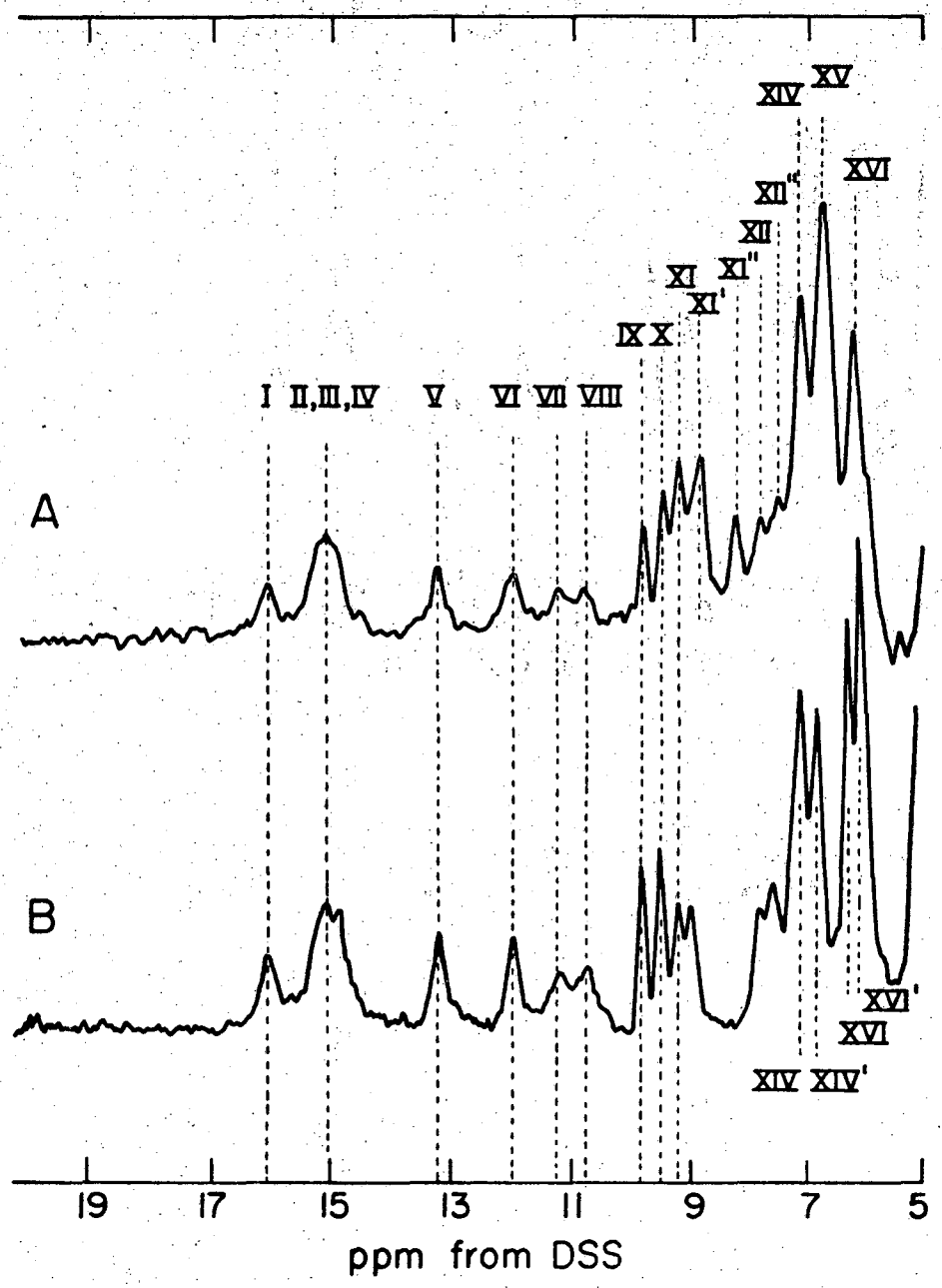
XV
XIV
XVI
XII''
XII
XI''
XI
XI'
IX X
I II,III,IV V VI VII VIII
A
B
XVI'
XVI
XIV XIV'
19 17 15 13 11 9 7 5
ppm from DSS

Fig. 33. ^{1}H-NMR (15° C) of C. acidi-urici [Phe^{2}]-ferredoxin (A) and C. acidi-urici native ferredoxin (B). Conditions are the same as in Fig. 28B.

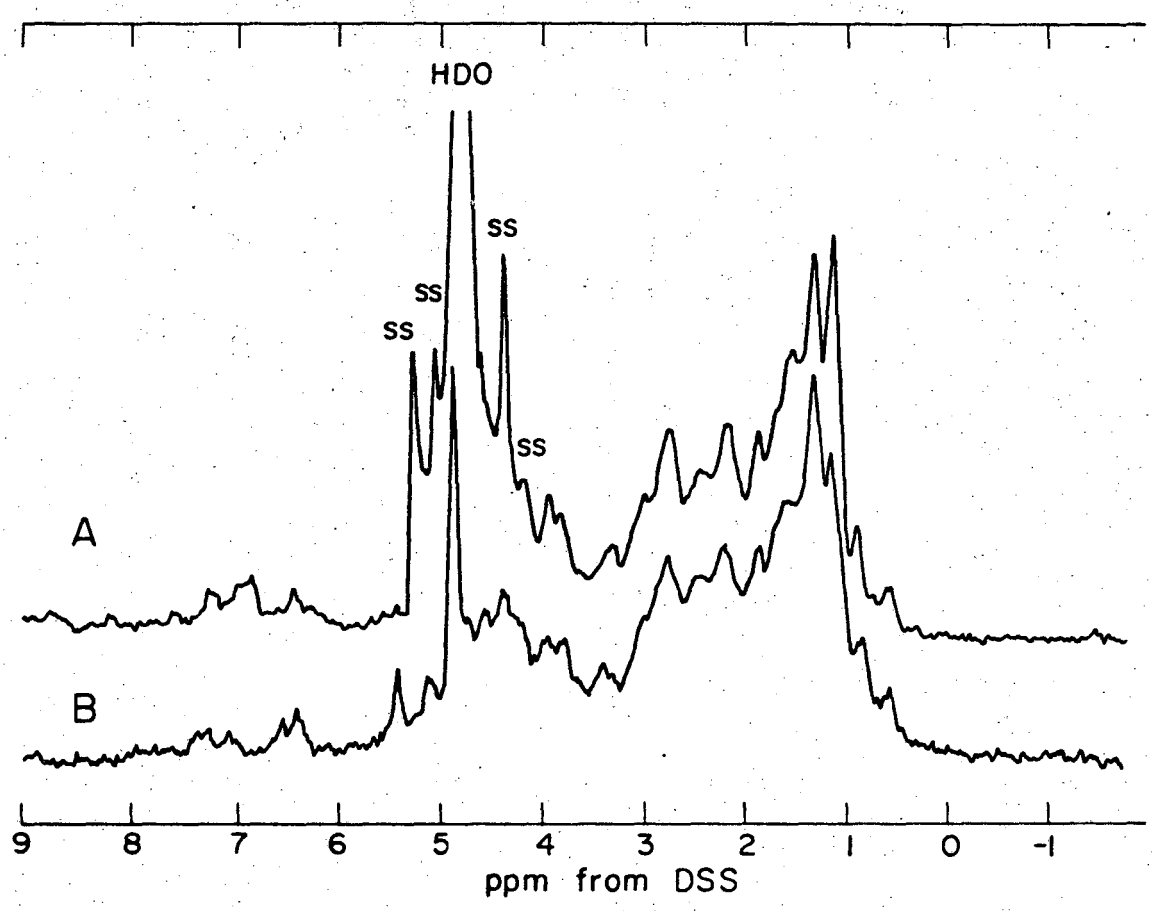
HDO
SS
SS
SS
SS
A
B
9
8
7
6
5
4
3
2
1
0
-1
ppm from DSS

Fig. 34. ^{1}H-NMR (15° C) of C. pasteurianum ferredoxin (A) and C. acidi-urici [Phe^{2}] -ferredoxin (B). Conditions are the same as in Fig. 28B.

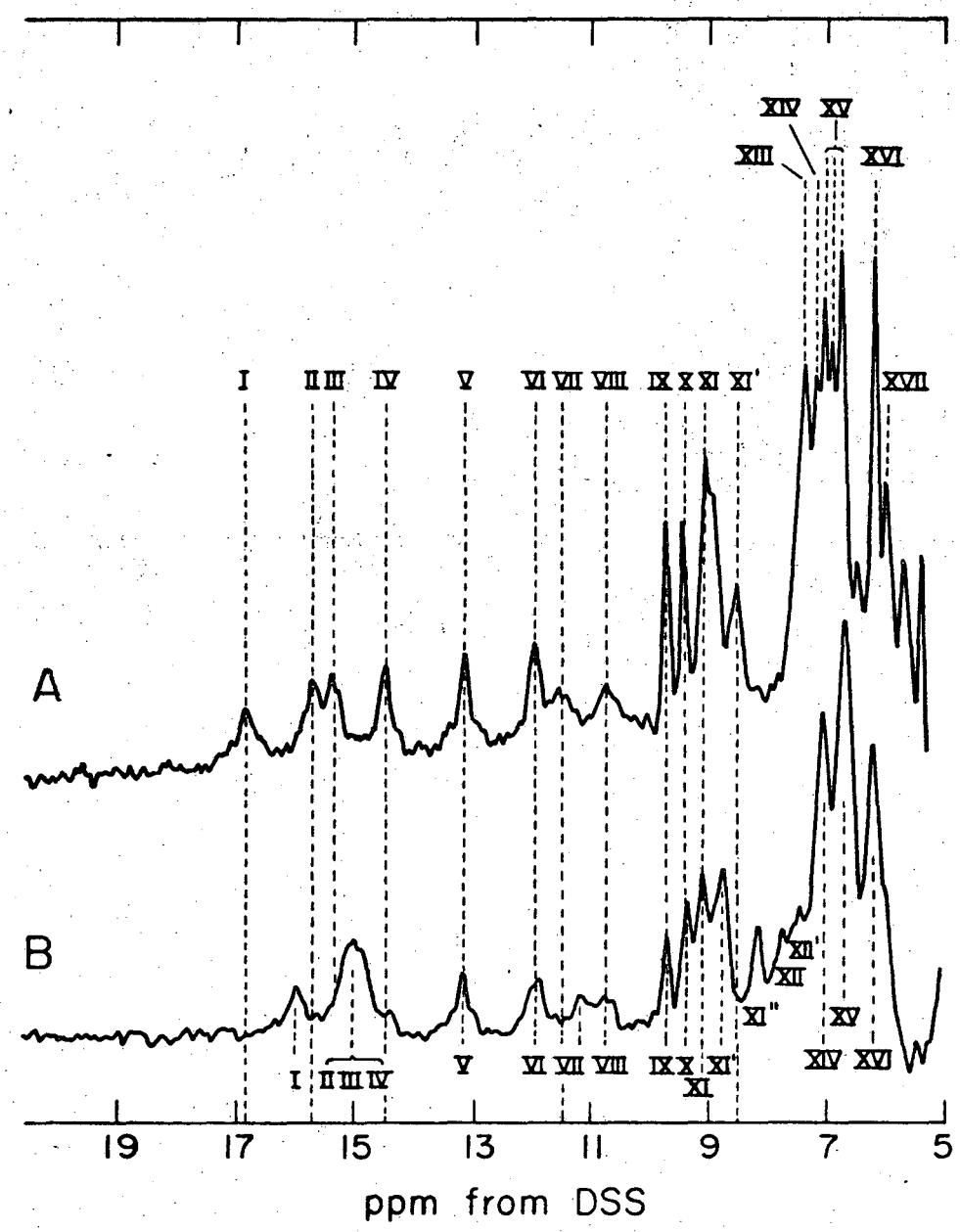
XIV
XV
XIII
XVI
I
II III
IV
V
VI
VII
VIII
IX
X
XI
XI'
XVII
A
B
XII'
XII
XI"
XI
19
17
15
13
11
9
7
5
ppm from DSS

Table 6. ^{1}H-NMR shifts (4° C) of oxidized C. acidiurici ferredoxin in the presence of H_2O and D_2O.

Peak (Fig. 26)	Number of Protons[a]	H_2O (ppm)[b]	D_2O (ppm)[b]	Difference[c] (ppm)[b]
I	1	16.0	15.5	+0.5
II	4 ± 1	15.0	14.7 ± 0.4[d]	+0.3 ± 0.4
III		14.8	14.7 ± 0.4	+0.1 ± 0.4
IV		14.6	14.7 ± 0.4	+0.1 ± 0.4
V	1	12.8	12.8	0
VI	1	11.7	11.7	0
VII	1	11.0	11.0	0
VIII	1	10.5 ± 0.1	10.7	-0.2 ± 0.1

a. Integrated area.

b. Shifts ± 0.05 ppm relative to DSS unless otherwise indicated.

c. (H_2O-D_2O)

d. In D_2O resonances II, III and IV are coalesced, and this position is an average position.

Table 7. ^{1}H-NMR shifts (15° C) of oxidized *C. acidiurici* ferredoxin in the presence of H_2O and D_2O.

Peak (Fig. 28)	Number of Protons[a]	H_2O (ppm)[b]	D_2O (ppm)[b]	Difference[c] (ppm)[b]
I	1	16.3	16.1	+0.2
II		15.4	15.1	+0.3
III	4 ± 1	15.1	15.0	+0.1
IV		14.9	14.9	0
V	1	13.1	13.3	-0.2
VI	1	12.0	12.0	0
VII	1	11.2	11.3	-0.1
VIII	1	10.6	10.8	-0.2

a. Integrated area.

b. Shifts (ppm) are ± 0.05 ppm relative to DSS.

c. (H_2O-D_2O)

d. Integrated area of this cluster of resonances in H_2O is equivalent to 4 ± 1 protons, but in D_2O it is equivalent to 3 protons.

Table 8. ^{1}H-NMR shifts (22° C) of oxidized C. acidi-urici ferredoxin in the presence of H_2O and D_2O.

Peak (Fig. 29)	Number of Protons[a]	H_2O (ppm)[b]	D_2O[c] (ppm)[b]	Difference[c] (ppm)[b]
I	1	16.7	16.4	+0.3
II	4 ± 1[e]	15.6	15.4	+0.2
III		15.3	15.3	0
IV		15.2	15.2	0
V	1	13.3	13.3	-0.3
VI	1	12.2	12.3	-0.1
VII	1	11.2	11.4	-0.2
VIII	1	10.7	10.9	-0.2

a. Integrated area.

b. Shifts ± 0.05 ppm relative to DSS.

c. Extrapolated shifts observed for ferredoxin dissolved in D_2O from 4° and 15° C spectra (Figs. 26, 28).

d. (H_2O-D_2O)

e. Integrated area of this cluster of resonances in H_2O is equivalent to 4 ± 1 protons, but in D_2O it is equivalent to 3 protons.

Table 9. ^{1}H-NMR shifts (15° C) of oxidized C. acidiurici ferredoxin in the presence and absence of 0.58 M NaCl.

Peak (Fig. 31)	Number of Protons[a]	+NaCl (ppm)[b]	-NaCl (ppm)[b]	Difference[c] (ppm)[b]
I	1	16.4	16.1	+0.3
II	1	15.8	15.1	+0.6 ± 0.1[d]
III	1	15.1	15.0	±0.1
IV	1	14.9	14.9	±0.1
V	1	13.3	13.3	0
VI	1	12.0	12.0	0
VII	1	11.3	11.3	0
VIII	1	10.9	10.8	+0.1
IX	1	10.2	10.0	+0.2
X	1	9.8	9.7	+0.1
XI[e]	2	9.3	9.35	-0.05
XI'[e]		9.3	9.25	+0.05
XII[e]	3	7.9	8.0	-0.1
XII'[e]		7.9	7.8	+0.1
XIV	4 ± 1	7.3[f]	7.3[f]	0
XIV'	4 ± 1	7.1[g]	7.1[g]	0
XVI	4 ± 1	6.6[h]	6.6[h]	0
XVI'	4 ± 1	6.4[i]	6.4[i]	0

a. Integrated area.

b. Shifts ± 0.05 ppm relative to DSS.

c. (+NaCl)-(-NaCl)

d. This value depends upon which of the three resonances in peaks II, III and IV in Fig. 31B one chooses

Notes to Table 9 continued.

d. (continued) to subtract from the corresponding peaks in Fig. 31A.

e. Slowly exchangeable proton region (See Experiment 6b).

f. 2',6'-Tyr^{30} proton resonance position (Experiment 7b).

g. 2',6'-Tyr^{2} " " " " "

h. 3',5'-Tyr^{30} " " " " "

i. 3',5'-Tyr^{2} " " " " "

Table 10. ^{1}H-NMR shifts (15° C) of oxidized C. acidi-urici native ferredoxin and C. acidi-urici [Phe^{2}]-ferredoxin.

Peak (Fig. 32)	Number of Protons[a]	Ferredoxin		
		Native (ppm)[b]	[Phe^{2}] (ppm)[b]	Difference[c] (ppm)[b]
I	1	16.1	16.1	0
II	1	15.2	15.2	0
III	1	15.1	15.1	0
IV	1	15.0	15.0	0
V	1	13.3	13.3	0
VI	1	12.0	12.0	0
VII	1	11.3	11.4	-0.1
VIII	1	10.8	10.8	0
IX	1	10.0	9.9	+0.1
X	1	9.7	9.6	+0.1
XI	1[d]	9.3	9.4	+0.1
XI'	2[d]	9.2	9.0	0
XI''	1[d]	-	8.4	0
XII	1[d]	8.0	8.0	0
XII'	2[d]	7.8	7.8	0
XIV	4 ± 1	7.3[e]	7.3[e]	0
XIV'	4 ± 1	7.1[f]	-	-
XV	5 ± 1	-	7.0[g]	-
XVI	4 ± 1	6.6[h]	-	-
XVI'	4 + 1	6.4[i]	6.5[h]	-0.1
XVII	1	-	5.7	-

a. Integrated area.

Notes to Table 10 continued.

b. Shifts ± 0.05 ppm relative to DSS.
c. (Native - [Phe^2])
d. Slowly exchangeable proton resonance region.
e. 2',6'-Tyr^{30} proton resonance position.
f. 2',6'-Tyr^2 " " "
g. 2',6',3',5',4'-Phe^2 proton resonance position.
h. 3',5'-Tyr^{30} proton resonance position.
i. 3',5'-Tyr^2 " " "

Table 11. ^{1}H-NMR (15° C) of oxidized *C. pasteurianum* ferredoxin and *C. acidi-urici* [Phe^{2}]-ferredoxin.

Peak (Fig. 34)	Number of Protons[b]	Ferredoxin		
		C. pasteurianum (ppm)[a]	*C. acidi-urici* [Phe^{2}]- (ppm)[a]	Difference[c] (ppm)[a]
I	1	17.0	16.1	+0.9
II	1	16.0	15.2	+0.8
III	1	15.6	15.1	+0.5
IV	1	14.8	15.0	-0.2
V	1	13.4	13.3	+0.1
VI	1	12.2	12.0	+0.2
VII	1	11.9	11.4	+0.5
VIII	1	10.9	10.8	+0.1
IX	1	9.9	9.9	0
X	1	9.6	9.6	0
XI	3[c]	9.3	9.4	-0.1
XI'	1[c]	8.9	9.0	-0.2
XII		7.6	8.4	-0.8
XII'	4 ± 1[d]	7.5	8.0	-0.5
XII''		-	7.8	-
XIII	4 ± 1	7.4[e,k]	-	-
XIV	4 ± 1	7.2[e,k]	7.3[f]	-0.1
XIV'	4 ± 1	7.1[e,k]	-	-
XV	5 ± 1	-	7.0[g]	-
XV'	5 ± 1	7.0[h]	-	-
XVI	4 ± 1	-	6.5[i]	-
XVI'	4 ± 1	6.4[j]	-	-

Table 11. continued

XVII	?	6.3	5.7	+0.6
XVII'		6.1	-	-

a. Shifts ± 0.05 ppm relative to DSS.

b. Integrated area.

c. (C. pasteurianum ferredoxin - C. acidi-urici [Phe^2]-ferredoxin.)

d. Slowly exchangeable proton region.

e. 2',6'-Tyr^2 ring proton position(s) (tentative assignment).

f. 2',6'-Tyr^{30} ring proton position.

g. 2',6',3',5',4'-Phe^2 ring proton positions of C. acidi-urici [Phe^2]-ferredoxin.

h. 2',6',3',5',4'-Phe^{30} ring proton positions (tentative assignment).

i. 3',5'-Tyr^{30} ring proton position of C. acidi-urici ferredoxin.

j. 3',5'-Tyr^2 ring proton position of C. pasteurianum ferredoxin.

k. These resonances overlap so the area cannot be assigned to any single peak.

Experiment 6b.

Slowly exchangeable protons of *Clostridium acidi-urici* ferrodoxin

SUMMARY:

Comparison of ^{1}H-NMR spectra of oxidized *C. acidi-urici* ferredoxin reconstituted in H_2O with that of oxidized *C. acidi-urici* ferredoxin reconstituted in D_2O shows that two resonances with area corresponding to three or four and one or two protons respectively are missing from the N-H proton region. Thus only three or four protons (which only exchange rapidly with solvent if *C. acidi-urici* ferredoxin is denatured to the apoferredoxin) can be designated as very slowly exchangeable protons in H_2O-reconstituted ferredoxin.

The resonances corresponding to the very slowly exchangeable protons are shifted in the ^{1}H-NMR spectrum of methyl viologen-reduced (H_2O-reconstituted) *C. acidi-urici* ferredoxin. When this ferredoxin is reoxidized, most of the resonances assigned to the very slowly exchangeable protons reappear in their unshifted positions, a result which suggests that some of the slowly exchangeable protons are very close to the Fe-S clusters in reduced *C. acidi-urici* ferredoxin.

INTRODUCTION:

^{1}H-NMR measurements of proteins require that most of the H_2O associated with the protein be exchanged with D_2O. Otherwise the proton resonance from H_2O will obscure most of the protein proton resonances. During D_2O exchange, any rapidly exchangeable protons,

such as N-H protons, will be replaced by deuterons. The resonances of slowly exchangeable protons have characteristic resonance positions, and the area of these resonances, (which is proportional to the number of protons) will vary from sample to sample, depending on how long the protein has been exposed to D_2O.

In clostridial-type ferredoxin, part of the Fe-S clusters may be surrounded by a hydrophobic environment and thus some slowly exchangeable protons may be close to an Fe-S cluster. Such protons can be identified by ^{1}H-NMR techniques because slowly exchangeable proton resonances will be magnetically shifted from their positions in free amino acids if these protons are close to the Fe-S clusters. To do these measurments one must reconstitute apoferredoxin in the presence of D_2O. The class of very slowly exchangeable protons in reconstituted ferredoxin is thus defined as those protons that rapidly exchange with solvent when the protein is denatured into an apoferredoxin (Fig. 35B).

METHODS AND MATERIALS:

C. acidi-urici apoferredoxin was reconstituted by methods described in the General Methods and Materials section, except that all reagents were lyophilized in D_2O several times to remove any exchangeable protons. The DEAE cellulose column used to purify the reconstituted ferredoxin was cooled by a water jacket and run outside the cold room to prevent H_2O from the air from exchanging with D_2O solutions.

RESULTS:

OXIDIZED FERREDOXIN:

Comparison of ^{1}H-NMR spectra of oxidized C. acidi-urici ferredoxin reconstituted in H_2O (Fig. 36B) with that of ferredoxin reconstituted in D_2O (Fig. 36A) shows that at 9.3 and 8.0 ppm two resonances are diminished by an area corresponding to three or four and one or two proton resonances, respectively (Fig. 36C). N-H proton resonances of proteins usually occur between 7.8-8.6 ppm from DSS(18). Hydrogen bonds tend to shift N-H resonances downfield (56, 67, 112), so it is possible that the resonances at 9.3 ppm correspond to the three or four very slowly exchangeable protons which are involved in hydrogen bonding (2). The one or two missing resonances at 8.0 ppm may correspond to very slowly exchangeable protons that are not hydrogen-bonded.

^{1}H-NMR spectra of oxidized C. acidi-urici ferredoxin reconstituted in H_2O (Fig. 37A) and D_2O (Fig. 37B) show that the areas and positions of the shifted resonances between 9.7 to 16.1 ppm are essentially identical. Thus we can say that the shifted resonances in ths region are not those of slowly exchangeable protons.

REDUCED FERREDOXIN:

In the ^{1}H-NMR spectra of methyl viologen-reduced (H_2O-reconstituted C. acidi-urici ferredoxin the proton resonances at 9.3 and 8.0 ppm (that had been assigned to the slowly exchangeable protons) are either shifted or the protons they represent are rapidly exchanged. These interpretations are based on the fact that when one

compares the ^{1}H-NMR spectrum of the exchangeable proton region of oxidized (H_2O-reconstituted) ferredoxin (Fig. 38A) with that of reduced ferredoxin (Figs. 38B, 38C, 38D), an area corresponding to three or four and one or two protons is missing from the resonances at 9.3 and 8.0 ppm respectively in the ^{1}H-NMR spectrum of the oxidized protein (Fig. 38A).

The slowly exchangeable proton resonances are also missing from the spectrum of 20% (methyl viologen-) reduced C. acidi-urici ferredoxin (Fig. 39B), but when this protein is reoxidized and the methyl viologen is removed by desalting on a Sephadex G-25 column, one or two and possibly one proton resonances reappear in the 9.3 and 8.0 ppm peaks respectively (Fig. 39C). (The error in determing the areas of these resonances is due to the uncertain base line in these spectra.) Thus at least one or two of the very slowly exchangeable proton resonances are shifted in the reduced protein and the protons they represent must be close to the Fe-S clusters.

Since the slowly exchangeable proton region is defined by the fact that it contains a variable number of proton resonances, one cannot yet be sure if reduction of ferredoxin causes the remaining three to five very slowly exchangeable protons to be rapidly exchanged with the D_2O solvent. All of the downfield-shifted resonances move further downfield with increasing reduction (Figs. 40, 41, and Table 12). If one assumes that the resonance at 12.2 ppm in the ^{1}H-NMR spectrum of the 45% methyl viologen-reduced (D_2O-reconstituted) ferredoxin (Fig. 38E) corresponds to the resonance at 11.5 ppm in 24% reduced (H_2O-reconstituted) ferredoxin (Fig. 38D), then one can assign this

resonance to some of the very slowly exchangeable protons. This is because the area of the resonance at 12.2 ppm (Fig. 38E) is much smaller than the 11.5 ppm resonance (Fig. 38D). When one compares the ^{1}H-NMR spectrum of 45% reduced (D_2O-reconstituted) ferredoxin (Fig. 42B), with that of 50% reduced (H_2O-reconstituted) ferredoxin (Fig. 42C), the resonances at 36.0 and 30.5 ppm in the spectrum of the H_2O-reconstituted ferredoxin (Fig. 42C) may be missing from that of the D_2O-reconstituted ferredoxin (Fig. 42B). These missing resonances (each corresponding to a single proton) can also be assigned to the slowly exchangeable protons.

One must use caution when one compares the intensities of resonances in partially reduced ferredoxin however, because with increasing reduction some of these resonances shift even further downfield and may overlap other resonances, which are not shifting downfield at the same rate. This is because the spectrum of partially reduced ferredoxin represents an averaged spectrum of oxidized and reduced protein, since the reducing electron is rapidly exchanged between oxidized and reduced forms of the protein (see Section 4). If for example the position of resonance I is upfield of resonance II in the oxidized protein, but is downfield from resonance II in the reduced protein, at some intermediate degree of reduction resonance II will overlap resonance I and increase its intensity.

The fact that some shifted proton resonances are missing or variable in the 45% reduced ferredoxin that had been reconsitututed in D_2O (Figs. 38E, 42B) suggests that some of the very slowly exchangeable protons are close to the Fe-S clusters.

Variable and missing proton resonances are also observed by Phillips in dithionite-reduced C. acidi-urici ferredoxin. When the ferredoxin is fully reduced by dithionite, as many as 16 proton resonances are significantly shifted (111). These protons have been tentatively assigned by Phillips to the β-protons of the 8 cysteinyl residues in the ferredoxin (111). The shifted proton resonance positions of dithionite-reduced C. acidi-urici ferredoxin are published as a table (111) and these published resonance positions are replotted in Fig. 43B. Phillips recently repeated this experiment with C. acidi-urici ferredoxin, supplied by the author, and the (unpublished) ^{1}H-NMR spectrum of this more recently (dithionite-) reduced ferredoxin appears in Fig. 42A.

Phillips' latest (unpublished) ^{1}H-NMR spectrum (Fig. 43A) of dithionite-reduced C. acidi-urici ferredoxin shows essentially all but three of the resonances he previously reported (Table 13). The new resonances, missing from the first report (111) occurred at 65.4, 55.0, and 19.3 ppm. Two of the most shifted resonances could have been newly discovered because Phillips expanded the range of his NMR spectrometer. Also, in the first report, there is at least one resonance (at 43.0 ppm) that is not seen in the more recent results. Thus, in our different samples of methyl viologen-reduced C. acidi-urici ferredoxin (Figs. 38E, 42B) and in Phillips' different samples of dithionite-reduced ferredoxin (Fig. 43) at least one or two significantly shifted resonances are variable. These variable resonances may either be so broadened, in the fully reduced protein that they are difficult to detect or they could represent slowly exchangeable protons.

Before one can be sure that the "missing" shifted proton resonances are exchangeable protons, these experiments must be repeated by adding H_2O to the reduced ferredoxin samples.

DISCUSSION:

Three classes of exchangeable protons are observed with the tritium-proton technique of Englander (44). In this technique, a protein is equilibrated with T_2O and the exchange-out of T_2O with solvent H_2O is measured.)

Class II protons have fairly rapid exchange rates and correspond to the relatively unhindered peptide-bond protons, Class III protons have intermediate exchange rates and correspond H-bonds protons or sterically protected protons or both, Class IV protons have very slow exchange rates and correspond to "masked" or bonded amino acid side chains (44).

Class IV protons are only rapidly exchanged in denatured proteins, such as C. acidi-urici apoferredoxin. The experiments we do are analogous to those reported by Englander (44) and Hong and Rabinowitz (60) except that we exchange D_2O for H_2O and directly measure the very slowly exchanged protons by comparing the ^{1}H-NMR spectra of ferredoxins that had been reconstituted in D_2O and H_2O. Before our ^{1}H-NMR measurements the ferredoxin samples are equilibrated with D_2O solvent for several weeks or months. Thus in the ferredoxin that had been reconstituted in H_2O, Class II and III protons can rapidly exchange with the solvent, leaving only Class IV protons in the protein. When the ^{1}H-NMR spectrum of ferredoxin reconstituted

in D_2O is subtracted from that of the ferredoxin reconstituted in H_2O an area corresponding to 4-6 protons remains and this number is consistent with the five Class IV protons/per molecule ferredoxin Hong and Rabinowitz measure in their T_2O-H_2O exchange experiments.

When we reduce the ferredoxin with methyl viologen, the resonances corresponding to these Class IV protons are either shifted or diminished. The fact that ^{1}H-NMR spectra of the slowly exchangeable proton region of reduced and reoxidized ferredoxins exhibit variable resonances suggests that the reduced protein can exchange 1-4 more protons than the oxidized protein. This observation is also consistent with the T_2O-H_2O exchange data of Hong and Rabinowitz. (In their experiments dithionite-reduced ferredoxin was equilibrated with T_2O and the reduced protein released three or four less T_2O molecules per molecule of protein than the oxidized protein.) Hong and Rabinowitz state that their data is consistent with the hypothesis that the reduced protein has less sites for equilibration with tritium and thus propose that the reduced protein has a more compact conformation. We believe that their data are also consistent with the hypothesis that the reduced protein has a more open conformation. Our hypothesis assumes that the one to four very slowly exchangeable protons (Class IV protons) in the oxidized protein become rapidly exchangeable protons (Class II protons) in the reduced protein and thus cannot be easily measured by the technique of Hong and Rabinowitz. Both interpretations however are tenable and consistent with the hypothesis that the reduced protein and oxidized protein have different conformations.

RAPIDLY EXCHANGEABLE PROTONS:

Phillips has just reported (104) that (unnamed) iron-sulfur proteins dissolved in H_2O, rather than D_2O, show additional contact-shifted resonances. He attributes these to (rapidly) exchangeable protons that are close to the paramagnetic centers. He does not mention whether this protein was oxidized or reduced, but if his measurments apply to reduced C. acidi-urici ferredoxin, then the reduced protein must have an open structure. His results are also consistent with our independent observations, which suggest that some of the very slowly exchangeable protons are also close to the Fe-S clusters.

CENTRAL WATER MOLECULE:

The x-ray crystal structure of oxidized P. aerogenes ferredoxin reveals that a single H_2O molecule is found trapped in the center of the protein molecule 3-5Å from each Fe-S cluster (64). Our data suggest that a H_2O molecule may be similarly trapped in oxidized C. acidi-urici ferredoxin if some of the resonances corresponding to the slowly exchangeable protons can be associated with this single H_2O molecule.

If electron transfer occurs between Fe-S clusters within the ferredoxin, then perhaps this single H_2O molecule (or any rapidly exchangeable H_2O molecules) may serve as a bridging intermediate for such an electron transfer reaction (see General Discussion).

Fig. 35. ^{1}H-NMR of C. acidi-urici ferredoxin (A); reconstituted in D_2O (15° C, 30 mg/ml ferredoxin dissolved in 0.2 M KD_2PO_4-K_2DPO_4 buffer, pD 7.0), and C. acidi-urici apoferredoxin; (B); (20° C, 80 mg/ml apoferredoxin dissolved in 0.2 M KD_2PO_4-K_2DPO_4 buffer, pD 7.8). The apoferredoxin was prepared under reducing conditions to eliminate intramolecular mixed disulfides with 0.05 M Na_2S and dialized anaerobically against 0.05 M KD_2PO_4-K_2DPO_4 pD 7.0 buffer and 0.01 M EDTA. The NMR sample was also anaerobic.

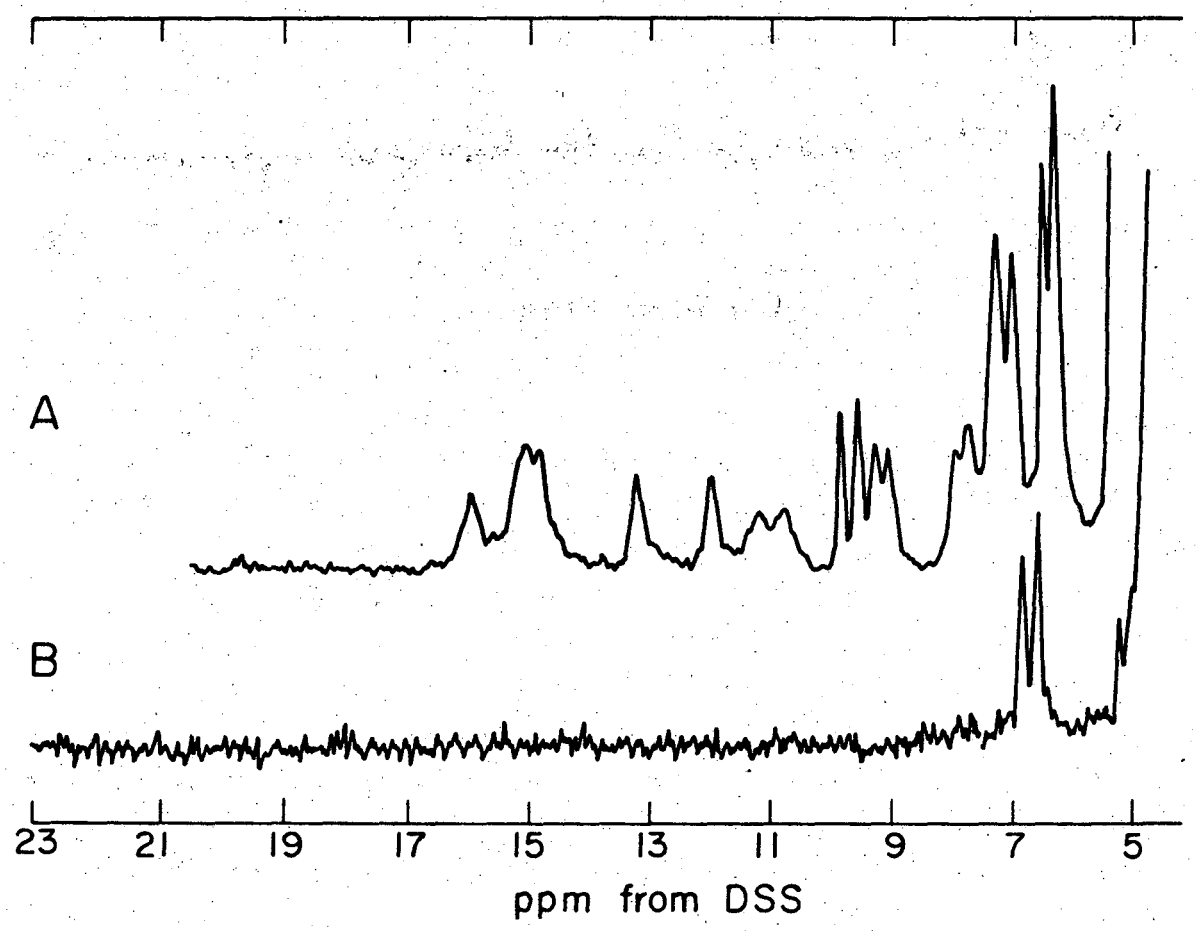
A
B
23
21
19
17
15
13
11
9
7
5
ppm from DSS

Fig. 36. ^{1}H-NMR (15° C) of the exchangeable proton region of C. acidi-urici ferredoxin. (30 mg/ml in 0.2 M KD_2PO_4-K_2DPO_4 buffer, pD 7.0) (A): Reconstituted in D_2O. (B): Reconstituted in H_2O.

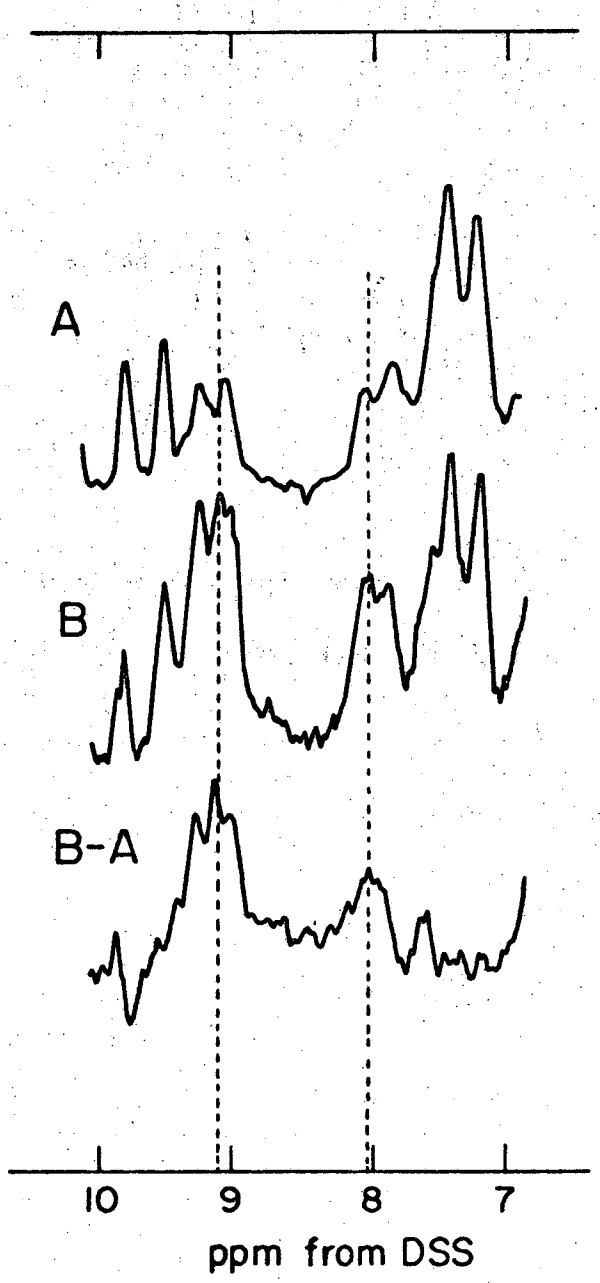
A
B
B-A
10
9
8
7
ppm from DSS

Fig. 37. ^{1}H-NMR (15°C) of oxidized C. acidi-urici ferredoxin. (A): Reconstituted in H_2O. (B): Reconstituted in D_2O. Conditions as in Fig. 36.

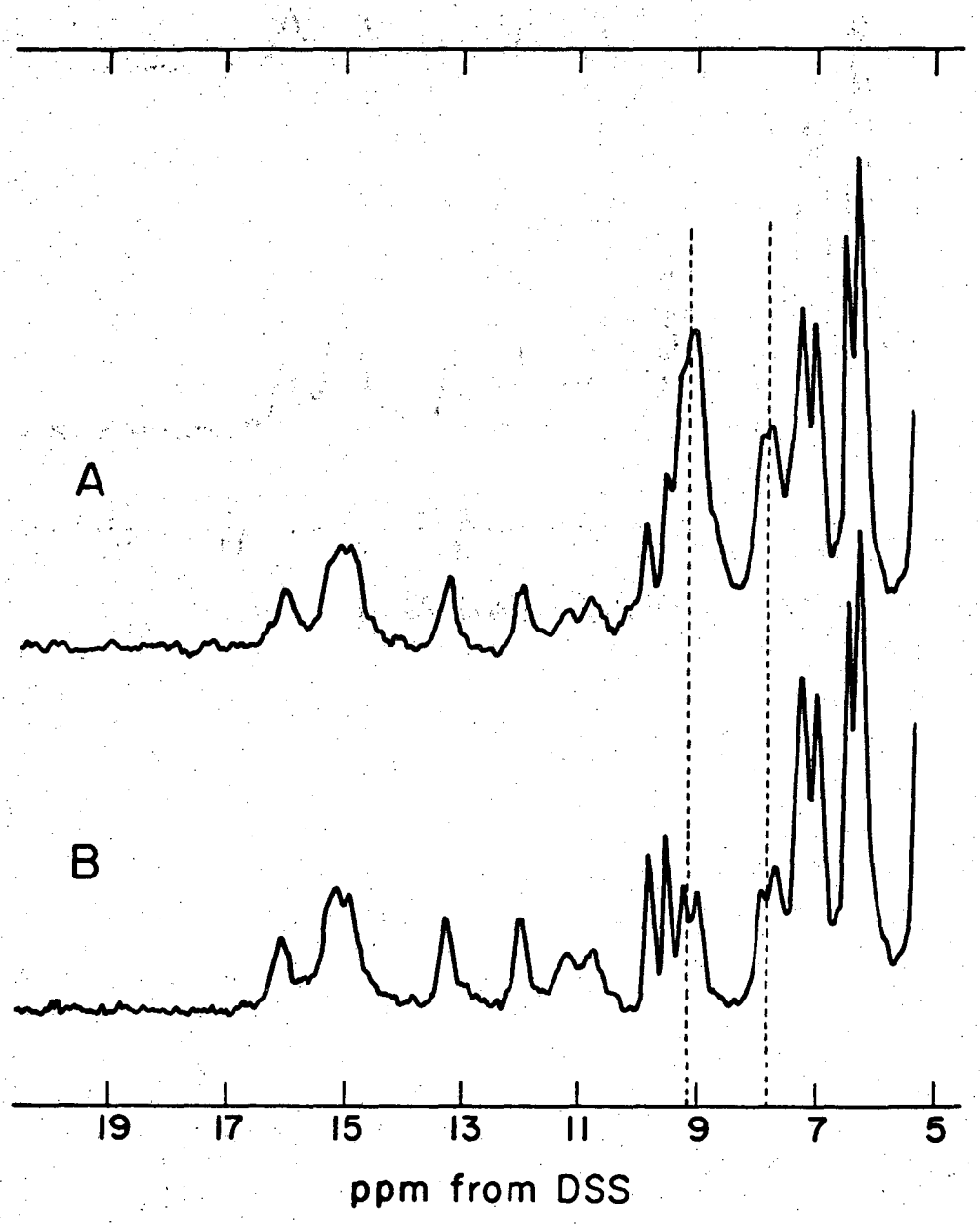
A
B
19
17
15
13
11
9
7
5
ppm from DSS

Fig. 38. ^{1}H-NMR (15° C) of the aromatic and exchangeable proton region of H_2O- and D_2O-reconstituted oxidized and reduced C. acidi-urici ferredoxins. (A): Oxidized, reconstituted in H_2O. (B): Oxidized, reconstituted in D_2O. (C): 6% reduced, reconstituted in H_2O. (D): 24% reduced, reconstituted in H_2O. (E): 45% reduced, reconstituted in D_2O.

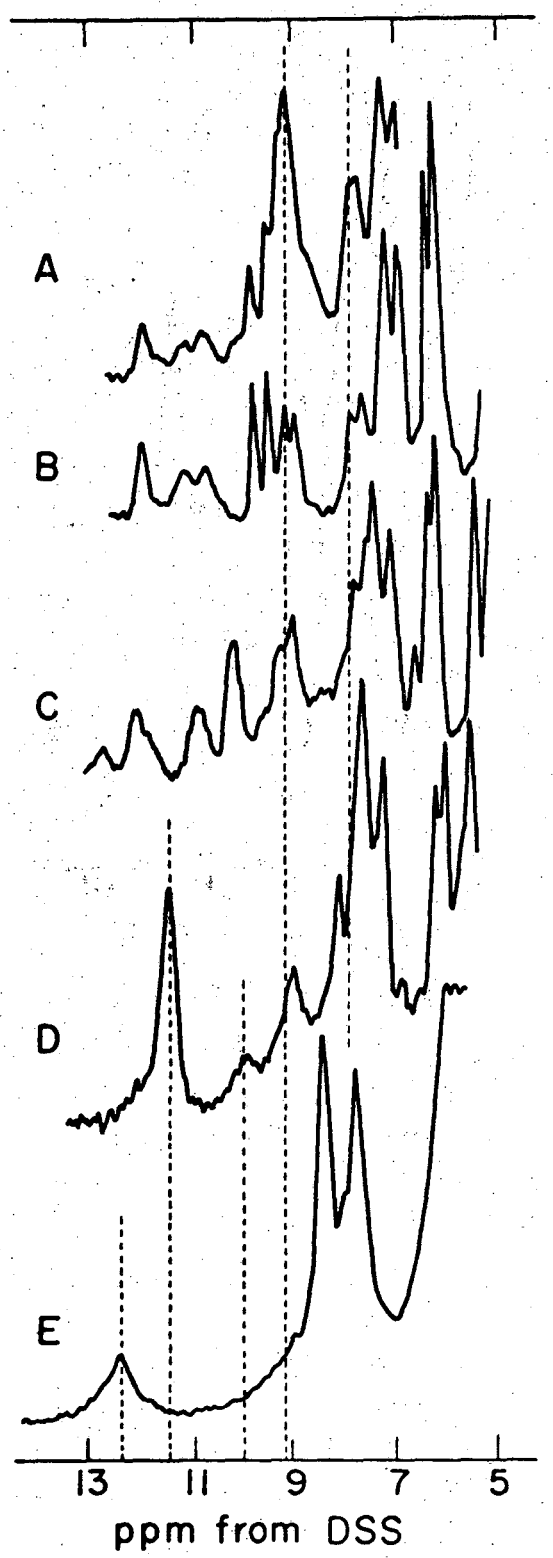
A
B
C
D
E
13
11
9
7
5
ppm from DSS

Fig. 39. ^{1}H-NMR (15° C) of the aromatic and exchangeable proton region of oxidized and methyl viologen-reduced *C. acidi-urici* ferredoxin. (A): Oxidized, reconstituted in H_2O. (B): 20% reduced, reconstituted in H_2O. (C): Re-oxidized *B.*, reconstituted in H_2O (methyl viologen was removed by a Sephadex G-75 desalting column). (D): Oxidized reconstituted in D_2O.

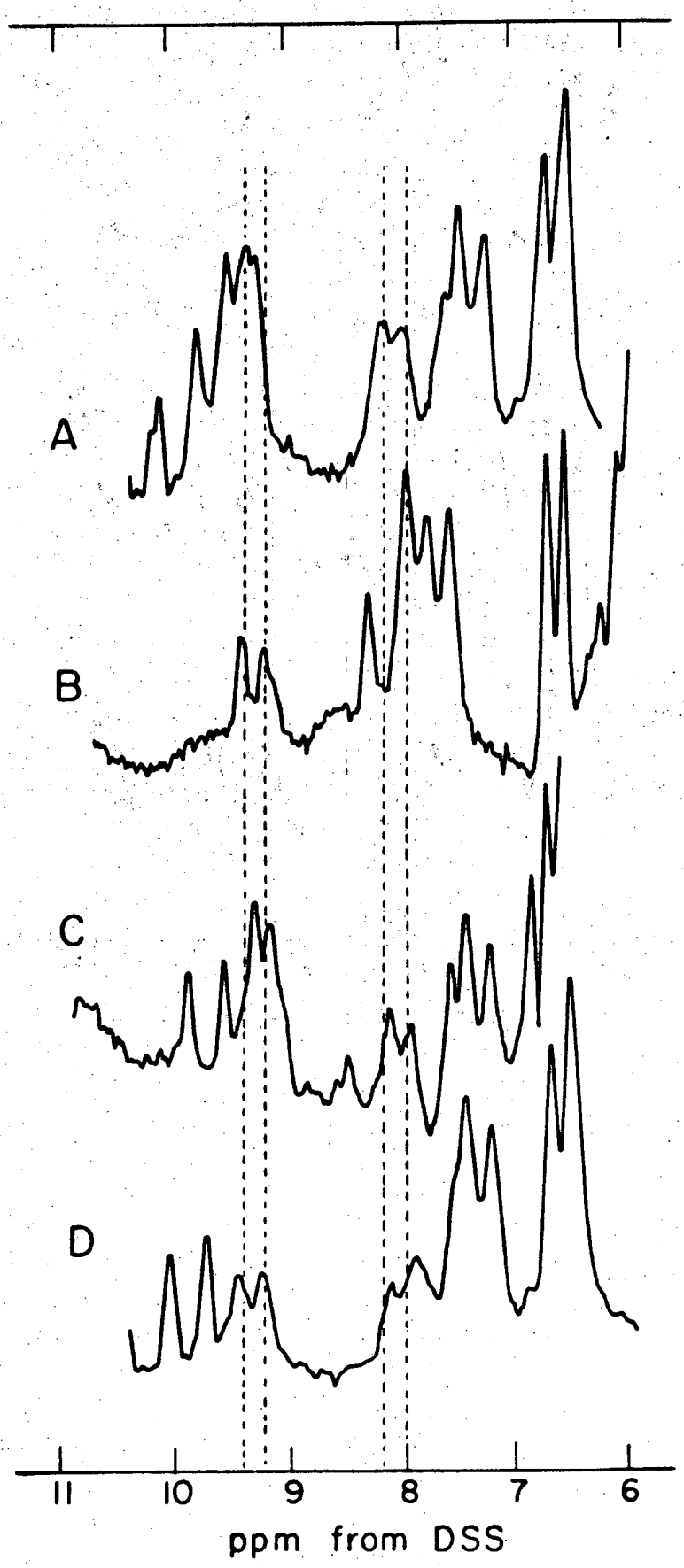
A
B
C
D
11
10
9
8
7
6
ppm from DSS

Fig. 40. ^{1}H-NMR (15° C) of oxidized and methyl viologen-reduced C. acidi-urici ferredoxins (reconstituted in H_2O). (A): Oxidized. (B): 5% Reduced. (C): 6.3% Reduced. (D): 20% Reduced. (E): 24% Reduced.

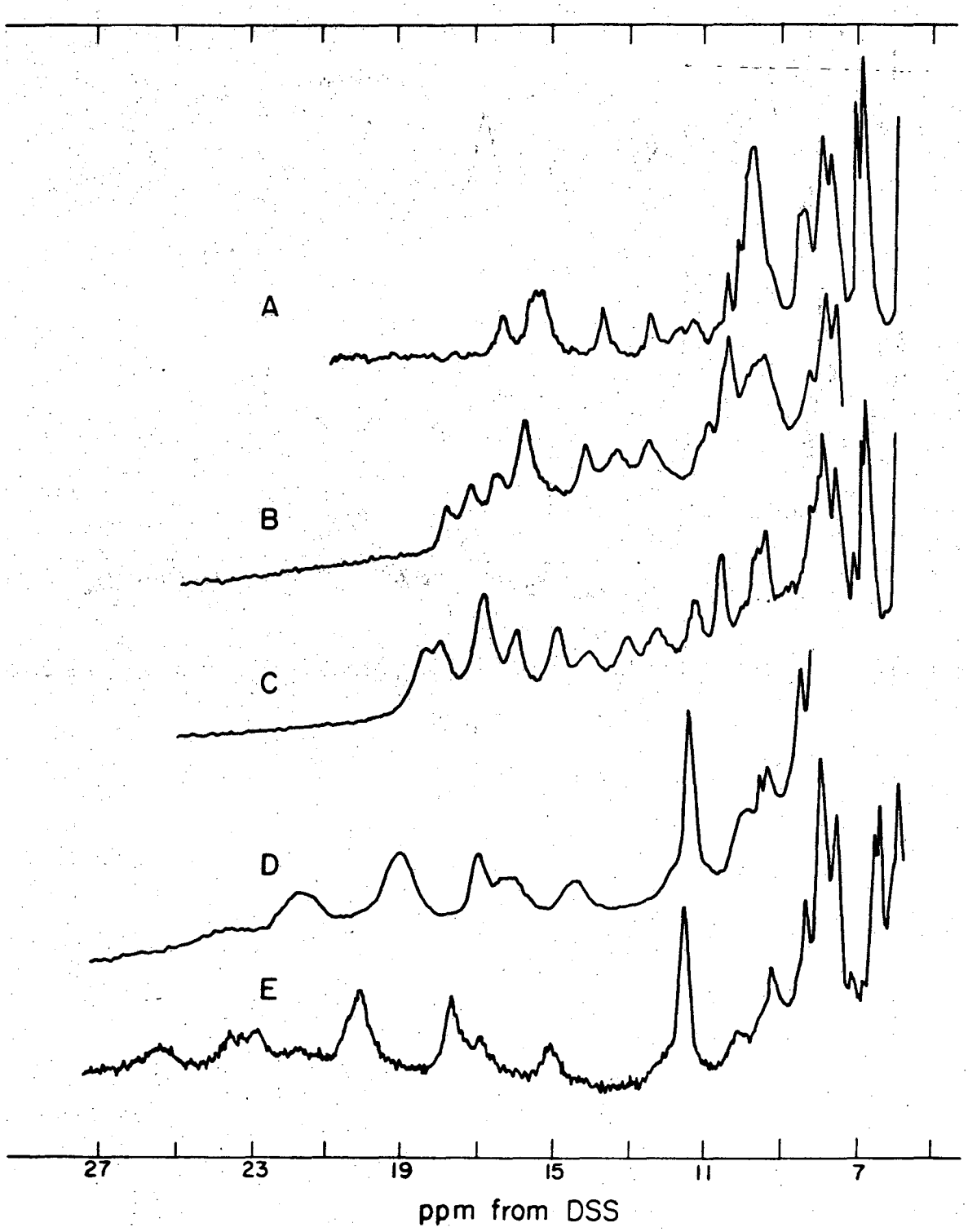
A
B
C
D
E
27
23
19
15
11
7
ppm from DSS

Fig. 41. ^{1}H-NMR (15° C) of oxidized and methyl viologen-reduced C. acidi-urici ferredoxins (reconstituted in H_2O). (F): 30% Reduced. (G): 35% Reduced. (H): 40% Reduced. (I): 50% Reduced.

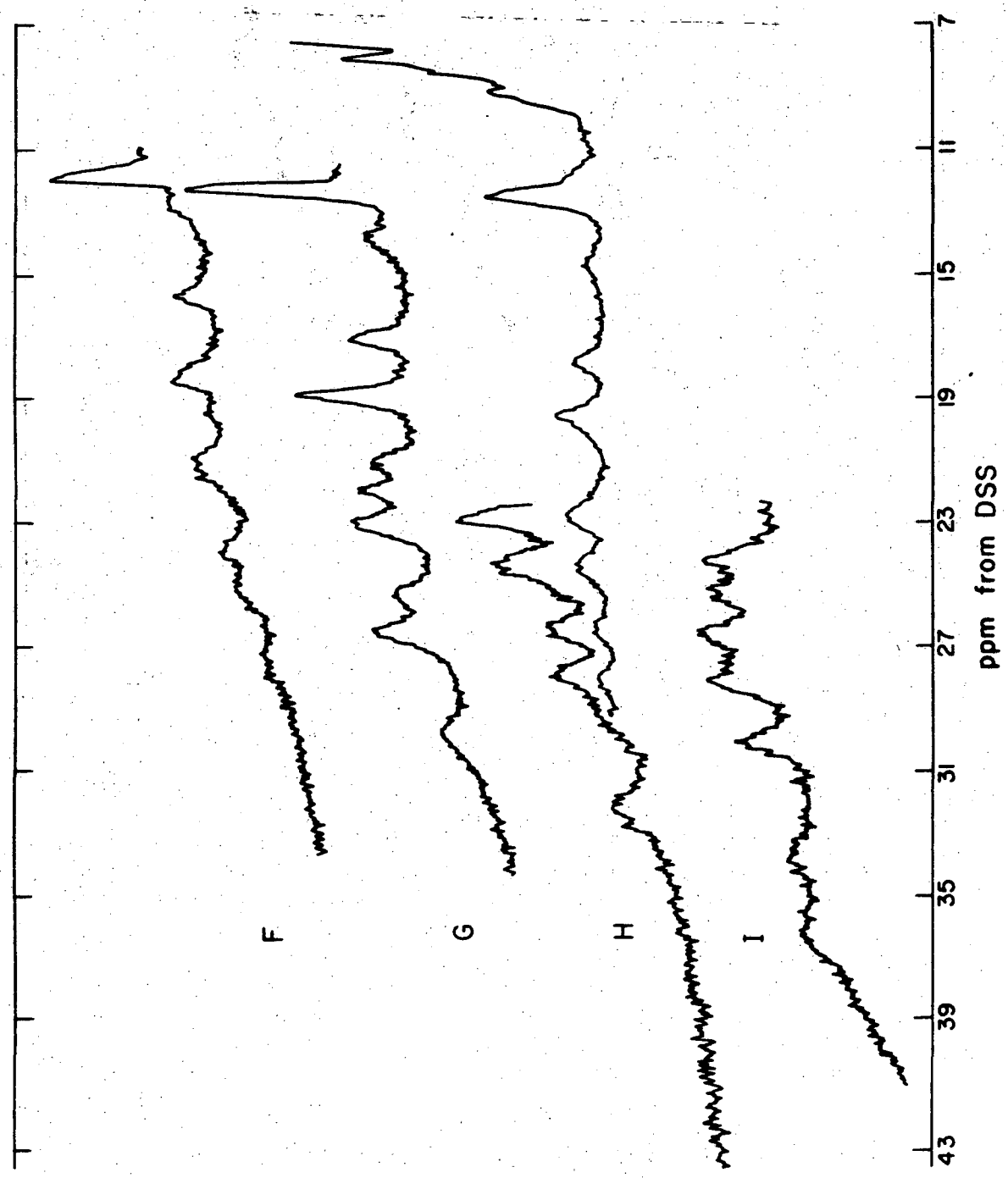
F
G
H
I
7
11
15
19
23
27
31
35
39
43
ppm from DSS

Fig. 42. ^{1}H-NMR (15°C) spectra of methyl viologen-reduced C. acidi-urici ferredoxins. (A): 40% Reduced ferredoxin (reconstituted in H_2O). (B): 45% Reduced ferredoxin (reconstituted in D_2O). (C): 50% Reduced ferredoxin (reconstituted in H_2O). Arrows point to the possible missing resonances.

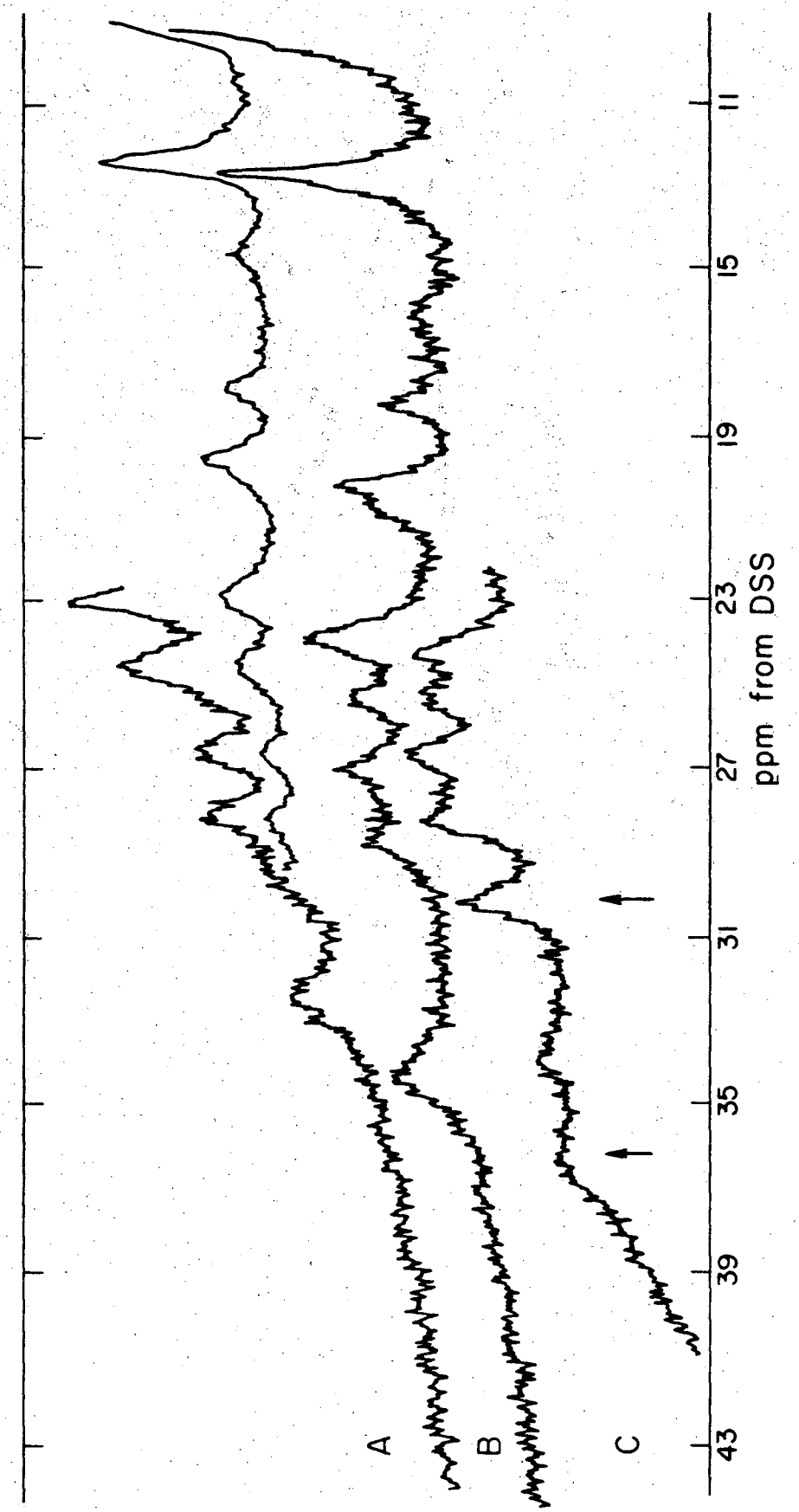
A
B
C
11
15
19
23
27
31
35
39
43
ppm from DSS

Fig. 43. ^{1}H-NMR spectrum of dithionite-reduced C. acidiurici ferredoxin as published in reference (111) (A) and as determined by Phillips on ferredoxin supplied by the author (3). The ferredoxin is assumed to be fully reduced (see text).

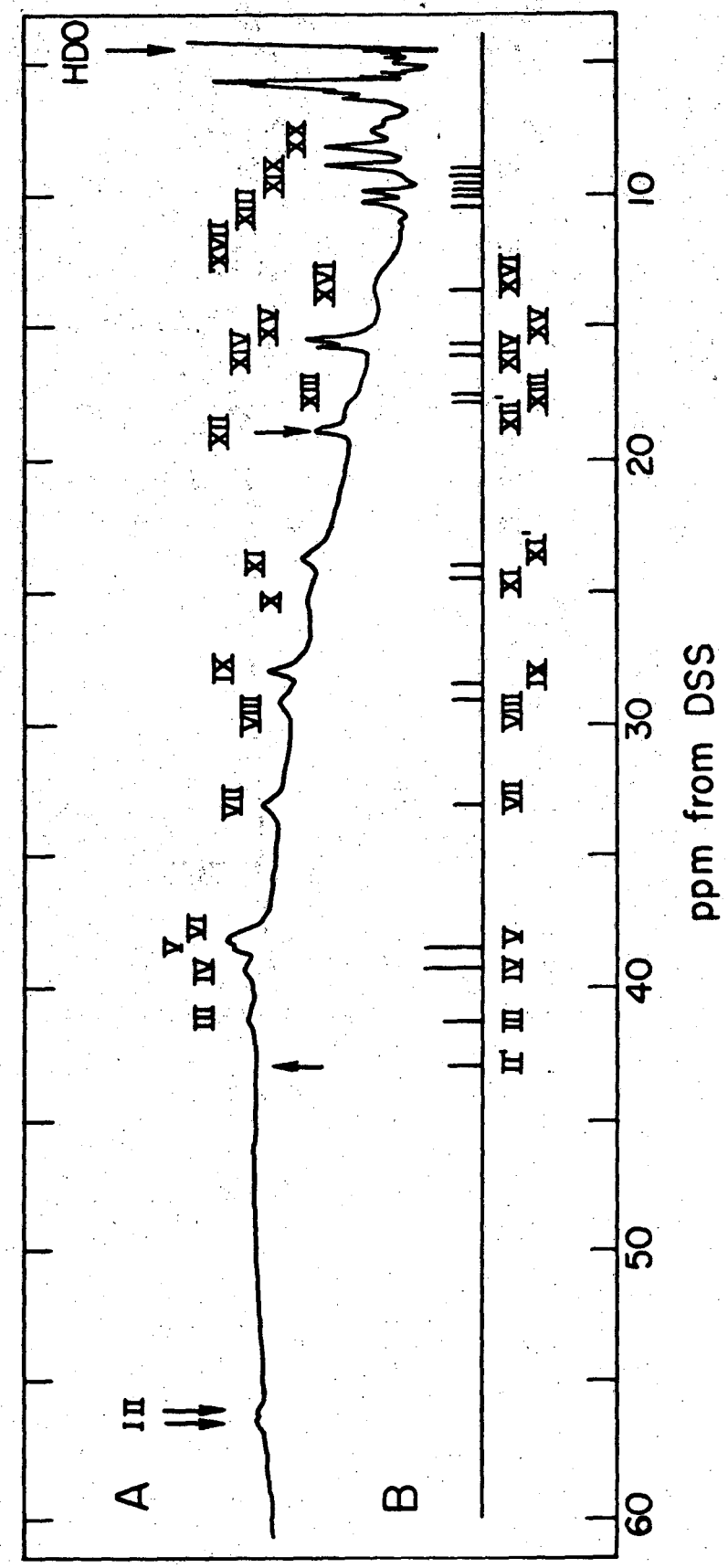
HDO
A
B
II
III
IV
V
VI
VII
VIII
IX
X
XI
XII
XIII
XIV
XV
XVI
XVII
XIII
XIX
XX
II'
XI'
10
20
30
40
50
60
ppm from DSS

Table 12. ^{1}H-NMR (15° C) of methyl viologen-reduced *C. acidi-urici* ferredoxins.

Spectrum (Figs. 40 and 41)	Most downfield shifted resonances (ppm)[a]	Shifts (reduced-oxidized) (ppm)	Degree of reduction[b] (%)
A	16.0	-	0
B	18.0	2.0	5
C	18.5	2.5	6
D	24.0	8.0	20
E	25.5	9.5	24
F	28.0	12.0	30
G	30.0	14.0	35
H	32.5	16.5	40
I	36.0	20.0	50

a. Shifts ± 0.5 ppm relative to DSS.

b. Degree of reduction calculated from the shift of the most downfield-shifted resonance of the dithionite-reduced *C. acidi-urici* ferredoxin relative to the most downfield shift in the oxidized protein (See Experiment 7b).

Table 13. ^{1}H-NMR (22° C) of dithionite-reduced *C. acidi-urici* ferredoxin reported by Phillips.

Peak (Fig. 43)	Number of Protons[a] (Fig. 43A)	Shift (ppm)[b]	Number of Protons[c] (Fig. 43B)	Shift (ppm)[b]
I	1	56.4	-	-
II	1	56.0	-	-
II'[d]	-	-	1	43.0
III	1	41.2	1	41.3
IV	1	39.4	2	39.3
V	1	38.6	1	38.5
VI	1	38.3	-	-
VII	1	33.3	1	33.1
VIII	1	29.4	1	29.0
IX	1	28.3	1	28.4
X	1	25.6	-	-
XI	1	24.1	1	24.5
XI'[d]	-	-	1	23.9
XII	1	19.3	-	-
XII'[d]	-	-	1	18.8
XIII	1	18.5	1	18.7
XIV	1	16.1	1	15.9
XV	1	15.9	1	15.4
XVI	1	13.7	1	13.5
XVII	1	10.8	-[e]	10.3
XVII'[d]	-	-	-[e]	10.0
XVIII	1	10.2	-[e]	9.8
XIX	2	9.3	-[e]	9.4
XIX'[d]	-	-	-[e]	9.1
XX	2	8.6	-[e]	8.8

a. Integrated area estimated by the author.

b. Shift ± 0.5 ppm relative to DSS.

c. Estimated by Phillips (111).

d. Present in ref. (111) only.

e. The number of protons in this region was considered variable by Phillips (111).

Section 4. ^{13}C-NMR Experiments

Experiment 7a.

^{13}C-NMR of the aromatic residues of *Clostridium acidi-urici* ferredoxin.

SUMMARY:

The ^{13}C-resonances of the 1' - and 2', 6' - ring carbon atoms of both tyrosyl residues of *C. acidi-urici* ferredoxin are shifted downfield in the oxidized and reduced protein relative to their resonance positions in *C. acidi-urici* apoferredoxin. Upon reduction the magnitude of these shifts increases. The resonances of the 3',5' - and 4' - carbons, which are unshifted in the oxidized protein, are significantly shifted in the reduced protein. These resonance shifts indicate that both tyrosyl residues in the oxidized and reduced protein are in magnetically equivalent environments, and suggest that both tyrosyl residues are close to the two iron-sulfur (Fe-S) clusters in the reduced and oxidized proteins, and that each cluster is equally accessible to one reducing electron. The observed shifts can be explained by a pseudocontact mechanism only if each tyrosyl residue is in a special symmetric orientation, or a Fermi-contact mechanism if there is electron delocalization from the Fe-S cluster to produce spin density in the tyrosine ring, or both.

INTRODUCTION:

C. acidi-urici ferredoxin was used for this study of the role of aromatic residues in electron transport because this protein contains two tyrosyl residues and its amino acid sequence is known (117). Recently Jensen and coworkers (2) have reported the 2.5 Å resolution x-ray structure of oxidized *Peptococcus aerogenes* ferredoxin. This ferredoxin

also contains two tyrosyl residues and has an amino acid sequence similar to that of C. acidi-urici ferredoxin (134). The x-ray structure reveals that each tyrosyl residue is similarly oriented with respect to each Fe-S cluster in the oxidized protein. Each of the two tyrosine residues is close to one Fe-S cluster and is approximately parallel to a face of the Fe-S cluster. The tyrosine rings are approximately 4 Å from the cube-like cluster face. The two cluster centers are 12 Å apart.

The fact that both tyrosyl residues in oxidized P. aerogenes ferredoxin have a similar orientation with respect to the Fe-S cluster suggests that this orientation is important to the structure or function of the protein, of both.

METHODS AND MATERIALS:

C. acidi-urici was grown and the NMR samples were prepared according to previously described procedures. C. acidi-urici ferredoxin was reduced by Zn-reduced methyl viologen because reduced methyl viologen is a stable free radical (87), and fast electron exchange between equilibrium mixtures of oxidized and reduced methyl viologen produces broad and shifted methyl viologen resonances which do not interfere with magnetic resonance measurements of the reduced ferredoxin. ESR and ^{1}H-NMR measurements of reduced and reoxidized ferredoxin show that methyl viologen reduction does not detectably denature ferredoxin (96).

RESULTS:

^{13}C-NMR of oxidized and reduced C. acidi-urici ferredoxin (Fig. 44A and 44B respectively) and C. acidi-urici apoferredoxin (Fig. 44C) show

significant differences in the resonances of the carbonyl, aliphatic, and aromatic regions, but this experiment will only discuss the resonances in the aromatic region. The proton-decoupled and proton-coupled ^{13}C-NMR spectra of the aromatic region of C. acidi-urici apoferredoxin is different from that of oxidized holoferredoxin (Fig. 45). The resonances at 38 and 77 ppm occur in the spectrum of apoferredoxin (Fig. 45A) and oxidized holoferredoxin (Fig. 45B), but the resonances at 64.9 and 62.2 ppm in the apoferredoxin spectrum do not appear in these positions in the spectrum (Fig. 45B) of the oxidized holoferredoxin. In the oxidized protein spectrum, however, three new resonances occur at 58.8, 59.5, and 60.4 ppm.

ASSIGNMENT OF RING CARBON RESONANCES:

OXIDIZED FERREDOXIN: Ring carbon resoances are assigned (identified) through the use of reference compounds and resonance-decoupling techniques. In Table 14 the ring carbon resonance positions of reference compounds, which consist of model polypeptides and C. acidi-urici apoferredoxin, are listed. If a ring carbon resonance in the spectrum of a ferredoxin occurs at the same position in the spectrum of a reference compound, it is initially assigned this resonance position and is designated an unshifted resonance.

The assignment is then checked by on-and-off proton resonance decoupling techniques (128). In proton-coupled ^{13}C-NMR spectra, the number of protons (n) bonded to a carbon atom split the carbon resonance into (n + 1) resonances, while carbons that are not bonded to protons remain as single resonances. The effect of protons on carbon resonances can be removed, or decoupled, by saturating all the proton resonances with an applied magnetic field, giving rise to a proton-(noise-)

decoupled ^{13}C-NMR spectrum, in which all carbon resonances appear as singlets. By comparing proton-coupled with proton-decoupled spectra, carbon resonance assignments can be checked.

For example, the two resonances at 58.8 and 59.5 ppm in the proton-decoupled ^{13}C-NMR spectrum (Fig. 45B) are assigned to the 1'- ring carbons because they are not split in the proton-coupled spectrum (Fig. 45C). (In this proton-coupled spectrum (Fig. 45C) the 1'- ring carbon resonances are seen as one unresolved resonance at 59.2 ppm, the average position of the two narrow 1'- carbon resonances in the proton-coupled spectra).

The resonance at 60.4 ppm in the proton-decoupled spectrum (Fig. 45B) collapses into a doublet* in the proton-coupled spectrum (Fig. 45C). This is assigned to the 2',6'- tyrosyl ring carbons because the doublet is centered about the original (decoupled) resonance (Fig. 45B).

The same techniques are used to confirm the positions of the unshifted 3',5'- and 4'- carbon resonances. (The single resonance at 36.1 ppm in Fig. 45B and 45C corresponds to the ϵ-carbon of the single arginyl residue in ferredoxin. Its position is unshifted from that of the free amino acid.)

A further check of resonance assignments is provided by consideration of the observed resonance line widths and intensities. The intensity and integrated area of the resonance is proportional to the number of carbons

*The J-coupling, the separation in Hertz between the two doublet resonances, observed for this doublet is also characteristic of ring carbon atoms (74).

it represents, and the line widths of resonances of carbons, not bonded to protons tend to be narrower than the resonances of carbons bonded to protons.

REDUCED FERREDOXIN: Figure 46 shows the aromatic region of oxidized and methyl viologen-reduced ferredoxin under various conditions of proton decoupling. In both oxidized (Fig. 46A) and reduced (Fig. 46D, E) ferredoxin the 1'- and 2', 6'-ring carbon resonances experience a large shift relative to the resonances of these carbons in diamagnetic reference compounds such as N-acetyltyrosine (Fig. 46F, G) or C. acidi-urici apoferredoxin (Fig. 44A).

SIMILAR MAGNETIC ENVIRONMENTS: Both tyrosyl residues are represented in the ^{13}C-NMR spectra of oxidized ferredoxin. This can be seen in Fig. 44B, in which two 1'- and two 4'- carbon resonances are visible. It can be concluded that the 1'- ring carbons are in similar magnetic environments because the 1'- carbon resonances are separated by only 0.7 ± 0.15 ppm in the oxidized and reduced proteins (Figs. 44, 47). Similarly, the 4'- ring carbon resonances, separated by only 0.4 ± 0.15 ppm, indicate that the 4'- ring carbons are in similar magnetic environments.

Further evidence that both tyrosyl residues are represented in the ^{13}C-NMR spectra of oxidized and reduced ferredoxin and are in similar magnetic environments comes from ^{1}H-NMR studies of oxidized and reduced ferredoxin containing [3', 5' -$^{2}H_2$]tyrosyl residues (See Experiment 2). If the ^{13}C-NMR spectrum of C. acidi-urici ferredoxin

(e.g., Fig. 45B) had shown the ring carbon resonances of only one tyrosyl residue, then one would have to conclude that the ring carbon resonances of the other tyrosyl residue were so dramatically broadened or shifted that they completely disappeared from the aromatic region of spectrum. The same would be true for the corresponding ring protons in a ^{1}H-NMR spectrum. To assign the tyrosyl ring protons resonances, the ^{1}H-NMR spectrum of oxidized C. acidi-urici [[3', 5' - $^{2}H_2$] Tyr] - ferredoxin (see Experiment 2) was compared with that of normal ferredoxin (Fig. 16, Experiment 2). This comparison showed that an area corresponding to four protons was missing from the aromatic region in the ^{1}H-MNR spectrum of [[3', 5' - $^{2}H_2$] Tyr]-ferredoxin. If the 3', 5'- proton resonances from one of the tyrosyl residues had been broadened or shifted out of the aromatic region, a resonance having an area corresponding to only two protons would have been missing from the spectrum.

An area corresponding to four protons was also missing from reduced [[3', 5' -$^{2}H_2$] Tyr] -ferredoxin (Fig. 17 Experiment 2). Thus these results confirm that both tyrosyl residues are represented in the ^{13}C- and ^{1}H-NMR spectra.

SYMMETRY ABOUT 1', 4'- RING CARBON AXIS: The carbon resonances of each half of each tyrosyl ring were observed to have essentially identical magnetic shifts but the proton resonances experience relatively small shifts (Table 15). The ring proton resonance shifts were determined by double resonance experiments which involve coherent proton decoupling techniques. These techniques are used to determine the resonance frequency of a proton bonded to a particular carbon. In a coherently decoupled spectrum all the carbons that are bonded to protons which have resonance frequencies of the applied coherent pulse

frequency will show collapsed multiplet structures. Thus, only carbons not bonded to protons or carbons bonded to protons which resonate at the coherent pulse frequency will appear as single resonances. For example, the 2', 6'- ring proton position in apoferredoxin was assumed to be within 0.5 ± 0.1 ppm of the 3', 5' -ring proton position (119) (See Experiment 2), and then a coherent pulse frequency, corresponding to the proton resonance position midway between the 3', 5' - and 2', 6' - proton resonances, was applied. Since the error of the pulse frequency is ± 0.5 ppm, this pulse should decouple both the 2', 6' - and 3', 5' - ring protons if the 3', 5'- and 2', 6' -proton resonances in the oxidized or reduced ferredoxins are not shifted (± 0.5 ppm) from their positions in apoferredoxin.

When one saturates the 2', 6' - and 3', 5' -ring protons with this coherent frequency, the two carbon resonances at 60.4 and 77.4 ppm in the oxidized protein (Fig. 46B) remain as single uncollapsed resonances. These resonances thus correspond to the 2', 6' - and 3', 5' -ring carbons respectively.

In the ~ 8% reduced ferredoxin spectra (Fig. 47), when one applies a coherent frequency that is just a little above or below the bonded proton resonance frequency, these ring carbon resonances will split into doublets. The separation of these doublets will increase the further the applied coherent proton frequency is from the proton resonance of the bonded proton. Thus, if the 2', 6-ring proton resonance is shifted as much as the 2', 6' -ring carbon resonance is in reduced ferredoxin (e. g., 7 ppm in Fig. 46D), applying a coherent pulse at the ring proton resonance frequency of the free amino acid (unshifted) position should cause the 2', 6' -carbon resonance

to split into a doublet. This splitting was not observed because in the (~ 38%) reduced ferredoxin spectrum (Fig. 56D) the 2', 6'-ring proton resonance is not shifted 7 ppm from its free amino acid position.

These results suggest that:

(i) the two tyrosyl rings of oxidized and reduced C. acidi-urici ferredoxin are equivalently oriented with respect to their neighboring Fe-S cluster, since both tyrosyl residues experience the same magnetic perturbations. This is consistent with the x-ray structure of oxidized P. aerogenes ferredoxin (64);

(ii) the magnetic perturbation produced by the Fe-S cluster is symmetric about the 1', 4' - ring carbon axis, and the magnitude of this perturbation is larger for the 1' - and 2', 6' - carbons than for the 3', 5'- and 4'-carbons in both the oxidized and reduced ferredoxins. (In P. aerogenes ferredoxin the 1' - and 2', 6' - tyrosyl carbons are closer to the Fe-S cluster than are the 3', 5'- and 4'- tyrosyl carbons (64);

(iii) the proton resonance positions remain essentially unshifted from their positions in free tyrosine;

(iv) in our most reduced ferredoxin samples (Fig. 46D) each ferredoxin molecule has approximately one reducing electron yet both tyrosyl residues are perturbed equivalently. This produces an averaged ^{13}C spectrum.

Double resonance techniques can also be used to determine the resonance positions of the protons bonded to specific ring carbons (128). Comparison of the noise decoupled ^{13}C-NMR spectrum (Fig. 47A) of the aromatic region of (8±2)% reduced C. acidi-urici ferredoxin with the proton coupled spectrum of this ferredoxin (Fig. 47E) shows that

the resonances at 58.8 and 77.1 ppm correspond to the 2',6'- and 3',5'- ring carbon atoms respectively, since the single resonances at 58.8 and 77.1 ppm in Fig. 47A are split into doublets in Fig. 47E. When one applies a coherent pulse which specifically decouples the 3',5'-proton resonances (at ~ 7.0 ppm from DSS (Fig. 47B)), then the 2',6'- ^{13}C resonance just begins to split. Thus the 3',5'-proton resonance is closer to 7 ppm (from DSS) than is the 2',6'-proton resonance. From the magnitudes of the splittings (J_r) of these doublets, one can calculate the proton resonance positions from the relation (128):

$$\Delta f = \frac{J_r}{J} F$$

where

Δf = the separation (in Hertz) of the proton resonance from the applied decoupling frequency

J_r = magnitude of residual splitting (Hz).

J = ^{13}C-H coupling constant (160 Hz for aromatic carbon atoms).

F = decoupling field strength (560 Hz for our experiments).

From the data presented in Fig. 47, we conclude that in (8±2)% reduced C. acidi-urici ferredoxin the 3',5'- and 2',6'- ring proton resonances (of both tyrosyl residues) are shifted +(0.2±0.1) ppm and -(0.7±0.5) ppm from their positions in apoferredoxin (Table 15). (Positive shifts are upfield shifts relative to the apoferredoxin resonances.) Thus in reduced C. acidi-urici ferredoxin (as in the oxidized ferredoxin) the resonances of protons bonded to ring carbons are shifted 5-10 times less than that of the corresponding ring carbon resonances. These proton

shifts are also symmetric about the 1',4'- ring carbon axis and are essentially equal for both aromatic residues (see Experiment 7b).

TWO STATE HYPOTHESIS: Oxidized ferredoxin is characterized by certain ring carbon shifts (Table 15). If we assume that the fully reduced ferredoxin is characterized by a different set of ring carbon shifts then any shifts that are intermediate between the oxidized and fully reduced shifts represent a mixture of oxidized and reduced proteins. This is because the electron is exchanging between the oxidized and reduced forms of the protein at a rate faster than the NMR time scale (112). From this we assume that the magnitude of the shifts increases linearly with the degree of reduction. This assumption is supported by an independent measurement of ^{1}H-NMR shifts of aliquots of partially reduced ferredoxin samples used for ^{13}C-NMR experiments. The ^{1}H-MNR spectra (see Experiment 6b) of partially reduced ferredoxin showed many shifted proton resonances. The most shifted proton resonance in the methyl viologen-reduced ^{13}C-NMR samples was never shifted as much as that reported by Phillips and coworkers for dithionite-reduced C. acidi-urici ferredoxin (111). If we assume that the most shifted proton resonance seen by Phillips represents a fully reduced ferredoxin, the degree of reduction can be calculated from the most downfield-shifted proton resonance position of the reduced ferredoxin samples used for the ^{13}C-NMR measurements, since the magnitude of the most downfield-shifted aliphatic proton shift increases linearly with the magnitude of each ring carbon shift of the tyrosyl residues in C. acidi-urici ferredoxin (See Experiment 7b). (The mechanism that produces the magnetic shifts is probably different for

aliphatic protons and aromatic carbons because they have different absolute magnitudes.) The simplest explanation for this correlation is that the intermediate shifts represent intermediate reduction in a two-state system, i.e., the shifts for protons and carbons is a linear function of the degree of reduction (see Experiment 7b).

The fact that the tyrosyl ring carbon resonance shifts increase monotonically with increasing reduction indicates that in the reduced protein the reducing electron is exchanging between clusters at a rate > 10,000 sec^{-1} at 10°C. This exchange rate is a low estimate (112) and is based on the fact that the 2', 6' - carbon resonance shift increases with increasing reduction, and that the linewidth of the 2', 6' -carbon resonance in the reduced ferredoxin (Fig. 46D) is less than the estimated frequency difference between the positions of the 2', 6' -carbon resonances of the oxidized and reduced proteins. Intra- and intermolecular electron exchange between reduced and oxidized Fe-S clusters cannot be distinguished at present (See General Discussion).

The fact that the ring carbon shifts increase linearly with reduction also facilitates the assignment of ring carbon resonances at different degrees of reduction.

DISCUSSION:

PARAMAGNETIC SHIFTS:

In diamagnetic proteins (proteins which contain no unpaired electrons), carbon and proton resonance diamagnetic shifts are the result of changes in protein conformation and local pH or charge variations (119). In the ferredoxins, there are also paramagnetic shifts that are caused by magnetic interactions between a specific proton or carbon nucleus and an

unpaired electron. These paramaanetic shifts fall into two classes (105): (i) Fermi-contact shifts, which are produced by interactions that proceed through orbitals and require that electron spin density be non-zero at the perturbed nucleus and (ii) Pseudo-contact shifts, which are produced by direction interactions through space, are the result of an electron spin-nuclear spin dipolar interaction and a nuclear spin-electron orbital interaction or both. The magnitude of pseudocontact shifts depends on the geometrical orientation of the perturbed nucleus and the unpaired electron. The diamagnetic and paramagnetic shift mechanisms need not be independent of each other since protein conformational changes, for example, can influence paramagnetic shifts in paramagnetic proteins.

RING CARBON RESONANCE SHIFTS: Paramagnetic shifts are usually distinguished from diamagnetic shifts by the strong, 1/T, temperature dependence of paramagnetic shifts. But the ring carbon resonance shifts in reduced and oxidized ferredoxin are not expected to show a large (detectable) temperature dependence of the type observed for aliphatic proton resonance shifts of ferredoxins (106). (Phillips and coworkers (111) report $\leq$ 0.02 ppm proton resonance shifts per degree C and $\leq$ 0.05 ppm shifts per degree C for oxidized and reduced C. acidi-urici ferredoxin, respectively.) The linewidths of the 2', 6'-carbon resonances, for example, are greater than the maximum calculated temperature shift of 0.5 ppm expected for ring carbon resonances of the oxidized and reduced proteins between 8-20° C (Fig. 1, reference 97).

The large shift in the 2', 6'- tyrosyl ring carbon atoms in oxidized C. acidi-urici ferredoxin can only be explained by a paramagnetic

mechanism because only the 2',6'- carbon resonances in the tyrosyl ring are significantly shifted in oxidized ferredoxin, while the 2',6'-ring carbon resonances in N-acetyltyrosine and Gly-Gly-Tyr-Gly-Gly are not shifted over the pH range 1-14 (52). Thus, there is no local pH effect producing the observed shifts. Protein conformational changes would be expected to perturb proton resonances more than the corresponding carbon resonances; the opposite effect is observed for the tyrosyl residues in ferredoxin.

WEAK CHEMICAL BOND: If the interaction of the aromatic residues and Fe-S complex is important to the structure and function of bacterial ferredoxin it would be of interest to know whether the interaction is only electrostatic or involves a weak chemical bond. Demonstration of a Fermi-contact interaction producing a magnetic shift of the aromatic nuclei would implicate a chemical bond. By unravelling the contribution from each paramagnetic shift mechanism one could determine: (i) the extent that the interaction of the aromatic residues with the Fe-S complex* is needed for protein stability and function; (ii) which energetic factors stabilize the alignment of the aromatic residues; and (iii) the extent that the reducing electron is shared by the atoms in each Fe-S complex.

POSSIBLE SHIFT MECHANISMS: The pseudocontact and Fermi-contact models require that each tyrosyl residue be within 4-5 Å from an Fe-S cluster. This occurs in oxidized P. aerogenes ferredoxin (2). The pseudocontact model also requires that each tyrosyl residue be in a special symmetric orientation in the oxidized and reduced protein. This orientation requires that each tyrosyl residue be at a distance and

*The Fe-S complex includes the cysteinyl sulfur atoms.

orientation that gives the same pseudocontact shift for all 2',6'-carbons and essentially no shift for the 2',6'- protons. The 2',6'-carbons could be in equivalent magnetic environments if the tyrosyl rings of C. acidi-urici ferredoxin were rotating about the 1',4'- carbon axis. In this case, the 1',4'- carbon axis of each tyrosyl ring would still have the same distance and orientation to the Fe-S clusters. Since the 2',6'- proton resonances are not shifted, rotation about the 1',4'-carbon axis is not possible if the 2',6'- carbon shifts are caused by a pseudocontact interaction. This is because the pseudocontact interaction depends on R^{-3} where R is the distance between the nucleus and unpaired electron. (105) Furthermore, if the solution structure of C. acidi-urici ferredoxin is the same as the crystal structure of oxidized P. aerogenes ferredoxin, rotation of the tyrosyl ring would be prevented by steric hindrance (64).

Both the pseudocontact and Fermi-contact interactions would explain the ^{13}C-NMR shift data if the orientation of the tyrosyl residues in oxidized ferredoxin is preserved in the reduced ferredoxin. If, however, x-ray studies of the reduced clostridial ferredoxins show that the special symmetric orientation of the tyrosyl residues is not preserved, then only an electron spin delocalization model could explain the observed ^{13}C-tyrosyl ring carbon shifts.

Contact mechanisms: Spin density in the tyrosyl orbitals:

Positive electron spin density can appear in the tyrosyl ring by partial transfer of an electron spin to or from the Fe-S cluster. Table 15 shows the observed carbon and proton shifts for the tyrosyl residues in oxidized and reduced C. acidi-urici ferredoxin. The shifts for the fully reduced

protein were obtained by a linear extrapolation from the observed shift values for lower degrees of reduction. In the oxidized protein the magnitude of the 1'- carbon resonance shift is larger than that of the 2', 6'-carbon, while in the reduced protein the reverse is true. The magnitude of the aromatic ring proton resonance shifts is 5 to 10 times smaller than the corresponding carbon resonance shifts.

In the case of the 3', 5'- nuclei, the 3', 5'- proton and 3', 5'-carbon resonance shifts are of opposite sign. This sign difference is what one expects from spin delocalization from the Fe-S clusters into the tyrosine orbitals. Thus a Fermi-contact model could account for the observed large carbon resonance shifts and relatively small proton resonance shifts (Table 15).

Electron spin delocalization could occur through overlap of the sigma (σ) and pi (π) orbitals of the tyrosyl residue with the 3p and 3d orbitals of the cysteinyl and acid-labile sulfur andiron atoms, respectively. This overlap may result in a small amount of electronic delocalization from the Fe-S cluster into the tyrosyl ring to give an energetically more favorable electronic distribution. The tyrosyl residues are 6 and 7 amino acid residues away from the Fe-S clusters in C. acidi-urici ferredoxin. Delocalization of spin through the sigma (σ)-electron framework from cysteinyl residues through the 5 and 6 intervening amino acids into the tyrosyl residue would not be detected, since a 5-10 fold attenuation in spin density occurs for each intervening σ-bond (33).

In the delocalization model the tyrosyl rings need not be in a symmetric orientation to the Fe-S clusters to account for the observed magnetic

equivalence of each half of each tyrosyl ring in both the oxidized and reduced proteins. Unpaired spin could proceed through the σ-orbitals of the 1'-carbon into the σ-framework of the tyrosyl ring and would show a 2-fold symmetry about the 1' - and 4' -ring carbon axis. σ-delocalization would result in decreasing shifts of the carbon resonances in the order of 1' > 2',6' > 3',5' > 4'. The corresponding proton resonance shifts would follow the same order, but their magnitudes would be 5 to 10 times smaller (33). This is observed (Experiment 7b).

If delocalization occurred into the tyrosyl π-orbitals the resulting unpaired electron spin distribution would also show a 2-fold symmetry in its distribution about the ring. The π-delocalization shift pattern would not be the same as the σ-delocalization pattern.

Reorthogonalization contact mechanism (83)

Unpaired spin density may also appear in the tyrosyl ring because of a reorthogonalization of the tyrosyl and Fe-S cluster orbitals. At large separations the Fe-S orbitals and tyrosyl orbitals are orthogonal; i.e., no overlap occurs. At small separations (< 4 Å) overlap between the Fe-S and tyrosyl orbitals can occur, and these orbitals are no longer orthogonal. A small admixture of molecular orbital occurs, and this restores the orthogonality. This admixture introduces spin into the tyrosyl ring. This can be a nearly isoenergetic process and would involve the σ-orbitals of the tyrosyl residues.

Fermi-contact mechanism (39)

If one assumes that the observed carbon shifts are primarily Fermi-contact in origin and arise from spin transfer into the empty (antibonding) π-orbitals of the tyrosyl ring, one can estimate the ratios of magnetic

shifts relative to the apoferredoxin. These predicted ratios for the Bg, Au_1 and Au_2 π-antibonding orbitals can be compared with the observed ratios (Table 16). The predicted shift patterns are based on the Karplus-Fraenkel equation (68), which relates the carbon hyperfine (Fermi-contact) constants to carbon spin densities. Estimates of electron spin densities used in these predictions were obtained from the ESR literature (19, 136).

We find that there is no agreement between the predicted and observed values. This suggests that mechanisms other than spin transfer into the antibonding π-orbitals of the tyrosyl ring contribute to the observed shifts. A similar conclusion is reached if one also considers the alternative possibility of spin transfer from the filled π-orbitals of the tyrosyl ring into the Fe-S complex (the Fe-S cluster plus the cysteinyl sulfur atoms).

Since the magnetic shift pattern of the carbons observed in oxidized and reduced C. acidi-urici ferredoxin is not characteristic of spin delocalization exclusively into the tyrosyl π-orbital, there must either be appreciable spin delocalization into the σ-orbitals of the tyrosyl residue (in addition to spin delocalization into the π-orbitals) or pseudocontact interactions or combinations of all three processes.

Pseudocontact mechanism

The pseudocontact mechanism is a direct magnetic interaction through space. For this model one assumes that in oxidized clostridial ferredoxins the electron spins of the Fe-S clusters are paired at low temperatures (110) and unpaired by thermal excitation at room temperature; and in the reduced protein the ground state is paramagnetic at all

temperatures. The proton and carbon atoms, however, have nuclear spins which are aligned along the external magnetic field. A dipolar magnetic field is produced at the proton and carbon nuclei by the electron spin and by the orbital motion of the unpaired electrons (71). This dipolar field averages to zero with the tumbling motion of the protein if the electron spins and nuclear spins are both aligned along the external magnetic field. The unpaired electron spins in oxidized and reduced ferredoxin need not be aligned along the direction of the external magnetic field, however, and pseudocontact shift only occurs if the electron and nuclear spins have different alignments, since then the dipolar field does not average to zero at the nuclei.

In C. acidi-urici ferredoxin a pseudocontact shift could occur if the unpaired electron spins of the Fe-S complex are not aligned along the external magnetic field because of $\underset{\sim}{g}$-tensor anisotropy or zero field splitting, or both. (Zero field splitting is the residual splitting of the energy levels of the unpaired electron when there is no applied magnetic field.) Zero field splitting could be produced by a slightly distorted Fe-S complex where the distorted ligands affect the spin-orbital coupling of the unpaired electron (24). $\underset{\sim}{g}$-tensor anisotropy occurs when the effect of the applied magnetic field on the electron spin is anisotropic because of the orientation of this spin (relative to the symmetry axis of the Fe-S clusters).

Pseudocontact ring carbon resonance shifts in C. acidi urici ferredoxin would depend on the geometric and electronic structure of the Fe-S cluster, and the orientation and distance of the tyrosine ring relative to the cluster (98). In the dipole limit (71), the shifts will depend

on R^{-3} and an angular orientation factor. (The dipole limit requires that the unpaired electron spin of the Fe-S cluster be effectively confined to a space of small diameter when compared with the distance ($R \geq 4$ Å) between the proton or carbon nucleus and the unpaired electron spins.)

If the observed 2',6'- carbon shifts are caused by the pseudocontact mechanism and if the tyrosyl residues are far from the Fe-S clusters, one would expect essentially the same magnitude of pseudocontact shifts for the 2',6'- protons as observed for the 2',6'- carbons. If the tyrosyl residues are close to the Fe-S clusters, large differences in the magnitude of the pseudocontact shifts would occur for carbon atoms and their corresponding protons. Under these circumstances only a very special orientation of the tyrosyl ring relative to its nearby Fe-S cluster would make it possible for each half of each tyrosyl ring to be in almost identical magnetic environments and for the ring carbons to experience a relatively large shift while the ring protons experience essentially no shift. It is not clear that such an orientation can physically exist at the presumed separation of ~ 4 Å between the Fe-S face and the tyrosyl ring. (See Table 17).

The magnetic equivalence of each half of each tyrosyl ring suggests that the reducing electron spin is shared by more than one iron atom per cluster (see Experiment 8). This hypothesis is consistent with the molecular orbital description (72) of the Fe-S cluster. It is also consistent with a dipolar (Heisenberg-Dirac-van Vleck) model (72) of the Fe-S cluster which assumes that the Fe atoms are in mixed valence states (57). To be consistent with this latter model, the spin states of each iron atom would be rapidly exchanged in the Fe-S cluster in order

to account for the magnetic equivalence of each half of each tyrosyl ring.

The resonance shifts observed for the 3', 5'- and 4'- ring carbon atoms are smaller than that of the 2', 6'- and 1'-carbon resonances. This is consistent with a pseudocontact mechanism if we assume that these carbon atoms are further away from the Fe-S cluster than are the 2', 6'-carbon atoms in both oxidized and reduced proteins.

Since tritium-hydrogen exchange (60) studies indicate that the conformations of the reduced and oxidized C. acidi-urici ferredoxins differ, the special orientation of the tyrosyl residues must be maintained in both redox states to be consistent with the pseudocontact mechanism, even if the protein changes shape upon reduction. The special orientation of the tyrosyl residues, suggested by the ^{13}C-NMR data, is seen in the oxidized P. aerogenes ferredoxin (2), and this orientation could be stabilized by a type of van der Waals interaction between the Fe-S cluster and the potentially polarizable tyrosyl rings (50).

Calculation of pseudocontact shifts

The observed ring carbon shifts cannot be solely due to pseudocontact shifts if one ignores the zero field splitting terms. (This assumes that the interaction between the unpaired electron and the nucleus can be considered a simple dipole-dipole interaction and the system has axial symmetry--an oversimplification if the carbon nucleus is $\leq$4 Å from the electron and the electron spin is distributed over all of the Fe and S atoms).

The expression for pseudocontact shifts (71) is proportional to differences between g-values, i.e., those parameters which describe the orientation of an electron spin. In clostridial-type ferredoxins (100) $g_{\parallel} = g_{\perp}$ for the oxidized protein and $(g_{\parallel}^2 - g_{\perp}^2)$ is small for the reduced protein (at temperatures <40°K). if we assume this is also true for higher temperatures (283°K) and if one ignores the zero field terms

one would expect no pseudocontact shifts in the oxidized protein, and small pseudocontact shifts in the reduced protein. Furthermore, the calculated ratios of shifts (relative to the oxidized protein) one expects for the different ring carbon atoms and protons in reduced ferredoxin (Table 17), do not correlate with the ratios of the observed shifts. (The range of these calculated ratios we limited by the fact that the shifts have to be symmetric about the 1',4'- ring carbon axis and be positive (i.e., shift upfield) for the 3',5'- proton and 4' -carbon resonances.) In order to resolve this lack of correlation between calculated and observed shifts, one could change ratios by adding the same fixed parameter (e.g., a correction due to zero field splitting) to the numerator and denominator of the shift ratio.

The magnitude of pseudocontact shifts including the zero field terms can be calculated (Table 11) with the limitation of the following assumptions: (i) in oxidized ferredoxin only the first excited spin level, S = 1, significantly contributes to the pseudocontact interaction and does so through the zero field term; (ii) in the reduced protein the ground S = 1/2 spin level contributed to the pseudocontact interaction through its anisotropic $\underset{\sim}{g}$-tensor while the first excited S = 3/2 level contributes through its zero field term.

Kurland and McGarvey (71) have derived equations for the pseudocontact shift assuming an anisotropic $\underset{\sim}{g}$-tensor or a zero field term of both. The zero field term depends on a parameter D. Their derivation is valid for the solid state case in the dipole limit. The solid state case corresponds to one where the electron spin relaxation time is less than the protein rotational correlation time (τ_r), and the anisotropy of the electron

spin energy is much greater than $\hbar\tau_r$ ($\hbar$ is Planck's constant divided by 2π). These conditions are expected to be filfilled for the various spin levels of the Fe-S cluster.

We calculate a range of pseudocontact shifts for various D and $\underset{\sim}{R}$ values (Table 18). The pseudocontact interaction could account for the observed shifts if $D \geq 30\ cm^{-1}$ for the S = 3/2 level of the reduced protein and $D \geq 90\ cm^{-1}$ for the S = 1 level of the oxidized protein. $D \geq 30\ cm^{-1}$ for the reduced protein is consistent with $D \sim 4\text{-}20\ cm^{-1}$ values obtained for compounds having a high spin Fe^{2+} (49, 42). But the unrealistically (16) high D values of $\geq 90\ cm^{-1}$ suggests that a significant pseudocontact interaction is not present in the oxidized protein. The need for this unrealistic D value may also reflect the limitations of the simple model proposed for the oxidized protein. We have excluded the possibility that the iron atoms in the Fe-S cluster are in mixed valence states (57) and have neglected spin-orbit contributions to the Fe^{3+} $\underset{\sim}{g}$-tensor from the neighboring organic and inorganic sulfur atoms.

Thus the factors responsible for the observed carbon and proton shifts are not understood. In the case of the pseudocontact mechanism, very approximate estimates of the pseudocontact contribution suggest that this mechanism may be responsible for the observed shifts in the reduced protein. If the pseudocontact mechanism is dominant, it is very difficult to understand why the magnetic shifts should show a symmetry about the tyrosyl 1', 4'- ring carbon axis and why the ring carbon resonance shifts should be significantly larger than those of the ring protons. The Fermi-contact explanation is an attractive alternative to the pseudocontact explanation in that it can readily explain the symmetry of magnetic shifts

about the tyrosyl 1',4'-ring carbon axis and also account for the large ring carbon shifts relative to those of the ring protons.

Since spin delocalization into the tyrosyl π-orbitals is not solely responsible for the observed shifts there must be delocalization into the tyrosyl ring σ-orbitals if the contact mechanism is primarily responsible for the observed shifts. We do not know if the orientation of the aromatic residues in clostridial ferredoxins, relative to the Fe-S complex, energetically permits this σ-delocalization.

The observed tyrosyl resonance shifts may be due to a sum of Fermi-contact and pseudocontact interactions, and thus may be difficult to unravel. ^{19}F-NMR of 3-fluorotyrosine-enriched ferredoxin, however, could help unravel the contributions from each shift mechanism (see General Discussion).

Fig. 44. ^{13}C-NMR (10° C) of C. acidi-urici apoferredoxin, oxidized and reduced C. acidi-urici ferredoxin. Apoferredoxin (80 mg/ml) (C) was prepared under reducing conditions to eliminate intramolecular mixed disulfides with 0.05 M Na_2S and dialized anaerobically against 0.05 M KD_2PO_4-K_2DPO_4 pD 7.0 buffer and 0.01 M EDTA. Oxidized (A) and reduced (B) ferredoxin (80 mg/ml) was prepared by dialysis against 0.05 M KD_2PO_4-K_2DPO_4 pD 7.0 buffer. Protons were simultaneously decoupled from carbon atoms by noise modulation. Carbon resonance assignments [ppm from CS_2]: carbonyl and carboxyl carbons [0-25], tyrosyl ring carbons [38-78], aliphatic carbons [125-190].

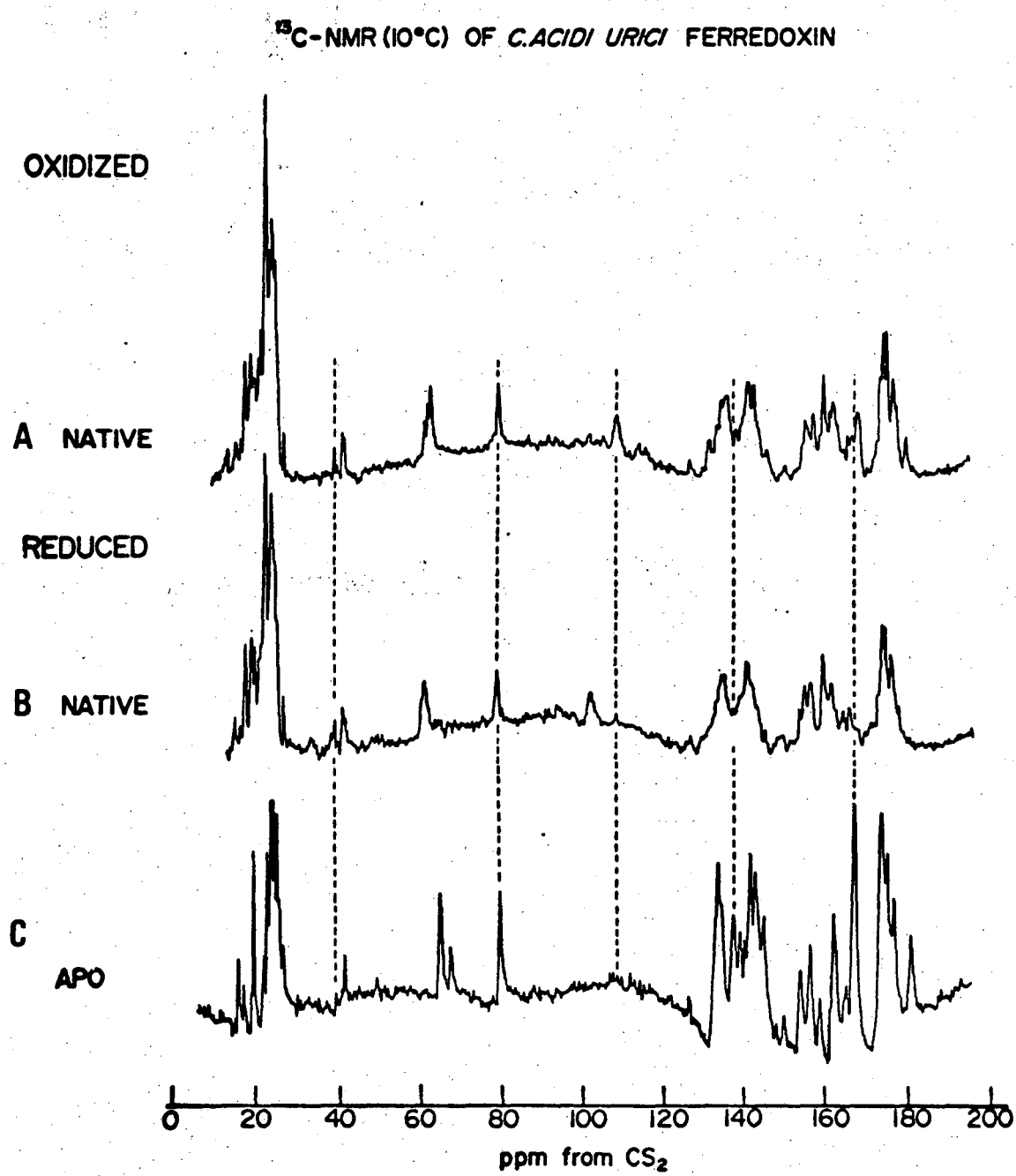
^{13}C-NMR (10°C) OF *C.ACIDI URICI* FERREDOXIN
OXIDIZED
A NATIVE
REDUCED
B NATIVE
C
APO
0
20
40
60
80
100
120
140
160
180
200
ppm from CS_2

Fig. 45. ^{13}C-NMR (10° C) of the aromatic region of C. acidi-urici apoferredoxin and oxidized C. acidi-urici ferredoxin. Protons were noise-decoupled in (A) and (B). Apoferredoxin (C) and oxidized ferredoxin (A) and (B) were prepared as in Fig. 44.

^{13}C- NMR (10°C) OF THE AROMATIC RESIDUES OF *C. Acidi Urici* FERREDOXIN

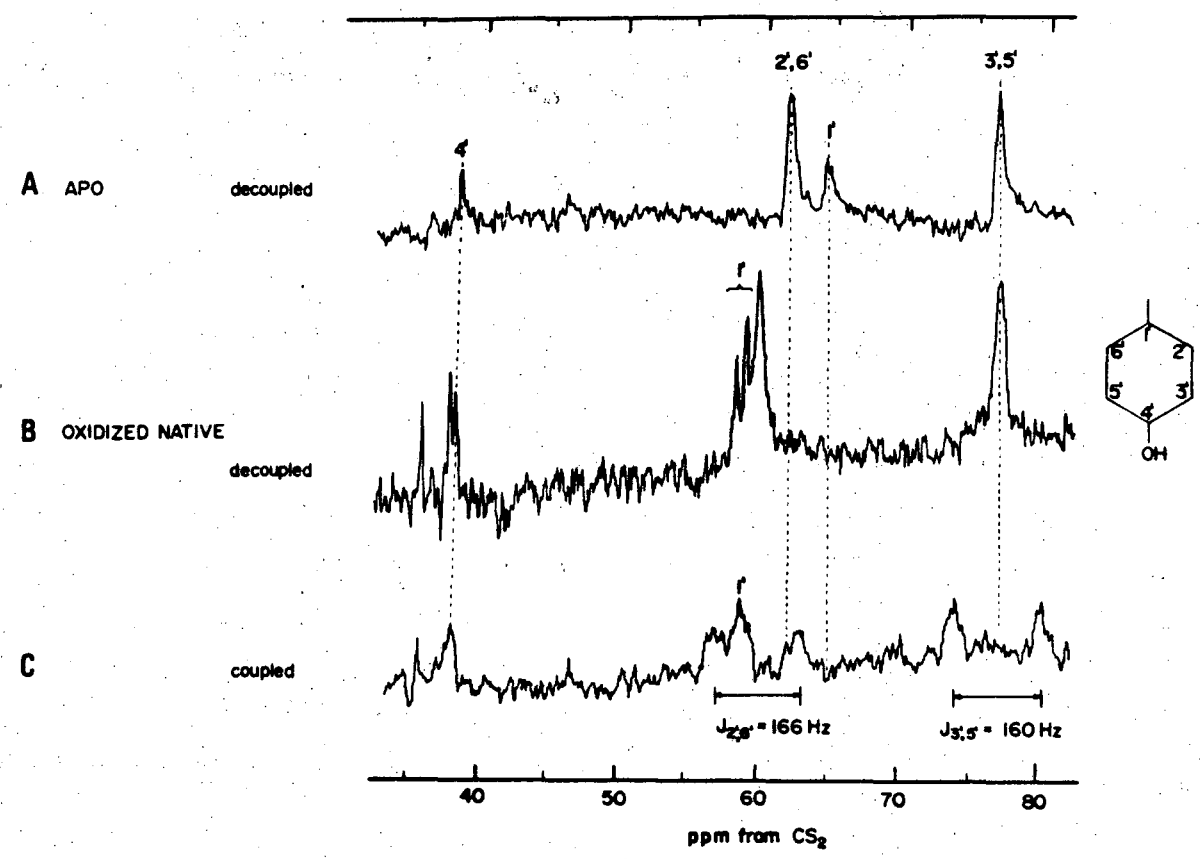

Fig. 46. ^{13}C-NMR (8-10°) of C. acidi-urici ferredoxin and N-acetyltyrosine. (Sample; Preparation): (A): Oxidized ferredoxin, all protons decoupled; prepared as in Fig. 44, (B): Oxidized ferredoxin, 3', 5'- tyrosyl protons decoupled; $(ND_4)_2SO_4$-free ferredoxin (30 mg/ml) prepared by dialysis against 0.05 M KD_2PO_4-K_2DPO_4 pD 7.0 buffer. (C): Oxidized ferredoxin, 3', 5'- tyrosyl protons incompletely decoupled; prepared as in B. (D): Methyl viologen reduced-ferredoxin, all protons decoupled; prepared as in B, except that 0.5 ml of 75 mM Zn-reduced methyl viologen was added to 0.5 ml of deaerated ferredoxin (60 mg/ml). (E): Methyl viologen reduced-ferredoxin, 3', 5'- tyrosyl protons decoupled; same as D. (F) N-acetyltyrosine plus 100 mM Zn-reduced methyl viologen, all protons decoupled; dissolved in 10 mM KD_2PO_4-K_2DPO_4, pD 7.0 buffer, to give 25 mM final concentration. (G): N-acetyltyrosine, all protons decoupled; dissolved in 10 mM KD_2PO_4-K_2DPO_4, pD 7.0 buffer, to give 250 mM final concentration.

Double resonance experiments with the following decoupling conditions: (A) and (D): proton noise decoupling; (C): coherent decoupling using ^1H decoupling field strength of about 550 Hz. With this decoupling field strength and the carbon resonance splittings observed in C, the 2', 6'- and 3', 5'-tyrosyl ring proton resonances were calculated (128) to occur within a few tenths of a ppm of that observed for N-acetyltyrosine in spectra (F) and (G). This is confirmed in B, where no detectable splittings occur. In reduced ferredoxin (E), the 2', 6'- and 3',5'-ring proton resonances are within 1 ppm of that of the oxidized ferredoxin (B). The observed shifted resonances represent an averaged position between that of the oxidized and fully reduced ferredoxins that indicates a rapid electron exchange between oxidized and reduced forms of the protein (see text).

^{13}C-NMR OF *C. ACIDI URICI* FERREDOXIN (8-10°C)
DOUBLE RESONANCE EXPERMENTS

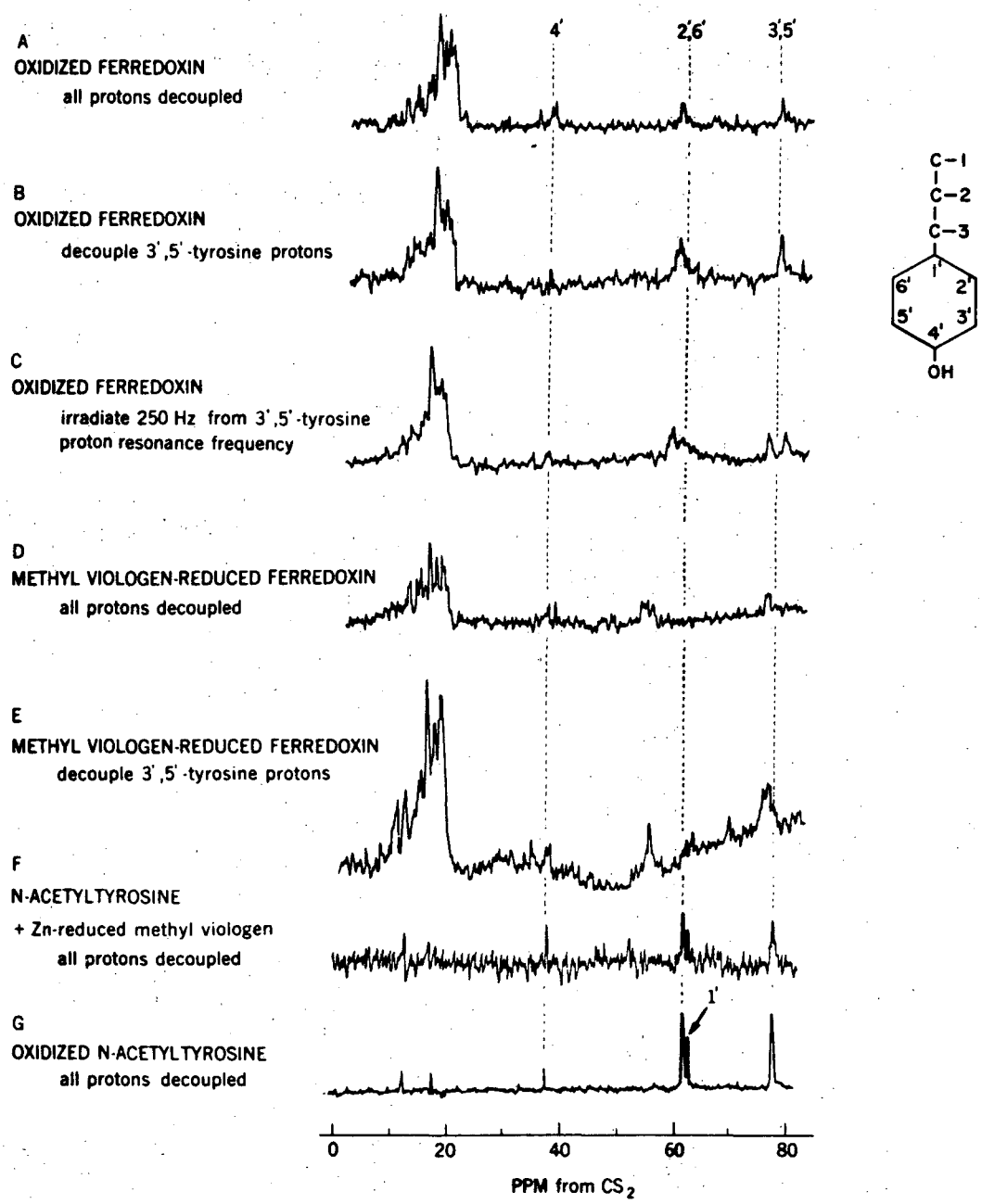

Fig. 47. ^{13}C-NMR (10°C) of the aromatic region of (8±2)% reduced C. acidi-urici ferredoxin. (A): Noise decoupled, all protons decoupled. (B): Coherent decoupled spectrum, coherent pulse frequency at 7.0 ppm from DSS (~ 0.5 ppm downfield of 3', 5' - ring proton resonance). (C): Coherent decoupled spectrum. Coherent pulse frequency at ~ 9.0 ppm from DSS (~ 2 ppm downfield of frequency which decouples 3', 5' - ring protons). (D): Coherent decoupled spectrum, coherent pulse frequency at 11.0 ppm from DSS (~ 2 and ~ 4 ppm downfield of frequency which decouples 2', 6' - and 3', 5' - ring protons respectively). (E): Coupled spectrum, all protons coupled to carbon atoms.

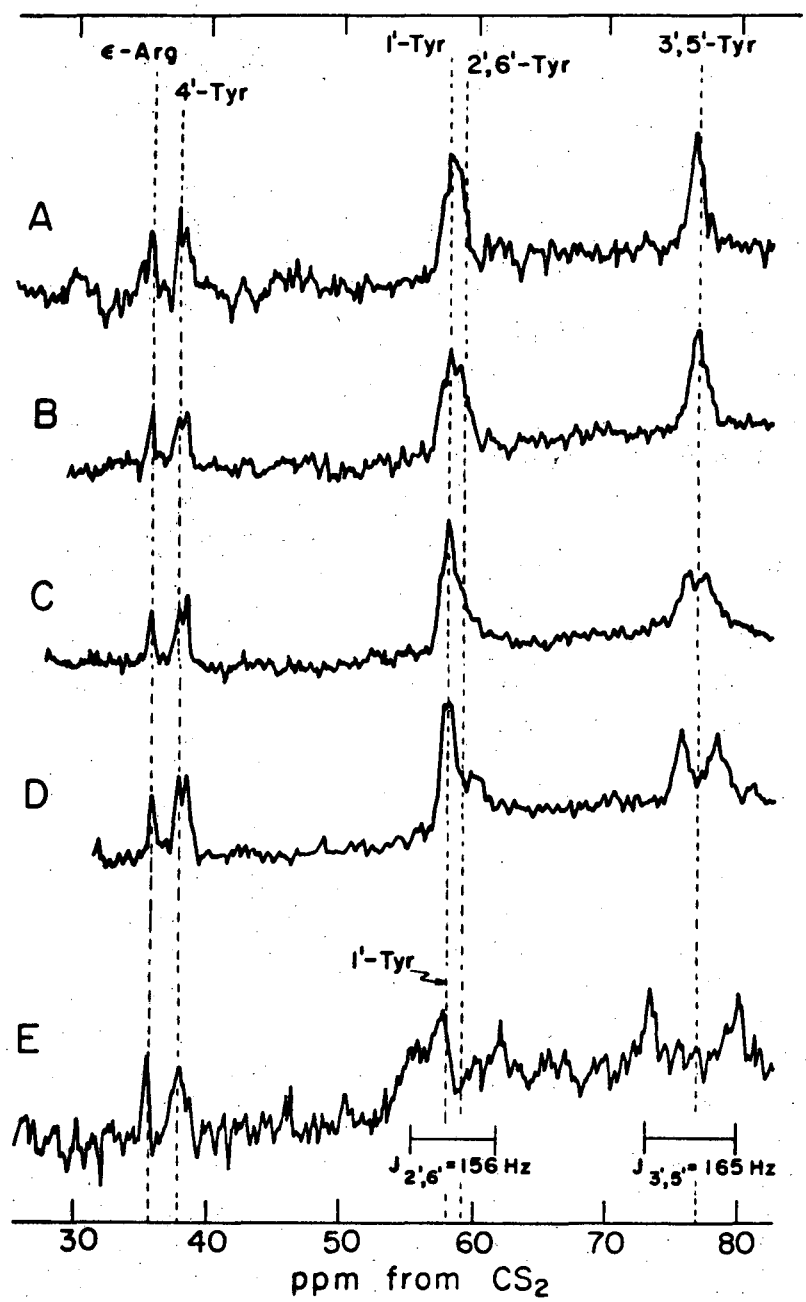
ε-Arg
4'-Tyr
1'-Tyr
2',6'-Tyr
3',5'-Tyr
A
B
C
D
E
1'-Tyr
$J_{2',6'}$ = 156 Hz
$J_{3',5'}$ = 165 Hz
30
40
50
60
70
80
ppm from CS_2

Table 14. ^{13}C-tyrosyl ring carbon shifts[a].

Sample	Ring carbon 1'	2',6'	3',5'	4'
Reference compound:				
Apoferredoxin[b]	64.9	62.2	77.3	38.0
GlyGlyTyrGlyGly (52)	64.9	62.4	77.4	38.2
Oxidized *C. acidi-*	59.5	60.4	77.3	38.5
urici ferredoxin[c]	58.8			38.0

a. Shifts (ppm relative to CS_2) are accurate to $\pm$ 0.2 ppm. (All shifts in this table are positive, that is, upfield of CS_2.)

b. Based on Fig. 45A.

c. Based on Fig. 45B.

Table 15. Observed shifts[a] of the tyrosyl ring carbon and ring proton resonances of oxidized and reduced C. acidi-urici ferredoxin relative to those in apoferredoxin.

	Ring carbon				Ring proton	
Oxidation state	1'	2',6'	3',5'	4'	2',6'	3',5'
Oxidized	-5.6	-1.9	0	0	-0.2±0.1[d]	-0.2±0.1[d]
(8 ± 2)% reduced[b]	-6.5	-3.3	-0.4	0	-0.7±0.5[e]	+0.2±0.1[c,d]
(40 ± 5)% reduced[b]	-8.5	-7.4	-1.3	+0.5[c]	-1.0±0.5[e]	+0.3±0.1[c,d]
100% reduced[f]	-14±1	-16±2	-4±0.5	+2.5±0.5[c]	-3.0±0.5[f]	+0.5[c,d,f]

a. Shifts (ppm) are accurate to ±0.2 ppm unless otherwise indicated.

b. Estimate of degree of reduction based on ^{1}H-NMR measurements of aliquots of ^{13}C-NMR samples (See Experiment 7b).

c. Positive shifts are upfield shifts (relative to the ring carbon resonances in C. acidi-urici apoferredoxin).

d. Estimate from ^{1}H-NMR spectra (See Experiment 7b).

e. Estimate from double resonance experiments.

f. Extrapolated from Fig. 55 (Experiment 7b).

Table 16. Predicted ratios of magnetic shifts[a] of tyrosyl ring carbon resonances in oxidized and reduced *Clostridium acidi-urici* ferredoxin assuming a Fermi-contact mechanism and that electron spin delocalization from the Fe-S clusters occurs exclusively into the tyrosine π-orbitals

	ρ_i^π, the π-electron[b] spin density at carbon i			$(\Delta H/H_0)_i/(\Delta H/H_0)_{2',6'}$ carbon				
	Antibonding orbital[c]			Predicted			Observed (Table 15)	
Carbon i	B_g	Au_1	Au_2	B_g	Au_1	Au_2	Oxidized	Reduced
1'	0	0.33	0.25	-1.3	-2.6	6.0	3.0	0.8
2' or 6'	0.25	0.05	0.17	1.0	1.0	1.0	1.0	1.0
3' or 5'	0.25	0.09	0.14	1.0	0.5	1.0	~ 0	0.2
4'	0	0.36	0.14	-1.3	-2.4	2.0	~ 0	-0.1

[a]Shifts are relative to the ring carbon resonances of *C. acidi-urici* apoferredoxin.

[b]π-spin densities are expressed in units of λ where $\lambda \leq 1$ and denotes the fraction of an electron spin transferred from the Fe-S cluster. The ρ_i^π are typical values.

[c]Energy ordering of the antibonding orbitals is $Au_2 > Au_1 > B_g$.

Notes for Table 16. (continued)

The shift in ppm relative to apoferredoxin is given by (23):

$$(\Delta H/H_0) \times 10^6 \text{ppm} = A_i \langle S_z \rangle \times 10^6/\gamma_I H_0 \qquad (1)$$

A_i is the hyperfine, or Fermi-contact, coupling constant at nucleus i and is related to the electron spin density at i. H_0 is the magnetic field at resonance in the absence of the electron coupling term (i. e., $A_i = 0$). $H_0 + \Delta H$ denotes the magnetic field at resonance in the presence of the electron coupling term. γ_I is the gyromagnetic constant for nuclear spin i. The carbon gyromagnetic constant is approximately a factor of 4 smaller than the proton gyromagnetic constant. $\langle S_z \rangle$ is the thermal average of the component of the electron spin magnetization parallel to the applied field $H_0 + \Delta H$. The Fe-S cluster contains antiferromagnetically coupled ions and $\langle S_z \rangle$ is more complicated (35) than the usual Curie expression (39). The Karplus-Fraenkel equation (68) relates the carbon hyperfine constant, A_c, to the π-electron spin densities:

$$A_c \simeq 35.6 \, |\gamma_e| \, \rho_i^\pi - 13.9 \, |\gamma_e| \sum_{j \text{ (neighbors)}} \rho_j^\pi \text{ Rad/sec.} \qquad (2)$$

γ_e is the electron gyromagnetic constant. ρ_i^π denotes the π electron density at carbon i. The sum over j is restricted to the bonded carbon neighbors of carbon i. Estimates of the π-electron spin distribution for for the various antibonding π-orbitals of tyrosine can be made using Hückel molecular orbital theory (124). The above equations together with estimates for ρ_i^π can be used to predict the ratios of carbon shifts relative to the apoferredoxin. Thus,

$$(\Delta H/H_0)_{\text{carbon } \underline{i}} \,/\, (\Delta H/H_0)_{\text{carbon } 2',6'}$$

$$= \left[35.6\, \rho_i^{\pi} - 13.0 \sum_{\substack{j \\ (\underline{i} \text{ neighbors})}} \rho_j^{\pi} \right] \Big/ \left[35.6\, \rho_{2',6'}^{\pi} - \sum_{\substack{j \\ (2',6' \text{ neighbors})}} \rho_j^{\pi} \right] \qquad (3)$$

Table 17. Predicted ratios of ring carbon and ring proton pseudocontact shifts for the reduced ferredoxin, neglecting possible zero field splitting terms.

	Calculated[b]			Observed[d] (Table 15)
$r(\mathring{A})^c$ =	2.9	3.5	4.0	
Shift ratio:				
$C_2':C_1'$	4.6	5.2	0.6	1.6 ± 0.4
$C_2':C_3'$	1.0	6.1	4.9	3.9 ± 0.6
$C_2':C_4'$	-30.5	-18.9	-13.3	-7 ± 1
$C_1':C_3'$	2.2	2.1	1.0	2.8 ± 0.6
$C_2':H_2'$	2.0	1.0	0.9	6 ± 1
$C_3':H_3'$	-2.2	-5.4	-4.1	-5 ± 1

a. Shifts are relative to those of the oxidized protein. Ratios were calculated from the ratios of pseudocontact expressions (71) for each nucleus (assuming dipole-dipole interactions). This expression neglects the zero field terms.

$$\frac{\text{H Nucleus i}}{\text{H Nucleus j}} = \frac{(3\cos^2\theta_i-1)(R_j)^3}{(3\cos^2\theta_j-1)(R_i)^3}$$

where R_i is the distance the electron is from the nucleus i and θ_i is the angle R_i makes with the axis parallel to a plane perpendicular to the ring. The above expression assumes:

(i) $\tau_{rot} >> T_{1e}$ (where τ_{rot} is the correlation time of the protein and T_{1e} is the relaxation time of the electron) so that any given state of the electron sees a fixed nuclear orientation.

Notes to Table 17 continued.

a. (continued)

(ii) Detectable pseudocontact shifts are produced at:

$r = 2.9$ Å (R_i ranges from 3.2 - 5.5 Å)

$r = 3.5$ Å (R_i ranges from 4.1 - 6.3 Å)

$r = 4.0$ Å (R_i ranges from 5.0 - 7.2 Å)

(iii) ψ is $\geq 45^{\circ}$ (ψ is the angle (120') the projection of $\mathbf{R}$ makes on the xy plane, and in this case the xy plane is the plane of the aromatic ring.) If this angle were $< 45^{\circ}$, then there could be no upfield shifts for the 4'-carbon and 3',5'-protons at the above values of r. Thus we can neglect the term containing cos 2ψ in the expression used for calculating pseudocontact shifts (71).

b. Since the ring carbon and proton resonance shifts are symmetric about the 1',4'-ring carbon axis, the electron was assumed to be on a plane perpendicular to the plane of the ring and intersecting the 1',4' axis of the ring.

c. r is the perpendicular distance the unpaired electron spin is to the plane of the ring, so that the angle it makes with the z axis (also perpendicular to the ring) is $\geq 56 \pm 1^{\circ}$ to the 4'-carbon atom and 3'- or 5'- proton. This will permit the 4'-carbon and 3',5'-proton resonance shifts to occur upfield as observed. r cannot be much less than 3 Å if the above constraints are to be fulfilled. At $r < 2.9$ Å the unpaired electron could overlap the ring orbitals and produce a contact shift.

d. Observed shifts are shifts extrapolated to the dithionite end-point for the "fully" reduced <u>C. acidiurici</u> ferredoxin (See Experiment 7b).

Table 18. Calculated range of pseudocontact shifts[a] (including zero field splitting terms) for the ring carbon resonances of oxidized and reduced *C. acidi-urici* ferredoxin.

	R(Å)[b]	D(cm^{-1}) 3	9	27
Oxidized	5	-0.02 to +0.04	-0.06 to +0.1	-0.2 to +0.3
	4	-0.04 to +0.08	-0.1 to +0.2	-0.3 to +0.6
Reduced	5	-1 to +0.7	-1 to +1	-2 to +2
	4	-2 to +1	-3 to +2	-4 to +5

a. Shifts (ppm) are relative to the ring carbon resonances in model polypeptides.

The pseudocontact contribution to the ^{13}C-shifts can be estimated if one uses Eqs. 20, 41, and 43 of reference (71) and assumes, as observed in the plant ferredoxins (35), that the iron atoms of the oxidized *C. acidi-urici* ferredoxin are antiferromagnetically coupled high spin Fe^{3+} (S = 5/2) ions, while the reduced form has a high spin Fe^{2+} (S = 2) ion, antiferromagnetically coupled to high spin Fe^{3+} ions. These antiferromagnetically coupled systems have spin levels S = 0, 1, 2, ... in the oxidized protein, and S = 1/2, 3/2, 5/2,... in the reduced protein. The dominant contribution to the ^{13}C-shift

Notes to Table 18 continued.

a. (continued) in the oxidized protein is assumed to come from S = 1, the first thermally (110) excited spin level of the Fe-S cluster. This level was taken to be $\approx 350\ cm^{-1}$ above the diamagnetic ground level (S = 0). In the reduced protein, both the ground S = 1/2 level and the thermally excited S = 3/2 level contribute to the observed ^{13}C-shift. The S = 3/2 level is assumed to be $\approx 250\ cm^{-1}$ above the S = 1/2 level. The S = 1 level of the oxidized protein is assumed to have an isotropic $\underset{\sim}{g}$-tensor with a principal value of 2.01. To the extent that the spin-orbit contributions from the neighboring organic and inorganic sulfur atoms can be ignored, this is a reasonable assumption for high spin Fe^{3+} in the tetrahedral or distorted tetrahedral environment occurring in ferredoxin. The S = 1/2 level has an anisotropic $\underset{\sim}{g}$-tensor with principal values 2.04, 1.94, and 1.88 (96, 100). The S = 3/2 level is assumed to have an isotropic g-tensor with a principal value of 2.2. This value was calculated using the Gibson model (49) for plant ferredoxin and the known $\underset{\sim}{g}$-tensor of the ground S = 1/2 level. A zero field term can appear for spin states for $S \geq 1$. This term was assumed to have the simple form $D[S_z^2 - S(S+1)/3]$ where D is the coupled value for the Fe-S cluster and S_z is the component of the electron spin (S = 1, or S = 3/2) along the unique z-axis in the Fe-S cluster. The orientation of this unique axis is not known.

b. This range of shifts is for a carbon atom at a distance R from the Fe-S cluster where the orientation of $\underset{\sim}{R}$ relative to the cluster is varied.

c. The estimated range includes a contribution from the $\underset{\sim}{g}$-tensor anisotropy of the ground S = 1/2 level.

Experiment 7b

The possible formation of a weak chemical bond between the aromatic residues and the Fe-S clusters of clostridial-type ferredoxins

SUMMARY:

The 2', 6'-and 1'-ring carbon resonances of the aromatic residues in oxidized C. acidi-urici native ferredoxin, C. acidi-urici [Phe^2]-ferredoxin and C. pasteurianum ferredoxin are significantly shifted relative to the corresponding resonances of model peptides. We conclude that the aromatic residues of the three oxidized proteins have essentially identical magnetic environments because the corresponding resonance shifts of the two tyrosyl residues of oxidized C. acidi-urici native ferredoxin and the phenylalanyl and tyrosyl residues of oxidized C. acidi-urici [Phe^2]-ferredoxin and oxidized C. pasteurianum ferredoxin are essentially identical. All the ring carbon resonances are significantly shifted in the three methyl viologen-reduced ferredoxins and the magnitudes of these shifts are larger in the reduced protein than in the oxidized protein. The aromatic residues of reduced C. acidi-urici native and C. acidi-urici [Phe^2]-ferredoxin maintain similar magnetic environments because the magnitudes of the shifts of the corresponding ring carbon atoms are similar. The aromatic residues of reduced C. pasteurianum ferredoxin, however, do not maintain similar magnetic environments.

The magnitudes of the ring proton resonance shifts, in all of the above oxidized and reduced ferredoxins are five to ten times smaller

than the magnitudes of the corresponding (bonded) ring carbon resonance shifts. This result suggests that the aromatic residues of these ferredoxins may form a weak chemical bond with their neighboring iron-sulfur clusters.

INTRODUCTION:

In Experiment 7a, we observed that the two tyrosyl residues of oxidized C. acidi-urici native ferredoxin are in similar magnetic environments. Upon reduction the aromatic residues are magnetically perturbed but both aromatic residues in this ferredoxin remain in similar magnetic environments. This fact indicates that each Fe-S cluster is equally accessible to one reducing electron since each tyrosyl residue is perturbed by the unpaired electron spins in a neighboring Fe-S cluster. This poses two immediate questions:

(i) are the two Fe-S clusters also equally accessible to the reducing electron when there is a phenylalanyl residue near the Fe-S cluster? and

(ii) do the aromatic residues of other oxidized and reduced clostridial type ferredoxins experience similar magnetic environments?

The answers to these questions may help elucidate whatever structural or functional role (or both) the aromatic residues have in clostridial-type ferredoxins.

METHODS AND MATERIALS:

C. acidi-urici [Phe^2]-ferredoxin* was synthesized by Dr. Eglis T. Lode (77) from C. acidi-urici apoferredoxin containing no free sulfhydryl groups. (The superscript refers to the amino acid position starting from the N-terminal residue of the protein (63)). Ala^1 and Tyr^2 were removed by Edman degradation (41). The t-BOC-p-introphenyl esters of alanine and tyrosine were used to couple Ala^1 and Phe^2 to des-Ala^1-Tyr^2-apoferredoxin by a previously described method (61). C. acidi-urici [Phe^2]-ferredoxin was then reconstitued (59) from the synthetic C. acidi-urici [Ala^1, Phe^2]-apoferredoxin (77).

C. acidic urici native ferredoxin and C. acidi-urici [Phe^2]-ferredoxin have the same biological activity (77) in the phosphoclastic assay (116) and Cytochrome c-reductase assay (102), and have identical optical (76), ^{1}H-NMR and ^{13}C-NMR spectra (see Experiment 8), excluding the absorptions of the different aromatic residues.

RESULTS:

^{13}C-NMR OF THE AROMATIC RESIDUES:

OXIDIZED FERREDOXIN: The resonances of the corresponding ring carbon atoms of the phenylalanyl and tyrosyl residues in diamagnetic reference compounds (Table 19) resonate at different frequencies. This is also true for the resonances of corresponding ring carbon atoms of the phenylalanyl and tyrosyl residues of C. pasteurianum ferredoxin and C. acidi-urici [Phe^2]-ferredoxin (Table 19), but the

*This nomenclature of [Phe^2]-ferredoxin is based on (63), recommended tentative rule 1 for the naming of synthetic modifications of natural peptides of the IUPAC-IUB approved by the commission on Biochemical Nomenclature in July, 1966.

2', 6'- and 1' ring carbon resonances of these oxidized ferredoxins are shifted from their positions in the peptide reference compounds.

In both oxidized C. acidi-urici [Phe^2]-ferredoxin and oxidized C. pasteurianum ferredoxin the shifts of the corresponding ring carbon atoms are essentially equal to each other. These shifts are also essentially equal to those of oxidized C. acidi-urici native ferredodin (Table 20). With this fact one can distinguish the corresponding ring carbon resonances of Tyr^2 and Tyr^{30} in C. acidi-urici native ferredoxin.

In native C. acidi-urici ferredoxin (Fig. 48C) the ring carbon resonances were assigned, as described in Experiment 7a by comparing the observed resonance positions of the holoferredoxin with those of the apoferredoxin (Fig. 48B). In C. acidi-urici apoferredoxin the four groups of ring carbon resonances seen at 78, 62, 65 and 77 ppm correspond to the 4'-, 2',6'-, 1'- and 3',5'-ring carbons respectively (Table 19). In oxidized C. acidi-urici native ferredoxin, two of these groups of resonances are shifted from their positions in apoferredoxin. These groups of shifted resonances occur at 59 and 60.4 ppm and are assigned to the 1'- and 2' 6'-ring carbons. This assignment is based on the following observations:

(i) proton-coupled ^{13}C-NMR spectra (Fig. 45C Experiment 7a) of the aromatic region of the C. acidi-urici native holoferredoxin show that the resonance at 60.4 ppm collapses into a doublet, centered about 60.4 ppm. The separation of this doublet is 166 Hz and is characteristic of ring carbons (74). The other resonances at 58.8 and 59.5 ppm do not collapse into doublets and these resonances correspond to

carbons that are not bonded to protons. They are thus assigned to the two 1' - carbon atoms of the two tyrosyl residues in the oxidized protein. The resonances at 38.0 and 38.5 ppm also do not collapse in the proton-coupled ^{13}C-NMR spectra (Fig. 45C). These resonances are assigned to the 4' - carbons of the two tyrosyl residues, since these resonances are within 0.25 ppm of the resonance position of the 4' - carbon of the apoferredoxin:

(ii) double resonance or coherent proton-decoupling techniques (see Experiment 7a) show that the resonance at 60.4 ppm (in Fig. 45B) corresponds to a carbon that is bonded to the 2', 6'-ring protons of the ferredoxin tyrosyl residues;

(iii) comparison of line widths shows that the assignments of the 1'-carbons are consistent with the fact that carbons not bonded to protons have narrower resonances;

(iv) comparison of resonance intensities (in Fig. 45B), which are proportional to the number of carbons they represent, shows that the 2', 6' - and 3',5' - carbon resonances are two times those of the 1' - and 4' - carbon resonances in each aromatic residue.

In oxidized C. acidi-urici [Phe^2]-ferredoxin (Fig. 48D) one sees resonances at 38.2, 58.8, 60.4, 77.4 ppm, and they correspond to the 4'-, 1'-, 2',6' - and 3',5' - ring carbons of Tyr^{30} respectively. The resonances at 38.5 and 59.5 ppm present in oxidized C. acidi-urici native ferredoxin (Fig. 48C) do not appear in the spectrum (Fig. 48C) of oxidized C. acidi-urici [Phe^2] - ferredoxin. These missing resonances thus correspond to the 4' - and 1'-ring carbons (respectively) of C. acidi-urici native ferredoxin.

The other resonances in the ^{13}C-NMR spectrum of the aromatic region of C. acidi-urici [Phe^2]-ferredoxin correspond to the ring carbons of its phenylalanyl residue. The phenylalanyl resonances are assigned by comparing the C. acidi-urici [Phe^2]-ferredoxin with that of the reference compound (glycylphenylalanylamide acetate, Fig. 48 A), and by on-and-off resonance decoupling techniques, line width and intensity analysis, as was done to assign the tyrosyl ring carbon resonances in Experiment 7a. The assignment is illustrated in Fig. 48 where the dotted lines connect tyrosyl ring carbon resonances and the solid lines connect phenylalanyl ring carbon resonances. Table 19 lists these assignments and shows that the magnetic shifts of the 1'- and 2',6'-ring carbons in C. acidi-urici native, and [Phe^2]-ferredoxin and C. pasteurianum ferredoxin are essentially identical.

REDUCED FERREDOXIN: In reduced C. acidi-urici [Phe^2]-ferredoxin the shifts of the corresponding ring carbon atoms in phenylalanyl and tyrosyl residues are similar to each other and to the shifts of the corresponding ring carbon atoms of the tyrosyl residues of C. acidi-urici native ferredoxin at the same extrapolated degree of reduction. In reduced C. pasteurianum ferredoxin the shifts of the Tyr^2 residue are similar to the corresponding shifts of the Tyr^2 residue in C. acidi-urici native ferredoxin and of the Phe^2 residue of C. acidi-urici [Phe^2]-ferredoxin at the same extrapolated degree of reduction (Table 21). The shifts of the corresponding ring carbons of the Phe^{30} residue, however, are not similar to the Tyr^2 residue or to the Tyr^{30} residues in C. acidi-urici native and [Phe^2]-ferredoxin (Table 21).

Assignment of ring carbon resonances in the reduced ferredoxins was made by using the assignment techniques described above and in Experiment 7a. In Experiment 7a the resonance positions of protons covalently bound to specific ring carbon atoms were determined by coherent proton-decoupling techniques. These techniques can be used to determine the resonance positions of the ring carbon atoms as well. In (proton-) coupled spectra, carbon resonances are split into (n + 1) resonances, where n is the number of protons bonded to each carbon. (The resonances of carbon atoms not bonded to protons will appear as single resonances in coupled and decoupled spectra.) If one applies a coherent frequency to the coupled spectrum, this frequency will decouple only the protons resonating at the applied frequency, and the resonances of the carbon atoms (bonded to this proton) will appear as single resonances.

For example, the resonances at 45.1 and 54.4 ppm in the noise-decoupled ^{13}C-NMR spectrum of the aromatic region of (fully-) reduced C. pasteurianum ferredoxin (Fig. 50B) collapse into doublets when a coherent frequency specifically decouples the 3', 5'-ring proton resonances (Fig. 50C) of the phenylalanyl and tyrosyl residues. The ^{13}C resonances, which are not collapsed in Fig. 50C, occur at 40.4, 44.4, 51.6, 62.1, and 73.4 ppm. The ^{13}C resonances at 62.1 and 73.4 ppm are broad, and collapse into doublets when a coherent frequency specifically decouples the 2', 6'-ring proton resonances (Fig. 50A). This enables us to assign the ^{13}C resonances at 62.1 and 73.4 ppm to the 3', 5'-ring carbon atoms. The ^{13}C resonances at 45.1 and 54.4 ppm do not collapse when the coherent frequency, that specifically

decouples the 2', 6'-ring protons, is applied and do collapse, when the coherent frequency that specifically decouples 3', 5'-protons is applied. This fact permits us to assign the ^{13}C resonances at 45.1 and 54.4 ppm to the 2', 6'-ring carbon atoms. The ^{13}C resonances at 40.4, 44.4, and 51.6 ppm do not collapse when one applies coherent frequencies which decouple the 3', 5'-and 2', 6'-ring protons. The ^{13}C resonances at 40.4, 44.4, and 51.6 ppm are thus assigned to ring carbon atoms not bonded to protons. (The ^{13}C resonance at 44.1 ppm (Fig. 50C), obscured by the resonance at 45.1 ppm in the noise decoupled spectrum (Fig. 50B), is revealed in the coherently decoupled spectrum (Fig. 50 C).) The final assignments (Table 22 and Figs. 49B, 50B) are confirmed by comparison of line widths and intensities by following each resonance position at different degrees of reduction (see Experiment 7c).

The resonance positions of the protons bonded to the ring carbon atoms of "fully" reduced C. pasteurianum ferredoxin were also determined by measuring the separation (in Hertz) of each collapsed doublet in the coherently decoupled spectra (Fig. 50A, 50C). (See Experiment 7a).

C. pasteurianum ferredoxin was assumed to be "fully" reduced in Fig. 49B because: (i) the most downfield-shifted proton resonance in the ^{1}H-NMR spectra of an aliquot of this methyl viologen-reduced sample (Fig. 51B) occurred at essentially the same position it appears in ^{1}H-NMR spectra of dithionite-reduced C. pasteurianum ferredoxin and C. acidi-urici ferredoxin (Fig. 51A) (Phillips, personal communication); (ii) the magnitude of the ring carbon shifts increased with the

magnitude of the shift of the most shifted proton resonance (Table 23) in ^{1}H-NMR spectra of aliquots of the reduced ferredoxin ^{13}C-NMR samples; and (iii) the Tyr^{2} ring carbon resonances of this "fully" reduced C. pasteurianum ferredoxin occur just where one would predict for the corresponding ring carbon resonances of fully reduced C. acidi-urici ferredoxin (Fig. 52).

^{1}H-NMR OF THE AROMATIC RESIDUES:

OXIDIZED FERREDOXIN: Comparison of ^{1}H-NMR spectra of the aromatic region of C. acidi-urici native and [Phe^{2}]-ferredoxin also permits one to assign the proton resonances of each aromatic residue in each ferredoxin. The resonance at 6.57 ppm in C. acidi-urici native ferredoxin (Fig. 53C) is missing in C. acidi-urici [Phe^{2}]-ferredoxin (Fig. 53B). The missing resonance at 6.57 ppm is assigned to 3', 5'-protons of the Tyr^{2} residue because the resonances at 6.57 and 6.39 ppm were previously assigned to the 3', 5'-tyrosyl ring protons from C. acidi-urici [[3', 5'-$^{2}H_{2}$] Tyr]-ferredoxin (Experiment 2). Similarly, the proton resonance at 7.07 ppm of C. acidi-urici native ferredoxin is missing from C. acidi-urici [Phe^{2}]-ferredoxin, and this resonance is assigned to the 2', 6'-protons of the Tyr^{2} residue in C. acidi-urici native ferredoxin. The Phe^{2} ring proton resonances occur at 7.0 ppm.

Similarly, the proton resonance at 7.07 ppm in the ^{1}H-NMR spectrum (Fig. 53C) of C. acidi-urici native ferredoxin is missing from the spectrum (Fig. 53B) of C. acidi-urici [Phe^{2}]-ferredoxin, and this resonance is assigned to the 2', 6'-protons of the Tyr^{2} residue in

C. acidi-urici native ferredoxin. (The Phe^2 ring-proton resonance occur at 7.0 ppm in the spectrum of C. acidi-urici [Phe^2]-ferredoxin). The integrated areas of the above-mentioned resonances are also consistent with their assignments.

The resonances in the ^{1}H-NMR spectrum (Fig. 53A) of the aromatic region of oxidized C. pasteurianum ferredoxin cannot be assigned as precisely. Qualitatively the ring-proton resonances in this ferredoxin also have small shifts, relative to the free amino acid positions (Table 24), and both aromatic residues are also in similar magnetic environments.

The 2', 6'-ring proton resonances of the three oxidized ferredoxins are shifted ~ 0.4 ppm from the corresponding positions of the ring proton resonances of free amino acids (Table 24) but these shifts are ~5 times less than the shifts of the corresponding ring carbon resonances in the three oxidized proteins (Table 20). The 3', 5'-ring proton resonances however, like the 3', 5'-ring carbon resonances, are not significantly shifted in the three oxidized ferredoxins.

REDUCED FERREDOXIN: ^{1}H-NMR spectra (Fig. 54) of the aromatic region of methyl viologen-reduced C. acidi-urici ferredoxin confirm the ^{13}C-NMR double resonance measurements (see Experiment 7a) by showing that the resonances of the 2', 6'-tyrosyl ring protons shift ~3 ppm downfield and the 3', 5'-protons shift ~ 0.5 ppm upfield (relative to the oxidized protein positions) with "full" reduction.

In the ^{1}H-NMR spectrum (Fig. 51A) of Phillips' dithionite-reduced C. acidi-urici ferredoxin, two resonances, each corresponding to about two protons, appear at 10.3 and 9.8 ppm. We propose that

these resonances correspond to the 2', 6'-ring protons since we predicted the 2', 6'-resonances to occur at 10.0 and 9.6 ppm in the (extrapolated) fully-reduced ferredoxin from an extrapolation of Fig. 55 (see Table 25). This estimate was obtained by extrapolating the ring proton resonances of partially (methyl viologen) reduced ferredoxin to full reduction, using the most downfield shifted aliphatic proton resonances as an index of reduction (Fig. 52). The shifts of the ring proton resonances of each tyrosyl residue can be distinguished and show that: (i) the magnitude of these shifts is 5-10 less than that of the corresponding ring carbon resonance shifts; (ii) the magnitude of the shifts of the ring protons of each residue is the same for the corresponding ring protons (this confirms the ^{13}C-NMR observation that upon reduction each aromatic residue maintains a similar magnetic environment and that this environment is symmetric about the 1', 4'-ring carbon axis); and (iii) the magnitude of the shifts increases linearly with reduction for each aromatic residue (this strengthens the two state hypothesis because the ring carbon resonances also shift linearly with reduction if one uses the most downfield shifted resonance of an aliphatic proton as an index of reduction).

The magnitudes of the ring proton resonance shifts of the (extrapolated) fully-reduced C. acidi-urici ferredoxin are essentially the same as the magnitudes of the observed (Fig. 56B) ring proton resonance shifts of fully-reduced C. pasteurianum ferredoxin. Double resonance experiments (Fig. 50) predict that the 2', 6'-proton resonances of the Tyr^{2} and Phe^{30} residues in the fully reduced C. pasteurianum ferredoxin should occur at ~ 9 ppm from DSS and that the 3', 5'-phenylalanyl

and tyrosyl proton resonances should occur at ~ 6 and ~ 8 ppm from DSS respectively. The direct ^{1}H-NMR observation (Fig. 56B) of the fully-reduced C. pasteurianum, used in the ^{13}C-NMR double resonance study, shows that proton resonances occur at the predicted positions. Thus the 2', 6'-ring proton resonances of Tyr^{2} and Phe^{30} shift 2.0±0.4 and 1.4±0.4 ppm downfield, and the 3', 5'-ring proton resonances of Tyr^{2} and Phe^{30} shift 0.8±0.4 ppm upfield and 0.5±0.4 ppm downfield respectively from their resonance positions in the oxidized protein.

Table 26 shows that, in reduced C. pasteurianum ferredoxin (as in C. acidi-urici ferredoxin) the ring carbon resonance shifts are 5 to 10 times that of the corresponding ring proton resonance shifts. Furthermore the absolute magnitudes of the ratios of the ring carbon shifts to their corresponding proton shifts are essentially the same for the nuclei of each aromatic residue in reduced C. pasteurianum ferredoxin. (The corresponding ratios of the extrapolated values of C. acidi-urici ferredoxin have larger errors, but still show that the absolute magnitudes of the ratios of carbon to proton shifts for the 2', 6'- and 3', 5'-ring atoms are similar.)

DISCUSSION:

MAGNETIC AND ELECTRONIC PROPERTIES OF THE Fe-S CLUSTERS:

The unpaired electron spins in the ground and thermally excited spin energy levels of the Fe-S clusters should perturb ^{13}C- and ^{1}H-nuclei of neighboring aromatic and aliphatic residues. Aliphatic resonance shifts relative to their positions in apoferredoxin are observed, and these will be discussed in Experiment 8. The mechanism for this magnetic perturbation is not understood and probably involves both

pseudocontact and contact interactions (98). To the extent that the pseudocontact interaction dominates the observed shifts of the neighboring residues, these shifts are expected to depend on electron spin g-values, zero-field splittings, and the strength of the antiferromagnetic coupling (150) between the iron atoms of the Fe-S cluster. To the extent that the contact interaction dominates the observed shifts of the neighboring residues, these shifts are expected to depend on the strength of the antiferromagnetic coupling (150) and the degree of electron orbital overlap between the neighboring residues and the Fe-S clusters (83). Regardless of the mechanism responsible for the observed shifts, the magnetic shifts of the nuclei of neighboring amino acid residues should be sensitive to the electronic properties of the Fe-S clusters. We assume that the ring carbon resonances are shifted in C. acidi-urici and C. pasteurianum ferredoxin because the aromatic residues are each close to a single Fe-S cluster.

FORMATION OF A WEAK BOND:

A weak bond could occur if the probability of electron spin transfer from the Fe-S cluster into an orbital of a neighboring atom is approximately one percent. The fact that the ratios of the carbon:proton shifts are similar for a particular ring carbon and its bonded proton, even if the magnitudes of these shifts differ, suggests that some delocalization of spin occurs into the aromatic ring, and that for C. acidi-urici and C. pasteurianum ferredoxins the contact interaction and not the pseudocontact interaction may be mostly responsible for the observed shifts. The symmetrical shift pattern about the 1', 4'-ring

carbon axis and 5 to 7 fold attenuation of proton shifts is also consistent with a contact shift mechanism involving some small overlap of orbitals of the Fe-S cluster and the aromatic ring, and this overlap is essentially a weak chemical bond.

The fact that such a bond could exist suggests that: (i) the aromatic residues could stabilize the Fe-S clusters in oxidized and reduced clostridial-type ferredoxins; or (ii) electron delocalization can occur *via* the aromatic residues to the Fe-S clusters; or (iii) both. This delocalization could affect the rate of electron transfer between Fe-S clusters between ferredoxin molecules (with and without a mediator) or within a ferredoxin molecule (see General Discussion). It does not necessarily require that the reducing electron be transferred through the orbitals of the aromatic ring.

Other (aliphatic) amino acid residues that are within 4-5 Å of an Fe-S cluster may also form weak chemical bonds with the Fe-S clusters. This question will be discussed in Experiment 8.

TYROSYL RADICAL:

Takana *et al.*, (127) proposed that electron transfer could occur *via* a tyrosyl radical in cytochrome *c*. A tyrosyl radical electron should produce appreciable ring carbon resonance shifts but our results suggest that the tyrosyl residues in *C. acidi-urici* and *C. pasteurianum* ferredoxins do not exhibit any appreciable tyrosyl radical character (at 10° C).

We do not believe a tyrosyl radical is produced at 10° C because the ring carbon and proton resonance shifts of tyrosyl residues (relative to their positions in free amino acids and model polypeptides) are

not different from the corresponding ring carbon and proton resonance shifts of the phenylalanyl residues in C. pasteurianum ferredoxin and C. acidi-urici [Phe^2]-ferrodoxin. (If a tyrosyl radical is produced at 10°C, the ring carbon and ring proton resonance shifts of tyrosyl residues (relative to their positions in free amino acids and model polypeptides) should be different from the corresponding ring carbon and proton resonance shifts of the phenylalanyl residues in C. pasteurianum ferredoxin and C. acidi-urici [Phe^2]-ferredoxin.) Furthermore, the 2', 6'-ring carbon resonances would be shifted upfield in a tyrosyl radical, and this is not observed.

ACCESSIBILITY OF THE REDUCING ELECTRON:

The essentially identical shift patterns seen for the aromatic residues of C. acidi-urici native and [Phe^2]-ferredoxin at the same (extrapolated) degree of reduction suggest that each Fe-S cluster in both ferredoxins is essentially equally accessible to one reducing electron, and confirms the hypothesis (46, 85, 122) that the ferredoxin can receive two reducing electrons. The shift pattern for each aromatic residue of reduced C. pasteurianum ferredoxin is not the same. This suggests that (even though a total of two reducing electrons can be received by the protein) each Fe-S cluster in C. pasteurianum ferredoxin is not equally accessible to a reducing electron.

The redox potential is higher for an Fe-S cluster that is more accessible to a reducing electron. The measurement of the redox potentials of C. pasteurianum and C. acidi-urici ferredoxins is the subject of Experiment 7c.

Fig. 48. Proton-decoupled ^{13}C-NMR (10°) of the aromatic residues of C. acidi-urici ferredoxin. (Sample; Preparation): (A): Glycylphenylalanylamide acetate; 62 mg/ml, pD 7.2. (B): C. acidi-urici apoferredoxin; 80 mg/ml, pD 7.8. (C): Oxidized native C. acidi-urici ferredoxin; ~100 mg/ml pD 7.0. (D): Oxidized C. acidi-urici [Phe^2]-ferredoxin; ~25 mg/ml, pD 7.6. (E): (20±5)% Reduced C. acidi-urici [Phe^2]-ferredoxin. Conditions same as D except that 0.25 M Zn-reduced methyl-viologen has been added to reduce the ferredoxin. Broken and unbroken lines connect tyrosyl and phenylalanyl residues respectively.

^{13}C-NMR (10°C) OF THE AROMATIC RESIDUES OF *C. ACIDI URICI* FERREDOXIN

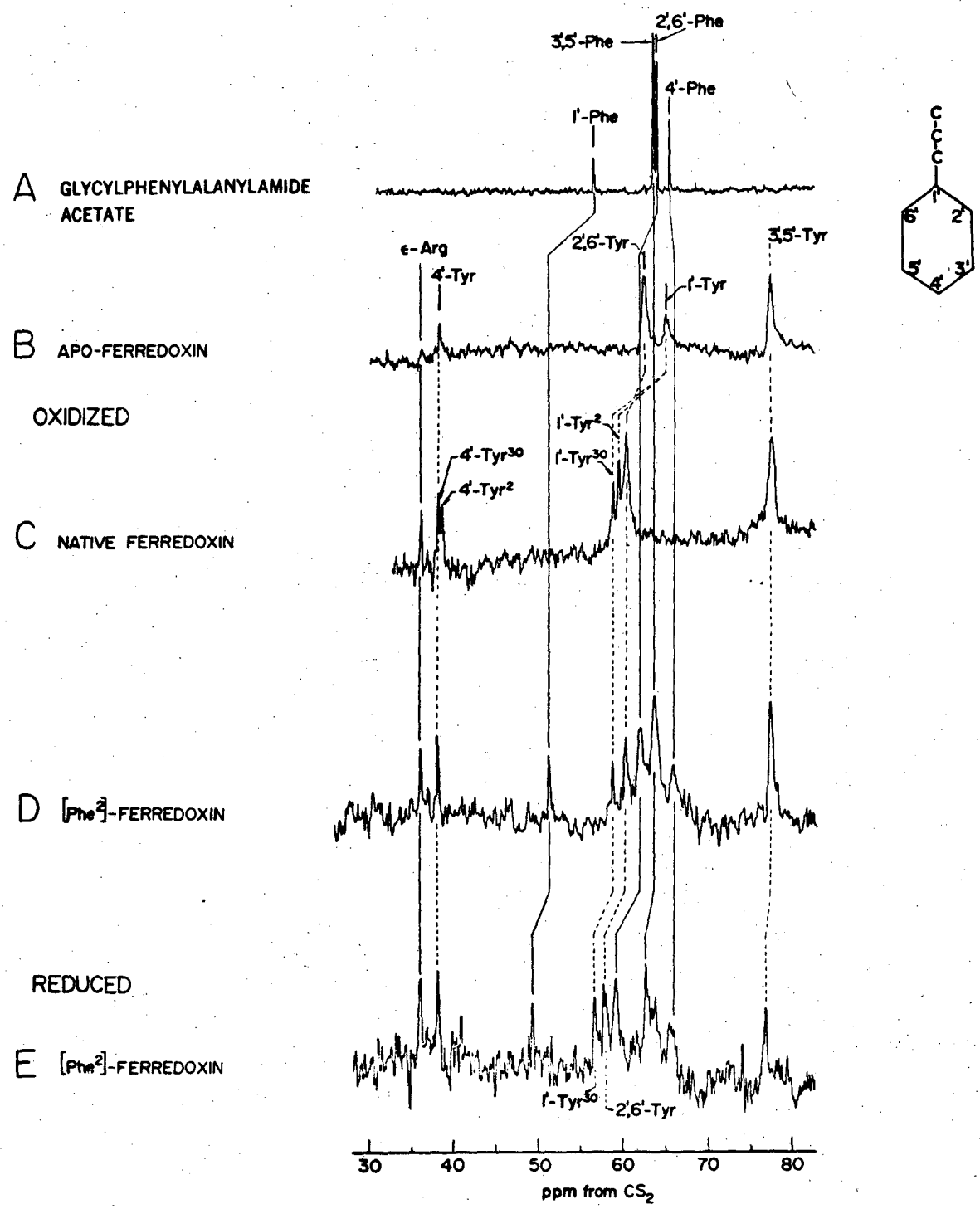

Fig. 49. ^{13}C-NMR (10°) of the aromatic residues of C. pasteurianum ferredoxin. (Sample; Preparation): (A): Oxidized C. pasteurianum ferredoxin; 80 mg/ml, pD 7.6 (pH 8.0). (B): (90±10)% reduced C. pasteurianum ferredoxin; ~40 mg/ml, pD 7.6. Protons were noise-decoupled in A and B. Broken and unbroken lines connect tyrosyl and phenylalanyl ^{13}C resonances respectively.

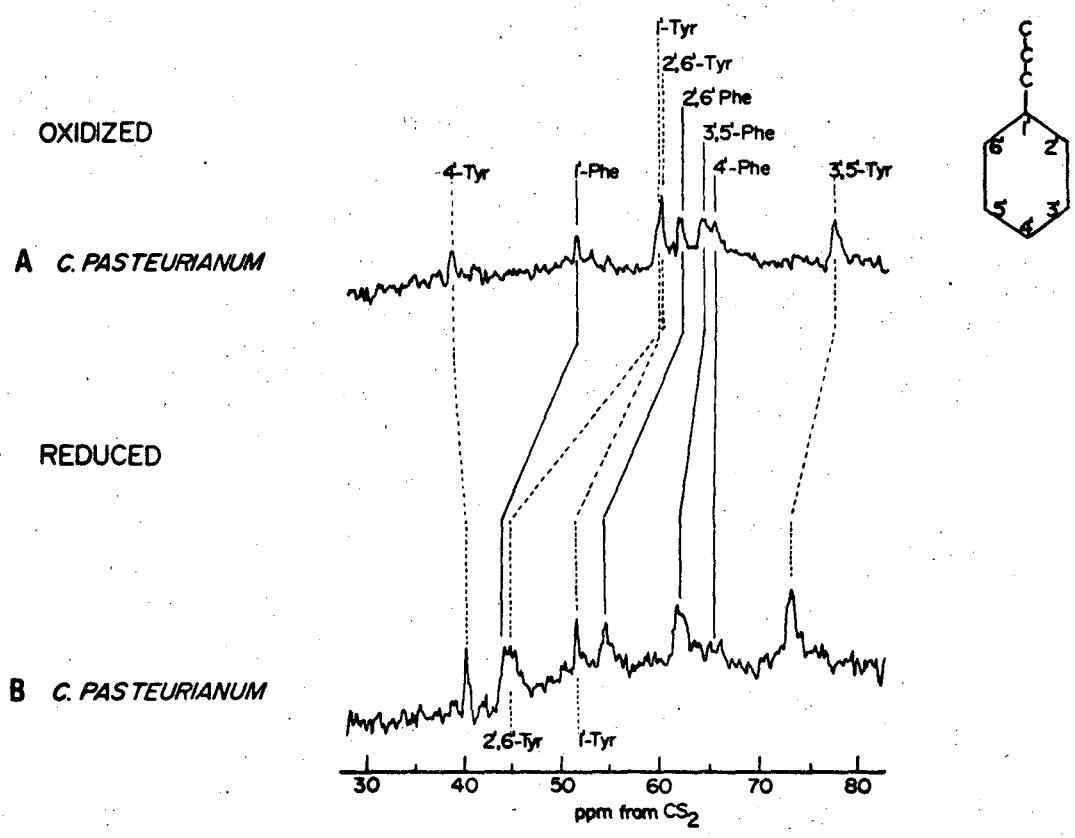
OXIDIZED
A C. PASTEURIANUM
REDUCED
B C. PASTEURIANUM
1-Tyr
2',6'-Tyr
2',6' Phe
3',5'-Phe
4'-Phe
4-Tyr
1-Phe
3',5'-Tyr
2',6'-Tyr
1-Tyr
30
40
50
60
70
80
ppm from CS2
C
C
C
C
1'
2'
3'
4'
5'
6'

Fig. 50. Coherent and noise-decoupled ^{13}C-NMR (10°C) spectra of the aromatic residues of (90±10)% reduced C. pasteurianum ferredoxin, 40 mg/ml, pD 7.6. (A): Coherent decoupled, decoupling frequency is 9.0 ppm from DSS or (2.0±0.5) ppm downfield from 3', 5'-tyrosyl ring proton resonance. (B): Noise-decoupled. (C): Coherent decoupled, decoupling frequency is 7.0 ppm or (0.5±0.5) ppm downfield from the 3', 5'-tyrosyl ring proton resonance. Broken and unbroken lines connect tyrosyl and phenylalanyl ^{13}C resonances, respectively.

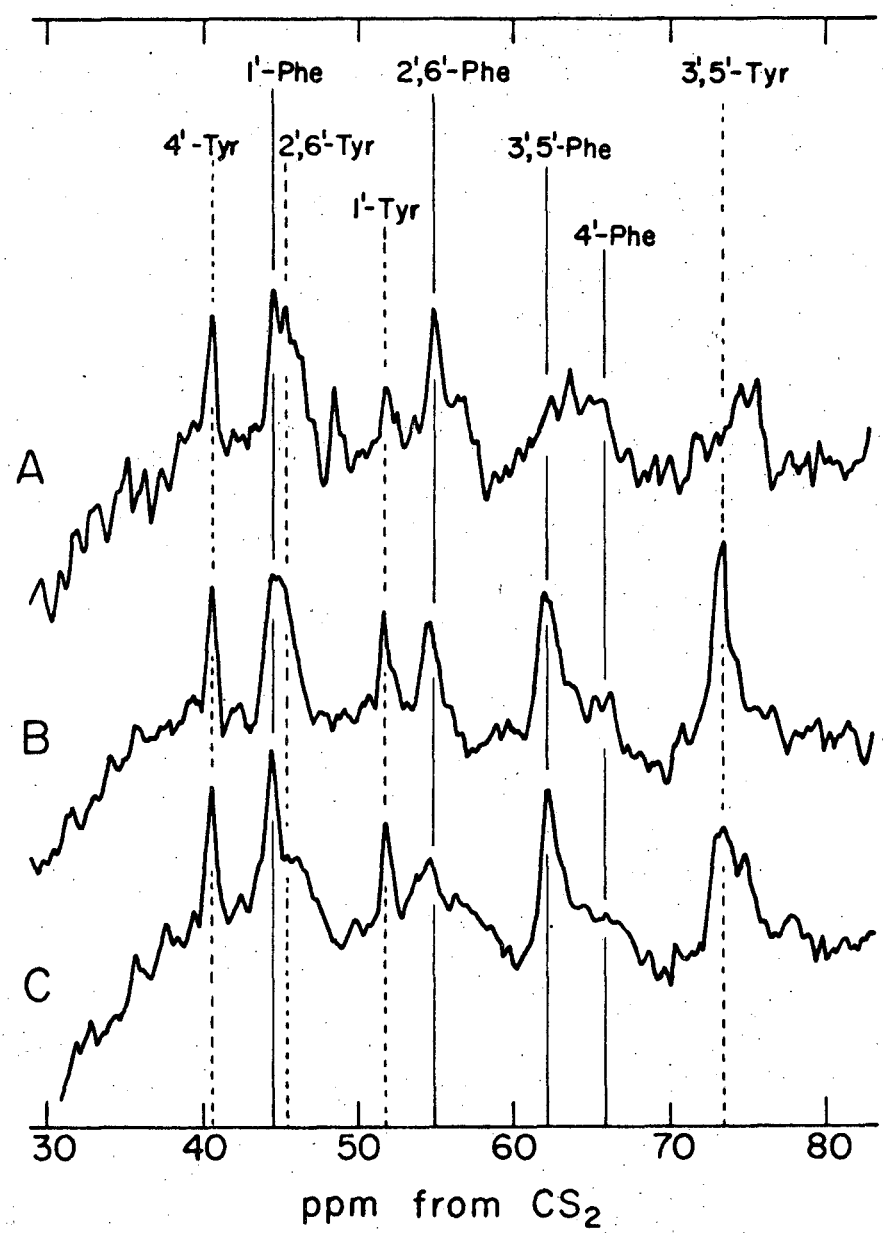
1'-Phe
2',6'-Phe
3',5'-Tyr
4'-Tyr
2',6'-Tyr
3',5'-Phe
1'-Tyr
4'-Phe
A
B
C
30
40
50
60
70
80
ppm from CS_2

Fig. 51. ^{1}H-NMR spectra of reduced C. acidi-urici ferredoxin (A) and (90±10)% reduced C. pasteurianum ferredoxin (B). C. acidi-urici ferredoxin (22°C) was reduced with dithionite by Phillips (recent unpublished data), and C. pasteurianum ferredoxin (10°C) was reduced by methyl viologen and is an aliquot of the ^{13}C-NMR sample (Fig. 49B).

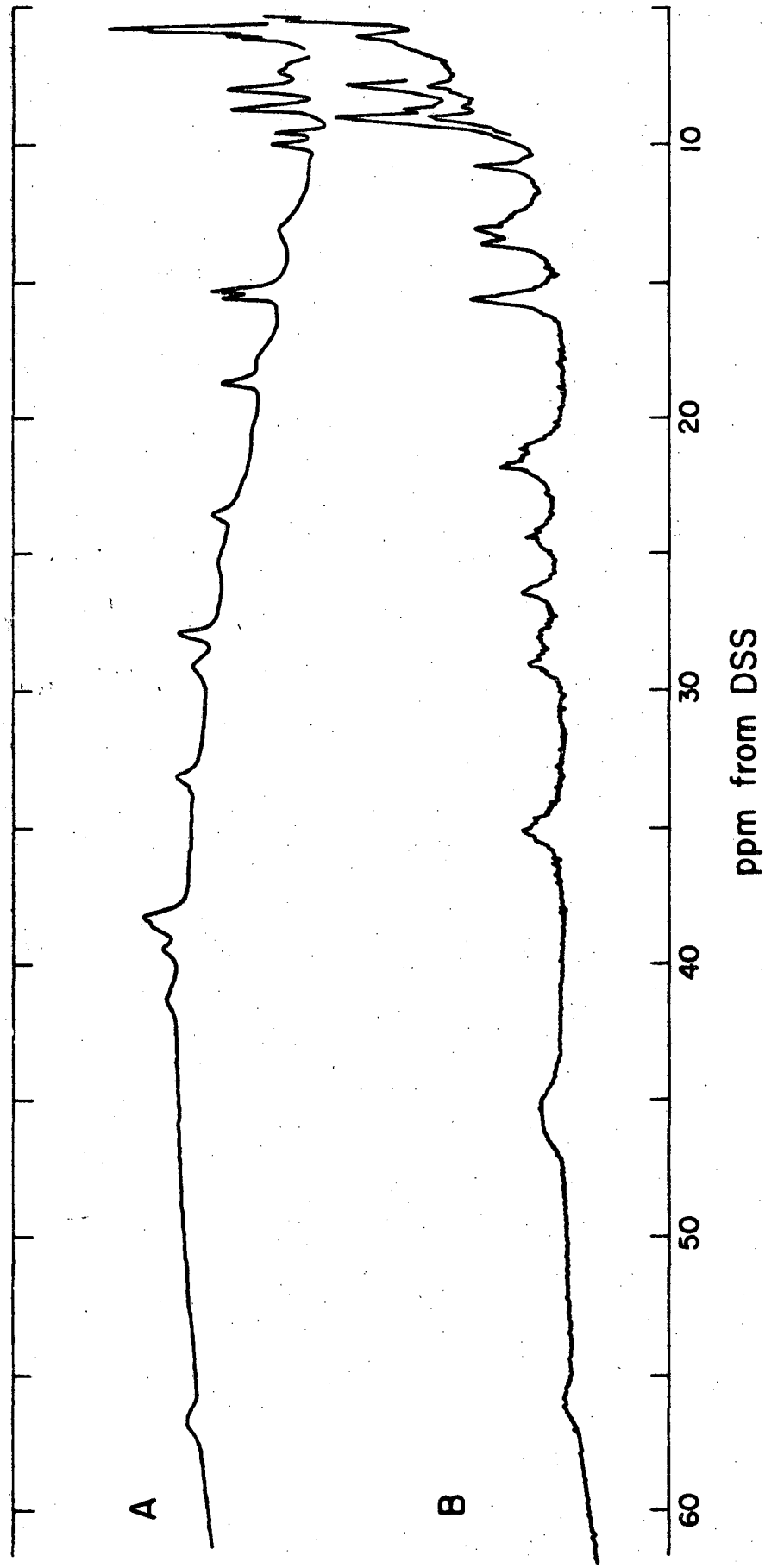
A
B
10
20
30
40
50
60
ppm from DSS

Fig. 52. ^{13}C-shifts of the tyrosyl residues in reduced C. acidi-urici and C. pasteurianum ferredoxin as a function of the most downfield aliphatic ^{1}H-shifts at different degrees of reduction. ^{13}C-shifts are relative to the corresponding ring carbon resonance positions in the oxidized protein at 10° C. The most downfield ^{1}H-shifts are relative to the most downfield ^{1}H-resonance position in the oxidized protein at 15-17° C (Figures 41 and 42 Experiment 6b). Arrows point to the ring carbon resonances of the Tyr^{2} residues of partially (↙) and "fully" (↙) reduced C. pasteurianum ferredoxins.

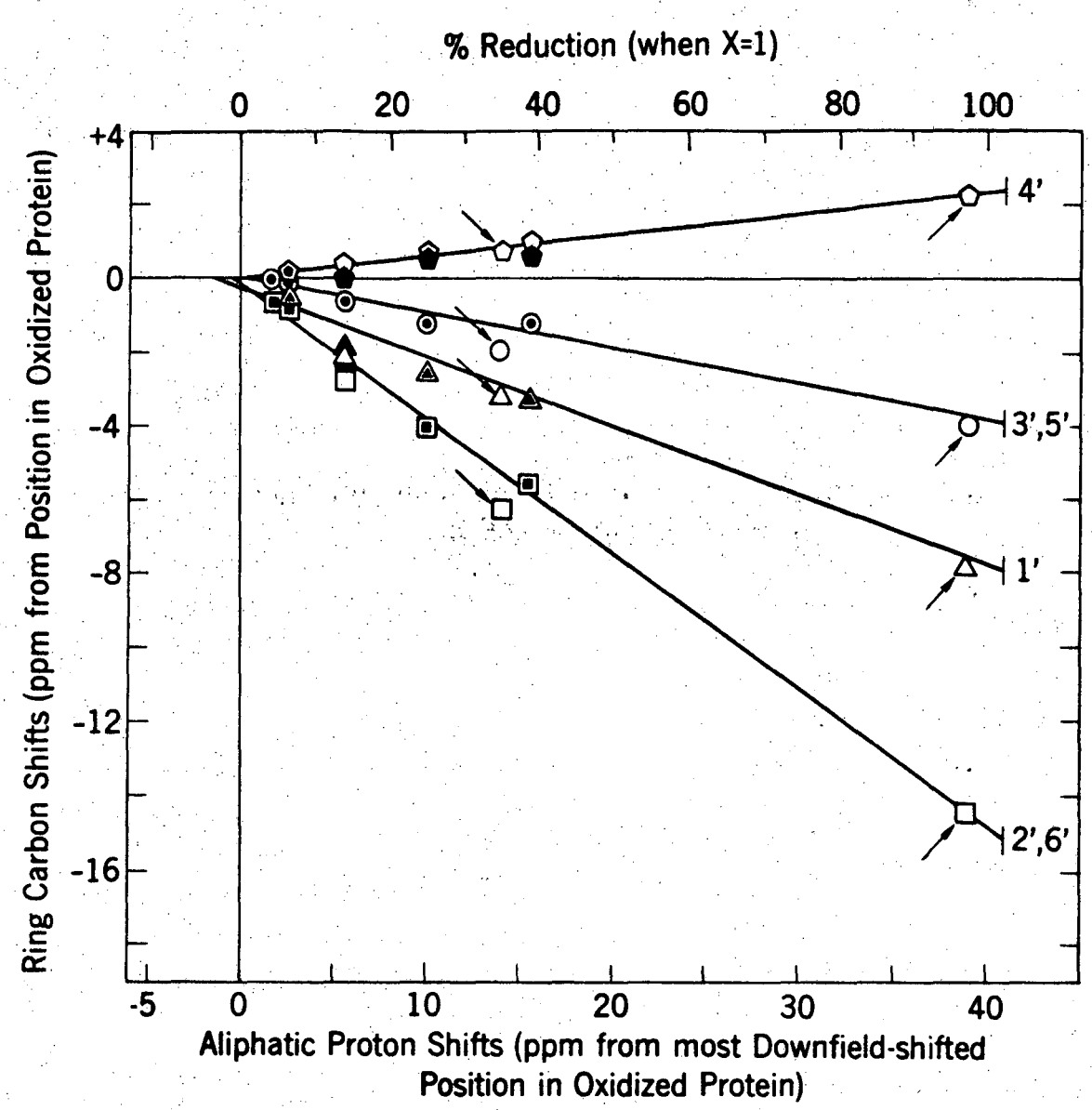
% Reduction (when X=1)
0
20
40
60
80
100
+4
0
-4
-8
-12
-16
Ring Carbon Shifts (ppm from Position in Oxidized Protein)
4'
3',5'
1'
2',6'
-5
0
10
20
30
40
Aliphatic Proton Shifts (ppm from most Downfield-shifted Position in Oxidized Protein)

Fig. 53. ^{1}H-NMR (15°C) of the aromatic region of oxidized (A) C. pasteurianum ferredoxin, ~40 mg/ml, pD 7.6; (B) C. acidi-urici [Phe^{2}]-ferredoxin, ~40 mg/ml, pD 7.6; and (C) C. acidi-urici native ferredoxin, ~40 mg/ml, pD 7.0. All ferredoxins were dissolved in 0.2 M K_2DPO_4-KD_2PO_4 buffer.

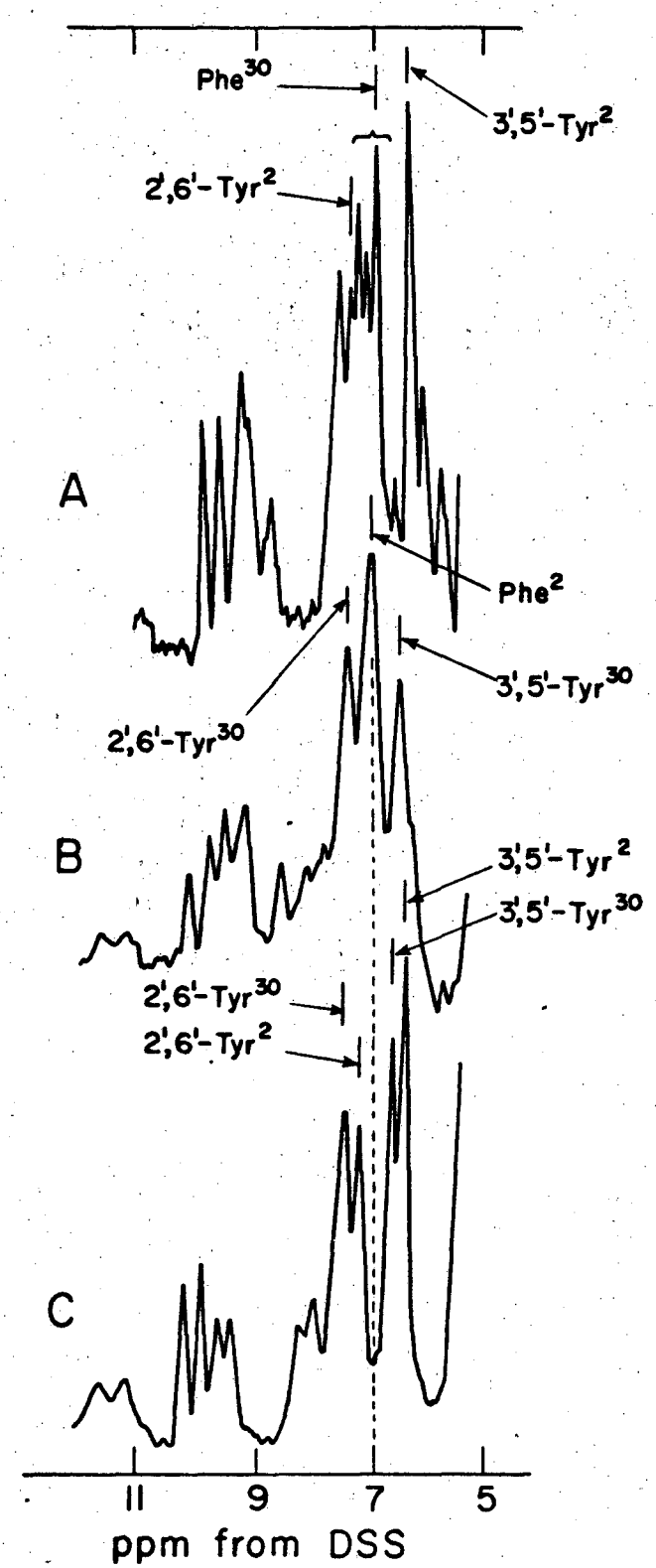
Phe30
3',5'-Tyr2
2',6'-Tyr2
A
Phe2
3',5'-Tyr30
2',6'-Tyr30
B
3',5'-Tyr2
3',5'-Tyr30
2',6'-Tyr30
2',6'-Tyr2
C
11
9
7
5
ppm from DSS

Fig. 54. ^{1}H-NMR (15° C) of the aromatic region of oxidized and methyl viologen-reduced C. acidi-urici ferredoxin (A): Oxidized, (B): 20% Reduced, (C): 50% reduced. The resonances upfield and downfield of 7.0 ppm from DSS are the 3', 5' - and 2', 6' - tyrosyl proton resonances respectively. (The arrows point to tentatively assigned 2', 6'-proton resonances.)

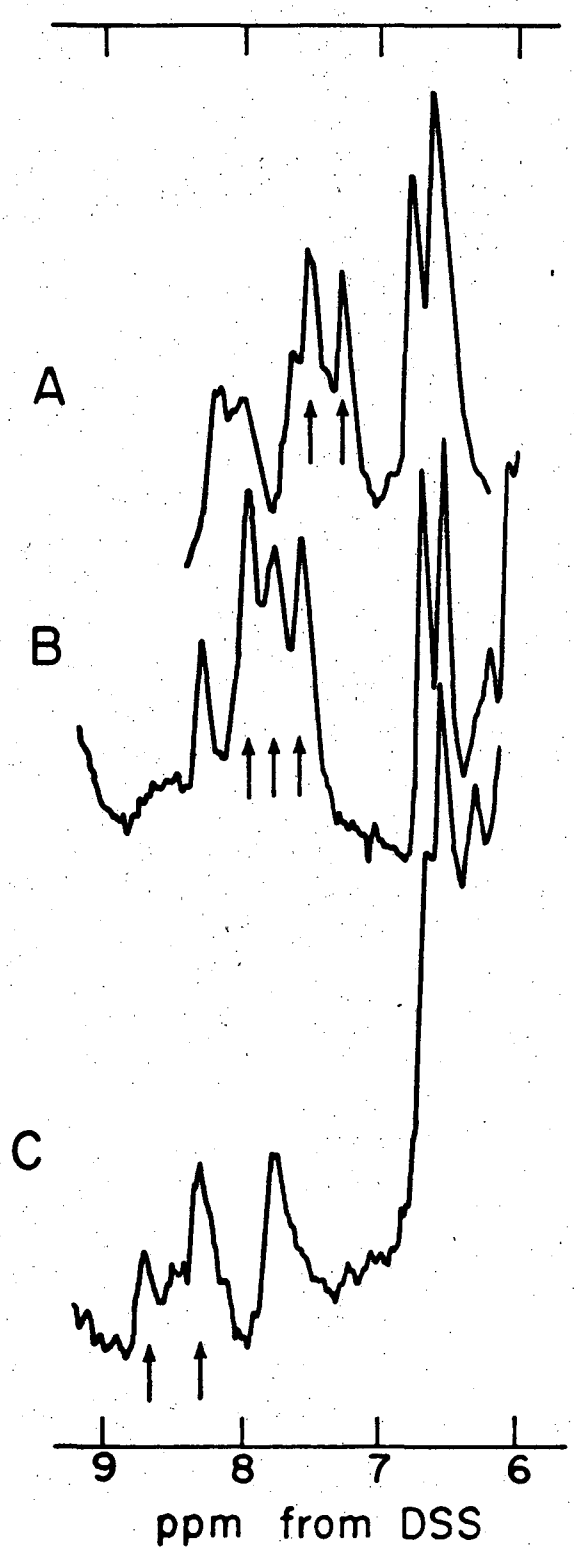
A
B
C
9
8
7
6
ppm from DSS

Fig. 55. ^{1}H-NMR shifts of the tyrosyl residues in reduced C. acidiurici ferredoxin relative to DSS. The percent reduction was determined from the most downfield shifted aliphatic proton resonance (see Experiment 6b).

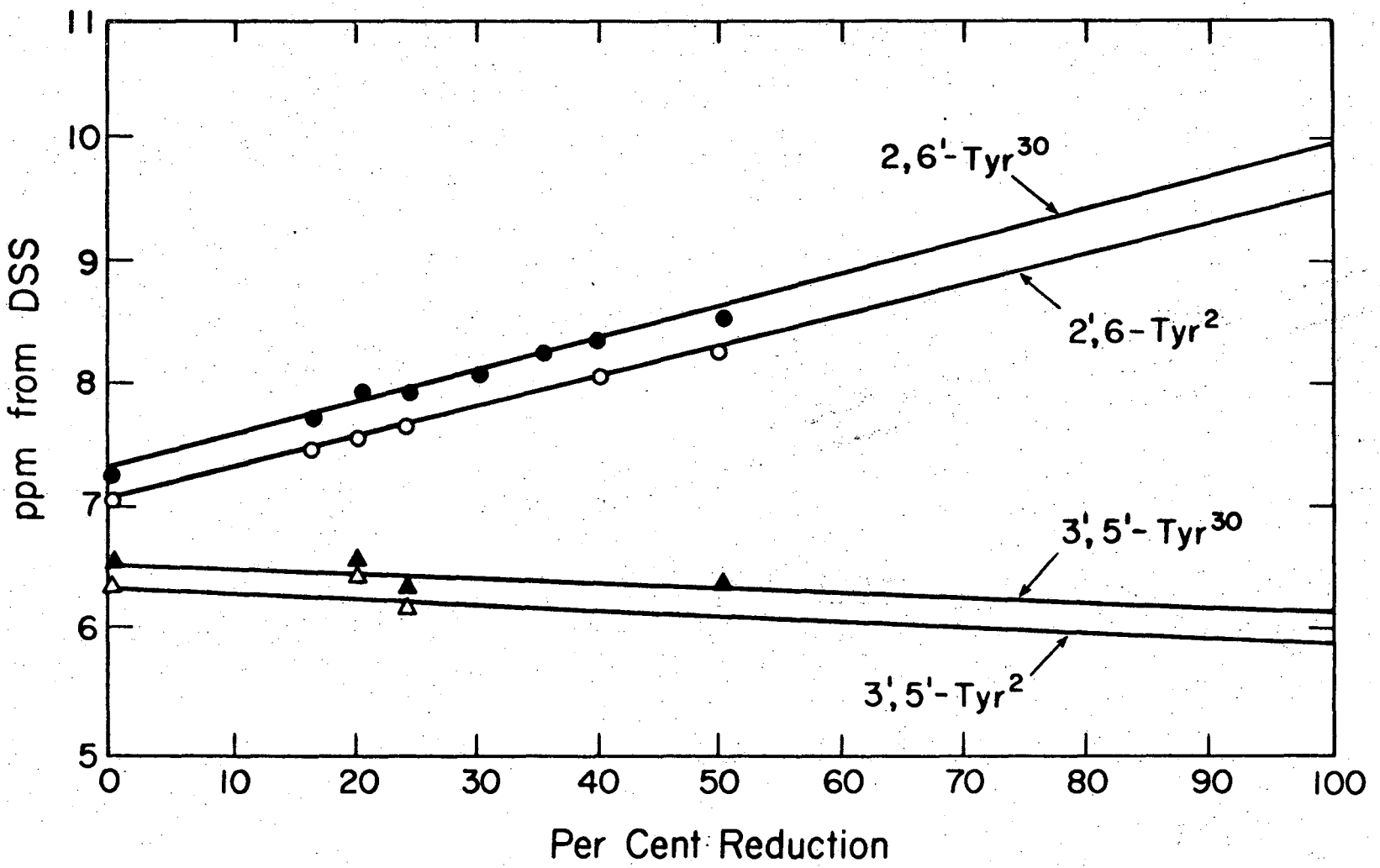
ppm from DSS
Per Cent Reduction
2,6'-Tyr30
2',6-Tyr2
3',5'-Tyr30
3',5'-Tyr2
11
10
9
8
7
6
5
0
10
20
30
40
50
60
70
80
90
100

Fig. 56. ^{1}H-NMR (15° C) of the aromatic region of oxidized (A) and fully reduced (B) C. pasteurianum ferredoxin. Reduction was by methyl viologen. Peak numbers XIV and XV refer to the 2', 6' protons of the tyrosyl and phenylalanyl residues respectively and peak numbers XV' and XVI refer to the 3', 5' protons of the phenylalanyl and tyrosyl residues respectively.

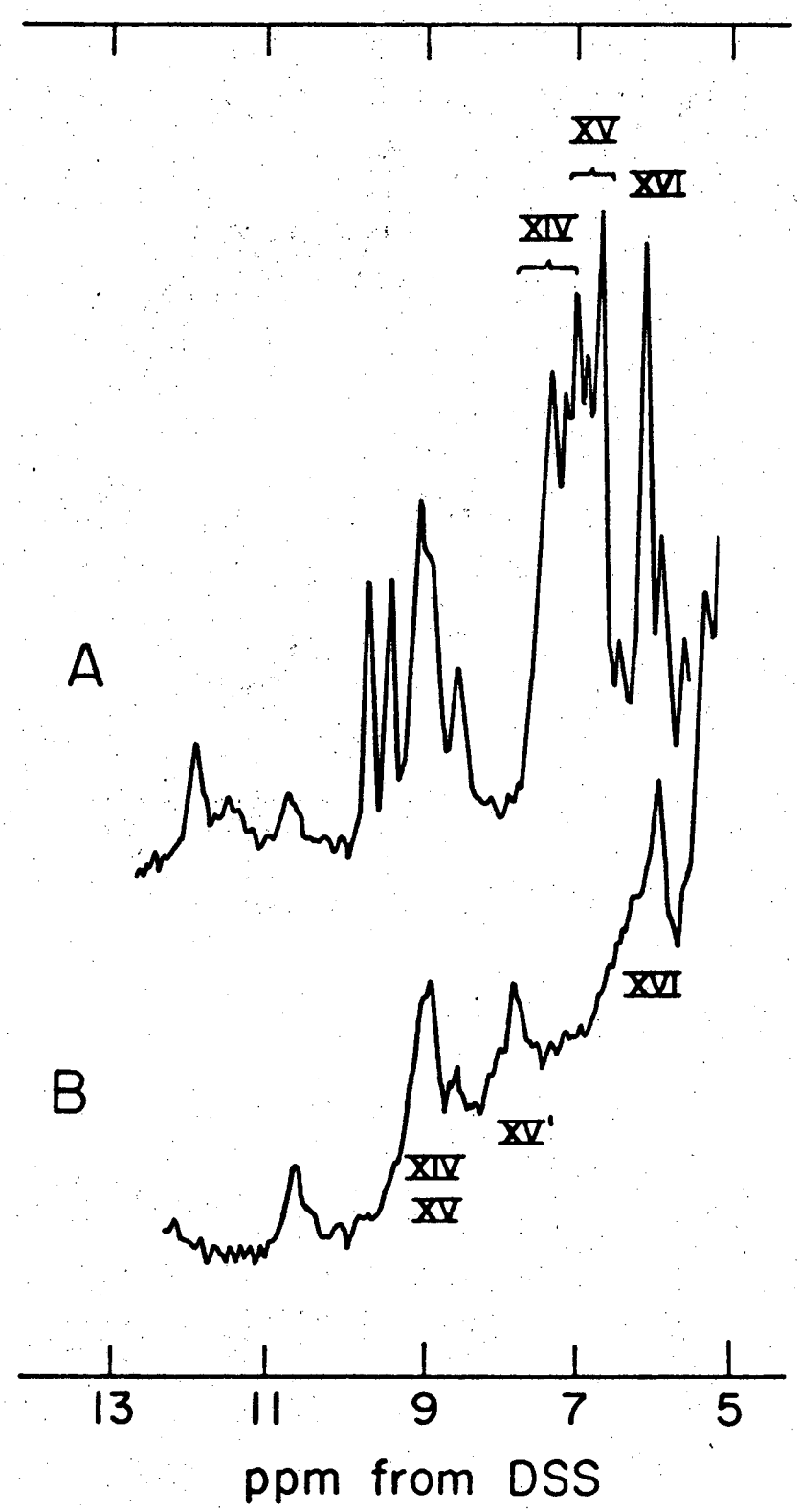
XV
XVI
XIV
A
XVI
B
XV'
XIV
XV
13
11
9
7
5
ppm from DSS

Table 19. ^{13}C-ring carbon shifts[a] of diamagnetic reference compounds and three oxidized clostridial-type ferredoxins.

Compound	Ring carbon 1'	2',6'	3',5'	4'
Diamagnetic reference compound:				
Tyrosyl residue:				
C. acidi-urici apoferredoxin	64.9	62.2	77.3	38.0
GlyGlyTyrGlyGly (52)	64.9	62.4	77.4	38.2
Phenylalanyl residue:				
Glycylphenylalanyl-amide acetate	56.5	63.6	64.0	65.5
model peptide (26,53)	56.4	63.5	63.9	65.6
Paramagnetic compound:				
Oxidized ferredoxins:				
C. acidi-urici				
Native:				
Tyr^2	59.5	60.4	77.3	38.5
Tyr^{30}	58.8	60.4	77.3	38.0
[Phe^2]-:				
Phe^2	51.3	62.0	63.8	65.8
Tyr^{30}	58.7	60.4	77.4	38.2
C. pasteurianum				
Native:				
Tyr^2	59.3	59.6	77.4	38.2
Phe^{30}	51.2	61.1	64.0	65.4

a. Shifts (ppm, relative to CS_2) are accurate to $\pm$ 0.2 ppm. Positive shifts are upfield of the reference compound. (In this table all shifts are positive.)

Table 20. Observed ^{13}C ring carbon resonance shifts[a] of the aromatic residues of oxidized *C. acidi-urici* and *C. pasteurianum* ferredoxins.

Ferredoxin	Ring carbon 1'	2',6'	3',5'	4'	Ring carbon 1'	2',6'	3',5'	4'
		Tyr^{2}				Phe^{30}		
C. pasteurianum	-5.6	-2.6	+0.1	+0.2[b]	-5.7	-2.0	0	-0.3
		Tyr^{2}				Tyr^{30}		
C. acidi-urici native	-5.6	-2.1	0	+0.6[b]	-6.3	-2.1	0	0
		Phe^{2}				Tyr^{30}		
C. acidi-urici [Phe^{2}]	-5.3	-1.7	-0.2	+0.3[b]	-6.1	-1.9	-0.1	+0.2[b]

a. Shifts are accurate to ± 0.2 ppm. Tyrosyl shifts are relative to the shifts of the tyrosyl residues in *C. acidi-urici* apoferredoxin, pD 7.8, and phenylalanyl shifts are relative to the shifts of the phenylalanyl residue in glycylphenylalanylamide acetate, pD 7.4 (Table 19).

b. Positive shifts are upfield shifts.

Table 21. Observed ^{13}C-shifts[a] of the aromatic residues of reduced C. acidi-urici ferredoxin and reduced C. pasteurianum ferredoxin relative to the shifts of the corresponding oxidized protein.

Ferredoxin	% Protein reduced[b]	Ring carbon 1'	Ring carbon 2',6'	Ring carbon 3',5'	Ring carbon 4'	Ring carbon 1'	Ring carbon 2',6'	Ring carbon 3',5'	Ring carbon 4'
C. acidi-urici			Phe^{2}				Tyr^{30}		
[Phe^{2}]-	(17 ± 5)[c]	-2.1	-2.8	-1.0	+0.2[d]	-2.0	-2.5	-0.6	+0.3
C. acidi-urici			Tyr^{2}				Tyr^{30}		
native	100[e]	-8±0.7	-14±1.5	-4±0.5	+2.4±0.5	-8±0.4	-14±1.5	-4±0.5	+2.4±0.5
C. pasteurianum	(90 ± 10)[f]		Tyr^{2}				Phe^{30}		
		-7.7	-14.5	-4.0	+2.2	-6.5	-7.2	-2.0	+0.8[d]

a. Shifts are ± 0.2 ppm if not indicated otherwise. Positive shifts are upfield shifts.
b. Based on ^{1}H-NMR spectra of aliquots of the ^{13}C-NMR samples (See Table 23).
c. Based on Fig. 48E.

Notes to Table 21 continued.

d. These values could have large errors, since the positions of these resonances were difficult to determine in the reduced protein.

e. Based on extrapolation to dithionite end-point (See Fig. 52).

f. Based on Fig. 49B.

Table 22. ^{13}C-ring carbon resonance shifts[a] of reduced C. acidi-urici [Phe^2]-ferredoxin and reduced C. pasteurianum ferredoxin.

Ferredoxin	% Protein reduced[b]	Ring carbon 1'	2',6'	3',5'	4'
C. acidi-urici[c] [Phe^2]-	17 ± 5				
Phe^2		49.2	59.2	62.8	65.6
Tyr^{30}		56.7	57.9	76.8	38.2
C. pasteurianum[d]	90 ± 10				
Tyr^2		51.6	45.1	73.4	40.4
Phe^{30}		44.4	54.4	62.1	66.0

a. Shifts are ± 0.2 ppm relative to CS_2.

b. Based on ^1H-NMR of aliquots of samples used for ^{13}C-studies (See Table 23).

c. Based on Fig. 48E.

d. Based on Figs. 49B, 50B.

Table 23. The fractional degree of reduction calculated from ^{1}H-NMR spectra of aliquots of methyl viologen-reduced ferredoxin used for ^{13}C-NMR studies.

^{1}H-NMR spectra[a]	^{13}C-NMR spectra[b]				
	Ring carbon				Average
	1'[c]	2',6'	3',5'	4'	
0.05	0.04	0.08	0	0	0.03
0.06	0.05	0.09	0.05	0	0.05
0.14[d]	0.27	0.19	0.25	0.09	0.20
0.24	0.33	0.28	0.31	0.24	0.29
0.35	0.39	0.41	0.31	0.39	0.38

a. To calculate the fractional degree of reduction of partially reduced ferredoxins (Figs. 40 and 41, Experiment 6b) from the ^{1}H-NMR spectra of aliquots of the ^{13}C-NMR samples, one subtracts 16 ppm (the resonance position of the most downfield-shifted proton resonance in the oxidized protein) from the resonance position of the most downfield-shifted proton in the reduced protein. This difference is then divided by 40.4 ppm (the difference between the most downfield resonance in the oxidized protein and the most downfield resonance position (recently observed by Phillips)) in dithionite-reduced ferredoxin (Fig. 51). This 40.4 ppm difference is assumed to represent 100% reduction.

b. To calculate the fractional degree of reduction of partially reduced ferredoxins from ^{13}C-NMR spectra one subtracts the resonance position of the corresponding ring carbon resonances of Tyr^{2} in oxidized protein from the observed ring carbon resonance of Tyr^{2} in partially reduced ferredoxin and divides this by the corresponding ring carbon shift (relative to the oxidized protein) of

Notes to Table 23 continued.

b. (continued) the Tyr^2 residue in "fully" reduced *C. pasteurianum* ferredoxin.

c. For *C. acidi-urici* native ferredoxin this is an average of both 1'-ring carbon resonances.

d. This is *C. acidi-urici* [Phe^2]-ferredoxin, and the percent reduction is calculated from the Phe^2 ring carbon resonance shifts of *C. acidi-urici* [Phe^2]-ferredoxin and the Tyr^2 resonance shifts of "fully" reduced *C. pasteurianum* ferredoxin.

Table 24. ^{1}H-NMR shifts[a] of the aromatic residues of oxidized C. acidi-urici native ferredoxin, C. acidi-urici [Phe^{2}]-ferredoxin, and C. pasteurianum ferredoxin.

	Ring protons		Difference from Reference compound: Ring protons	
	2',6'	3',5'	2',6'	3',5'
Reference compound:				
Amino acid				
Phenyl-alanine[b]	7.37	7.37	-	-
Tyrosine[b]	7.19	6.90	-	-
Peptide[c] tyrosine	7.10	6.80	-	-
C. acidi-urici apoferredoxin tyrosine[d]	6.93	6.66	+0.3[e]	+0.2[e,f]
Sample:				
C. acidi-urici native				
Tyr^{30}	7.32	6.57	-0.4[g]	+0.1[g]
Tyr^{2}	7.07	6.39	-0.1[g]	+0.3[g]
C. acidi-urici [Phe^{2}]-				
Tyr^{30}	7.32	6.49	-0.4[f]	+0.2[f]
Phe^{2}	7.00[i]	7.00[i]	+0.4[h]	+0.4[h]
C. pas-teurianum				
Phe^{30}	7.2±0.2[j]	7.2±0.2[j]	-0.2±0.2[h]	-0.2±0.2[h]
Tyr^{2}	7.2±0.2[j]	6.40	-0.2±0.2[f]	+0.3[f]

Notes to Table 24.

a. Shifts are ± 0.05 ppm relative to DSS unless otherwise indicated.

b. From reference (119).

c. From reference (86).

d. From Fig. 15, Experiment 2.

e. Difference = (amino acid shift - apoferredoxin shifts)

f. Positive shifts (relative to reference) are upfield shifts.

g. Difference = (apoferredoxin shift - ferredoxin shift).

h. Difference = (amino acid shift - ferredoxin shift).

i. Includes all Phe^2-ring proton resonances.

j. This region contains resonances at 7.00, 7.17, 7.27, and 7.39 ppm.

Table 25. ^{1}H-NMR shifts of the aromatic residues of reduced C. acidi-urici ferredoxins.

Percent reduction	Shift[a] relative to DSS Ring proton 2',6' Tyr^{30}	2',6' Tyr^{2}	3',5' Tyr^{30}	3',5' Tyr^{2}	Shift[b] relative to oxidized protein Ring proton 2',6' Tyr^{30}	2',6' Tyr^{2}	3',5' Tyr^{30}	3',5' Tyr^{2}
0	7.3	7.1	6.6	6.4	-	-	-	-
16	7.8	7.5	-	-	-0.5	-0.4	-	-
20[c,d]	8.0	7.6	6.6	6.5	-0.7	-0.5	0	-0.1
24[c]	8.0	7.7	6.4	6.2	-0.7	-0.6	+0.2	+0.2
30[e]	8.1	-	-	-	-0.8	-	-	-
35[e]	8.3	-	-	-	-1.0	-	-	-
40[e]	8.4	8.1	-	-	-1.1	-1.0	-	-
50[d,e]	8.6	8.3	6.4	-	-1.3	-1.1	+0.3	-
100[f]	10.0	9.6	6.2	5.9	-2.7	-2.4	+0.4	+0.5
100[g]	10.3	9.8	-	-	-3.0	-2.9	-	-

a. Shifts are ± 0.1 ppm relative to DSS and are based on tentative assignments.

b. Negative shifts relative to the oxidized protein are downfield shifts. Positive shifts relative to the oxidized protein are upfield shifts.

Notes to Table 25 continued.

c. Based on Fig. 40.
d. Based on Fig. 54.
e. Based on Fig. 41.
f. Extrapolated to 100% reduction (Fig. 52).
g. From dithionite-reduced C. acidi-urici ferredoxin (Fig. 51A).

Table 26. Ring carbon and proton resonance shifts[a] of "fully" reduced *C. acidi-urici* and *C. pasteurianum* ferredoxin.

Ferredoxin	Aromatic residue	Ring atom	Shift	Ratio[b] C:H
C. pasteurianum	Tyr^{2}	2',6'-C	-(14.5 ± 0.2)[c]	+(7 ± 2)
		2',6'-H	-(2.1 ± 0.5)[d]	
		3',5'-C	-(4.0 ± 0.2)[c]	-(7 ± 4)
		3',5'-H	+(0.8 ± 0.5)[d]	
	Phe^{30}	2',6'-C	-(7.2 ± 0.2)[c]	+(6 ± 2)
		2',6'-H	-(1.4 ± 0.5)[d]	
		3',5'-C	-(2.0 ± 0.2)[c]	+(4 ± 2)
		3',5'-H	-(0.5 ± 0.5)[d]	
C. acidi-urici	Tyr^{2},Tyr^{30}	2',6'-C	-(14 ± 1.5)[e]	+(5 ± 1)
	Tyr^{30}	2',6'-H	-(2.7 ± 0.1)[f]	
	Tyr^{2}	2',6'-H	-(2.4 ± 0.1)[f]	
	Tyr^{2},Tyr^{30}	3',5'-C	-(4 ± 0.5)[e]	-(12 ± 7)
	Tyr^{30}	3',5'-H	+(0.4 ± 0.1)[f]	
	Tyr^{2}	3',5'-H	+(0.5 ± 0.1)[f]	

Notes to Table 26.

a. Shifts (ppm) are relative to that of the oxidized protein. Positive shifts are upfield shifts.
b. Ratio of ring carbon atom shift to corresponding ring proton shift.
c. Based on Fig. 49B.
d. Based on double resonance experiments (Fig. 50).
e. Extrapolated from ^{13}C-NMR spectra of partially reduced C. acidi-urici ferredoxins (Fig. 52, Table 23).
f. Extrapolated from ^{1}H-NMR spectra of partially reduced C. acidi-urici ferredoxins (Fig. 55).

Experiment 7c.

The redox potential of each Fe-S cluster of Clostridium acidi-urici and Clostridium pasteurianum ferredoxins

SUMMARY:

^{13}C-NMR of oxidized and reduced C. acidi-urici and C. pasteurianum ferredoxin show that: (i) the midpoint redox potential of C. acidi-urici ferredoxin is (47 ± 10) mV less than that of C. pasteurianum ferredoxin; (ii) in both proteins each iron-sulfur (Fe-S) cluster can be distinguished, (iii) in both proteins cluster II produces essentially the same magnetic shifts on its neighboring aromatic residue, at the same degree of reduction, and (iv) in C. pasteurianum ferredoxin the midpoint redox potential of cluster II is ~ 10 mV less than that of cluster I. This difference in redox potentials can be attributed to differences in protein conformation.

INTRODUCTION:

The midpoint redox potentials of proteins containing "cube-like" Fe-S clusters can be very different. Midpoint redox potentials have been measured for clostridial ferredoxins from Chromatium (7) and C. pasteurianum (126) and for the high potential iron protein from Chromatium (36). They are approximately -490, -390, and +350 mV (relative to the H_2 electrode, pH 7), respectively.

The bond lengths of the two Fe-S clusters in P. aerogenes and the and the single Fe-S cluster in Chromatium high potential iron protein are essentially identical (25). If we assume that the Fe-S clusters have the same geometrical structure in all clostridial-type ferredoxins, then the above mentioned differences in redox potential cannot be soley

attributed to the geometrical structure of the Fe-S clusters. The difference in redox potentials may be due to the differences in amino acid sequence and conformation among clostridial ferredoxins and Chromatium high potential iron protein.

Carter et al. (25) have recently hypothesized that the differences in redox potentials of Chromatium high potential iron protein and P. aerogenes ferredoxin are due to differences in the oxidation states of iron within the Fe-S clusters in each protein. They further assume that a possible role of the protein conformation of these proteins is to prevent the Fe-S clusters in each protein from achieving all of its potential oxidation states [a cluster could have more than two oxidation states (25, 57)]. They state that the redox potentials of these proteins is only slightly influenced by the differences in protein conformation.

We would like to know if two clostridial ferredoxins which have very similar amino acid sequences have similar redox potentials, and if small differences in the sequences of such similar ferredoxins correlate with differences in redox potential. For this purpose we did ^{13}C-NMR studies of the aromatic residues of C. acidi-urici and C. pasteurianum ferredoxins.

With ^{13}C-NMR techniques we can distinguish each Fe-S cluster in C. pasteurianum and C. acidi-urici ferredoxin by using the aromatic residues as probes. The ring carbon resonances shift with increasing protein reduction, suggesting that the ring carbon atoms are close to Fe-S clusters, a fact which is consistent with the ESR experiment which showsthat the reducing electron is associated with the iron atoms in these proteins (see Experiment 4). This allows us to determine the relative midpoint redox potentials of each protein and of

each Fe-S cluster within each protein, because the redox potential is proportional to the degree of Fe-S cluster reduction.

Jensen (2) has determined that in P. aerogenes ferredoxin Fe-S clusters II and I are physically close to aromatic residues 2 and 28 respectively. We assume that in C. acidi-urici ferredoxin Fe-S clusters II and I are physically close to aromatic residues 2 and 30 respectively, because C. acidi-urici ferredoxin and P. aerogenes ferredoxin have similar amino acid sequences (See General Introduction).

RESULTS:

To determine the relative redox potentials of C. acidi-urici and C. pasteurianum ferredoxin, a sample of reduced C. acidi-urici ferredoxin (Fig. 57B) and reduced C. pasteurianum ferredoxin (Fig. 57D) was mixed to give a new equilibration mixture (Fig. 57C). The protein concentration ratio of the two reduced ferredoxins in this mixture was 3:1, [C. acidi-urici ferredoxin] :[C. pasteurianum ferredoxin] , and this facilitated the assignment (Table 27) of the ring carbon resonances of each ferredoxin, since the intensity of each resonance is proportional to the corresponding protein concentrations. Thus the smaller resonance peaks seen in Fig. 57C represent the ring carbon resonances of the C. pasteurianum ferredoxin in the equilibrium mixture and the larger resonances at 57.8, 58.5, 59.1 and 77.2 in Fig. 57B represent the ring carbon resonances of the C. acidi-urici ferredoxin in this mixture. The C. acidi-urici ferredoxin resonances in this mixture have been assigned by techniques described in Experiments 7a and 7b.

Deconvolution techniques (47) can further aid in assigning ^{13}C resonances. These techniques increase the resolution of ^{13}C-NMR

spectra by artifically narrowing all the resonances, but this increase in resolution is accompanied by a corresponding loss in the signal to noise ratio. Nevertheless, it is very unlikely that the increased noise in the deconvoluted spectrum should produce noise spikes at exactly the same positions in the convoluted (normal) spectrum. For example, in the ^{13}C-NMR spectra of the aromatic region of the equilibrium mixture of C. acidi-urici and C. pasteurianum ferredoxins (Fig. 58A, 58B), the sharp resonances at 39.0 and 59.1 are not noise spikes, for they appear in the same positions in the deconvoluted (Fig. 58A) and convoluted (Fig. 58B) spectra. (The Fig. 58A spectrum is the deconvoluted form of the Fig. 58B spectrum). These resonances are assigned to the 4' -Tyr^{2} and 1' -Phe^{30} ring carbon atoms of C. pasteurianum ferredoxin respectively. The resonance at 56.2 ppm is narrower in both deconvoluted and convoluted spectra than any of the other resonances corresponding to the ring carbons of C. pasteurianum ferredoxin in this equilibrium mixture, and thus this resonance is assigned to the C. pasteurianum ferredoxin 1' -Tyr^{2} ring carbon atom.

Other techniques described in Experiments 7a and 7b such as comparison of noise decoupled, coherent decoupled and coupled spectra of the aromatic region of the equilibrium mixture confirm the assignments listed in Table 27. From these assignments we conclude that in the equilibrium mixture of reduced methyl viologen and two reduced ferredoxins the ring carbon resonances of Tyr^{2} and Phe^{30} of C. pasteurianum ferredoxin are more shifted than the ring carbon resonances of Tyr^{2} and Tyr^{30} in C. acidi-urici ferredoxin (Table 28). Thus, under the same reducing conditions, C. pasteurianum ferredoxin is more reduced and

has a higher midpoint redox potential than C. acidi-urici ferredoxin.

DEGREE OF REDUCTION:

The magnitude of the ring carbon shifts of a single aromatic residue reflects the degree of reduction of its neighboring Fe-S cluster and the redox potential of the Fe-S cluster is proportional to the degree of reduction of this cluster (see Appendix B). Each aromatic residue can be distinguished in C. pasteurianum ferredoxin and C. acidi-urici [Phe^2] -ferredoxin (see Experiment 7b). Since each aromatic residue is close to one Fe-S cluster and the reducing electron is associated with each cluster, the ring carbon shifts of each (distinguishable) aromatic residue can be used to determine the redox potential of each cluster.

MIDPOINT REDOX POTENTIAL:

The midpoint redox potential of the two ferredoxins and of each of the two clusters in each protein can be estimated if one assumes that the two distinguishable clusters are reduced independently and do not interact (See Appendix C), and ring carbon resonance shifts (relative to the oxidized protein shifts) are proportional to the degree of reduction. We assume that clusters I and II of "fully" reduced C. acidi-urici ferredoxin and cluster II of "fully" reduced C. pasteurianum ferredoxin are essentially equally reduced, because the extrapolated resonance shifts (See Experiment 7b) of the corresponding ring carbon atoms of both aromatic residues in C. acidi-urici ferredoxin are essentially equal to the observed resonance shifts of the corresponding ring carbon atoms of Tyr^2 in "fully" reduced C. pasteurianum ferredoxin.

CALCULATION OF MIDPOINT REDOX POTENTIAL: In the "fully" reduced proteins, the percent reduction of cluster II in C. pasteurianum ferredoxin and clusters I and II in C. acidi-urici ferredoxin is 100X, and it is 100Y for cluster I of C. pasteurianum ferredoxin. Cluster and protein midpoint redox potentials both depend on X and Y.

The ferredoxins are in equilibrium with methyl viologen. Thus, for each protein the electrode potentials E_I and E_{II}, of clusters I and II respectively, are equal to each other. E_I and E_{II} (at 10 °C) are defined by and calculated from the Nernst equation (140):

$$E_I(\text{volts}) = E_I^{0'} - 0.056 \log_{10} \left(\frac{mX}{1-mX} \right) \quad (1)$$

$$E_{II}(\text{volts}) = E_{II}^{0'} - 0.056 \log_{10} \left(\frac{kY}{1-kY} \right) \quad (2)$$

where m and k are the fractional degrees of reduction of clusters I and II respectively relative to the "fully" reduced protein. $E_I^{0'}$ and $E_{II}^{0'}$ are the cluster-midpoint redox potentials. The protein midpoint redox potential is $(E_I^{0'} + E_{II}^{0'})/2$ and is the observed redox potential when the protein is reduced by one electron. The difference in cluster midpoint redox potentials in each protein can be calculated from Eqs. (1) and (2) and is the same for all observed m and k values. For $X \leq 1$ in C. pasteurianum ferredoxin the difference in cluster midpoint redox potentials, $E_{II}^{0'} - E_I^{0'}$, is ≥ 10 mV.

The validity of the dithionite endpoint

In ^{1}H-NMR spectra of dithionite-reduced C. acidi-urici ferredoxin, (Fig. 51A, Experiment 7b) and dithionite-reduced C. pasteurianum ferredoxin (103), the most downfield-shifted proton resonances are shifted

to the same extent. We observe similar proton shifts for methyl viologen-reduced C. pasteurianum ferredoxin (Fig. 51B, Experiment 7b). If sodium dithionite did not fully reduce these proteins one would not expect similar magnitudes of proton shifts for both ferredoxins. Nevertheless it is possible that the high concentrations of ferredoxin required for NMR experiments does not permit the protein to become fully reduced. We cannot at present (by optical methods) independently measure the degree of reduction of the methyl viologen-reduced ^{13}C-NMR ferredoxin samples since it is difficult to obtain reproducibly diluted aliquots of these samples. Until we can do such measurements we must either assume that the ^{1}H-NMR spectra of dithionite-reduced ferredoxins is the reduction endpoint and that cluster II is 100% reduced (X = 1) or that cluster II is not 100% reduced (X < 1). Either assumption does not invalidate the observation that C. acidi-urici ferredoxin has a lower midpoint redox potential than cluster II in C. pasteurianum (and perhaps in C. acidi-urici) ferredoxin. Only the calculated magnitudes of the differences in these redox potentials will change depending on whether we assume X = 1 or X < 1.

Calculation if X = 1

Cluster midpoint redox potential

The degree of reduction of each cluster is proportional to the ratio of the corresponding ring carbon resonance shifts of the partially reduced ferredoxin to that of the "fully" reduced ferredoxin. From this ratio we calculate that in partially reduced C. pasteurianum ferredoxin (Fig. 57C) cluster I (near Phe^{30}) is (32 ± 3.5)% reduced, cluster II (near Tyr^{2}) is (42 ± 3)% reduced. The difference between the midpoint

redox potentials of each Fe-S cluster in C. pasteurianum ferredoxin is on the order of 10 mV.

Similarly, from the ratios of the magnitude of the 1' - and 2', 6' - ring carbon shifts of partially and (extrapolated) "fully" reduced C. acidi-urici ferredoxin we calculate that in partially reduced native C. acidi-urici ferredoxin (Figs.57B, 57C), both clusters are (8±2)% reduced, and, in C. acidi-urici [Phe^2] -ferredoxin (Experiment 7b, Fig. 48E), cluster I (near Tyr^{30}) and II (near Phe^2) are (20±4)% and (23±3)% reduced, respectively. From these estimates (Table 29) the difference between the midpoint redox potential of each Fe-S cluster in C. acidi-urici ferredoxin is calculated to be < 10 mV.

The degree of cluster II reduction calculated from ring carbon resonances (Table 29) correlates well with the degree of protein reduction calculated from the most downfield shifted proton resonances (See Table 23, Experiment 7b).

Protein midpoint redox potential

In the equilibrium mixture (Fig. 57C) of C. acidi-urici (CA) and C. pasteurianum (CP) ferredoxin, the electrode potentials E_I and E_{II} of Eqs. (1) and (2) of both proteins are all equal to each other. To determine the difference in protein midpoint redox potentials from this mixture, we calculate:

$$\left[(E_{II}^{0'}{}_{(CA)} - E_{II}^{0'}{}_{(CP)}) - (E_I^{0'}{}_{(CA)} - E_I^{0'}{}_{(CP)})\right]/2$$

This difference is estimated to be (47±10) mV. Adding this to -383 mV (pH 7.4, 23°) the midpoint redox potential of C. pasteurianum ferredoxin (43), we calculate the midpoint redox potential of C. acidi-urici ferredoxin

to be - (430 ± 10) mV (pH 8.0, 25°). This assumes that X = 1 and that both protein midpoint redox potentials are independent of pH between pH 7.4 and 8.0 (see below).

DISCUSSION:

DISTINGUISHABLE REDUCTION SITES:

Eisentein and Wang (43) conclude that C. pasteurianum ferredoxin is reduced in two reduction steps. They assume that the reduction sites are indistinguishable and calculate two different midpoint redox potentials, $E_1^{0'}$ and $E_2^{0'}$, for each step. To fit their optical data they calculate that $(E_1^{0'} - E_2^{0'}) = (31 \pm 3)$mV and attribute this difference to a statistical factor equaling 36 mV. This statistical factor stems from their assumption that the reduction of C. pasteurianum ferredoxin involved two equivalent independent and indistinguishable reduction sites. This statistical factor vanishes as soon as one can distinguish each reduction site. The ability to distinguish each reduction site does not, of course, invalidate the hypothesis that ferredoxin is reduced in two reduction steps.

INTERACTION BETWEEN FE-S CLUSTERS: A large (~ 25 mV) difference between cluster midpoint redox potentials in C. pasteurianum ferredoxin would imply that, after one cluster is reduced, it interacts with the other Fe-S cluster by making it easier (or harder) to reduce. If there is no interaction between Fe-S clusters, a large difference between the cluster midpoint redox potentials of C. pasteurianum ferredoxin would be inconsistent with the data of Eisenstein and Wang (43). This conclusion is based on a recalculation of their data (Table 30), assuming distinguishable noninteracting sites (see Appendix C).

pH-INDEPENDENT MIDPOINT REDOX POTENTIAL:

Sobel and Lovenberg (122) show a large pH-dependence for the midpoint redox potential of C. pasteurianum ferredoxin and report the protein midpoint redox potential to be -450 mV at pH 8.0. If our C. pasteurianum ferredoxin is almost fully reduced with methyl viologen at pH 8.0 (Fig. 57D), the pH-dependent redox potential reported by Sobel and Lovenberg is inconsistent with our results, because the pH-dependent (87, 133) midpoint redox potential of methyl viologen is -444 mV (43, 133).

COUNTING ELECTRONS: Stoichiometric investigations show that two electrons can be transferred to clostridial-type ferredoxins (46, 85, 122). This has led Sobel and Lovenberg (122) to represent the reduction of C. pasteurianum ferredoxin with hydrogenase as:

$$Fd(ox) + H_2 \rightleftharpoons Fd(red) + 2H^+ \qquad (1a)$$

or

$$(0\text{-}0) + H_2 \rightleftharpoons (R\text{-}R) + 2H \qquad (1b)$$

Similarly, one could represent the reduction of C. acidi-urici ferredoxin with methyl viologen (mv) as:

$$Fd(ox) + 2mv^+ \rightleftharpoons Fd(red) + 2mv^{++} \qquad (2a)$$

or

$$(0\text{-}0) + 2mv^+ \rightleftharpoons (R\text{-}R) + 2mv^{++} \qquad (2b)$$

(In Eqs. (1b) and (2b) we denote the oxidation states of the two iron-sulfur clusters in clostridial-type ferredoxin as (0-0), (R-R), for the oxidized and fully reduced proteins, respectively.)

The protein midpoint redox potentials $E^{0'}$ can be calculated from Eqs. (1) and (2). At 25°C Eqs. (3) and (4) follow from Eqs. (1) and (2) respectively.

$$E^{0'} - \frac{0.059}{2} \log \frac{[R\text{-}R]}{[0\text{-}0]} = -\frac{0.059}{2} \log \left(\frac{p_{H_2}}{[H^+]^2} \right) \tag{3}$$

$$E^{0'} - \frac{0.059}{2} \log \frac{[R\text{-}R]}{[0\text{-}0]} = E^{0'}_{(mv)} - \frac{0.059}{2} \log \left(\frac{[mv^+]}{[mv^{++}]} \right)^2$$

$$= 0.444 - 0.059 \log \beta \tag{4}$$

where $\beta = [mv^+]/[mv^{++}]$.

The reduction of the clostridial-type ferredoxins most likely proceeds in two one-electron transfer steps. This was shown by Eisenstein and Wang for methyl viologen reduction of C. pasteurianum ferredoxin (43). Therefore, Eqs. (1) and (2) do not describe a physically real situation, since Eqs. (1) and (2) imply a single step reduction which involves the simultaneous transfer of two electrons into ferredoxin.

With methyl viologen reduction of ferredoxin, neglect of [0-R] and [R-0] would cause $E^{0'}$ to be a function of β and to become more positive with decreasing reduction (See Appendix B). Thus, if the estimate of $E^{0'}$ of -430 ± 10 mV for C. acidi-urici ferredoxin obtained from the ^{13}C-NMR measurements (which assumes single electron transfer steps) is correct, then a neglect of [0-R] and [R-0] in the estimate of [R-R]/[0-0] would cause $E^{0'}$ (in Eq. (4)) to be more positive than -430 mV for potential measurements where $\alpha < 1/2$ and to be more negative than -430 mV for potential measurements where $\alpha > 1/2$. At $\alpha = 1/2$, $E^{0'}$ would be equal to -430 ± 10 mV.

Nevertheless, a correct $E^{0'}$ is obtained from Eqs. (3) and (4) if the concentration of the two intermediate states of reduction in ferredoxin, [0-R] and [R-0], is considered. (There are two intermediate states since only one electron can reduce one or the other Fe-S clusters in the protein.) If these intermediate states are considered one can correctly estimate the ratio of [R-R] /[0-0] from the experimental determination of α, the degree of ferredoxin reduction (See Appendix B). Since the intermediate reduction states are not explicitly considered in Eqs. (1) and (2), Sobel and Lovenberg ignored these intermediate reduction states in estimating the ratio [R-R] /[0-0]. This neglect causes $E^{0'}$ (as calculated from Eqs. (3) and (4)) to become a function of α, the degree of reduction.

In Sobel and Lovenberg's calculations $E^{0'}$ was reported to be a function of pH between pH 7 and 8 (Table 31) (i. e., $E^{0'}$ was reported to become more positive with decreasing pH). In their pH study the α they used in estimating [R-R] /[0-0] was that obtained from hydrogenase reduction. The α values they report were near 1 (i. e., near 100% ferredoxin reduction), but α decreased with decreasing pH. (The hydrogen electrode potential becomes more positive with decreasing pH. A consequence of this is to cause α, the percent reduction of ferredoxin, to decrease with decreasing pH.) (Table 31). This in turn caused their calculated $E^{0'}$ to become more positive, which they mistakenly interpreted as indicating that $E^{0'}$ had a pH-dependence.

Sobel and Lovenberg set α, the observed fraction of reduced ferredoxin, equal to (the equivalent of):

$$[R\text{-}R]/([R\text{-}R] + [0\text{-}0]) \tag{5a}$$

which can be rearranged to give:

$$\frac{[R\text{-}R]}{[0\text{-}0]} = \frac{\alpha}{1-\alpha} \tag{5b}$$

Because of the intermediate states present in partially reduced clostridial ferredoxin, α should not be represented by Eq. (5a) but rather by:

$$\frac{2[R\text{-}R] + [0\text{-}R] + [R\text{-}0]}{2[R\text{-}R] + 2[0\text{-}R] + 2[0\text{-}R] + 2[R\text{-}0]} \tag{6}$$

In this case $[R\text{-}R]/[0\text{-}0]$ is equal to $(\alpha/(1-\alpha))^2$ (See Appendix B.).

Setting $[R\text{-}R]/[0\text{-}0] = \alpha/(1-\alpha)$, as was done by Sobel and Lovenberg, gives a pH-dependent $E^{0'}$ that disagrees with the observations of Eisenstein and Wang (43) and Tagawa and Arnon (126). Curiously, Tagawa and Arnon obtained essentially the correct $E^{0'}$ for C. pasteurianum ferredoxin, and concluded that $E^{0'}$ is independent of pH between pH 6.5-7.4.

These correct conclusions were obtained because Tagawa and Arnon incorrectly assumed that ferredoxin is reduced by one electron. How did they reach the right $E^{0'}$ for the wrong reasons? (It is now generally agreed that clostridial-type ferredoxins take up two electrons.) The answer is as follows. The two clusters of C. pasteurianum ferredoxin are essentially equivalent and are essentially independently reduced. Thus, assuming each ferredoxin contains two identical clusters (each cluster may be either oxidized or reduced), we can write:

$$2[\text{ oxidized clusters}] + H_2 \rightleftharpoons 2\,[\text{ reduced clusters}] + 2H^+; \tag{7}$$

$$E^{0'} - 0.059 \log \frac{[\text{ reduced clusters}]}{[\text{oxidized clusters}]} = - \frac{0.059}{2} \log\left(\frac{p_{H_2}}{[H^+]^2}\right) \tag{8}$$

Furthermore

$$\alpha = \frac{[\text{reduced clusters}]}{[\text{reduced clusters}] + [\text{ oxidized clusters}]}$$

$$\alpha = \frac{2[\text{ R-R}] + [\text{ 0-R}] + [\text{ R-0}]}{(2[\text{ R-R}] + [\text{ 0-R}] + [\text{ R-0}]) + (2[\text{ 0-0}] + [\text{ 0-R}] + [\text{ R-0}])} \tag{9}$$

and

$$\frac{\alpha}{(1-\alpha)} = \frac{[\text{ reduced clusters}]}{[\text{ oxidized clusters}]} \tag{10}$$

Therefore the correct estimate for $E^{0'}$ using Sobel and Lovenberg's data is:

$$E^{0'} = 0.059 \log \left(\frac{\alpha}{(1-\alpha)}\right) - \frac{0.059}{2} \log\left(\frac{p_{H_2}}{[H^+]^2}\right)$$

$$= 0.394 \pm 0.010 \text{ volts} \tag{11}$$

and is essentially pH independent between pH 7.0-8.0 (See Table 31).

Tagawa and Arnon assume:

$$2\,Fd(ox) + H_2 \rightleftharpoons 2\,\overline{F}d(red) + 2H^+ \tag{12}$$

where $\overline{F}d(red)$ is a one electron reduced protein. $E^{0'}$ is given by:

$$E^{0'} = 0.059 \log \frac{[\text{ Fd(red)}]}{[\text{Fd(ox)}]} - \frac{0.059}{2} \log\left(\frac{p_{H2}}{[H^+]^2}\right). \tag{13}$$

They then set

$$\frac{Fd(red)}{Fd(ox)} = \frac{\alpha}{(1-\alpha)} \tag{14}$$

This gives an expression for $E^{0'}$ that is idential to Eq. (11) and is pH independent.

One can also take Eisenstein and Wang's α vs β data (Table II in Ref. (43)) and use Eq. (2) and Eq. (4) in estimating $E^{0'}$. In the process one can set

$$\frac{[R\text{-}R]}{[0\text{-}0]} = \frac{\alpha}{(1-\alpha)}$$

i.e., neglect [0-R] and [R-0] to show what problems are encountered. These results are in Appendix B.

PROTEIN CONFORMATION CHANGES UPON REDUCTION:

C. acidi-urici and C. pasteurianum ferredoxin have different protein midpoint redox potentials, but the differences in the magnetic properties of the corresponding Fe-S clusters are small. Changes in protein conformation upon reduction may be responsible for the observed difference in protein midpoint redox potentials. Tritium-hydrogen exchange (60) studies indicate that the conformations of reduced and oxidized C. acidi-urici ferredoxins differ. Slightly different conformational changes upon reduction may also occur in C. pasteurianum ferredoxin.

PROTEIN CONFORMATION CHANGES WITH pH:

When one recalculates Sobel and Lovenberg's data (Table 31), one sees that at pH 9.0 and at pH values less than 6.5, the protein midpoint redox potential, $E^{0'}$, deviates significantly from the essentially constant $E^{0'}$ value between pH 7.0-8.5. This deviation in the calculated $E^{0'}$ value could be due to changes in protein conformation at the extreme pH values. Slight changes in $E^{0'}$ with pH have been observed for other proteins (144); and the variation of $E^{0'}$ with pH (and ionic strength) for

cytochrome c has been attributed to changes in protein conformation (82). We thus propose that the different amino acid sequences (and conformations) of different proteins primarily account for differences in protein midpoint redox potentials.

The aromatic residues of oxidized C. pasteurianum ferredoxin are presumably identically oriented to their neighboring Fe-S clusters, since the corresponding ring carbon resonances are equivalently shifted (relative to the resonances in diamagnetic reference compounds), and this magnetic equivalence is not maintained in reduced C. pasteurianum ferredoxin (See Experiment 7b). This fact suggests that in reduced C. pasteurianum ferredoxin there could be: (i) a change in protein conformation which affects clusters I and II differently; or (ii) a change in the orientation of the aromatic residues relative to their neighboring Fe-S clusters; or (iii) both. Any conformational changes responsible for this nonequivalence must occur > 10,000 sec^{-1}, since this is the rate the reducing electron is exchanged between the oxidized and reducing electron is exchanged between the oxidized and reduced states of the Fe-S clusters (See Experiment 7a).

The suggestion that the aromatic residues have different orientations in the reduced protein is not inconsistent with the fact that in reduced C. pasteurianum ferredoxin the difference in the percent reduction of each Fe-S cluster is a measure of the difference in cluster midpoint redox potentials. The difference in cluster midpoint potentials is independent of the mechanism which produces the shifts because of the two state hypothesis which assumes that there are only two classes of shifts, one corresponding to the oxidized clusters and the other corresponding to the reduced clusters.

AMINO ACID SEQUENCE HOMOLOGY:

Similar cluster II environments in C. acidi-urici and C. pasteurianum ferredoxin:

The shift parameters of the aromatic residue near Fe-S cluster II in reduced C. acidi-urici native ferredoxin, C. acidi-urici [Phe^2]-ferredoxin, and C. pasteurianum ferredoxin are essentially identical. The protein conformation around cluster II could be similar in the three proteins (assuming that their three-dimensional structures are similar to that of P. aerogenes ferredoxin). This is consistent with the fact that 7 of the 8 amino acid residues directly bonded to Cys^{37}, Cys^{40}, Cys^{43}, and Cys^{18} (which are coordinated to cluster II) are homologous in C. acidi-urici and C. pasteurianum ferredoxins (129) compared to 4 of the 8 amino acid residues bonded to Cys^{8}, Cys^{10}, Cys^{14} and Cys^{47}, coordinated to cluster I.

Symmetrical environments in C. acidi-urici ferredoxin:

The amino acid sequences of C. acidi-urici and C. pasteurianum ferredoxin are homologous to each other (40 out of 55 residues) (129). Each half of the sequence of each protein is also homologous to the other half. In C. acidi-urici the two halves are more homologous (14 homologous residues out of 27) than in C. pasteurianum (8 homologous residues out of 27). Thus C. acidi-urici ferredoxin can be said to be more symmetric with regard to amino acid sequence than C. pasteurianum ferredoxin is. C. acidi-urici ferredoxin may therefore have a more symmetric protein conformation than C. pasteurianum ferredoxin. (The amino acid sequence of P. aerogenes ferredoxin shows that 10 out of 27 residues are homologous for each half of the protein, and its three-dimensional structure is almost

symmetric about a 2-fold axis (2)). If this symmetry is important to the structure and function of the protein, the greater homology between the two halves of C. acidi-urici ferredoxin compared to that in C. pasteurianum ferredoxin may be partially responsible for the fact that magnetic properties and the midpoint redox potentials of the two Fe-S clusters in C. acidi-urici are more similar than they are in C. pasteurianum ferredoxin.

Fig. 57. Proton decoupled ^{13}C-NMR (10°C) of the aromatic residues of C. acidi-urici and C. pasteurianum ferredoxin. (Sample: Preparation): (A): Oxidized C. pasteurianum ferredoxin; ~ 80 mg/ml, pD 7.6 (pH 8.0). (B): ~ 8% reduced C. acidi-urici ferredoxin; ~ 90 mg/ml, pD 7.0. (C): Mixture of ~ 8% reduced C. acidi-urici ferredoxin and ~ 40% reduced C. pasteurianum ferredoxin; ~ 90 mg/ml and 30 mg/ml respectively, pH 7.6. (D): ~ 100% reduced C. pasteurianum ferredoxin; ~ 40 mg/ml, pD 7.6. Broken and unbroken lines connect tyrosyl and phenylalanyl residues respectively.

^{13}C-NMR (10°C) OF THE AROMATIC RESIDUES OF *C. ACIDI URICI* AND *C. PASTEURIANUM* FERREDOXIN

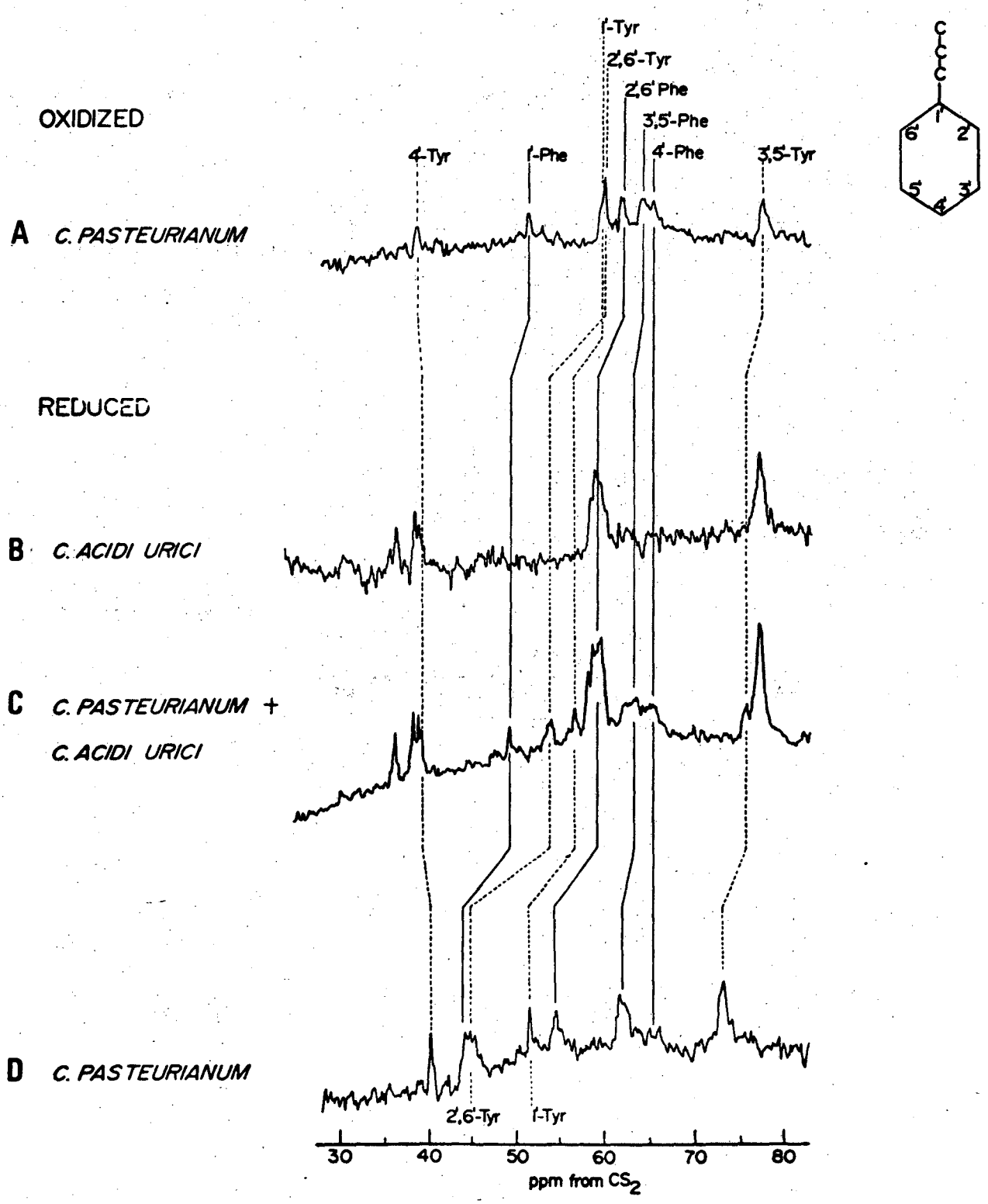

Fig. 58. ^{13}C-NMR (10°C) of the aromatic region of methyl viologen reduced C. pasteurianum and C. acidi-urici ferredoxins. (A): Deconvoluted spectrum of equilibrium mixture of C. acidi-urici and C. pasteurianum ferredoxins, conditions the same as in Fig. 57C.: (B): Convoluted (normal) version of A; (C): Convoluted (normal) spectrum of ~ 8% reduced C. acidi-urici ferredoxin, conditions the same as in Fig. 57B.

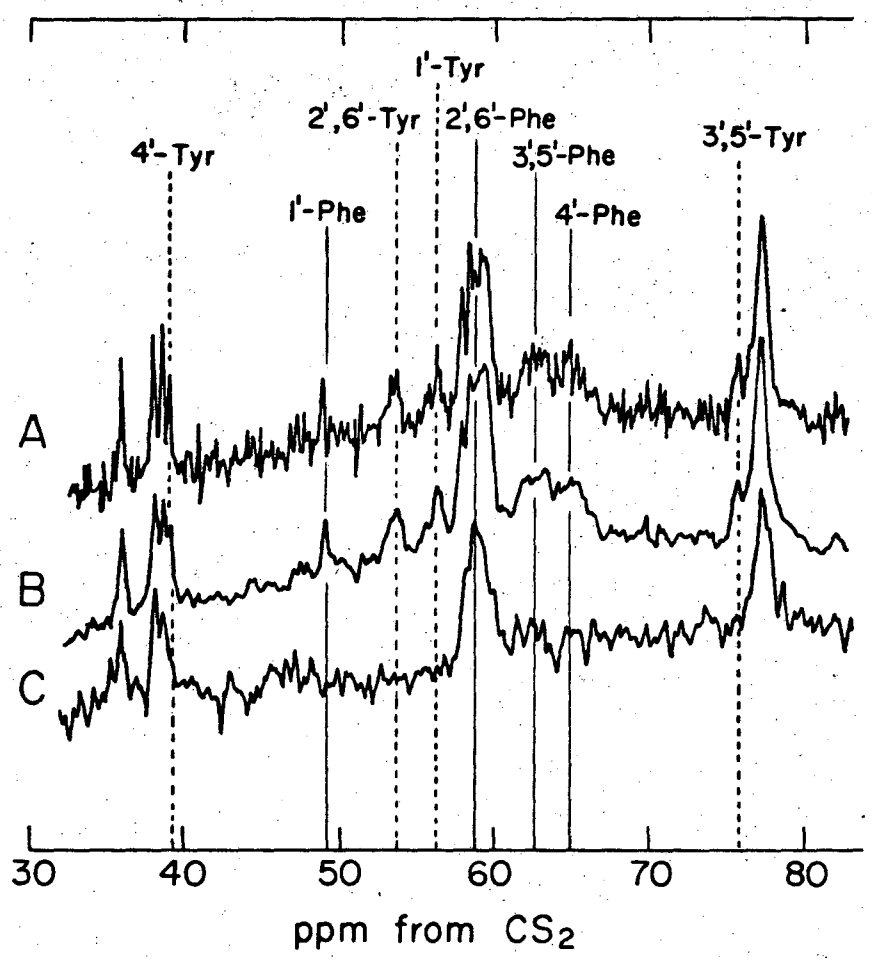
1'-Tyr
2',6'-Tyr
2',6'-Phe
4'-Tyr
3',5'-Phe
3',5'-Tyr
1'-Phe
4'-Phe
A
B
C
30
40
50
60
70
80
ppm from CS_2

Table 27. ^{13}C-ring carbon resonance shifts[a] (ppm, relative to CS_2) of oxidized and reduced C. acidi-urici and C. pasteurianum ferredoxin.

Ferredoxin	Ring carbon 1'	2',6'	3',5'	4'
Oxidized				
C. acidi-urici[b]				
Tyr^{2}	59.5	60.4	77.3	38.5
Tyr^{30}	58.8	60.4	77.3	38.0
C. pasteurianum[c]				
Tyr^{2}	59.3	59.6	77.4	38.2
Phe^{30}	41.2	61.1	64.0	65.4
Reduced				
C. acidi-urici[d]				
Tyr^{2}	58.2[e]	58.8	77.1	38.5
Tyr^{30}	58.2[e]	58.8	77.1	38.0
C. pasteurianum[f]				
Tyr^{2}	51.6	45.1	73.4	40.4
Phe^{30}	44.4	54.4	62.1	66.0
Reduced mixture				
C. acidi-urici[g]				
Tyr^{2}	58.5	59.1	77.2	38.8
Tyr^{30}	57.8	59.1	77.2	38.1
C. pasteurianum[g]				
Tyr^{2}	56.2	53.5	75.5	39.0
Phe^{30}	48.9	59.1	63.5	65.2

a. Shifts accurate to ± 0.2 ppm.

b. Based on Fig. 58C, Experiment 7b.

c. Based on Fig. 57A.

d. Based on Fig. 57B.

e. These resonances are unresolved in Fig. 57B.

f. Based on Fig. 57D.

g. Based on Fig. 57C.

Table 28. Observed ^{13}C-shifts[a] of the aromatic residues of reduced C. acidi-urici and reduced C. pasteurianum ferredoxin relative to the corresponding shifts of the oxidized protein.

Ferredoxin	% Protein reduced[b]	Ring carbon 1'	2',6'	3',5'	4'	Ring carbon 1'	2',6'	3',5'	4'
		Tyr^{2}				Phe^{30}			
C. pasteurianum	(37 ± 5)[c]	-3.1	-6.2	-1.9	+0.8	-1.9	-2.5	-0.6[d]	+0.1[d]
	(90 ± 10)[e]	-7.7	-14.5	-4.0	+2.2	-6.5	-7.2	-2.0	+0.8[d]
		Tyr^{2}				Tyr^{30}			
C. acidi-urici	(8 ± 2)[f]	-0.8	-1.0	-0.15	+0.17	-0.8	-1.0	-0.15	+0.16
		Tyr^{2}				Tyr^{30}			
	(100)[e]	-8±0.7	-14±1.5	-4±0.5	+2.4±0.5	-8±0.4	-14±1.5	-4±0.5	+2.4±0.5

a. Shifts are ± 0.2 ppm if not otherwise indicated.

b. Based on ^{1}H-NMR spectra of aliquots of the ^{13}C-NMR samples (See Experiment 7b).

c. Based on Fig. 57C.

d. These values could have large errors since the positions of these resonances were difficult to determine in the reduced protein.

e. Based on Fig. 57D.

f. Based on Fig. 57B.

g. Extrapolated to dithionite end-point (See Experiment 7b).

Table 29. Calculated percent reduction of the Fe-S clusters of C. pasteurianum and C. acidi-urici ferredoxin.

Ferredoxin	Cluster:	X = 1 % Reduction I	II
C. pasteurianum		(32 ± 3.5)[a]	(42 ± 2)[a]
		(90 ± 10)[b]	(90 ± 10)[b]
C. acidi-urici native		(8 ± 2)[c]	(8 ± 2)[c]
C. acidi-urici [Phe^2]-		(20 ± 4)[d]	(22 ± 3)[d]
C. acidi-urici native		(32 ± 4)[e,g]	(36.5± 4)[e,g]
C. acidi-urici native		100[f]	100[f]

a. Based on Fig. 57C.
b. Basec on Fig. 57D.
c. Based on Fig. 57B.
d. Based on Fig. 48E (Experiment 7b).
e. Based on Fig. 46D (Experiment 7a).
f. Dithionite end-point (Fig. 52, Experiment 7b).
g. This calculation (based on Fig. 46D) is tentative since it depends on the validity of: (i) our assignment of the resonance at 56.2 ppm to the 1'-ring carbon resonance and (ii) our assignment of the resonance at 54.6 ± 0.2 ppm to two 2',6'-ring carbon resonances at 54.2 and 54.6 ppm. The 2',6'-ring carbon resonance in Fig. 46D is broader than the usual ferredoxin 2',6'-ring carbon resonance, and this broadening suggests that the resonance is splitting into two resonances, each of which represents a single tyrosyl residue.

Table 30. Recalculation of Eisenstein and Wang's data (Table II in reference (43)), assuming that each reduction site is distinguishable.

Case	Distin-guishable[a]	Equi-valent[b]	Inter-acting[c]	Mean error[d] x 10^2
0	yes	yes	no	0.88
i	yes	no	no	1.00
ii	yes	no	yes	0.43
iii	yes	yes	yes	0.48
Wang[e]	no	yes	no	0.48

a. Fe-S clusters can be distinguished by NMR techniques but are not distinguishable by optical techniques.
b. Fe-S clusters are equivalent if they have the same midpoint redox potentials (i.e., are equally accessible to a reducing electron). Nonequivalent Fe-S clusters would have a midpoint redox potential difference of 16 ± 9 mV, if, for example, X = 0.7.
c. Fe-S clusters are interacting if reduction of one Fe-S cluster changes the redox potential of the other Fe-S cluster. This change can be as high as 10 ± 5 mV.
d. The mean error is the mean of the deviations between the calculated and observed degrees of reduction. The observed degree of reduction is based on data of Eisenstein and Wang (Table II in reference (43)), and the calculated degree of reduction is obtained from equations derived for distinguishable reduction sites (See Appendix C). The lower the error estimate, the better the fit to a particular case. This fit depends upon the precision of the data of Eisenstein and Wang.

Notes to Table 30 continued.

e. This case contains the assumptions Eisenstein and Wang make for C. pasteurianum ferredoxin. Their data make an excellent fit with a plot based on equations derived for distinguishable reduction sites. To the extent that their error estimates are meaningful, their optical data cannot (for example) determine if equivalent Fe-S clusters can interact (to change the cluster midpoint potential 10 ± 5 mV) or not. In fact if case (ii) is correct their data suggest that when one cluster is reduced the second cluster is easier to reduce by 7 mV (See Appendix C).

Table 31. Recalculation of the midpoint redox potential of *C. pasteurianum* ferredoxin from the data[a] of Sobel and Lovenberg (122).

Sobel and Lovenberg data			Recalculated[b]
pH of reaction mixture	E^o ferredoxin (mV)[c]	E_h (25°) hydrogen electrode (mV)[c]	$E^{o\prime}$ (25°) ferredoxin (mV)[c]
5.5	-346	-325	-367
6.0	-360	-354	-366
6.3	-375	-373	-377
6.5	-387	-384	-390
7.0	-395	-412	-398
7.3	-418	-430	-396
7.4[d]	-415	-435	-396
7.5	-425	-443	-407
8.0[e]	-450	-472	-406
8.5	-470	-502	-406
9.0	-496	-531	-416
		Average[f]	-394

a. From Fig. 2 and Table IV of reference (122).

b. Recalculation assuming n = 1 where n is the number of electrons (see text).

c. Accurate to ± 5 mV, referenced to the hydrogen electrode.

d. From experiments 1, 2 and 4 of Table IV in reference (122), where $\alpha = 0.82$. (α is the degree of reduction.)

e. From experiment 3 of Table IV in reference (122), where $\alpha = 0.93$.

Notes to Table 31 continued.

f. Between pH 7.0 and 8.5, the average $E^{o'} = -(402 \pm 5)$ mV. This is within the error of Fig. 2 in reference (122). Tagawa and Arnon (126) find that with hydrogenase $E^{o'} = -(385 \pm 1)$ mV for C. pasteurianum ferredoxin and is independent of pH between pH 6.5 and 7.4; and Eisenstein and Wang (43) find that $E^{o'} = -(383 \pm 3)$ mV (pH 7.4, 23°) for C. pasteurianum ferredoxin, reduced by Zn-reduced methyl viologen.

APPENDIX B

REDOX POTENTIAL MEASUREMENTS:

The electrode potential, E_h, is the voltage one needs to apply to a set of two half cell reactions in order to prevent a flow of electrons. For example, if two half cells (one consisting of H_2 gas in equilibrium with H^+, the standard cell, and the other consisting of another oxidized substance in quilibrium with its reduced form) are coupled by a KCl-agar bridge which permits electron flow, but no reactant flow, the potential difference between these cells is E_h.

E_h can be calculated from the Nernst equation:

$$E_{h(pH1)} = E^0 + \frac{RT}{nF} \ln \frac{[\text{oxidized substance}]}{[\text{reduced substance}]}$$

$$E_{h(pH7)} = E^{0'} + \frac{0.06}{n} \log_{10}\left(\frac{1-\alpha}{\alpha}\right)$$

where $E^0_{(pH1)}$ at pH 1 is zero and is the midpoint redox potential of the standard cell,

$E^{0'}_{(pH7)}$ at pH 7, 30° C is -0.42V for the H_2 electrode

n = number of electrons transfered in the reaction,

$$\alpha = \frac{[\text{reduced substance}]}{[\text{reduced substance}] + [\text{oxidized substance}]}$$

When solutions of different potentials are mixed, the reaction proceeds until equilibrium is attained, and the final solution has an intermediate electrode potential:

$$A_{(red)} + B_{(ox)} \rightleftharpoons A_{(ox)} + B_{(red)}$$

$$E^{0'}_{(B)} + \frac{0.06}{n} \log\left(\frac{[B_{(ox)}]}{[B_{(red)}]}\right) = E^{0'}_{(A)} \frac{0.06}{n} \log\left(\frac{[A_{ox}]}{[B_{red}]}\right)$$

$$E^{0'}_{(B)} - E^{0'}_{(A)} = \frac{0.06}{n} \log \frac{[A_{(ox)}]\,[B_{(red)}]}{[B_{(ox)}]\,[A_{(red)}]}$$

$$= \frac{0.06}{n} \log K_{eq} = \frac{0.06}{n} \log \left(\frac{1-\alpha}{\alpha} \right)$$

where K_{eq} the equilibrium constant.

A change of 7 mV in the redox potential is equivalent to a 35% change in the equilibrium constant.

In our treatment $[A_{(ox)}]$ and $[A_{(red)}]$ are the concentrations of the oxidized and reduced Fe-S clusters, respectively; and $[B_{(ox)}]$ and $[B_{(red)}]$ are the concentrations of oxidized and singly reduced methyl viologen, (mv^{++}) and (mv^{+}), respectively.

CONSEQUENCES OF NEGLECTING (0-R) AND (R-0):

Neglecting the intermediate reduction states, (0-R) and (R-0), in estimating $E^{0'}$ from methyl viologen reduction of C. pasteurianum ferredoxin (Fd) will cause $E^{0'}$ to be a function of α, and will only give correct $E^{0'}$ at $\alpha = 1/2$.

This can be shown by rewriting Eqs. (2) and (4) (in text, Experiment 7c) so that they correspond to reactions transferring two electrons in one step:

$$Fd_{(ox)} + 2\ mv^{+} \rightleftharpoons Fd_{(red)} + 2\ mv^{++} \qquad (b.1)$$

$$(0\text{-}0) + 2\ mv^{+} \rightleftharpoons (R\text{-}R) + 2\ mv^{++} \qquad (b.2)$$

The midpoint reduction potential, $E^{0'}$, is obtained from

$$E^{0'} - \frac{0.059}{2} \log \frac{[R\text{-}R]}{[0\text{-}0]} = -0.444 - \frac{0.059}{2} \log \beta^{2} \qquad (b.3)$$

*The derivations that follow in this Appendix and in Appendix C are by Dr. H. Sternlicht of Bell Telephone Laboratories, Inc.

where

$$\beta = [mv^{+}]/[mv^{++}].$$

Collecting terms,

$$E^{0'} = E^{0'}_{(mv)} - \frac{0.059}{2} \log \left(\frac{[0\text{-}0]\,\beta^2}{[R\text{-}R]} \right)$$

$$= -0.444 - \frac{0.059}{2} \log \bar{K}. \qquad \text{(b.4)}$$

The equilibrium constant, $\bar{K}$ (for the reactions consisting of one two-electron step), can be related to the equilibrium constants for the reactions consisting of two <u>one</u>-electron steps. If one assumes that the two clusters are nearly equilibrium and are reduced nearly independently in one-electron steps, then:

$$(0\text{-}0) + mv^{+} \rightleftharpoons (0\text{-}R) + mv^{++};\ K_{11} = K \qquad \text{(b.5)}$$

$$(0\text{-}R) + mv^{+} \rightleftharpoons (R\text{-}R) + mv^{++};\ K_{12} = K \qquad \text{(b.6)}$$

$$(0\text{-}0) + 2\,mv^{+} \rightleftharpoons (R\text{-}R) + 2mv^{++};\ \bar{K} \qquad \text{(b.7)}$$

$$\bar{K} = K_{11}K_{12} = K^2 \qquad \text{(b.8)}$$

(Note: we could have also used

$$(0\text{-}0) + mv^{+} \rightleftharpoons (R\text{-}0) + mv^{++};\ K_{21} = K$$

$$(R\text{-}0) + mv^{+} \rightleftharpoons (R\text{-}R) + mv^{++};\ K_{22} = K$$

$$(0\text{-}0) + 2mv^{+} \rightleftharpoons (R\text{-}R) + 2mv^{++};\ \bar{K} = K^2)$$

$E^{0'}$ is obtained by (setting $\bar{K} = K^2$)

$$E^{0'} = -0.444 - \frac{0.059}{2} \log \bar{K} = -0.444 - 0.059 \log K$$

$$= -0.3815 \text{ volts} \qquad \text{(b.9)}$$

if $K = 0.088$, $\bar{K} = K^2 = 0.0077$.

Thus, whether one assumes that the electrons are transferred in two one-electron steps (equilibrium constant, K = 0.088) or in one two-electron step (equilibrium constant $\overline{K} = K^2 = 0.0077$), the same $E^{0'}$ of -381.5 mV is obtained from Eisenstein and Wang's spectrophotometric measurement of α. The estimate of $\overline{K} = 0.0077$ was obtained by Eisenstein and Wang's postulating the existence of the intermediates (0-R) and (R-0).

If we do not recognize or use the intermediate states (0-R) and (R-0) in estimating $\frac{[R-R]}{[0-0]}$, we write:

$$\frac{[R-R]}{[0-0]} = \frac{\alpha}{(1-\alpha)} = \frac{\beta^2}{\overline{K}} \quad \text{or}$$

$$\alpha = \frac{[R-R]}{[0-0] + [R-R]} = \frac{\beta^2}{(\beta^2 + \overline{K})} \qquad \text{(b.10)}$$

$\overline{K}$ calculated from Eq. (b.10), where (0-R) and (R-0) are neglected, is a function of α and gives and $E^{0'}$ that becomes more positive with decreasing α. Only at $\alpha = 1/2$, $E^{0'} = -381.5$ mV. $\overline{K}$, calculated from Eq. (c29) in Appendix C, is essentially independent of α and gives $E^{0'} = (-381.5 \pm 1)$ mV for all α values. This is shown in Table 32.

CONSEQUENCES OF CONSIDERING (0-R) AND (R-0):

When one considers the intermediates (0-R) and (R-0), then

$$\frac{[R-R]}{[0-0]} = \left[\frac{\alpha}{(1-\alpha)}\right]^2$$

Proof:

If one assumes that the clusters are distinguishable, equivalent, and noninteracting, and that the reduction proceeds in single electron reduction steps, then

	Equilibrium Const.
$(0\text{-}0) + mv^{+} \rightleftharpoons (R\text{-}0) + mv^{++}$;	$K_{11} = K$
$(R\text{-}0) + mv^{+} \rightleftharpoons (R\text{-}R) + mv^{++}$;	$K_{12} = K$
$(0\text{-}0) + mv^{+} \rightleftharpoons (0\text{-}R) + mv^{++}$;	$K_{21} = K$
$(\text{-}0R) + mv^{+} \rightleftharpoons (R\text{-}R) + mv^{+}$;	$K_{22} = K$

(b.11)

$$[R\text{-}0] = [0\text{-}0]\ \beta/K; \tag{b.12}$$

$$[0\text{-}R] = [0\text{-}0]\ \beta/K\ . \tag{b.13}$$

where

$K = \bar{K}^{1/2}$ (see Appendix B).

$$\alpha = \frac{2[R\text{-}R] + [0\text{-}R] + [R\text{-}0]}{2[R\text{-}R] + 2[0\text{-}0] + 2[0\text{-}R] + 2[R\text{-}0]}\ . \tag{b.14}$$

Substituting $[0\text{-}0]\ \beta/K$ for $[0\text{-}R]$ or $[R\text{-}0]$ and dividing numerator and denominator by $[0\text{-}0]$

$$\alpha = \frac{\frac{[R\text{-}R]}{[0\text{-}0]} + \frac{\beta}{K}}{\frac{[R\text{-}R]}{[0\text{-}0]} + \frac{2\beta}{K} + 1} \tag{b.15}$$

Solving for $[R\text{-}R]/[0\text{-}0]$:

$$[R\text{-}R]/[0\text{-}0] = \frac{\alpha + (2\alpha - 1)\ \beta/K}{1-\alpha}\ . \tag{b.16}$$

However

$$\alpha = \frac{\beta}{\beta + K}\ ,$$

solving for β/K:

$$\frac{\beta}{K} = \frac{\alpha}{1-\alpha}\ . \tag{b.17}$$

Substituting $\alpha/1\text{-}\alpha$ for β/K in Eq. (b6)

$$\frac{[R\text{-}R]}{[0\text{-}0]} = \frac{\alpha + (2\alpha - 1)\left(\frac{\alpha}{1-\alpha}\right)}{(1-\alpha)} = \left[\frac{\alpha}{1-\alpha}\right]^2 \tag{b.18}$$

Table 32. Consequences of considering or ignoring intermediate reduction states (O-R) and (R-O) when calculating $E^{o\prime}$.

Eisenstein and Wang data (43)		Consider (O-R) and (R-O) states[a]		Ignore (O-R) and (R-O) states[b]	
β	α	$\overline{K} \times 10^3$	$E^{o\prime}$ (mV)	$\overline{K} \times 10^3$	$E^{o\prime}$ (mV)
0.0075	0.0764	8.23	-382.5	0.68	-350.6
0.0183	0.166	8.46	-382.9	1.68	-362.1
0.0300	0.247	8.37	-382.7	2.75	-368.5
0.0466	0.335	8.59	-383.0	4.32	-374.2
0.0669	0.424	8.28	-382.6	6.09	-380.2
0.0985	0.529	7.74	-381.7	8.67	-383.2
0.1328	0.604	7.57	-381.4	11.5	-386.8
0.1650	0.661	7.23	-380.8	14	-389.3
0.2050	0.718	6.4	-379.3	16	-391.0

a. $[R-R]/[O-O] = (\alpha/(1-\alpha))^2 = \beta^2/\overline{K}$, $\alpha = \beta/(\beta + \overline{K}^{1/2})$, and $\overline{K} = [\beta(1-\alpha)/\alpha]^2$.

b. $[R-R]/[O-O] = \alpha/(1-\alpha)$, $= \beta^2/\overline{K}$, $\alpha = \beta^2/(\beta^2 + \overline{K})$, and $\overline{K} = \beta^2(1-\alpha)/\alpha$.

APPENDIX C

MIDPOINT REDOX POTENTIALS OF DISTINGUISHABLE Fe-S CLUSTERS

The Fe-S clusters of clostridial type ferredoxins are reduced one step at a time. They can be equally accessible to the reducing electron and thus be considered equivalent. They are distinguishable by ^{13}C-NMR techniques or indistinguishable by optical techniques (Eisenstein and Wang (43)). If the reduction of the Fe-S cluster affects the reduction of the second Fe-S cluster, the two clusters are said to be interacting.

Eisenstein and Wang analyzed their data in terms of the assumption that the two reduction sites of C. pasteurianum ferredoxin are indistinguishable, equivalent, and noninteracting. They test their assumption by comparing a calculated α with the observed α. We also recalculated α for each of the following cases to determine whether these cases are consistent with the data of Eisenstein and Wang.

Case (o): two distinguishable, equivalent, and noninteracting clusters

(i): two distinguishable, nonequivalent, and noninteracting clusters

(ii): two distinguishable, nonequivalent, and interacting clusters

(iii): two distinguishable, equivalent, and noninteracting clusters.

Our recalculated α is compared with the α observed by Eisenstein and Wang by doing a least square fit of the calculated α against a plot of observed α vs. β. α denotes $(\alpha_I + \alpha_{II})/2$, for clusters I and II , and is the degree of reduction of C. pasteurianum ferredoxin. $\beta = [mv^+]/[mv^{++}]$ is the ratio of the concentrations of singly reduced and oxidized methyl viologen (Table 33).

In general, a least square plot of α vs. β for the Eisenstein and Wang methyl viologen reduced C. pasteurianum ferredoxin is not very sensitive to the assumptions made by cases (o), (i), (ii), (iii) or the Wang case and one must use mean error estimates of the fits to distinguish between cases. If indeed Wang's error in his $\alpha_{observed}$ vs. $\beta_{observed}$ is as small as he implies, then case (ii) would be probably correct.

Figures 59 and 60 show a least square plot for case (ii) using our ^{13}C-NMR estimate of a 10 mV difference in Fe-S cluster midpoint redox potentials. This was a two independent variable fit. The fit obtained was better than Eisenstein and Wang's two variable fit. The Eisenstein and Wang data together with 3 other limiting cases (case (o), (i) and (iii) are plotted in Fig. 61. Case (iii) gives the identical plot as the Wang case. Case (iii) assumes two distinguishable, equivalent, and interacting clusters and gives the best least square fit in Fig. 61. The assumption of distinguishable, nonequivalent, and interacting clusters (case (ii), Figs. 59 and 60) gives tbe best overall fit (Table 35).

Figure 62 shows a least square plot of the limiting case (i) of two distinguishable nonequivalent and noninteracting clusters where the protein midpoint potential is -383 mv, rather than the calculated least square value of -381.5 mv, and the difference in cluster potentials is 10 mv. The fit is excellent below $\alpha = 0.5$ and deviates for $\alpha > 0.5$. This suggests the second electron is more easily introduced than the first, and the two clusters are not independent.

The basis for our calculation is illustrated by a derivation of α vs. β for the general case (case (ii) of two distinguishable, nonequivalent and

interacting clusters which involves 3 independent and 1 dependent variables.

Derivation:

Case (ii)

$\alpha_{calc.}$ vs. β for nonequivalent, distinguishable and interacting sites.

Cluster: (II-I) (II-I)

$$\left.\begin{array}{ll} (0\text{-}0) + mv^{+} \rightleftharpoons (R\text{-}0) + mv^{++};\ K_{11} & \text{(c1)} \\ (0\text{-}0) + mv^{+} \rightleftharpoons (0\text{-}R) + mv^{++};\ K_{12} & \text{(c2)} \end{array}\right\} \text{1st electron}$$

$$\left.\begin{array}{ll} (R\text{-}0) + mv^{+} \rightleftharpoons (R\text{-}R) + mv^{++};\ K_{21} & \text{(c3)} \\ (0\text{-}R) + mv^{+} \rightleftharpoons (R\text{-}R) + mv^{++};\ K_{22} & \text{(c4)} \end{array}\right\} \text{2nd electron}$$

$$K_{11} = \frac{[0\text{-}0][mv^{+}]}{[R\text{-}0][mv^{++}]} = \frac{[0\text{-}0]}{[R\text{-}0]}\ \beta; \qquad \text{(c5)}$$

$$K_{12} = \frac{[0\text{-}0][mv^{+}]}{[0\text{-}R][mv^{++}]} = \frac{[0\text{-}0]}{[0\text{-}R]}\ \beta; \qquad \text{(c6)}$$

$$K_{21} = \frac{[R\text{-}0][mv^{+}]}{[R\text{-}R][mv^{++}]} = \frac{[R\text{-}0]}{[R\text{-}R]}\ \beta; \qquad \text{(c7)}$$

$$K_{22} = \frac{[0\text{-}R][mv^{+}]}{[R\text{-}R][mv^{++}]} = \frac{[0\text{-}R]}{[R\text{-}R]}\ \beta; \qquad \text{(c8)}$$

$$K_{11}K_{21} = K_{12}K_{22} \qquad \text{(c9)}$$

Fractional reduction of cluster II:

$$\alpha_{II} = \frac{[R\text{-}0) + [R\text{-}R]}{[0\text{-}0] + [R\text{-}R] + [0\text{-}R] + [R\text{-}0]} \qquad \text{(c10)}$$

$$\alpha_{II} = \frac{1 + \frac{[R\text{-}R]}{[R\text{-}0]}}{\frac{[0\text{-}0]}{[R\text{-}0]} + \frac{[R\text{-}R]}{[R\text{-}0]} + \frac{[0\text{-}R]}{[R\text{-}0]} + 1} \qquad \text{(c11)}$$

$$\alpha_{II} = \frac{1 + \frac{\beta}{K_{21}}}{\frac{K_{11}}{\beta} + \frac{\beta}{K_{21}} \frac{K_{11}}{K_{12}} + 1} \tag{c12}$$

$$\alpha_{II} = \frac{\beta K_{12}K_{21} + \beta^2 K_{12}}{K_{11}K_{12}K_{21} + \beta K_{11}K_{21} + \beta K_{12}K_{21} + \beta^2 K_{12}} \tag{c13}$$

Fractional reduction of cluster I:

$$\alpha_I = \frac{[0\text{-}R] + [R\text{-}R]}{[0\text{-}0] + [R\text{-}R] + [0\text{-}R] + [R\text{-}0]} \tag{c14}$$

$$\alpha_I = \frac{1 + \frac{[R\text{-}R]}{[0\text{-}R]}}{\frac{[0\text{-}0]}{[0\text{-}R]} + \frac{[R\text{-}R]}{[0\text{-}R]} + \frac{[0\text{-}R]}{[0\text{-}R]} + \frac{[R\text{-}0]}{[0\text{-}R]}} \tag{c15}$$

$$\alpha_I = \frac{1 + \frac{\beta}{K_{22}}}{\frac{K_{12}}{\beta} + \frac{\beta}{K_{22}} + 1 + \frac{K_{21}}{K_{22}}}$$

using Eq. (9),

$$\alpha_I = \frac{1 + \frac{\beta}{K_{22}}}{\frac{K_{12}}{\beta} + \frac{\beta}{K_{22}} + 1 + \frac{K_{12}}{K_{11}}} \tag{c16}$$

collecting terms,

$$\alpha_I = \frac{\beta K_{11}K_{22} + \beta^2 K_{11}}{K_{11}K_{12}K_{22} + \beta K_{11}K_{22} + \beta K_{12}K_{22} + \beta^2 K_{11}} \tag{c17}$$

Fractional reduction, α, of C. pasteurianum ferredoxin:

$$\alpha = \frac{(\alpha_{II} + \alpha_I)}{2} \tag{c18}$$

$$\alpha = \frac{1}{2}\left[(\beta K_{12}K_{21} + \beta^2 K_{12})/(K_{11}K_{12}K_{21} + \beta K_{11}K_{21} + \beta K_{12}K_{21} + \beta^2 K_{12})\right]$$

$$+ \frac{1}{2}\left[(\beta K_{11}K_{22} + \beta^2 K_{11})/(K_{11}K_{12}K_{22} + \beta K_{11}K_{22} + \beta K_{12}K_{22} + \beta^2 K_{11})\right] \tag{c19}$$

$$E^0_{ij}\ (\text{volts}) = -\ 0.444 - 0.0587 \log_{10} K_{ij},\ \text{at } 10°\text{C} \tag{c20}$$

$$E^0_{ij} - E^0_{i'j'} = 0.0587 \log_{10} \frac{K_{i'j'}}{K_{ij}} \tag{c21}$$

In case (ii) $E^0_{11} - E^0_{12} = 10$ mv; $\dfrac{K_{12}}{K_{11}} = 1.47$ (c22a)

Set $K_{11} = 0.076\kappa$, $K_{12} = 0.112\kappa$ (c22b)

Set $E^0_{22} - E^0_{21} = 10$ mv; $\dfrac{K_{21}}{K_{22}} = 1.47$ (c23a)

$K_{21} = 0.112\lambda$; $K_{22} = 0.076\lambda$

Equation (c23a) follows from Eq. (c22a) and Eq. (9) (in text, Experiment 7c).

Eisenstein and Want fit their data by treating the reduction sites as equivalent, indistinguishable, and noninteracting. But their α data can also be fitted quite accurately with:

$$\alpha = \frac{2[R\text{-}R] + [0\text{-}R] + [R\text{-}0]}{2[R\text{-}R] + 2[0\text{-}0] + 2[0\text{-}R] + 2[R\text{-}0]} = \frac{\beta}{\beta + K}$$

$$= \frac{\beta}{\beta + \bar{K}^{1/2}} \tag{c29}$$

This corresponds to case (o), the case of distinguishable, equivalent, and noninteracting clusters.

Fig. 59. Case (ii). Distinguishable, nonequivalent, and interacting clusters. Least square fit to Wang's data (o-points) using two variables, κ and λ to get the best fit. These least square values are $\kappa = 1.086$ and $\lambda = 0.83538$. The parameters for this least square plot are listed in Table 33.

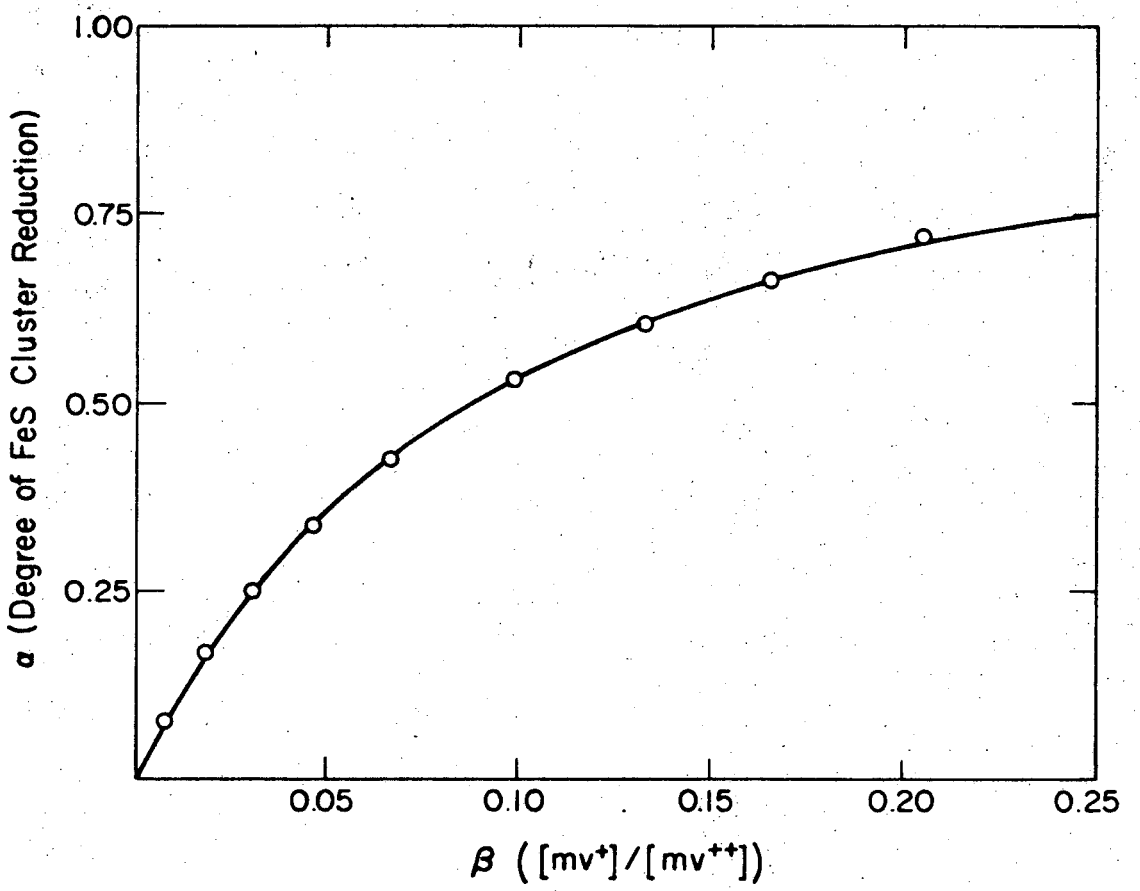
1.00
0.75
0.50
0.25
α (Degree of FeS Cluster Reduction)
0.05
0.10
0.15
0.20
0.25
β ([mv+]/[mv++])

Fig. 60. Case (ii). Same as Fig. 59 except that β is expanded to $\beta = 1.0$.

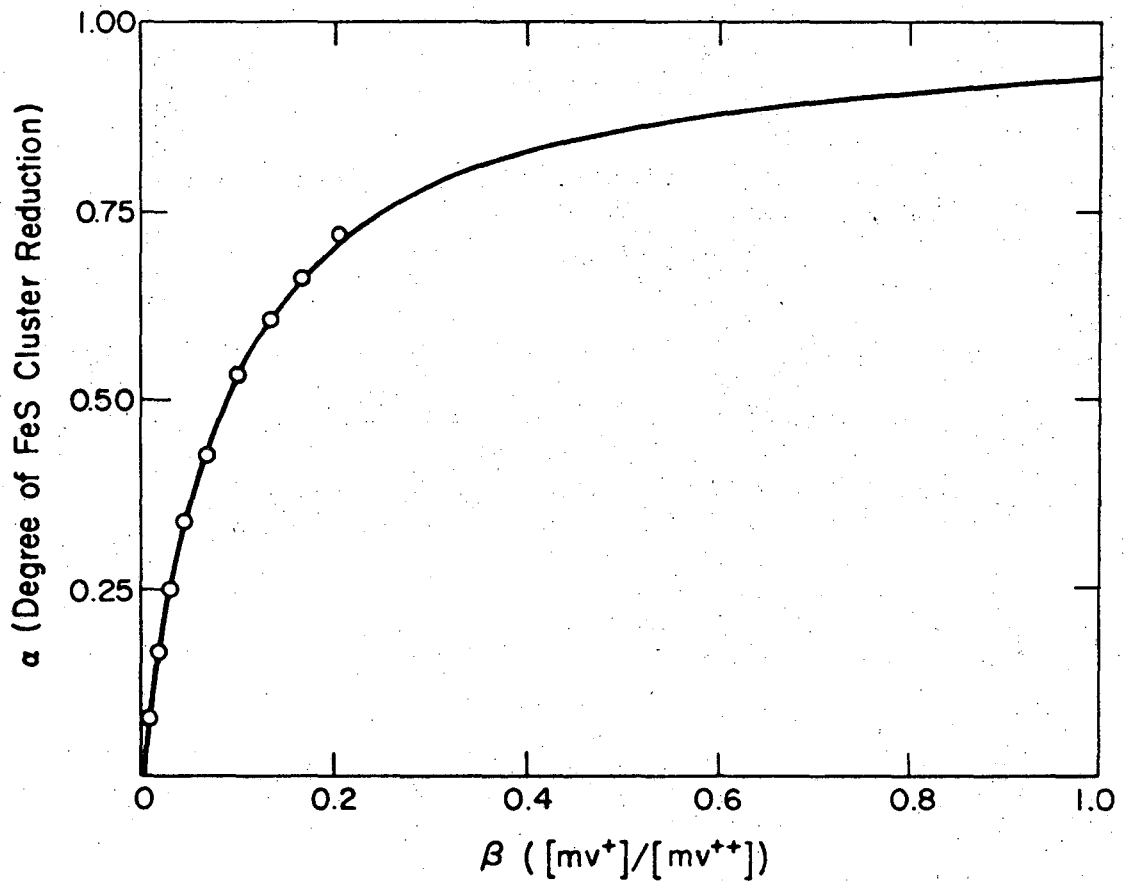
1.00
0.75
0.50
0.25
α (Degree of FeS Cluster Reduction)
0
0.2
0.4
0.6
0.8
1.0
β ([mv+]/[mv++])

Fig. 61. Least square fits (α_{calc}) to $\alpha_{obs.}$ (x-points) for limiting cases (o), (i), (iii) and (Wang). The general equations for α_{calc} are:

$$\alpha_{calc} = \frac{\beta}{\beta+K}$$

and for a two parameter fit,

$$\alpha = \frac{\frac{1}{2} + \frac{\beta}{K_{2(Wang)}}}{\frac{K_{1(Wang)}}{\beta} + \frac{K_{2(Wang)}}{\beta} + 1}$$

and

$$\alpha_{calc} = \frac{2\beta^2 + (K_{11} + K_{12})\beta}{2\beta^2 + 2(K_{11} + K_{12})\beta + 2K_{11}K_{12}}$$

The parameters for these least square plots are listed in Table 34.

○ = case (o)

△ = case (i)

▽ = case (iii)

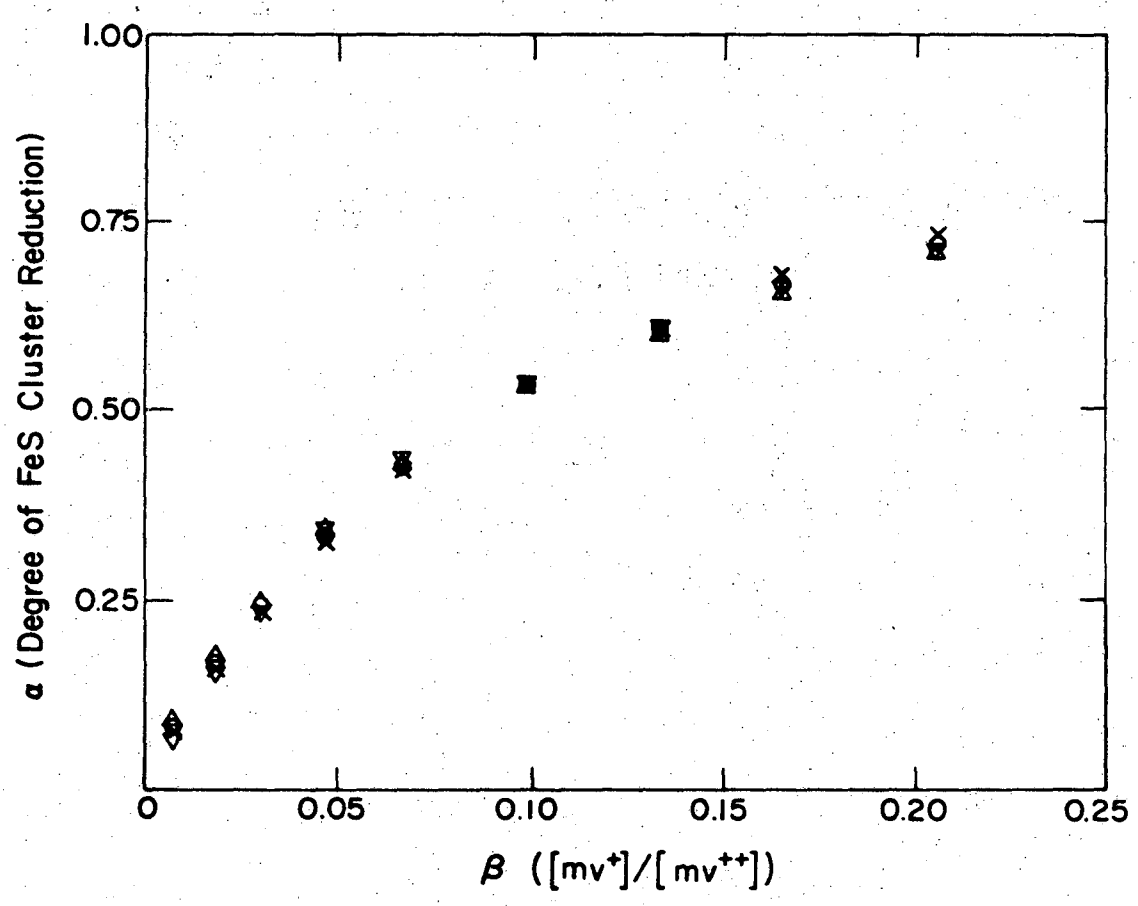
1.00
0.75
0.50
0.25
α (Degree of FeS Cluster Reduction)
0
0.05
0.10
0.15
0.20
0.25
β ([mv+]/[mv++])

Fig. 62. Comparison of α_{calc} for case (i) with Wang's α_{obs}, where $E_{II}^{0'} - E_{I}^{0'} = 10$ mV and $(E_{II}^{0'} + E_{I}^{0'})/2 = -383$ mV. The general equation for α_{calc} for a two parameter fit is:

$$\alpha_{calc} = \frac{2\beta^2 + (K_{11} + K_{12})\beta}{2\beta^2 + 2(K_{11} + K_{12})\beta + 2K_{11}K_{12}}$$

where $K_{11} = 0.076$ and $K_{12} = 0.112$.

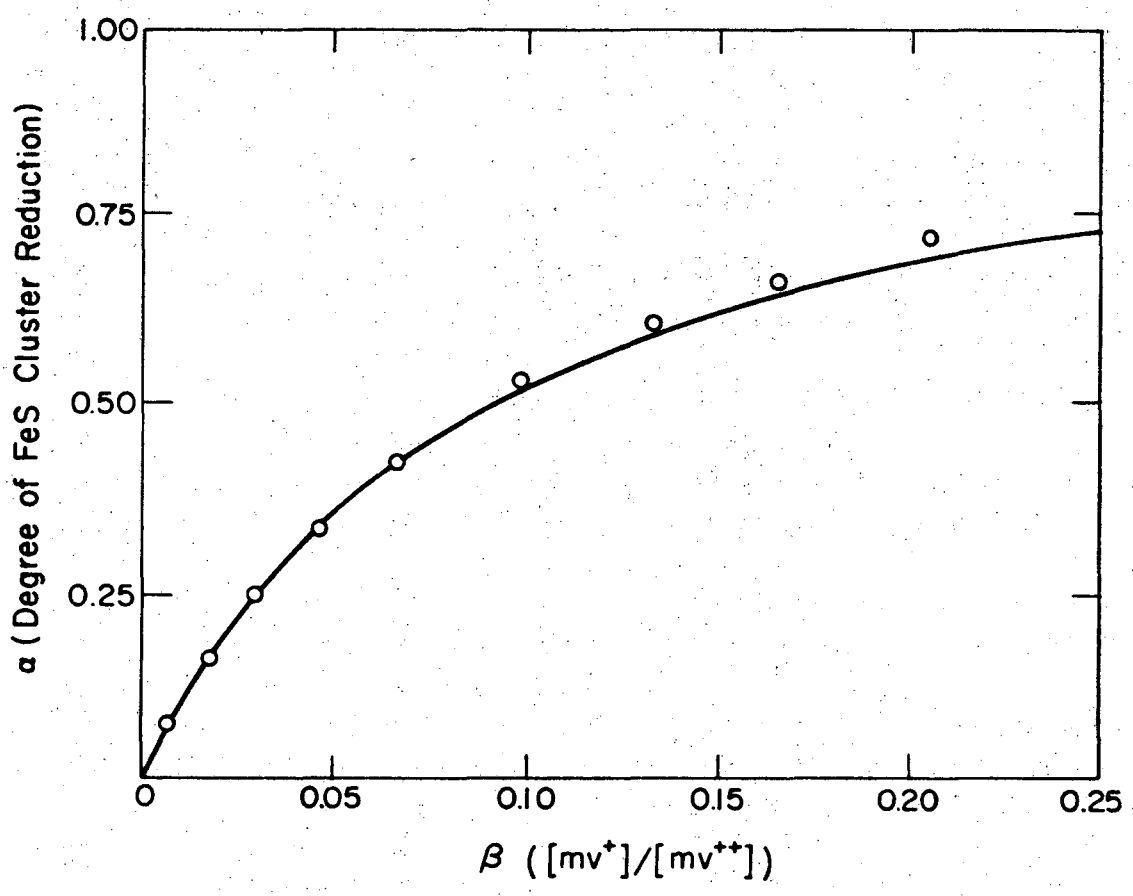
1.00
0.75
0.50
0.25
α (Degree of FeS Cluster Reduction)
0
0.05
0.10
0.15
0.20
0.25
β ([mv⁺]/[mv⁺⁺])

Table 33. Conditions (Fig. 59) for calculating best fits for case (ii)[a].

First electron		Second electron	
Equilibrium constants[b]			
K_{11}	K_{12}	K_{21}	K_{22}
0.0825	0.1216	0.09356	0.0635
Cluster midpoint redox potentials[c] (mV)			
E_{11}^{o}	E_{12}^{o}	E_{21}^{o}	E_{22}^{o}
-380	-390	-383	-373

a. Case (ii) is the case of distinguishable, non-equivalent and interacting Fe-S clusters.

b. The degree of reduction for case (ii) is calculated from equation (c19). The equilibrium constants K_{ij} that give a best fit to the data of Eisenstein and Wang (43) are calculated from two least square parameters, κ and λ. κ is used to determine K_{11} for (O-O)$\longrightarrow$(R-O), and K_{12} for (O-O)$\longrightarrow$(O-R), the first electron reactions in which only one cluster in the ferredoxin is reduced, and $\alpha < 0.5$. λ is used to determine the K_{21} for (R-O)$\longrightarrow$(R-R), and K_{22} for (O-R)$\longrightarrow$(R-R), the second electron reactions, in which both clusters in the ferredoxin are reduced and $\alpha > 0.5$. A smaller K_{ij} means that the reaction is faster and the corresponding cluster is easier to reduce (See Eqs. c20 to c23a).

c. From the least square parameters one calculates $E_{ij}^{o}{}_{(volts)} = 0.444 - 0.0587 \log_{10} K_{ij}$ and determines that the protein midpoint potential ($\alpha = 0.5$) is:

$$E^{o\prime}_{protein} = \frac{(E_{11}^{o\prime} + E_{12}^{o\prime} + E_{21}^{o} + E_{22}^{o\prime})}{4} = -381.5 \text{ mV}$$

Table 34. Parameters for Fig. 61

Case	Conditions	$(E_{II}^{o'} - E_{I}^{o'})$ (mV)	$\left(\frac{E_{I}^{o'} + E_{II}^{o'}}{2}\right)$ (mV)	Equilibrium constants K_{11}	K_{12}	K_{21}	K_{22}
(o)	Distinguishable, equivalent, and noninteracting clusters.	0	-383	.088	.088	.088	.088
(i)	Distinguishable, nonequivalent, and noninteracting clusters.	10	-381.5	.0725	.107	.107	.0725
(iii)[a]	Distinguishable, equivalent, and interacting[b] clusters.	0[b]	-383	.096[c]	.096[c]	.081[d]	.081[d]
(Wang)	Indistinguishable, equivalent, and noninteracting clusters.	5 ± 3[e]	-383	K_1 (Wang)[f] 0.048		K_2 (Wang)[f] 0.162	

a. Case (iii) and the Wang case have identical α vs β plots. Here the parameters are $K_{11} = K_{12} = 2K_1$ (Wang), and $K_{21} = K_{22} = (K_2)/2$ (Wang).

Notes to Table 34 continued.

b. Before reduction, $(E_{II}^{o\prime} - E_{I}^{o\prime}) = 0$, but if one cluster gets reduced the MV of interaction is 59 log $(\frac{0.096}{0.081})$ = 5 mV(i.e., the reduction of one cluster increases the midpoint redox potential of the other cluster by 5 mV).

c. First electron.

d. Second electron.

e. This is the difference between Eisenstein and Wang's observed and statistical values. From this difference they conclude that the two reducible iron atoms in each clostridial ferredoxin do not interact with each other "appreciably" (43).

f. K_1 (Wang) and K_2 (Wang) are the equilibrium constants Eisenstein and Wang calculate for their case of indistinguishable, equivalent, and noninteracting clusters.

Table 35. Least square calculation of α, the degree of reduction of C. pasteurianum ferredoxin based on the assumptions of cases (o), (i), (ii), and (iii).

β	$\alpha_{obs.}$	case (ii)[a] (Fig. 59)	case (iii)[b]	case (o)[b]	case (i)[b,c] (least square)	case (i)[d]
0.0075	0.0764	0.0720	0.0734	0.0785	0.0795	0.0763
0.0183	0.1660	0.1621	0.1641	0.1722	0.1735	0.1673
0.0300	0.2470	0.2441	0.2460	0.2542	0.2554	0.2471
0.0466	0.3350	0.3387	0.3398	0.3462	0.3468	0.3370
0.0669	0.4240	0.4284	0.4285	0.4319	0.4318	0.4211
0.0985	0.5290	0.5300	0.5288	0.5282	0.5271	0.5162
0.1328	0.6040	0.6072	0.6051	0.6014	0.5998	0.5892
0.1650	0.6610	0.6601	0.6575	0.6522	0.6501	0.6402
0.2050	0.7180	0.709	0.7063	0.6997	0.6974	0.6881
mean error ($\times 10^2$):		0.43	0.48	0.884	1.00	1.38

a. See Fig. 59.

b. See Fig. 61.

c. From this α_{calc} (least square) the protein midpoint redox potential is calculated to be -381.5 mV (See Fig. 59 caption).

d. α is recalculated assuming the protein midpoint redox potential is -383 mV.

Experiment 8.

The possible formation of a weak chemical bond between the aliphatic residues and the Fe-S clusters of clostrial-type ferredoxins

SUMMARY:

The ^{13}C-resonance positions of aliphatic amino acid residues in C. acidi-urici apoferredoxin do not significantly differ from the ^{13}C-resonance positions of aliphatic amino acids in model polypeptides. However in oxidized and reduced C. acidi-urici and C. pasteurianum ferredoxins some ^{13}C-resonances are significantly shifted from their positions in model polypeptides. The shifted resonances are tentatively assigned to amino acid residues that may be close to the Fe-S clusters of the oxidized and reduced ferredoxins.

INTRODUCTION:

Recently Adman et al. (2) have shown that eleven amino acid residues are closely packed around each Fe-S cluster in P. aerogenes ferredoxin. C. acidi-urici and C. pasteurianum ferredoxins, which are similar in sequence, are both homologous in sequence to P. aerogenes ferredoxin (129). The eleven above mentioned amino acid residues are homologous to the amino acid sequences of both C. acidi-urici and C. pasteurianum ferredoxin. (Only 2 and 3 of the 11 amino acid residues that may be packed around each Fe-S cluster in C. acidi-urici and C. pasteurianum ferredoxin, respectively, differ from those in P. aerogenes ferredoxin and these differing amino acids are similar in structure). This homology suggests that the three-dimensional orientation of the amino acid residues packed around the Fe-S clusters of these ferredoxins is similar.

The fact that both aromatic residues of C. acidi-urici (Experiment 7a) and C. pasteurianum (Experiment 7b) ferredoxins are magnetically perturbed by the unpaired electron spins in the Fe-S clusters is consistent with the fact that the two aromatic residues of P. aerogenes ferredoxin are each close to an Fe-S cluster.

^{13}C-resonances of the aliphatic amino acid residues close to the Fe-S clusters should also be magnetically shifted. The aliphatic region of oxidized and reduced C. acidi-urici and C. pasteurianum ferredoxin was thus examined by ^{13}C-NMR techniques to determine whether the aliphatic amino acid residues close to the Fe-S clusters in P. aerogenes ferredoxin are also close to the clusters in C. acidi-urici and C. pasteurianum ferredoxins.

The orientation and interaction of aliphatic and aromatic residues and Fe-S complexes may be important to the structure or function of bacterial ferredoxins. The magnitudes of the observed resonance shifts may depend on how the Fe-S cluster is oriented to neighboring protons and carbon atoms. Knowing the magnitudes of the shifts of aromatic and aliphatic ^{13}C resonances relative to the magnitudes of the shifts of their bonded protons can help one distinguish between the mechanisms which produce paramagnetic shifts. By unravelling the contribution from each paramagnetic shift mechanism one could determine: (i) the extent the interaction of these residues with the Fe-S complex is needed for protein stability and function; (ii) which energetic factors stabilize the alignment of these residues; and (iii) the extent the reducing electron is shared by the atoms in each Fe-S complex.

RESULTS:

RECONSTRUCTED ^{13}C-NMR SPECTRA:

One can reconstruct a ^{13}C-NMR spectrum of a denatured protein if one knows the amino acid composition and resonance position of each carbon atom in the amino acid residues. The ^{13}C resonances of the carbon atoms of most of the amino acid residues in model polypeptides have been assigned (Table 36), and, with the aid of a computer, we have reconstructed the ^{13}C-NMR spectrum of the aliphatic region of C. acidi-urici apoferredoxin (Fig. 63B) by assuming that the average half-width of each resonance is 15 Hz for the amino acid backbone-carbon atoms and 10 Hz for the amino acid side chain-atoms. This half-width assumption is arbitrary, but it is consistent with the fact that, in polypeptides (53), side chain atoms rotate more freely than do α-carbon (backbone) atoms and thus have narrower resonances.

The major discrepancies between the calculated (reconstructed) ^{13}C-NMR spectrum (Fig. 63B) and the observed spectrum (Fig. 63A) of C. acidi-urici apoferredoxin are: (i) the 1 ppm upfield displacement of the δ-carbon resonance of the five isoleucyl residues at 181.3 ppm, in the reconstructed spectrum, to 182.3 ppm in the observed spectrum (this shift for the isoleucyl δ-carbon resonance is also observed in denatured ribonuclease (53)), (ii) the 1 ppm upfield displacement of the α- and β-carbon resonances of the eight cysteinyl residues at 136.1 and 167.1 ppm, in the reconstructed spectrum, to 137.1 and 168.1 ppm in the observed spectrum respectively. (iii) the absence of a resonance at 153.8 ppm, which is present in the calculated spectrum. The intensity of the resonance at 156.3 ppm in the reconstituted spectrum is larger

than the corresponding resonance in the observed spectrum, and this may be due to differences in resonance positions of either the β-carbons of the five aspartyl residues, the five isoleucyl residues or the two tyrosyl residues. The extra resonance at 153.8 ppm in the observed spectrum may correspond to any of the above-mentioned β-carbon resonances.

C. acidi-urici FERREDOXIN:

When the ^{13}C-NMR spectrum of C. acidi-urici apoferredoxin (Fig. 64C) is compared with that of oxidized and methyl viologen-reduced C. acidi-urici ferredoxins (Fig. 64B and 64A, respectively), there are many significant differences. The δ-carbon resonance of the five isoleucyl residues and the α- and β-carbon resonances of the eight cysteinyl residues are the only resonances one can tentatively assign.

In (8±2)% reduced C.acidi-urici ferredoxin the isoleucyl δ-carbon resonances are shifted ~2 ppm downfield relative to their position in the oxidized protein. To the extent that one can accurately extrapolate this shift to full reduction, this represents a 20 ppm shift. This 20 ppm shift is of the same order of magnitude as some ring carbon shifts (Table 37). The resonances seen at 0.5 and 0.9 ppm from DSS in the ^{1}H-NMR spectra of oxidized C. acidi-urici ferredoxin (Fig. 65C) can be tentatively assigned to the δ-proton resonances of the isoleucyl residues since these resonances are near the resonance position of the δ-protons of isoleucyl residues in model polypeptides (119). These proton resonances only shift ~ 0.2 ppm downfield in the ^{1}H-NMR spectrum of 50% reduced ferredoxin. (Fig. 65A). Some (or all of) the α- and β-cysteinyl carbon resonances are missing in the ^{13}C-NMR spectrum

(Fig. 64B) of oxidized C. acidi-urici ferredoxin, and all of the β-cysteinyl carbon resonances are missing in the spectrum (Fig. 64A) of reduced C. acidi-urici ferredoxin.

A group of "eight" resonances, in the ^{13}C-NMR spectrum (Fig. 66B) of oxidized C. acidi-urici ferredoxin, is shifted between 20 and 40 ppm from the α-cysteinyl carbon resonance position in C. acidi-urici apoferredoxin (Fig. 64C). This group, of "eight" shifted resonances, shifts an additional 10 ppm (as a group) in the spectrum (Fig. 66D) of the ~ 8% reduced C. acidi-urici ferredoxin and this 10 ppm shift extrapolates to 100 ppm in the fully reduced ferredoxin. Double resonance experiments (Fig. 71) show small shifts for the resonances of the protons, bonded to the carbon atoms represented by these "eight" shifted carbon resonances (Table 37). The proton-coupled ^{13}C-NMR spectrum (Fig. 71) of ~ 8% reduced C. acidi-urici ferredoxin shows that some of these "eight" shifted carbon resonances split into doublets and thus these resonances correspond to α-carbon atoms.

C. pasteurianum FERREDOXIN:

To the extent that the calculated (reconstructed) ^{13}C-NMR spectrum of the aliphatic region of C. acidi-urici apoferredoxin agrees with that of the observed C. acidi-urici apoferredoxin spectrum, one can use the calculated ^{13}C-NMR spectrum (Fig. 67A) of the aliphatic region of C. pasteurianum apoferredoxin in lieu of an observed spectrum for C. pasteurianum apoferredoxin. Comparison of the calculated spectra of C. acidi-urici and C. pasteurianum apoferredoxins (Fig. 67) shows only small differences and these are due to the differences in amino acid composition. The differences between the observed ^{13}C-NMR spectra of the

alphatic region of oxidized C. acidi-urici and C. pasteurianum ferredoxins (Fig. 68A and 68B respectively) are greater than the differences between that of the calculated spectra of C. acidi-urici and C. pasteurianum apoferredoxins. This suggests that the conformations of oxidized C. acidi-urici and oxidized C. pasteurianum ferredoxins differ more than the conformations of C. acidi-urici and C. pasteurianum apoferredoxins. This difference is also reflected in the ^{1}H-NMR spectra (Fig. 72) of the aliphatic regions of oxidized C. acidi-urici and C. pasteurianum ferredoxins. The presence of a phenylalanyl residue in these ferredoxins is not responsible for the difference in the NMR spectra of oxidized C. acidi-urici and C. pasteurianum ferredoxins because the ^{1}H-NMR spectrum of the aliphatic region of C. acidi-urici native ferredoxin (Fig. 72C) is identical to that of C. acidi-urici [Phe^{2}]-ferredoxin (Fig. 72B). This is also true for the corresponding ^{13}C-NMR spectra of the aliphatic region. (Fig. 69).

Many of the same ^{13}C- and ^{1}H-resonance shifts observed for oxidized and reduced C. acidi-urici ferredoxins occur in oxidized and reduced C. pasteurianum ferredoxins as well. The α- and β-carbon resonances of the eight cysteinyl residues and the δ-carbon resonances of the five isoleucyl residues, in the ^{13}C-NMR spectra of oxidized and reduced C.pasteurianum ferredoxins (Figs. 68B and 68A respectively) are missing (or shifted) from their positions in the calculated spectrum (Fig. 68C) of C. pasteurianum apoferredoxin. The eight shifted carbon resonances (at ~ 100 ppm from CS_2) in the ^{13}C-NMR spectrum (Fig. 66C) of the oxidized C. pasteurianum ferredoxin are missing in the spectrum (Fig. 66E) of the fully reduced protein. Similarly the δ-proton resonances (at 0.5 and 0.9 ppm from DSS (Fig. 70B), tentatively assigned to the

isoleucyl residues of oxidized C. pasteurianum ferredoxin, is also missing in the ^{1}H-NMR spectrum (Fig. 70A) of the fully reduced protein.

DISCUSSION:

Some of the carbon and proton resonances of certain aliphatic and both aromatic amino acid residues are shifted in oxidized and reduced C. acidi-urici and C. pasteurianum ferredoxins (Table 37). Only the eight cysteinyl residues are directly bonded to the Fe-S clusters in these ferredoxins, and the α- and β-carbon and proton resonances of these residues should experience large shifts. These shifts would be primarily due to a Fermi-contact interaction involving spin delocalization. The shifts of ^{13}C- or ^{1}H-resonances of other amino acid residues very close to the Fe-S cluster should be primarily due to any combination of pseudocontact. Fermi-contact and reorthogonalization contact interactions (See Experiment 7a).

CYSTEINYL β-CARBON RESONANCES:

The β-carbon resonance of C. acidi-urici apoferredoxin is missing from the ^{13}C-NMR spectra of the aliphatic region. ^{1}H-NMR spectra of oxidized and reduced C. acidi-urici and C. pasteurianum ferredoxins show large proton resonance shifts relative to their free amino acid proton resonance positions of ~ 15 ppm and ~ 50 ppm for the oxidized and reduced proteins respectively (See Experiments 6b, and 7b.). Phillips and coworkers (111) have assigned these shifted resonances to the β-protons of the eight cysteinyl residues in both ferredoxins. If this assignment is correct, one would expect the cysteinyl β-carbon resonances of the cysteinyl residues is practical only with clostridial-type ferredoxin in which the cysteinyl residues are enriched with ^{13}C because the β-carbon resonances may be too broad to detect in ^{13}C natural abundance.

CYSTEINYL α-CARBON RESONANCES:

A group of seven or eight carbon resonances is shifted 20-40 ppm downfield (relative to the α-cysteinyl carbon resonance in model peptides (151) in oxidized C. acidi-urici and C. pasteurianum ferredoxins.

These "eight" shifted carbon resonances are tentatively assigned to the α-carbon resonances of the eight cysteinyl residues in C. acidi-urici and C. pasteurianum ferredoxins because:

(i) same of these shifted resonances are α-carbon resonances;

(ii) most, if not all, of the α-carbon resonances of the cysteinyl residues in the ^{13}C-NMR spectra of these oxidized and reduced ferredoxins are missing or shifted;

(iii) in the oxidized protein this group of "eight" carbon resonances is shifted (relative to the α-cysteinyl carbon resonance position in model peptides) ~ 35 ppm downfield, while the resonances of the protons (bonded to these carbon atoms) $\leq$ 2 ppm downfield from the β-proton position of the cysteinyl residues in model peptides;

(iv) in the reduced protein this group of "eight" carbon resonances shifts as a group, and the magnitude of this shift (extrapolated to the fully reduced protein) is ~ 100 ppm; and

(v) the large magnitude of the carbon resonance shifts (and the small magnitude of the proton resonance shifts) suggests that these carbon resonance shifts are caused by a Fermi-contact shift interaction which would be expected for carbon atoms of cysteinyl residues, since these residues are covalently bonded to the iron atoms of the Fe-S cluster.

The similar shift pattern observed for this group of "eight" shifted resonances in both oxidized C. acidi-urici and C. pasteurianum ferredoxins also indicates that, if the cysteinyl α-carbon assignment is correct, the cysteinyl sulfur atoms may be bonded similarly in each protein.

Even if our α-cysteinyl carbon resonance assignment is not correct, the fact that these "eight" resonances are shifted as a group suggests that the reducing electron is shared by all the iron atoms in each Fe-S cluster, since this group of resonances could correspond to the α-carbon atoms of other amino acid residues that are physically surrounding the Fe-S cluster.

ISOLEUCYL δ-CARBON RESONANCES:

If our isoleucyl δ-proton and δ-carbon resonance assignments are correct, then the shifts of the proton resonances of the isoleucyl residues in C. acidi-urici ferredoxin are much smaller than the shifts of their corresponding (bonded) carbon atoms. Large carbon and small proton resonance shifts are also observed for the aromatic residues (See Experiment 7b). Thus, we hypothesize that the aromatic residues and some of the isoleucyl residues in these ferredoxins may form weak chemical bonds with the Fe-S clusters, a hypothesis which is consistent with the fact that most of the ring carbon atoms and four isoleucyl δ-carbon atoms are close to an Fe-S cluster in oxidized crystalline P. aerogenes ferredoxin (64) (Table 39).

OTHER ALIPHATIC CARBON RESONANCES:

The carbon resonances of a few other aliphatic residues (Table 38) in both ferredoxins are also shifted downfield upon reduction. We have tentatively assigned these shifted resonances to the aliphatic residues that may be physically close to the Fe-S clusters of each protein (Table 39) (64). This is because there is a high probability that a shifted resonance corresponds to a nucleus of an amino acid residue close to an Fe-S cluster (Table 38). (Almost all of the shifted resonances correspond in number and kind to carbon nuclei of the aliphatic residues presumed to be close to the Fe-S clusters in oxidized C. acidi-urici and C. pasteurianum ferredoxin.) This tentative assignment is strengthened by the fact that upon reduction of both proteins some of these same resonances are shifted still further downfield (Fig. 38), and the resonances of amino acids not close to the Fe-S cluster tend not to be shifted in both oxidized and reduced proteins.

The differences in the NMR spectra of the aliphatic regions of oxidized C. acidi-urici and C. pasteurianum ferredoxins may be due to differences in the magnitudes of magnetic shifts produced by differences in the orientations within each protein of certain aliphatic side chains surrounding the Fe-S cluster.

Most of the shifts of the ^{13}C-resonances of aliphatic amino acid residues close to, but not directly bonded to, Fe-S clusters are downfield shifts. Shifts due to a pseudocontact interaction tend to be of the same sign (24), but the resonances of nuclei very close to the Fe-S cluster may also be shifted by a contact mechanism involving reorthogonalization of spins. (See Experiment 7a).

Weak bonds to the Fe-S clusters:

If some of the nuclei are close enough to the Fe-S clusters to be shifted by the (reorthogonalization) contact mechanism, these nuclei must form weak bonds with the Fe-S cluster. This is consistent with the fact that upon full reduction of C. pasteurianum and C. acidi-urici ferredoxins of assigned (aromatic) carbon atoms and tentatively assigned (δ-isoleucyl) carbon atoms, shift about 20 ppm from their positions in the oxidized proteins. In oxidized (crystalline) P. aerogenes ferredoxin (64) there are at least twenty other carbon atoms within 5 Å of the Fe-S clusters (Table 39). A conservative estimate would assume that if the structure of P. aerogenes ferredoxin is similar to that of C. acidi-urici ferredoxin at least twenty protons bonded to these assigned and unassigned carbon atoms should show similar ($\leq$ 20 ppm) downfield resonance shifts upon reduction (if the shifts were due to a pseudocontact interaction). These large proton shifts are not observed. (If the sixteen significantly shifted

proton resonances observed for fully reduced C. acidi-urici and C. pasteurianum ferredoxins represent the β-protons of the eight cysteinyl residues, then the resonances of the ~ 20 (noncysteinyl) protons must experience small shifts).

Some of the ring carbon atoms could form a weak bond with the Fe-S cluster (See Experiment 7a, b), since the proton shifts of the ring carbon resonances are five to ten times smaller than expected for a pseudocontact interaction. Thus if the resonances of protons bonded to aliphatic carbon atoms (that show large carbon resonance shifts) are small, then the perturbed aliphatic residues could also form weak bonds with the Fe-S clusters.

Fig. 63. ^{13}C-NMR (10°C) of the aliphatic residues of C. acidi-urici apoferredoxin. (A): Observed C. acidi-urici apoferredoxin spectrum, conditions same as Fig. 67A. (B): Calculated reconstructed C. acidi-urici apoferredoxin spectrum based on peptide amino acid residue assignments in Table 36. The resonances are plotted so that each resonance has a 15 Hz half width (i.e., width at half the resonance intensity) from 125-150 ppm and 10 Hz half-width from 150-180 ppm. The 10 Hz half-width region corresponds to resonances of side chain aliphatic carbon atoms.

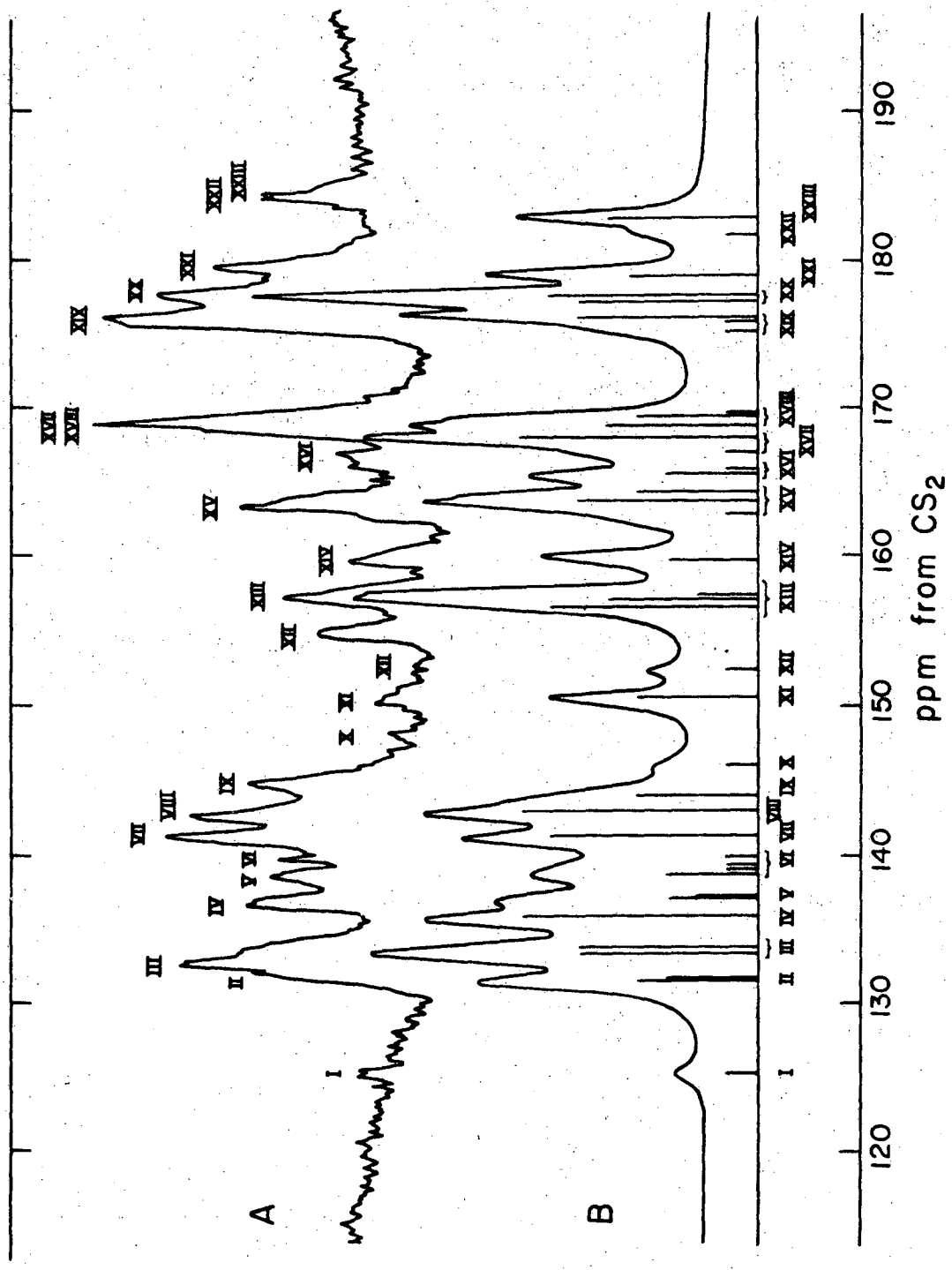
A
B
120
130
140
150
160
170
180
190
ppm from CS_2

Fig. 64. ^{13}C-NMR spectra of the aliphatic region of C. acidi-urici ferredoxin. (A): (20±5)% reduced ferredoxin (~ 30 mg/ml, dissolved in 0.2M KD_2PO_4-K_2DPO_4 buffer, pD 7.8 plus 0.25M Zn-reduced methyl viologen), (B): Oxidized ferredoxin (~ 40 mg/ml, dissolved in 0.2M KD_2PO_4-K_2DPO_4 buffer, pD 7.6), (C): Apoferredoxin (~ 80 mg/ml, dissolved in 0.2M KD_2PO_4 - K_2DPO_4 buffer, pD 7.8 plus 0.1M Na_2S).

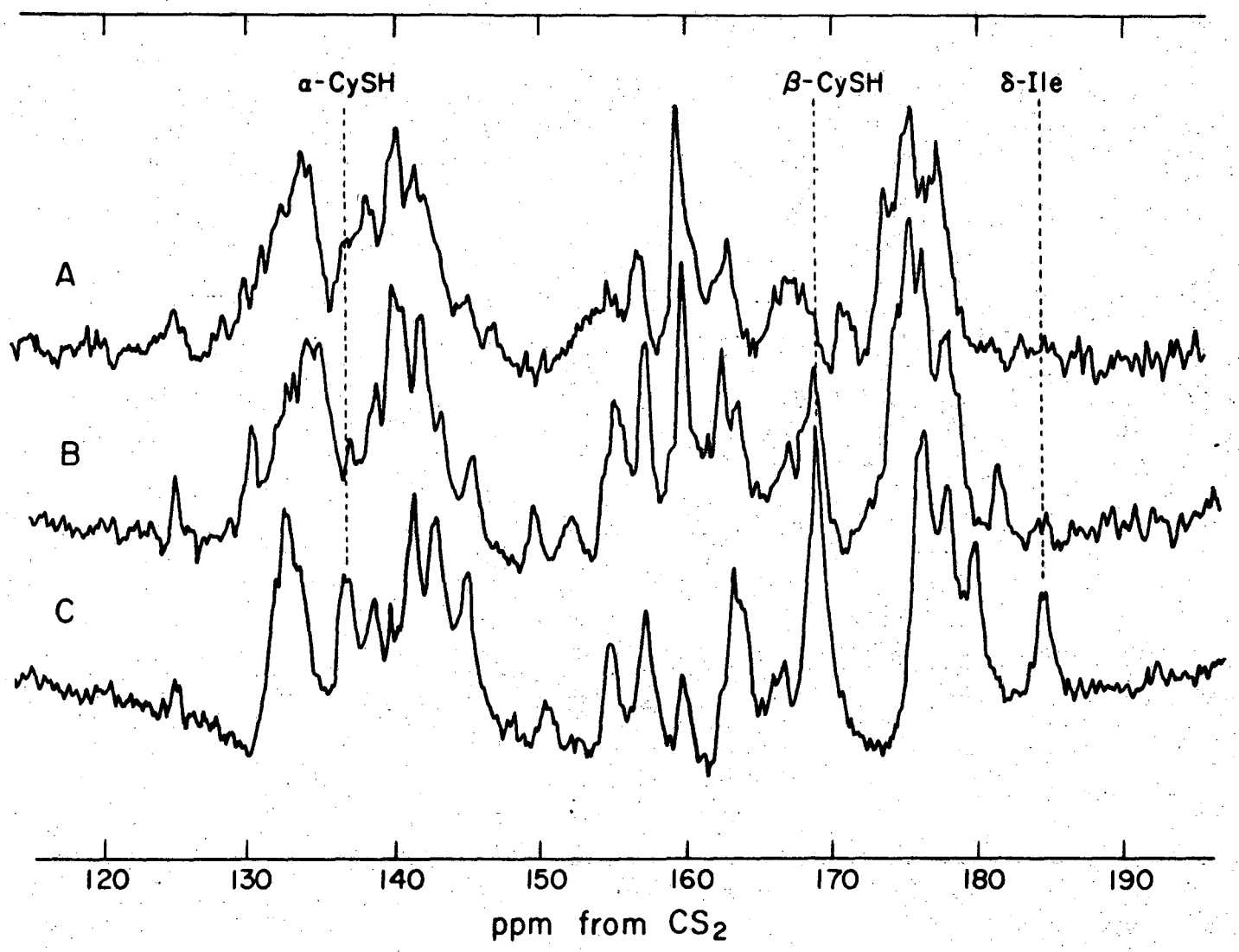
α-CySH
β-CySH
δ-Ile
A
B
C
120
130
140
150
160
170
180
190
ppm from CS_2

Fig. 65. ^{1}H-NMR (15°C) of the aliphatic region of oxidized and reduced C. acidi-urici ferredoxin. (A): 50% Reduced. (B): 20% Reduced. (C): Oxidized. Conditions same as described in Experiments 6a and 6b. (Arrows point to tentatively assigned isoleucyl δ-proton resonances.)

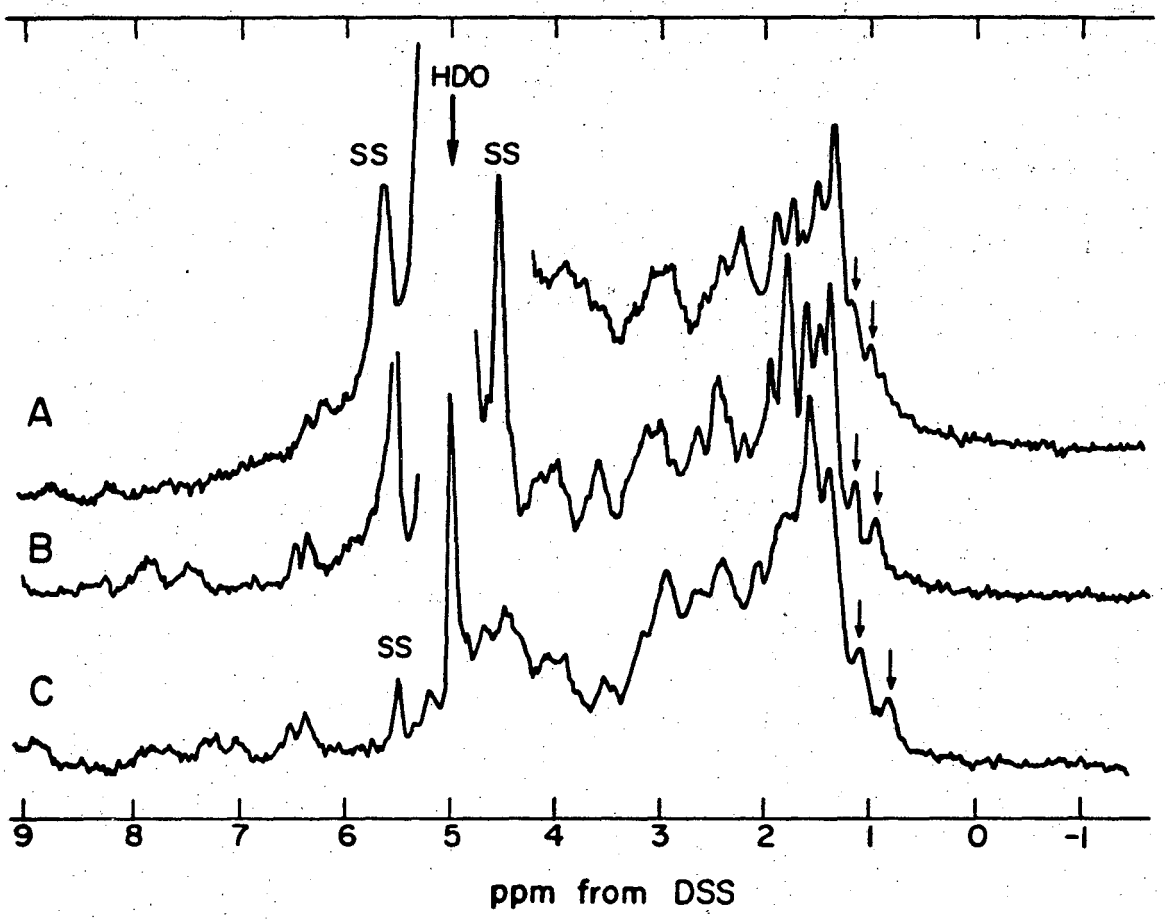
HDO
SS
SS
SS
A
B
C
9
8
7
6
5
4
3
2
1
0
-1
ppm from DSS

Fig. 66. ^{13}C-NMR (10° C) of the shifted aliphatic residues of oxidized and reduced C. acidi-urici and C. pasteurianum ferredoxins. (A): C. acidi-urici apoferredoxin ~ 80 mg/ml, 0.2 M KD_2PO_4-K_2DPO_4 buffer, pD 7.8 plus 0.1 M Na_2S. (B): Oxidized C. acidi-urici native ferredoxin, ~ 40 mg/ml, 0.2 M KD_2PO_4-K_2DPO_4 buffer, pD 7.0. (C): Oxidized C. acidi-urici [Phe^2]-ferredoxin ~40 mg/ml, 0.2 M KD_2PO_4-K_2DPO_4 buffer, pD 7.8. (D): Oxidized C. pasteurianum ferredoxin, conditions same as B. (E): (8 ± 2)% reduced C. acidi-urici ferredoxin, ~80 mg/ml, 0.2 M KD_2PO_4-K_2DPO_4 buffer, pD 7.6 plus 0.25 M Zn-reduced methyl viologen. (F): (90 ± 10)% reduced C. pasteurianum ferredoxin, 0.2 M KD_2PO_4-K_2DPO_4 buffer, pD 7.6 plus 0.25 M Zn-reduced methyl viologen.

^{13}C-NMR (10°C) OF *C.ACIDI URICI* AND *C.PASTEURIANUM* FERREDOXIN
α-CARBON RESIDUES

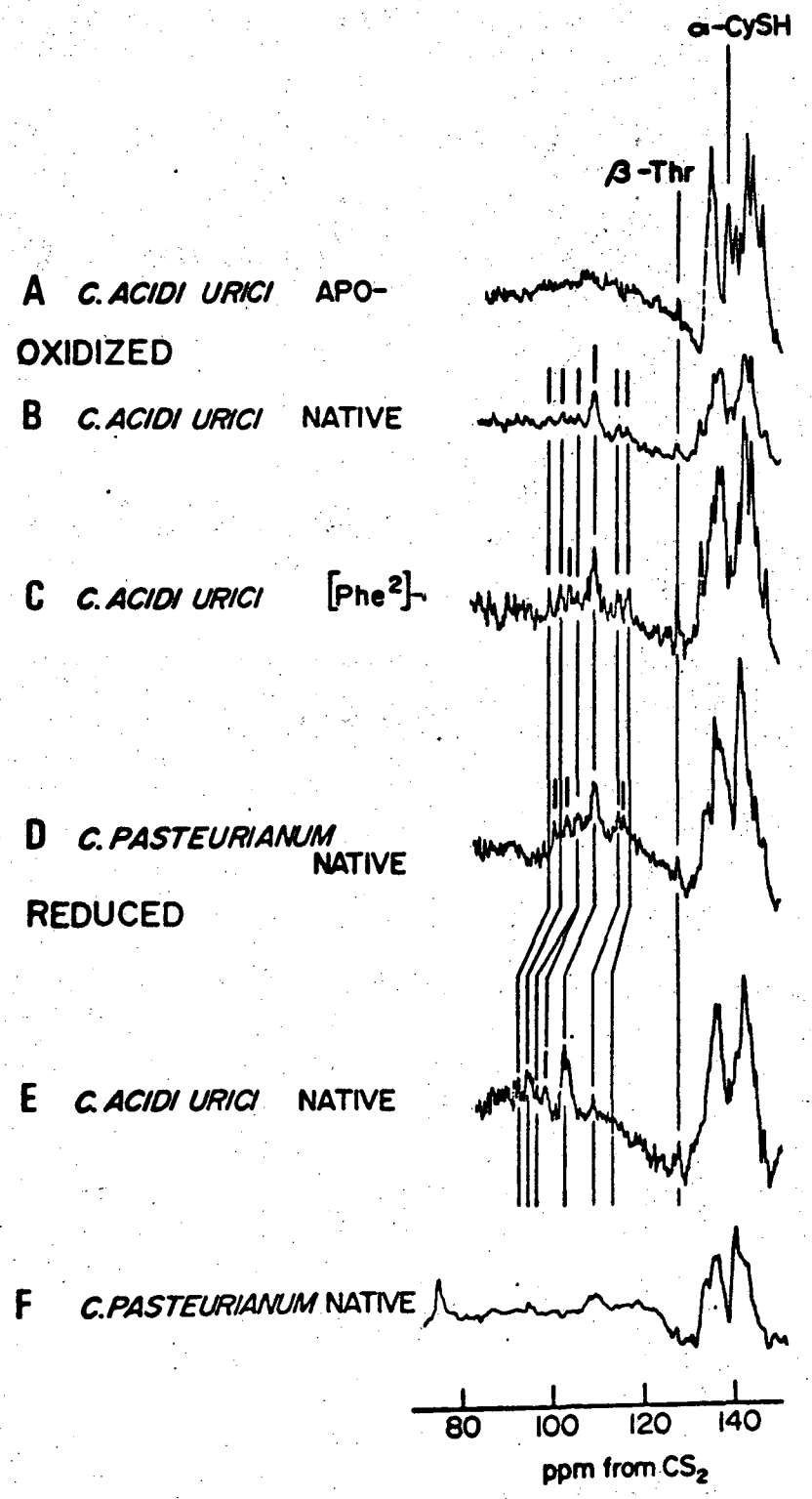

Fig. 67. ^{13}C-NMR (10°C) of the aliphatic region of clostridial-type ferredoxins. (A) Observed spectrum of oxidized C. pasteurianum ferredoxin. Conditions as in Fig. 66D. (B) Observed spectrum of oxidized C. acidi-urici ferredoxin. Conditions as in Fig. 66B. (C) Calculated spectrum of C. pasteurianum apoferredoxin based on assignments listed in Table 36 and assuming a resonance half-width of 15 Hz. (D) Calculated spectrum of C. acidi-urici apoferredoxin. Conditions as in A.

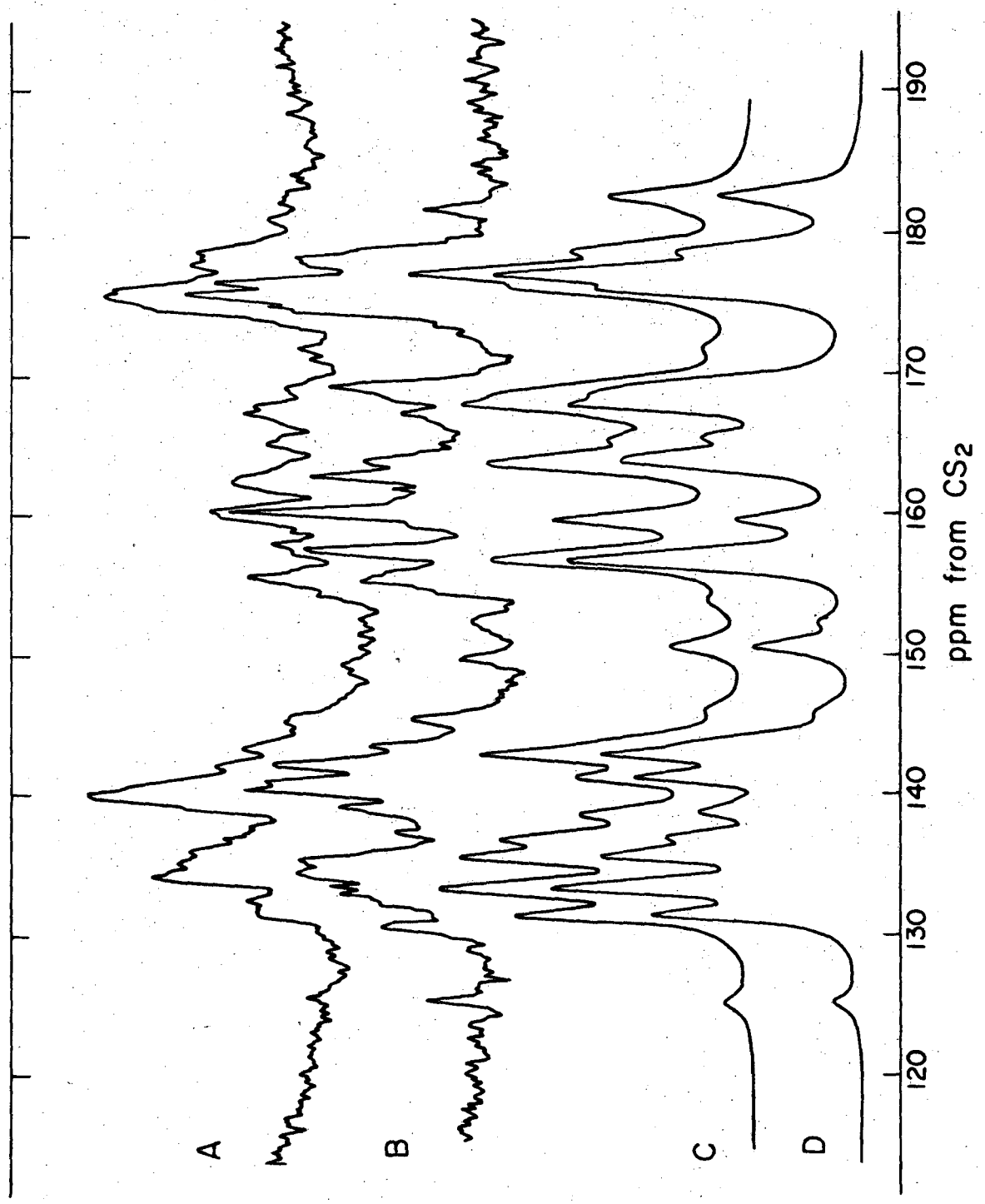
A
B
C
D
120
130
140
150
160
170
180
190
ppm from CS_2

Fig. 68. ^{13}C-NMR spectra of the aliphatic region of C. pasteurianum ferredoxin. (A) (90 ± 10)% Reduced ferredoxin, (B) Oxidized ferredoxin, and (C) Calculated (reconstructed) apoferredoxin, assignments based on Table 36 with an average half line-width of 15 Hz. Conditions same as in Fig. 66F, and 66D for the reduced and oxidized proteins respectively.

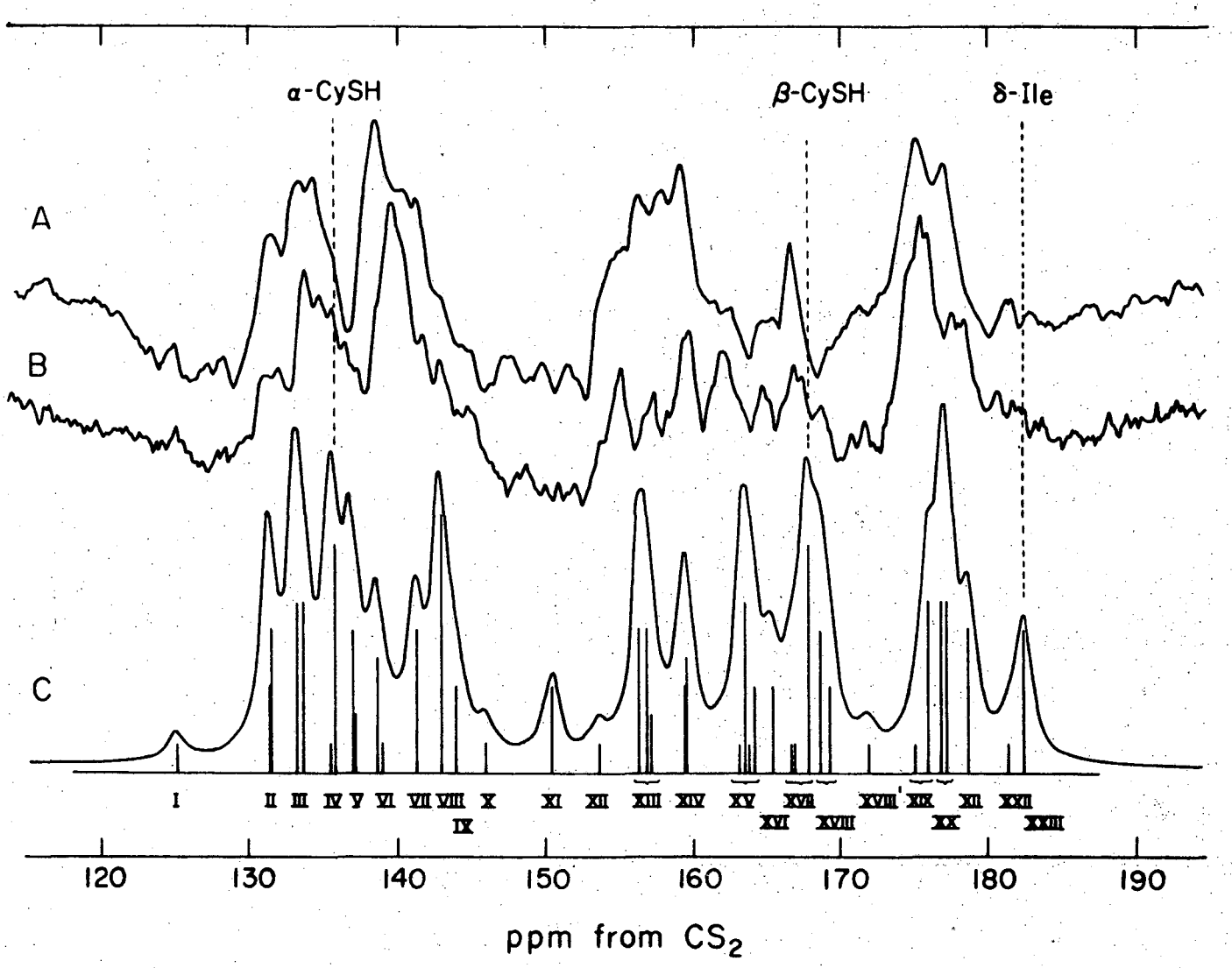
α-CySH
β-CySH
δ-Ile
A
B
C
I
II
III
IV
V
VI
VII
VIII
IX
X
XI
XII
XIII
XIV
XV
XVI
XVII
XVIII
XIX
XX
XXII
XXIII
120
130
140
150
160
170
180
190
ppm from CS_2

Fig. 69. ^{13}C-NMR of oxidized C. acidi-urici native ferredoxin (A) and C. acidi-urici [Phe^{2}]-ferredoxin (B). Conditions same as described in Figs. 66B and 66C respectively.

^{13}C-NMR (10°C) OF *C.ACIDI URICI* FERREDOXIN

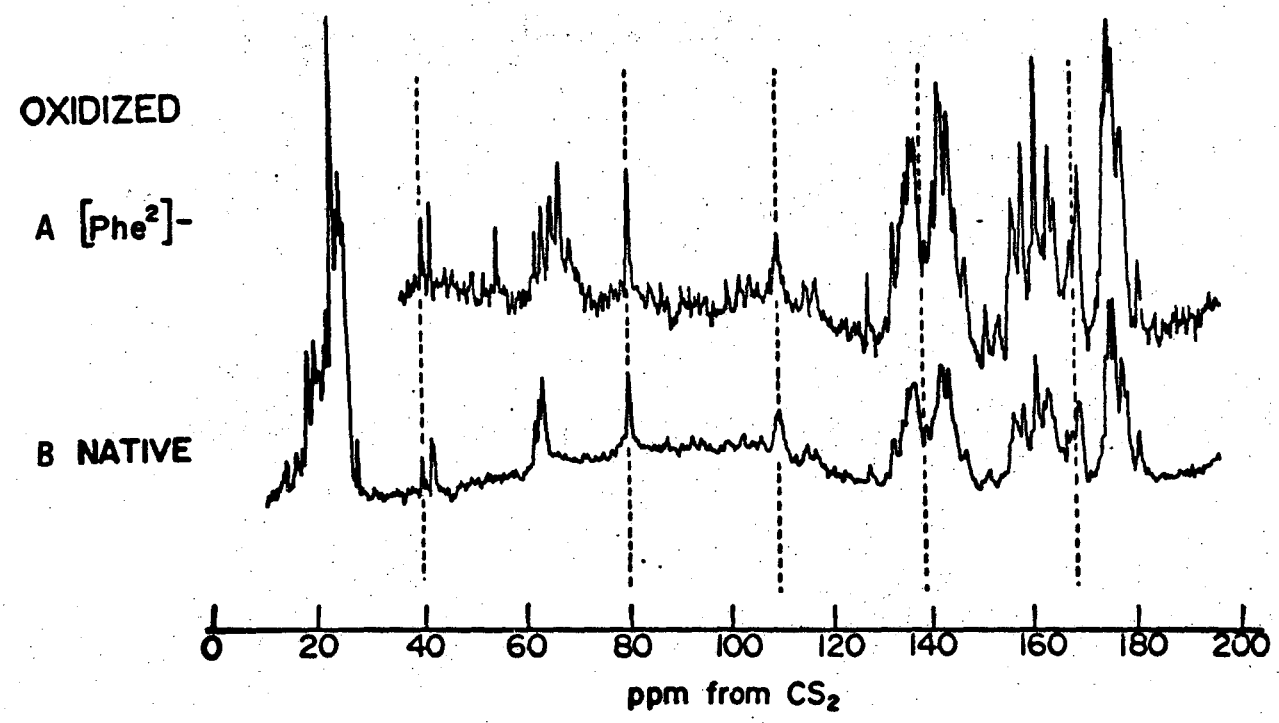

Fig. 70. ^{1}H-NMR (15°C) of the aliphatic region of oxidized and reduced *C. pasteurianum* ferredoxin. (B): Oxidized (A): (90 ± 10)% reduced. Conditions same as described in Experiment 7b. (Dotted lines designate the tentatively assigned isoleucyl δ-proton resonances.)

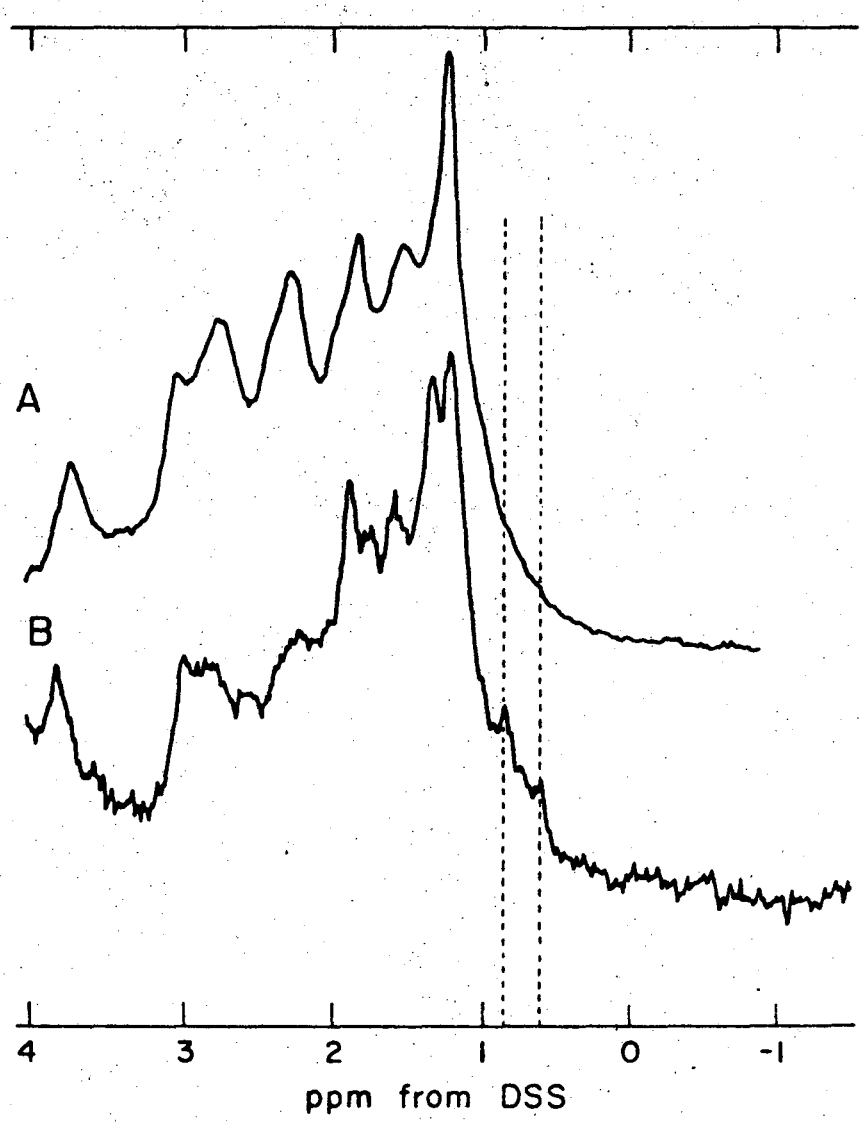
A
B
4
3
2
1
0
-1
ppm from DSS

Fig. 71. ^{13}C-NMR (10° C) of (8 ± 2)% reduced C. acidi-urici ferredoxin. (A): Noise decoupled. (B): Coherent decoupled, decoupling frequency 3 ppm from DSS. (C) Coherent decoupled, decoupling frequency 7 ppm from DSS. (D): Coherent decoupled, decoupling frequency 9 ppm from DSS; (E): Coherent decoupled, decoupling frequency 11 ppm from DSS; (F): Coupled.

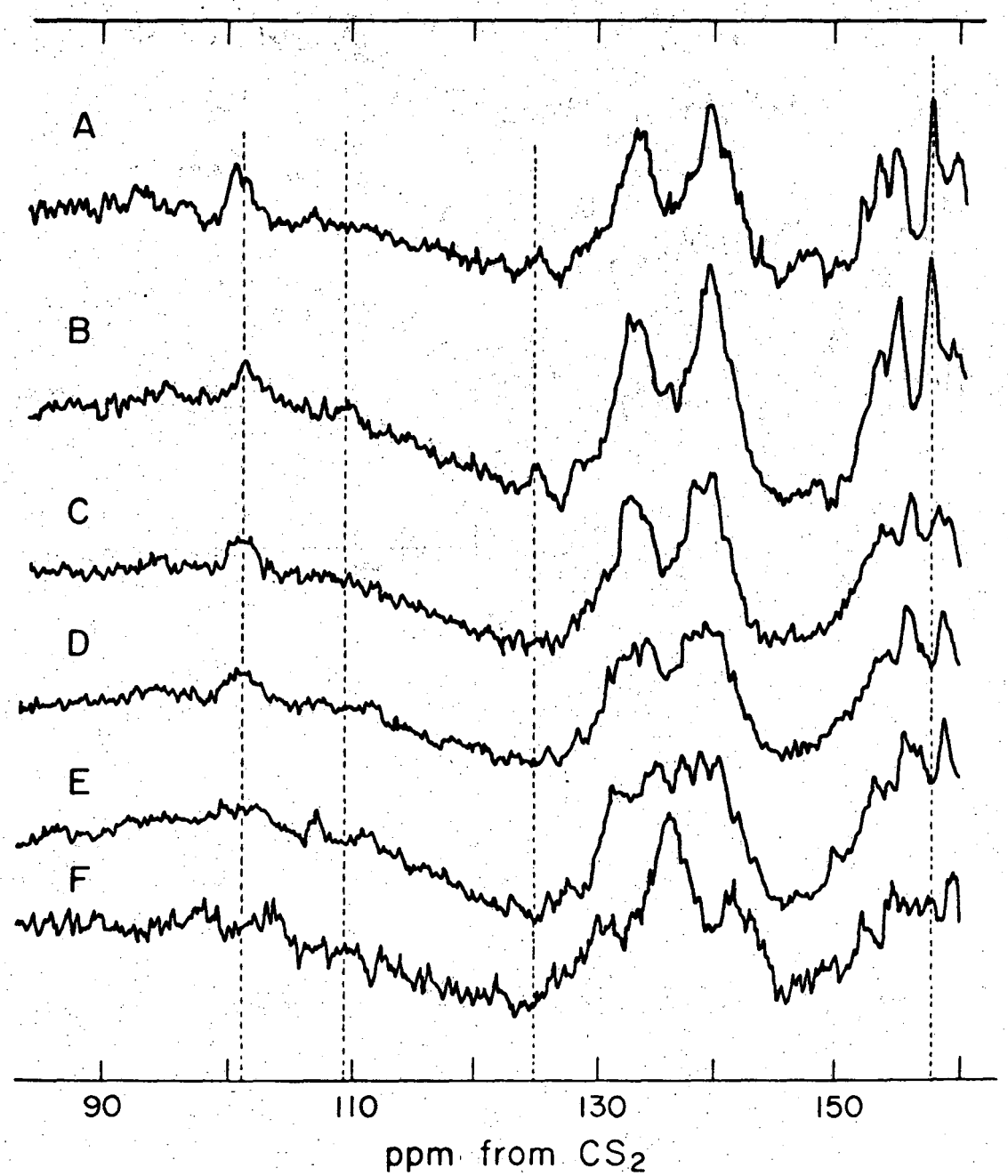
A
B
C
D
E
F
90
110
130
150
ppm from CS_2

Fig. 72. ^{1}H-NMR spectra (15°C) of the aliphatic region of oxidized *C. pasteurianum* ferredoxin (A), *C. acidi-urici* [Phe^{2}]-ferredoxin (B), and *C. acidi-urici* native ferredoxin (C).

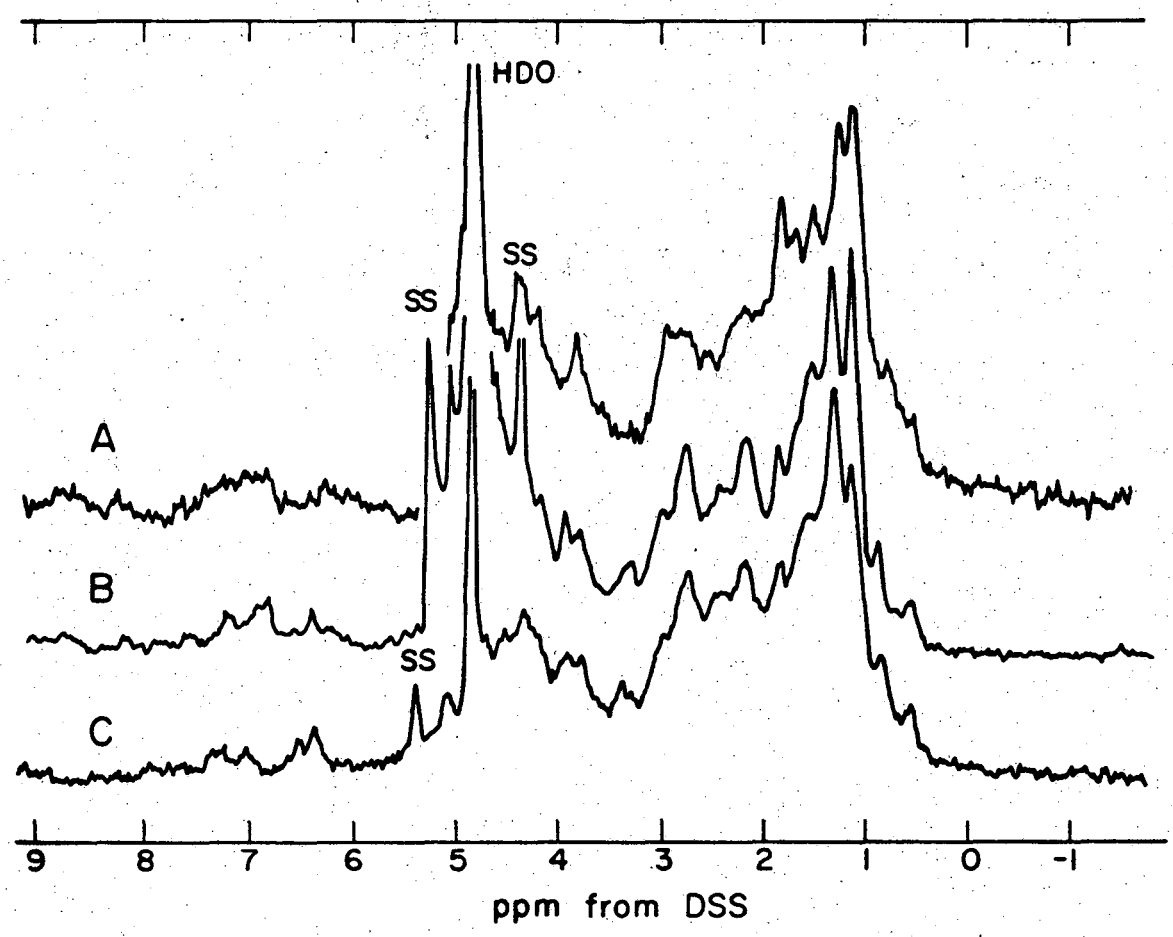
HDO
SS
SS
SS
A
B
C
9
8
7
6
5
4
3
2
1
0
-1
ppm from DSS

Table 36. Aliphatic carbon resonance shifts[a] (ppm relative to CS_2) in *Clostridium acidi-urici* and *Clostridium pasteurianum* ferredoxin.

Peak (Figs. 63, 64, and 67)	Position ppm from CS_2	Amino Acid Carbon	Number of Residues: *C. acidi-urici* (117)	Number of Residues: *C. pasteurianum* (130)
I	125.8	β-Thr	1	1
II	131.9	α-Pro	4	3
	132.0	β-Ser	3	5
III	133.7	α-Ile	5	5
	133.7	α-Thr	1	1
	134.1	α-Val	6	6
IV	135.9	α-Glu[b]	0	1
	136.1	α-CySH	8	8
V	137.3	α-Ser	3	5
	137.4	α-Tyr	2	1
	137.4	α-Phe	0	1
VI	138.9	α-Glu	3	3
	138.9	α-Lys	0	1
	139.2	α-Gln	1	1
VI'	139.5	α-Arg	1	0
	140.0	α-Ala[b]	1	0
VII	141.4	α-Asp	7	5
VIII	143.0	α-Ala	7	6
	143.0	α-Asn	1	3
IX	144.0	δ-Pro	4	3
X	146.0	α-Ala[c]	1	1
XII	150.3	α-Gly	4	3
XIII	152.1	δ-Arg	1	0
	153.4	ε-Lys	0	1
XIII'	156.0	β-Asp	7	5
	156.5	β-Ile	5	5
	156.8	β-Tyr	2	1
	156.8	β-Phe	0	1
XIV	159.0	β-Asn	1	3
	159.1	γ-Glu	3	3
	159.1	γ-Glu[b]	0	1

Table 36. (Continued)

	162.2	γ-Gln	1	0
	162.7	β-Lys	0	1
XV	163.0	β-Val	6	6
	163.3	β-Glu[b]	0	1
	163.6	β-Pro	4	3
	164.8	β-Glu	3	3
XVI	165.1	β-Arg	1	0
	166.2	β-Gln	0	1
	166.6	δ-Lys	0	1
XVII	167.1	β-CySH	8	8
	167.9	γ-Ile	5	5
XVIII	168.5	γ-Pro	4	3
	168.7	γ-Arg	1	0
XVIII'	170.9	γ-Lys	0	1
	174.1	γ-Thr	1	1
XIX	174.8	β-Ala[b]	1	0
	175.0	γ_1-Val	6	6
XX	176.0	γ_2-Val	6	6
	176.3	β-Ala	7	5
XXI	177.7	γ_2-Ile	5	5
XXII	180.3	β-Ala[c]	1	1
XXIII	181.3	δ-Ile	5	5

a. Based on peptide assignments of References 26 and 53.

b. C-terminal

c. N-terminal

Table 37. ^{13}C and ^{1}H resonance shifts[a] of C. acidi-urici and C. pasteurianum ferredoxin relative to their resonance positions in free amino acids.

Atom	Aromatic Residues							
	Oxidized				Reduced[b]			
	Tyr[2]	Tyr[30]	Phe[2]	Phe[30]	Tyr[2]	Tyr[30]	Phe[2]	Phe[30]
2',6'-C	-2.6	-2.4	-1.6	-2.0	-17.1	-17[c]	-17[c]	-9.2
2',6'-H	-0.4	-0.2	0	0	- 2.5	- 3[c]	- 2[c]	-1.4
3',5'-C	+0.1	0	-0.2	0	- 3.8	- 4	- 4	-2.0
3',5'-H	0	0	0	0	+ 0.8	+0.4	-0.5	-0.5

	Aliphatic Residues			
	Oxidized		Reduced[b]	
	CySH[d]	Ile[e]	CySH[d]	Ile[e]
α-C	range from -20 to -40	-	range from -80 to -100	-
α-H	range from +0.5 to -2.9 ± 0.6	-	n.d.[f]	
δ-C	-	-1	-	-25[g]
δ-H	-	<+0.2	-	<-0.2[g]

Notes to Table 37.

a. ^{13}C-shifts are $\pm$ 0.2 ppm relative to CS_2. ^{1}H shifts are $\pm$ 0.5 ppm relative to DSS unless otherwise indicated.
b. Of "fully" reduced ferredoxin (See Experiment 7b).
c. Extrapolated to full reduction (Fig. 52, Experiment 7b).
d. Tentatively assigned to seven or eight cysteinyl residues.
e. Tentatively assigned to three or four isoleucyl residues.
f. nd = not determined.
g. Extrapolated to full reduction from 8% and 20% reduced C. acidi-urici ferredoxin from ^{13}C-NMR spectra.
h. Extrapolated to full reduction from 20% and 50% reduced C. acidi-urici ferredoxin from ^{1}H-NMR spectra. (Fig. 65).

Table 38. Shifted[a] aliphatic carbon resonances in oxidized and reduced *Clostridium acidi-urici* and *Clostridium pasteurianum* ferredoxin.

Peak (Figs. 64 and 66)	Shifted Peak: Oxidized[b]	Shifted Peak: Reduced[c]	Amino Acid Carbon	Amino acids presumed to be near an Fe-S cluster: *C. acidi-urici*	Amino acids presumed to be near an Fe-S cluster: *C. pasteurianum*
I	-	-	β-Thr	0	0
II	+	d	α-Pro	2	2
			β-Ser	1(1)[e]	2(1)
III	+	d	α-Ile	2	1
			α-Thr	0	0
			α-Val	2	2
IV	-	-	α-Glu[f]	0	0
IV'	+[g,h]	+++[h,i]	α-CySH	8(8)	8(8)
V	-	-	α-Ser	1	2
			α-Thr	2	1
			α-Phe	0	1
VI	-	-	α-Glu	0	1
			α-Lys	0	0
			α-Gln	0	1
VI'	-	-	α-Arg	0	0
			α-Ala[f]	0	0
VII	-	+	α-Asp	1	1
VIII	+	++	α-Ala	2	1
			α-Asn	0	0
IX	+	++	δ-Pro	2(2)	2(2)
X	-	-	α-Ala[j]	0	0
XI	+	++	α-Gly	2(1)	1(1)
XII	-	-	δ-Arg	0	0
			ε-Lys	0	0
XIII	-	+	β-Asp	1	1
			β-Ile	2(2)	1(1)
			β-Tyr	2(2)	1(1)
			β-Phe	0	1(1)
			β-Asn	0	0
			γ-Glu	0	1
			γ-Glu[f]	0	0

Table 38. (continued)

XV	+	++	γ-Gln	0	1
			β-Lys	0	0
			β-Val	2(1)	2(2)
			β-Glu[f]	0	0
			β-Pro	2	2
XVI	-	+	β-Glu	0	1
XVII	-	-	β-Arg	0	0
			β-Gln	0	0
XVII'	-	-	δ-Lys	0	0
XVIII	+	++	β-CySH[g]	8(8)	8(8)
			γ_1-Ile	2(4)	1(3)
			γ-Pro	2(2)	2(2)
			γ-Arg	0	0
XVIII'	-	-	γ-Lys	0	0
XIX	+	+	γ-Thr	0	0
			β-Ala[f]	0	0
			γ_1-Val	2	2(1)
XX	d	++	γ_2-Val	2	2(1)
			β-Ala	2(2)	1(2)
XXI	-	+	γ_2-Ile	2(3)	1(2)
XXII	-	-	β-Ala[j]	0	0
XXIII	d	+	δ-Ile	2(3)	1(2)

Notes for Table 38.

a. Shift $\geq$ 2 ppm = +, no shift = -. (Shifts are based on tentative assignments).

b. Shift relative to free amino acid position.

c. Shift relative to oxidized protein position. C. acidi-urici ferredoxin was (20±5)% reduced and C. pasteurianum ferredoxin was (90±10)% reduced.

d. The number of amino acid residues in parenthesis refers to the number of nuclei that would be $\leq$ 5 Å from each Fe-S cluster in C. acidi-urici and C. pasteurianum ferredoxins, if one assumes that the three-dimensional structures of these proteins is similar to that of P. aerogenes ferredoxin (See Table 39).

e. Resonance shifts obscured by other resonances.

f. C-terminal.

g. 20-40 ppm shift.

h. Resonances were not observed in the reduced protein.

i. Resonances were not observed in the oxidized protein.

j. N-terminal.

Table 39. Proton and carbon atoms of amino acid residues within 5 Å of an Fe atom of the Fe-S clusters of P. aerogenes ferredoxin (64).

Amino Acid Residue	Atom	Atoms within 5 Å of an Fe atom in Cluster II		Amino Acid Residue	Atom	Atoms within 5 Å of an Fe atom in Cluster I	
		Fe^{35}-Fe^{41} face				Fe^{8}-Fe^{41} face	
		C	H			C	H
Tyr^{2}	β	1	2	Tyr^{30}	β	1	2
	1'	1	-		1'	1	-
	2', 6'	2	2		2', 6'	2	2
	3', 6'	2	2		3', 5'	2	2
	4'	1	-		1'	1	-
Ile^{30}	β	1	1	Ile^{4}	γ_1	1	2
	γ_1, γ_2	2	3		δ	1	3
		Fe^{38}-Fe^{18} face				Fe^{41}-Fe^{45} face	
		C	H			C	H
Val^{20}	β	1	1	Gly^{12}	α	1	1
Ile^{36}	γ_1, γ_2	2	6	Ile^{9}	β	1	0
	δ	1	3		γ_1, γ_2	2	3
					δ	1	3
Ser^{40}	β	1	2	Ala^{13}	β	1	3
Pro^{19}	γ, δ	2	2	Pro^{50}	γ, δ	2	4
				Ala^{49}	β	1	3

PART IV. GENERAL DISCUSSION

DISTINGUISHABLE Fe-S CLUSTERS:

^{13}C-NMR of the aromatic residues of C. acidi-urici [Phe^{2}]-ferredoxin and C. pasteurianum ferredoxins permits one to distinguish each Fe-S cluster within each protein. By using each aromatic residue as a probe of the magnetic environments of each Fe-S cluster, one can determine the relative midpoint redox potentials of each Fe-S cluster in the reduced proteins. The ^{13}C-NMR results suggest that the midpoint redox potentials of the two Fe-S clusters in C. acidi-urici ferredoxin differ by < 10 mV. The midpoint redox potentials of the two Fe-S clusters in C. pasteurianum ferredoxin, however, differ by (10± 5) mV. Thus one cluster is more easily reduced than the other cluster in C. pasteurianum ferredoxin; and it is still uncertain whether such a difference exists in C. acidi-urici ferredoxin.

^{13}C-NMR of an equilibrium mixture of methyl viologen-reduced C. acidi-urici and C. pasteurianum ferredoxin shows that the protein midpoint redox potential of C. acidi-urici ferredoxin is (47±10) mV lower than that of C. pasteurianum ferredoxin. This measurement has been independently confirmed by Eglis T. Lode by using the more conventional techniques (77). This confirmation strengthens the assumptions we used to calculate the above mentioned midpoint redox potentials with NMR methods.

AROMATIC RESIDUES:

SYMMETRIC SHIFTS:

^{13}C-NMR and ^{1}H-NMR of the aromatic residues of C. acidi-urici native and [Phe^{2}]-ferredoxin and C. pasteurianum ferredoxin also reveals that the aromatic ring nuclei experience symmetric magnetic perturbations about the 1', 4'-ring carbon axis in the oxidized and reduced proteins. This is consistent with the fact that the aromatic residues of oxidized crystalline P. aerogenes ferredoxin are each approximately parallel to and equidistant from a face of one Fe-S cluster (2). If this symmetric orientation of the aromatic residues in P. aerogenes ferredoxin occurs in C. acidi-urici and C. pasteurianum ferredoxin, then the symmetric orientation of the aromatic residues with respect to the Fe-S clusters may be responsible for the symmetric shifts observed in oxidized proteins.

These studies would then suggest that the solution structure of oxidized C. acidi-urici and C. pasteurianum ferredoxin is similar to that of oxidized crystalline P. aerogenes ferredoxin. The fact that the symmetry of the ring carbon and proton shifts is maintained in the reduced protein also suggests that the proposed symmetrical orientation of the aromatic residues is maintained in the reduced protein as well.

SHIFT MECHANISMS:

The above conclusions concerning the symmetric orientation of the aromatic residues are valid only if the ring carbon resonances were shifted by a pseudocontact interaction. The pseudocontact

shifts would be symmetric if the perturbed nuclei were symmetrically orientated about the unpaired electron spins.

The shifts of the ring proton resonances in the oxidized and reduced protein were 5 to 10 times less than the shifts of the corresponding ring carbon resonances. This ratio of C:H resonance shifts however is characteristic of a contact shift mechanism. The contact shift hypothesis is strengthened by the fact that the shifts of ring carbon and proton resonances are symmetric about the 1', 4' -ring carbon axis for both aromatic residues in both oxidized and reduced proteins. The aromatic residues need not maintain a symmetric orientation if they are perturbed by a contact interaction, since electron spin density would be transferred through overlapping orbitals. This implies that some of the ring carbons are weakly bonded to the Fe-S clusters. (A weak bond would occur if the probability of electron spin transfer from the Fe-S cluster into an orbital of neighboring atoms is approximately one percent.)

Determining which shift mechanism is primarily responsible for the observed ring carbon and proton shifts will help elucidate whatever structural and functional role the aromatic residues have in clostridial-type ferredoxins. For example, if the shifts are due to a contact interaction, the formation of a weak chemical bond between the aromatic residues and the Fe-S clusters could: (i) stabilize the protein and Fe-S cluster structure; (ii) affect the rate of electron transfer; (iii) affect the redox potentials of the Fe-S clusters, or; (iv) any combination of the above. The involvement of the aromatic residues in any one of the above roles does not necessarily exclude the existence of the other two.

If more than one of these roles exists, one can determine their relative importance and the conditions under which one role may be more important than another.

POSSIBLE FUNCTIONAL ROLE OF AROMATIC RESIDUES:

ELECTRON TRANSFER: The aromatic residues could be involved in inner-sphere or outer-sphere electron transfer reactions. Electron transfer reactions occur if the orbitals of the reactants overlap. In these reactions the coordination number and the coordinated ligands of the reaction partners do not change during the net reaction. If only a single element is involved, as in the reaction

$$*Fe^{2+} + Fe^{3+} \rightleftharpoons *Fe^{3+} + Fe^{2+}$$

it is called an electron exchange reaction.

If the coordination shells are unchanged, not only in the net reaction, but remain intact throughout its entire course, the reaction is called an outer-sphere electron transfer reaction. If, during the course of the reaction, one or more of the ligands become common to the coordination shells of both reactants the reaction is called inner-sphere (93).

In certain cases electron transfer reactions occur via bridged intermediate (81). The bridging groups are sometimes atoms and sometimes groups of atoms; the transfer mechanism is sometimes an atom transfer and sometimes an electron transfer (81).* (Atom transfer mechanisms are always inner sphere reactions (81).)

*This distinction is seen in the following pair of reactions (108):

$$+FeCl^{2+} + Fe^{2+} \xrightarrow{\text{electron transfer}} *FeCl^{+} + Fe^{3+}$$

$$+FeCl^{2+} + Fe^{2+} \xrightarrow{\text{atom transfer}} *Fe^{2+} + FeCl^{2+}$$

MODEL COMPOUNDS: Mixed-valence organometallic compounds containing aromatic ligands have high electron transfer rates and have been proposed as ferredoxin model compounds (31). The properties of these mixed-valence compounds depend upon the amount of delocalization (31) between the two moieties. One such model compound, biferrocene picrate,

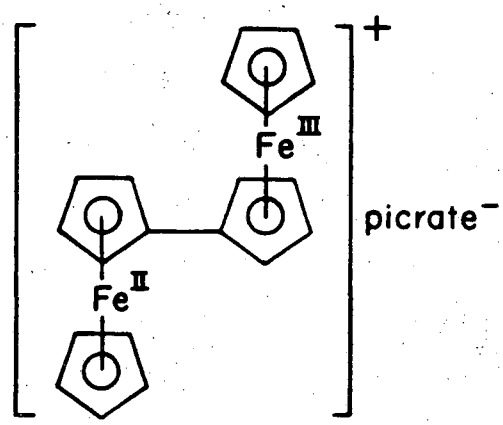

is characterized by an electronic transition in the visible and near infrared region. This transition corresponds to an intra-molecular electron transfer between two metal-like orbitals (ϵ_{2g}) that weakly interact with the π conjugated system of the molecule (31). The energy of this transition depends upon differences in geometry and bond lenghts of the donor and acceptor, and it is not very dependent upon the extent of delocalization in the ground state or upon the distance separating the donor and acceptor moieties. The intensity of the allowed transition, however, is proportional to the square of the probability of finding the electron on the acceptor (in the ground state) and upon the square of the distance between the acceptor and donor (31). The greater the extent of delocalization, the higher will be the electron transfer rate.

Electron transfer may be rate-limited by other factors, however, such as electrostatic charges between donor and acceptor moieties (55, 73, 101, 125). In this case kinetic studies alone will not determine the functional role of aromatic intermediate in electron transport.

THE ROLE OF AROMATIC RESIDUES IN OTHER ELECTRON-CARRIER PROTEINS: Circumstantial evidence suggests that aromatic residues in some electron carrier proteins may also have a functional role in electron transfer, in addition to a possible structural role. Aromatic residues are associated with the electron-carrying prosthetic groups of the following electron-carrier proteins: (i) two bacterial flavodoxins where part of the flavin moiety is exposed to the solvent; the planar flavin moiety is sandwiched between and approximately parallel to two aromatic residues (4, 138); (ii) P. aerogenes ferredoxin, where part of the two aromatic residues are exposed to the solvent and each aromatic residue is approximately parellel and close to an Fe-S cluster (65); (iii) Chromatium high potential iron protein, where the single Fe-S cluster is surrounded by several aromatic residues (70); (iv) Bacterial azurins, where aromatic residues are close to the Cu prosthetic group (16); (v) Cytochrome c, where the heme group is exposed to the solvent (143) (a tyrosyl* residue is also close to this heme group (34, 127).

---

*Takano et al. (127) observed that in cytochrome c the tyrosyl residue close to the heme group changes orientation upon reduction, and suggested that electron transfer occurs by way of a proton transfer from a tyrosyl radical. Electron transport by aromatic residues in clostridial ferredoxinx would have to operate by another mechanism, since there are clostridial ferredoxins that contain only phenylalanyl residues instead of tyrosyl residues (13, 28).

Bridging aromatic intermediates within the protein or small ions from the solvent or both can have a role in electron transport. Gupta et al. (55) have shown by ^{1}H-NMR methods that electron transfer between oxidized and reduced cytochrome c does not require the mediation of small ions because the electron exchange rate has a first-order dependence on the cytochrome c concentration. Electron exchange between oxidized and reduced cytochrome c thus results from binary collisions between proteins. The observed rate constant (at pH 10, the isoelectric point) is 2×10^{4} liter mole^{-1}second^{-1} and the calculated diffusion limited rate constant (assuming electron transfer during every binary collision) is 5×10^{9} liter mole^{-1}second^{-1} (55). Thus the colliding molecules must have a specific orientation before the electrons can be transferred.

X-ray studies show that one edge of a heme in cytochrome c is exposed to the solvent (34), and ^{1}H-NMR studies show that the unpaired electron is extensively delocalized to the heme periphery (143). This suggests that direct transfer of an electron could occur from the heme iron of one cytochrome c molecule to the other. This does not mean that electron transfer in cytochrome c cannot also be mediated by small ions. Sutin and coworkers (125) have recently shown that, depending on the conditions and nature of the medium, reduction of cytochrome c by Cr(II) can proceed by adjacent or remote attack. The remote attack is hypothesized to involve electron transfer to the exposed edge of the porphyrin ring system and the adjacent attack involves electron transfer to the Fe(III) atom of heme via a bridging anion intermediate. Thus electron transfer to electron carrier proteins need not

require aromatic intermediates in order to transfer electrons. The fact that aromatic intermediates are not necessary for electron transport does not mean that electron transfer does not occur via an aromatic intermediate.

ALIPHATIC RESIDUES:

CYSTEINYL CARBON RESONANCES:

^{13}C-NMR of the aliphatic residues of oxidized C. acidi-urici and C. pasteurianum ferredoxin (Experiment 8) indicate that the cysteinyl carbon resonances are shifted from their positions in apoferredoxin and in model polypeptides. (Most, if not all, of the β-carbon resonances of the eight cysteinyl residues are missing from the aliphatic region of both oxidized ferredoxins.)

A group of "eight" resonances is shifted 20-40 ppm downfield of the α-cysteinyl carbon resonance. ^{13}C-NMR double resonance techniques show that some of the carbon resonances in this group of shifted resonances represent α-carbon resonances, and these are tentatively assigned to the α-carbon atoms of the cysteinyl residues, because these resonances are assumed to be contact-shifted resonances. These shifts would be due to a contact mechanism because of: (i) the magnitudes of the shifts in the oxidized protein; (ii) the extrapolated magnitude of these shifts in the fully reduced protein; and (iii) the fact that the shifts of the carbon resonances are $\geqslant 10$ times those of the protons bonded to these carbons.

These "eight" carbon resonances also shift as a group upon reduction. This result is consistent with the hypothesis that the electron spin is delocalized over (or is rapidly exchanged with) all the Fe atoms in both Fe-S clusters. This hypothesis however does not require that all of

any of the "eight" shifted resonances represent the α-carbon atoms of the cysteinyl residues. The fact that as many as eight carbon resonances exhibit such large shifts suggests that bonds may form between the Fe-S complex and eight carbon atoms, and thus strengthens the above hypothesis, that the electron (spin) is delocalized over (or exchanged with) all the Fe atoms.

UNASSIGNED CARBON RESONANCES:

In both oxidized ferredoxins other (unassigned) carbon resonances are shifted; upon full reduction some of these resonances, corresponding to about 10-20 carbon atoms, are shifted as much as 10-20 ppm (relative to their positions in the oxidized protein). Most of the carbon resonances of amino acid residues that may be ≤ 5 Å from an Fe atom in an Fe-S cluster are shifted in C. acidi-urici and C. pasteurianum ferredoxin (Table 39, Experiment 8). (This assumes that their three-dimensional structures are similar to that of P. aerogenes ferredoxin.) The shifts of the unassigned (like the shifts of the tentatively assigned) carbon resonances may be due to a contact mechanism. If a pseudo-contact mechanism produced the unassigned carbon shifts, the ^{1}H-NMR spectrum of reduced ferredoxin should show 10-20 significantly shifted proton resonances (in excess of the sixteen resonances already tentatively assigned by Phillips (110) to the β-protons of the eight cysteinyl residues). If the unassigned carbon shifts are due to a contact mechanism then some of the carbon atoms of the aliphatic residues ≤ 5 Å from the Fe-S clusters may also be weakly bonded to Fe-S clusters. Certain aliphatic residues could thus have a role similar to that of the

aromatic residues, a role which does not require the delocalization properties of an aromatic residue.

SLOWLY EXCHANGEABLE PROTON RESONANCES:

If it is true that some of the significantly shifted proton resonances of fully reduced C. acidi-urici ferredoxin are represented by slowly exchangeable protons, then these protons may also be close enough to the Fe-S clusters to form weak chemical bonds.

Phillips has recently observed (104) additional contact shifted resonances in ^{1}H-NMR spectra of iron-sulfur proteins dissolved in H_2O instead of D_2O. This observation suggests that rapidly exchangeable protons can also form weak bonds with the Fe-S clusters.

CONFORMATIONAL CHANGES:

The magnitude of paramagnetic shifts in C. acidi-urici and in C. pasteurianum ferredoxin can be influenced by protein conformation. Protein conformation can cause: (i) a change in the conformation of the perturbed nuclei about the Fe-S cluster; (ii) a change in the conformation of the Fe-S cluster; (iii) a change in the electronic structure of the Fe-S cluster; or (iv) any combination of these.

The cube-like Fe-S cluster(s) of Chromatium high potential iron protein, P. aerogenes ferredoxin (25), and a model compound synthesized by Holm and coworkers (57) have identical three-dimensional structures, but different magnetic properties (6). Thus, even if the geometric structure of these clusters is insensitive to the differences in protein conformation of these proteins, this is not true for its magnetic properties or electronic structure. There can be a large change

in the electronic structure of the Fe-S clusters without a correspondingly large change in the geometry of the cluster. For example, the dihedral angles, the cysteinyl residues make with the cube-like Fe-S clusters in these proteins, may vary in each protein, and this difference in bonding could produce different amounts of overlap between p and d orbitals of the S and Fe atoms respectively, and this could change the electronic structures of the Fe-S clusters in each protein.

It would be of interest to determine to what extent the different magnetic shifts we observe for C. pasteurianum and C. acidi-urici ferredoxin are due to differences in the orientation and bonding of the perturbed nuclei to the Fe-S cluster or to changes in protein conformation that influence the electronic structure of the Fe-S cluster.

PROSPECTUS:

The NMR and ESR experiments discussed in this thesis have raised the following (testable) questions.

DO AMINO ACID RESIDUES FORM WEAK CHEMICAL BONDS WITH A NEIGHBORING Fe-S CLUSTER?

In order to answer this question one must determine to what extent the observed ring carbon shifts are due to pseudocontact and contact interactions. ^{19}F-NMR of C. acidi-urici [[3' $-^{19}F_1$] Tyr] -ferredoxin could help answer this question. This is because the monosubstituted F atom will break the electronic symmetry of the aromatic ring. The ring carbon and proton resonance shifts would no longer be symmetric about the 1', 4' -ring carbon axis if the observed shifts were due to a contact mechanism,

since ^{19}F, unlike ^{1}H, can participate in the π-orbital conjugation of the aromatic ring (37) and the spin densities on the ring carbon nuclei will be affected by the spin density of the p-orbital of ^{19}F (38, 40). If the observed ring carbon shifts were due to a pseudocontact mechanism then the symmetrical pattern of the shifts should not be altered. This assumes that the 3-fluoro-tyrosyl residue has the same orientation as the tyrosyl residue it replaced. The orientation of the 3-fluoro-tyrosyl residue, which can be checked by ^{1}H-NMR, should not be very different because the fluorine atom is not much bigger than a proton.

IS THE REDUCING ELECTRON TRANSFERRED BETWEEN Fe-S CLUSTERS WITHIN EACH FERREDOXIN OR BETWEEN FERREDOXINS WITHOUT A MEDIATOR OR BOTH?

With methyl viologen as a reductant and mediator the reducing electron is rapidly exchanging between oxidized and reduced forms of ferredoxins since the resonances seen in partially reduced ferredoxin represent an averaged spectrum between the fully reduced and oxidized protein spectrum. If the mediator, methyl viologen, can be removed, electron exchange between Fe-S clusters would be demonstrated if one sees an averaged spectrum of reduced and oxidized ferredoxin that is independent of protein concentration. If there is no exchange between Fe-S clusters one would see two spectra, each corresponding to the oxidized and reduced protein. In order to observe the presence or absence of averaged resonances as a function of protein concentration, it would be desirable to do ^{13}C-NMR of $[[1'-^{13}C_1]Phe^2]$-ferredoxin.

DO CHANGES IN PROTEIN CONFORMATION CHANGE THE MIDPOINT REDOX POTENTIALS OF EACH Fe-S CLUSTER?

This question can be answered by determining the degree of reduction of each Fe-S cluster (by the techniques discussed in Experiment 7) in ferredoxin solutions containing either D_2O or H_2O or salt concentrations known to change the conformation of the protein.

DOES SUBSTITUTION OF THE TYROSYL RESIDUES IN C. acidiurici FERREDOXIN FOR DIFFERENT AROMATIC OR ALIPHATIC RESIDUES AFFECT THE RATE OF ELECTRON TRANSFER OR MIDPOINT REDOX POTENTIALS OF THE Fe-S CLUSTERS OR BOTH?

This question may be answered by comparing the line widths of the ring carbon resonances of the unsubstituted aromatic residue (in position 30) of methyl viologen-reduced ferredoxins with and without a modified amino acid residue in position 2. The line width of the ring carbon resonances will change if the rate is $< 10{,}000\ sec^{-1}$.

ARE ELECTRONS TRANSFERRED BY AMINO ACID RESIDUES?

Before electrons can be transferred to amino acid residues, a chemical bond must be able to form between the amino acid nuclei and the Fe-S clusters. The magnitude of resonance shifts of these nuclei is proportional to the probability (or "strength") of such chemical bonds if the shifts are due to contact interactions. The cysteinyl residues are directly bonded to the Fe-S clusters and one would like to know the magnitudes of the cysteinyl β-carbon and β-proton resonance shifts. This can only be determined if the shifted resonances can be assigned. Assignment of these resonances will be facilitated by the incorporation of $[3\text{-}^{2}H_2]$cysteine and $[3\text{-}^{13}C_1]$cysteine into

C. acidi-urici ferredoxin. Also, the hypothesis that the reducing electron causes electron spin to be present in all the atoms of the Fe-S cluster would be strengthened if if could be shown that all of the cysteinyl carbon and cysteinyl proton resonances were shifted.

LITERATURE CITED

1. ADLER, H. I., and A. A. HARDIGREE (1965). Growth and division of filamentous forms of Escherichia coli. J. Bacteriol. 90: 223-226.

2. ADMAN, E. T., L. C. SIEKER, and L. H. JENSEN (1973). The structure of a bacterial ferredoxin. J. Biol. Chem., in the press.

3. AMES, G. F., and J. R. ROTH (1968). Histidine and aromatic permeases of S. typhimurium. J. Bacteriol., 96: 1742-1749.

4. ANDERSON, R. D., P. A. APGAR, R. M. BURNETT, G. D. DARLING, M. E. LEQUESNE, S. G. MAYHEW, and M. L. LUDWIG (1972). Structure of the new radical form of clostridial flavodoxin: a new molecular model. Proc. Nat. Acad. Sci. USA, 69: 3189-3191.

5. AVERILL, B. A., T. HERSKOVITZ, R. H. HOLM, and J. A. IBERS (1973). Synthetic analogues of the active sites of bacterial iron-sulfur proteins. II. Synthesis and structure of the tetra [mercapto-μ_3-sulfidoiron] clusters $[Fe_4S_4(SR)_4]^{2-}$. J. Am. Chem. Soc., in the press.

6. AYSEOUGH, P. G. (1967). Electron spin resonance in chemistry. London, Methuen and Co., Ltd., p. 105.

7. BACHOFEN, R., and D. I. ARNON (1966). Crystalline ferredoxin from the photosynthetic bacterium Chromatium. Biochim. Biophys. Acta, 120: 259-265.

8. BARKER, H. A., and W. H. PETERSON (1944). The nutritional requirements of Clostridium acidiurici. J. Bacteriol., 47: 307-308.

9. BASKERVILLE, E. N., and R. TWAROG (1972). Regulation of the tryptophan synthetic enzymes in Clostridium butyricum. J. Bacteriol., 112: 304-314.

10. BEARDEN, A. J. (1972). Unpublished observations.

11. BECKER, E. D., and T. C. FARRAR (1972). Fourier transform spectroscopy. Science, 178: 361-368.

12. BEINERT, H., and W. H. ORME-JOHNSON (1969). Electron-nuclear and electron-electron spin interactions in the study of enzyme structure and function. Ann. N. Y. Acad. Sci., 158: 336-360.

13. BENSON, A. M., H. F. MOWER, and K. T. YASUNOBU (1966). The amino acid sequence of Clostridium butyricum ferredoxin. Proc. Nat. Acad. Sci. USA, 55: 1532-1535.

14. BERGMANN, E. D., S. SICKER, and B. E. VOLCANS (1953). Action of substituted phenylalanine on Escherichia coli. Biochem. J., 54: 1-13.

15. BLOOMSTROM, D. C., E. KNIGHT, Jr., W. D. PHILLIPS, and J. F. WEIKER (1964). The nature of iron in ferredoxin. Proc. Nat. Acad. Sci. USA, 51: 1085-1092.

16. BLUMBERG, W. (1972). Personal communication.

17. BLUMBERG, W. E., and J. PEISACH (1965). Model complexes for the electron paramagnetic resonance in the electron transport system. In Non-heme iron proteins, San Pietro, A., Ed., Yellow Springs, Ohio, Antioch Press.

18. BOVEY, F. A. (1972). High resolution NMR of macromolecules. Chapter XIV. New York, Academic Press, in the press.

19. BOWERS, K. W. (1968). In Radical Ions, Kaiser, E. T., and L. Kevon, Eds., New York, Interscience Publishers.

20. BRANDTS, J. F. (1969). Conformational transitions of proteins in water and in aqueous mixtures. In Structure and stability of biological macromolecules, Timasheff, S. N., and G. D. Forman, Eds., New York, Marcel Dikker, Inc.

21. BRAY, G. A. (1960). A simple efficient liquid scintillator for counting aqueous solutions in a liquid scintillation counter. Anal. Biochem., 1: 279-285.

22. BROWN, K. D. (1970). Formation of aromatic amino acid pools in E. coli K-12. J. Bacteriol., 104: 177-188.

23. BUCHANAN, B., and D. I. ARNON (1971). Ferredoxins: chemistry and function in photosynthesis, nitrogen fixation, and fermentative metabolism. Advances in Enzymology 33: 119-176.

24. CARRINGTON, A., and A. D. McLACHLAN (1967). Introduction to magnetic resonance. New York, Harper and Row.

25. CARTER, C. W., Jr., J. KRAUT, S. T. FREER, R. A. ALDEN, L. C. SIEKER, E. ADMAN, and L. H. JENSEN (1972). A comparison of Fe_4S_4* clusters in high-potential iron protein and in ferredoxin. Proc. Nat. Acad. Sci. USA, 69: 3526-3529.

26. CHAIKEN, I. J., M. H. FREEDMAN, J. R. LYERLA, and J. S. COHEN (1973). Preparation and studies of ^{19}F-labeled and enriched ^{13}C-labeled semi-synthetic ribonuclease-S' analogues. J. Biol. Chem., 248: 884-891.

27. CHAMPION, A. B. (1971). Unpublished observations.

28. CHAMPION, A. B. (1972). Comparative study of clostridial purine fermenters. Ph.D. Thesis. University of California, Berkeley.

29. CHEN, C.-S. (1972). Glycine metabolism in purine-fermenting clostridial. Ph.D. Thesis. University of California, Berkeley.

30. COHEN, J. S., M. FEIL, and I. M. CHAIKEN (1971). Proton magnetic resonance studies of the tyrosine residues of staphylococcal nuclease using [3,5-$^2H_2$]tyrosine. Biochim. Biophys. Acta, 236: 468-478.

31. COWAN, D. O., C. L. LE VANDA, J. PARK, and F. C. KAURMAN (1973). Mixed-valence ferrocene chemistry. Accounts of Chem. Res., 6: 1-7.

32. CUMMINS, C. S., and J. L. JOHNSON (1971). Taxonomy of the clostridia: wall composition and DNA homologies in Clostridium butyricum and other butyric acid-producing clostridial J. Gen. Microbiol., 67: 33-46.

33. de BOER, E., and H. van WILLIGEN (1967). Nuclear magnetic resonance of paramagnetic systems. In Progress in nuclear magnetic resonance spectroscopy, 2, 111-161, London, Pergamon Press.

34. DICKERSON, R. E., T. TAKANO, D. EISENBERG, O. B. KALLAI, L. SAMPSON, A. COOPER, and E. MARGOLIASH (1971). Ferricytochrome c. I. General features of the horse and bonito proteins at 2.8 Å resolution. J. Biol. Chem., 246: 1511-1535.

35. DUNHAM, W. R., G. PALMER, R. H. SANDS, and A. J. BEARDEN (1971). On the structure of the iron-sulfur complex in the two iron ferredoxins. Biochim. Biophys. Acta, 253: 373-384.

36. DUS, K., H. de KLERK, K. SLETTEN, and R. G. BARTSCH (1967). Chemical characterization of high potential iron proteins from Chromatium and Rhodopseudomonas gelatinosa. Biochim. Biophys. Acta, 140: 291-311.

37. EATON, D. R., A. D. JOSEY, R. E. BENSON, W. D. PHILLIPS, and T. L. CAIRNS (1962). Unpaired electron distribution in π-systems. J. Am. Chem. Soc., 84: 4100-4106.

38. EATON, D. R., A. D. JOSEY, and W. D. PHILLIPS (1962). ^{19}F contact interaction shifts: effects of fluorine conjugation. Mol. Phys. 5: 407-466.

39. EATON, D. R., and W. D. PHILLIPS (1965). Nuclear magnetic resonance of paramagnetic molecules. In Advances in magnetic resonance, Waugh, J., Ed., Academic Press, 1: 103-139.

40. EATON, D. R., and W. A. SHEPPARD (1962). F^{19} chemical shifts of the sulfur pentafluoride, trifluoromethoxy, trifluoromethylthio and trifluoromethylsulfomyl groups in aromatic compounds. J. Am. Chem. Soc., 85: 1310-1313.

41. EDMAN, P. (1956). On the mechanism of the phenyl isothiocyanate degradation of peptides. Acta Chem. Scand., 10: 761-768.

42. EDWARDS, P. R., C. E. JOHNSON, and R. J. P. WILLIAMS (1967). Mössbauer spectra of some tetrahedral iron (II) compounds. J. Chem. Phys., 47: 2074-2082.

43. EISENSTEIN, K. K., and J. H. WANG (1969). Conversion to light to chemical free energy. J. Biol. Chem., 244: 1720-1728.

44. ENGLANDER, S. W. (1963). A hydrogen exchange method using tritium Sephadex: its application to ribonuclease. Biochemistry 2: 798-806.

45. ERNST, R. R., and W. A. ANDERSON (1966). Application of Fourier transform spectroscopy to magnetic resonance. Rev. Sci. Instrum., 37: 93-102.

46. EVANS, M. C. W., D. O. HALL, H. BOTHE, and F. R. WHATLEY (1968). The stoichoimetry of electron transfer by bacterial and plant ferredoxins.

Biochem. J., 110: 485-489.

47. FARRER, T. C., and E. D. BECKER (1971). Pulse and Fourier transform NMR. New York, Academic Press.

48. FISCHER, H. (1965). Magnetic properties of free radicals. In Numerical data and functional relationships in science and technology, Group II, atomic and molecular physics, Hellwege, K. H., and A. M. Hellwege, Eds., Londolt-Börnstein, 1: 58.

49. GIBSON, J. F., D. O. HALL, J. H. M. THORNLEY, and F. R. WHATLEY (1966). The iron complex in spinach ferredoxin. Proc. Nat. Acad. Sci. USA, 56: 987-990.

50. GLARUM, S. (1972). Personal communication.

51. GLICK, M. C., T. SALL, F. ZILLIKEN, and S. MUDD (1960). Morphological changes of Lactobacillus bificans var. pennsylvanicus produced by a cell wall precursor. Biochim. Biophys. Acta, 37: 361-363.

52. GLUSHKO, V. (1972). Personal communication.

53. GLUSHKO, V., P. J. LAWSON, and F. R. N. GURD (1972). Conformational states of bovine pancreatic ribonuclease A observed by normal and partially relaxed carbon 13 nuclear magnetic resonance. J. Biol. Chem., 247: 3176-3185.

54. GRULA, E. A., and M. M. GRULA (1962). Cell division in a species of Erwinia. V. Effect of metabolic inhibitors on terminal division and composition of a "division" medium. J. Bacteriol., 84: 492-499.

55. GUPTA, R. K., S. H. KOENIG, and A. G. REDFIELD (1972). On the electron transfer between cytochrome c molecules as observed by nuclear magnetic resonance. J. Magn. Resonance 7: 66-73.

56. HARTMAN, K. A., Jr. (1966). The structure of water and the stability of the secondary structure in biological molecules. An infrared and proton magnetic resonance study. J. Phys. Chem., 70: 270-276.

57. HERSKOVITZ, T., B. A. AVERILL, R. H. HOLM, J. A. IBERS, W. D. PHILLIPS, and J. F. WEIHER (1972). Structure and properties of a synthetic analogue of bacterial iron-sulfur proteins. Proc. Nat. Acad. Sci. USA, 69: 2437-2441.

58. HOFFMAN, H., and M. E. FRANK (1963). Temperature limits, geneological origin, developmental course and ultimate fate of heat-induced filaments in Escherichia coli microcultures. J. Bacteriol., 85: 1221-1234.

59. HONG, J.-S., and J. C. RABINOWITZ (1967). Preparation and properties of clostridial apoferredoxins. Biochem. Biophys. Res. Commun., 29: 246-252.

60. HONG, J.-S., and J. C. RABINOWITZ (1970). Immunological properties and conformational differences detected by tritium-hydrogen exchange of clostridial ferredoxin and apoferredoxins. J. Biol. Chem., 245: 4995-5000.

61. HONG, J.-S., and J. C. RABINOWITZ (1970). The effects of chemical modifications on the reconstitution, activity and stability of clostridial

ferredoxin. J. Biol. Chem., 245: 4988-4994.

62. HUGHES, W. H. (1956). The structure and development of the induced long forms of bacteria. Symp. Soc. Gen. Microbiol., 6: 341-360.

63. IUPAC-IUB Commission on biochemical nomenclative rules for naming synthetic modifications of natural peptides, tentative rules. (Tentative Rule No. 1). (1967). J. Biol. Chem., 242: 555-557.

64. JENSEN, L. H. (1972). Personal communication.

65. JENSEN, L. H., L. C. SIEKER, K. D. WATENPAUGH, E. T. ADMAN, and J. R. HERRIOTT (1973). Structures of two non-haem iron proteins. Rubredoxin at 0.15 mn (1.5 Å) resolution and ferredoxin at 0.20 mn (2.0 Å) resolution. Biochemical Society Transactions, 1: 27.

66. JOHNSON, C. E., R. COMMACK, K. K. RAO, and D. O. HALL (1971). The interpretation of the EPR and Mössbauer spectra of two-iron, one-electron, iron-sulfur proteins. Biochem. Biophys. Res. Commun., 43: 564-571.

67. JOHNSON, L. F., I. L. SCHWARTZ, and R. WATER (1969). Oxytocin and neurohypophyseal peptides: spectral assignment and conformational analysis by 220 MHz nuclear magnetic resonance. Proc. Nat. Acad. Sci. USA, 64: 1269-1275.

68. KARPLUS, M., and G. K. FRAENKEL (1961). Theoretical interpretation of carbon-13 hyperfine interactions in electron spin resonance spectra. J. Chem. Phys.,

35: 1312-1323.

69. KING, N. K., F. D. LOONEY, and M. E. WINFIELD (1967). Amino acid free radicals in oxidized metmyoglobin. Biochim. Biophys. Acta, 133: 65-82.

70. KRAUT, J. (1972). Personal communication.

71. KURLAND, R. J. and B. R. McGARVEY (1970). Isotropic NMR shifts in transition metal complexes: the calculation of the Fermi contact and pseudocontact terms. J. Magn. Resonance 2: 286-301.

72. LA MAR, G. N., G. R. EATON, R. H. HOLM, and F. A. WALKER (1972). Proton magnetic resonance investigation of antiferromagnetic oxo-bridged ferric dimers and related high-spin monomeric ferric complexes. J. Am. Chem. Soc., 95: 63-75.

73. LAND, E. J., and A. J. SWALLOW (1971). One-electron reactions in biochemical systems as studied by pulse radiolysis. V. Cytochrome c. Arch. Biochem. Biophys., 145: 365-372.

74. LEVY, G. C., and G. L. NELSON (1972). Carbon-13 nuclear magnetic resonance for organic chemists. New York, Wiley Interscience, p. 28.

75. LLINÁS, M. (1973). Metal-polypeptide interactions: the conformational state of iron proteins. Structure and bonding. In the press.

76. LODE, E. T. (1973). Modulation of clostridial ferredoxin via chemical substitution of amino acids in

the amino terminal portion. Abst. 1822. Federation proceedings. (FASEB) 32: 542.

77. LODE, E. T., and J. C. RABINOWITZ (1973). Unpublished observations.

78. LOVENBERG, W., B. B. BUCHANAN, and J. C. RABINOWITZ (1963). Studies on the chemical nature of clostridial ferredoxin. J. Biol. Chem., 238: 3899-3913.

79. MACLEAN, F. I., and R. J. MASON (1961). Some environmental factors affecting the length of Escherichia coli organisms in continuous cultures. J. Gen. Microbiol., 25: 17-27.

80. MALKIN, R., and A. J. BEARDEN (1971). Primary reactions of photosynthesis: photoreduction of a bound chloroplast ferredoxin at low temperature as detected by EPR spectroscopy. Proc. Nat. Acad. Sci. USA, 68: 16-19.

81. MARCUS, R. A. (1961). Chemical and electrochemical electron-transfer theory. Ann. Rev. Phys. Chem., 15: 155-196.

82. MARGALIT, R., and A. SCHEJTER (1973). Cytochrome c: a thermodynamic study of the relationships among oxidation state, ion-binding and structural parameters. 1. The effects of temperature, pH and electrostatic media on the standard redox potential of cytochrome c. Eur. J. Biochem., 32: 492-499.

83. MARSHALL, W. (1963). Hyperfine interactions with ligand nuclei in transition ion complexes. In Paramagnetic resonance, 1: 347-362. Low, W. Ed., New York, Academic Press.

84. MATSUBARA, H., R. M. SASAKI, D. K. TSUCHIYA, and and M. C. W. EVANS (1970). The amino acid sequence of Chromatium ferredoxin. J. Biol. Chem., 245: 2121-2131.

85. MAYHEW, S. G., D. PETERING, G. PALMER, and G. P. FONST (1969). Spectrophotometric titration of ferredoxins and Chromatium high potential iron protein with sodium dithionite. J. Biol. Chem., 244: 2830-2834.

86. McDONALD, C. C., and W. D. PHILLIPS (1969). Proton magnetic resonance spectra of proteins in random-coil configurations. J. Am. Chem. Soc., 91: 1513-1521.

87. MICHAELIS, L., and E. S. HILL (1933). The viologen indicators. J. Gen. Physiol., 16: 859-873.

88. MOODY, G. J., and J. D. R. THOMAS (1971). Selective ion sensitive electrodes. Watford, Herts., England, Menow Publishing Co., Ltd., p. 63.

89. MORTENSON, L. E., R. C. VALENTINE, and J. E. CARNABAN (1962). An electron transport factor from Clostridium pasteurianum. Biochem. Biophys. Res. Commun., 7: 448-452.

90. MUNIER, R., and G. N. COHEN (1959). Incorporation d'analogues structuraux d'amino acides dans les protéines bacteriénnes au cours de leur synthèse in vivo. Biochim. Biophys. Acta, 31: 378-391.

91. NESTER, E. W., and R. A. JENSEN (1966). Control of aromatic amino acid biosynthesis in Bacillus subtilis; sequential feedback inhibition. J. Bacteriol., 91: 1594-1598.

92. NESTER, E. W., R. A. JENSEN, and D. S. NASSER (1969). Regulation of enzyme synthesis in the aromatic amino acid pathway of Bacillus subtilis. J. Bacteriol., 97: 83-90.

93. NEWTON, T. W. (1968). The kinetics of oxidation-reduction reactions. J. Chem. Educ., 45: 571-575.

94. ORME-JOHNSON, W. H., and H. BEINERT (1969). Heterogeneity of paramagnetic species in two iron-sulfur proteins: Clostridium pasteurianum ferredoxin and milk xanthine oxidase. Biochem. Biophys. Res. Commun., 36: 337-344.

95. ORME-JOHNSON, W. H., R. M. SWEET, M. SUNDARALINGHAM, L. F. DAHL, and H. BEINERT (1972). Evidence for two iron-sulfur cluster systems in ferredoxin from Clostridium acidi-urici. submitted to J. Mol. Biol.

96. PACKER, E. L., and A. J. BEARDEN (1972). Unpublished observations.

97. PACKER, E. L., H. STERNLICHT, and J. C. RABINOWITZ (1972). The possible role of aromatic residues of Clostridium acidi-urici ferredoxin in electron transport. Proc. Nat. Acad. Sci. USA, 69: 3278-3282.

98. PACKER, E. L., H. STERNLICHT, and J. C. RABINOWITZ (1973). The possible structural and functional role of aromatic residues in bacterial ferredoxins. Ann. N. Y. Acad. Sci., in the press.

99. PALMER, G. (1967). The effect of the ^{57}Fe hyperfine interaction of the EPR spectrum of spinach ferredoxin. Biochem. Biophys. Res. Commun., 27: 315-318.

100. PALMER, G., R. H. SANDS, and C. E. MORTENSON (1966). Electron paramagnetic resonance studies on the ferredoxin from Clostridium pasteurianum. Biochem. Biophys. Res. Commun., 23: 357-362.

101. PECHT, I., and M. FARAGGI (1972). Electron transfer to ferricytochrome c: reaction with hydrated electrons and conformational transitions involved. Proc. Nat. Acad. Sci. USA, 69: 902-906.

102. PETERSON, J. A., and M. J. COON (1968). Enzymatic ω-oxidation. J. Biol. Chem., 243: 329-334.

103. PHILLIPS, W. D. (1972). Personal communication.

104. PHILLIPS, W. D. (1973). Nuclear magnetic resonance studies on iron-sulfur proteins. Biochemical Society Transactions 1: 31-32.

105. PHILLIPS, W. D., and M. POE (1972). Contact shifts and magnetic susceptibilities in iron-sulfur proteins as determined from nuclear magnetic resonance spectra. In Methods in Enzymology 24: 304-317.

106. PHILLIPS, W. D., and M. POE (1973). NMR spectroscopy of the iron-sulfur proteins. Chapter 17 in Iron-sulfur proteins. Lovenberg, W., Ed., New York, Academic Press, in the press.

107. PHILLIPS, W. D., M. POE, C. C. McDONALD, and R. G. BARTSCH (1970). Proton magnetic resonance studies of

Chromatium high potential iron protein. Proc. Nat. Acad. Sci. USA, 67: 682-687.

108. PLADZIEWICZ, J. R., and J. H. ESPENSON (1973). Kinetics and mechanisms of some electron transfer reactions of ferrocenes. J. Am. Chem. Soc., 95: 56-63.

109. POE, M., W. D. PHILLIPS, J. D. GLICKSON, C. C. McDONALD, and A. SAN PIETRO (1971). Proton magnetic resonance studies of the ferredoxins from spinach and parsley. Proc. Nat. Acad. Sci. USA, 68: 68-71.

110. POE, M., W. D. PHILLIPS, C. C. McDONALD, and W. LOVENGERG (1970). Proton magnetic resonance study of ferredoxin from Clostridium pasteurianum. Proc. Nat. Acad. Sci. USA, 65: 797-804.

111. POE, M., W. D. PHILLIPS, C. C. McDONALD, and W. H. ORME-JOHNSON (1971). PMR and magnetic susceptibility studies on Clostridium acidi-urici ferredoxin. Biochem. Biophys. Res. Commun., 42: 705-713.

112. POPLE, J. A., W. G. SCHNEIDER, and H. J. BERNSTEIN (1959). High resolution nuclear magnetic resonance. New York, McGraw-Hill Book Co., Inc., p. 79-82.

113. POOLE, C. P., Jr. (1967). Electron spin resonance. New York, Interscience, p. 27.

114. RABINOWITZ, J. C. (1963). Intermediates in purine breakdown. In Methods in Enzymology 4: 703-713.

115. RABINOWITZ, J. C. (1971). Clostridial ferredoxin: an iron-sulfur protein. Advances in Chemistry Series. Number 100. Bioinorganic Chemistry. American Chem.

Soc., p. 322-345.

116. RABINOWITZ, J. C. (1972). Preparation and properties of clostridial ferredoxins. In Methods in Enzymology 24: 431-446.

117. RALL, S. C., R. E. BOLINGER, and R. D. COLE (1969). The amino acid sequence of ferredoxin from Clostridium acidi-urici. Biochemistry 8: 2486-2496.

118. ROBERTS, R. B., P. H. ABELSON, D. B. COWIE, E. T. BOLTON, and R. J. BUTTER (1956). Studies of biosynthesis in Escherichia coli. Carnegie Institution of Washington Publication 607, 445-447.

119. ROBERTS, G. C. K. and JARDETSKY, O. (1970). Nuclear magnetic resonance spectroscopy of amino acids, peptides and proteins. Adv. Prot. Chem., 24: 448-545.

120. SHEARD, B. T., T. YAMINE, and R. G. SHULMAN (1970). Nuclear magnetic resonance study of cyanoferrimyoglobin; identification of pseudocontact shifts. J. Mol. Biol., 53: 35-48.

121. SIEKER, L. C., E. ADMAN, and L. H. JENSEN (1972). Structure of the Fe-S complex in a bacterial ferredoxin. Nature, 235: 40-42.

122. SOBEL, B. E., and W. LOVENBERG (1966). Characteristics of Clostridium pasteurianum ferredoxin in oxidation-reduction reactions. Biochemistry 5: 6-13.

123. STERNLICHT, H., and D. M. ZUCKERMAN (1972). Modification of the Varian XL-100 NMR spectrometer for

Fourier transform operation. Rev. Sci. Instrum., 43: 525-529.

124. STREITWIESER, A. (1961). Molecular orbital theory for organic chemists. New York, Wiley.

125. SUTIN, N., and J. K. YANDELL (1972). Mechanisms of the reactions of cytochrome c. Rate and equilibrium constants for ligand binding to horse heart ferricytochrome c. J. Biol. Chem., 247: 6932-6936.

126. TAGAWA, K., and D. I. ARNON (1968). Oxidation-reduction potentials and stoichoimetry of electron transfer in ferredoxins. Biochim. Biophys. Acta, 153: 602-613.

127. TAKANO, T., R. SWANSON, D. S. KALLAI, and R. E. DICKERSON (1971). Conformational changes upon reduction of cytochrome c. Cold Spring Harbor Symp. Quant. Biol. 36: 397-404.

128. TANAKE, M., T. HAMASAKI, D. THOMAS, and L. JOHNSON (1971). Biosynthetic studies with carbon 13. Asperlin. J. Am. Chem. Soc., 93: 273-274.

129. TANAKA, M., M. HANIU, G. MATSUEDA, K. T. YASUNOBU, R. H. HIMES, J. M. AKOGI, E. M. BARNES, and T. DEVANATHAN (1971). The primary structure of Clostridium tartarivorum ferredoxin, a heat stable ferredoxin. J. Biol. Chem., 246: 3953-3960.

130. TANAKA, M., T. NAKASHIMA, A. BENSON, H. MOWER, and K. T. YASUNOBU (1966). The amino acid sequence of Clostridium pasteurianum ferredoxin. Biochemistry 5: 1666-1681.

131. TERRY, D. R., A. GAFFAR, and R. D. SAGARS (1966). Filament formation in Clostridium acidi-urici. J. Bacteriol., 91: 1625-1634.

132. TRAVIS, J., D. J. NEWMAN, J. Le GALL, and H. D. PECK (1971). The amino acid sequence of ferredoxin from the sulfate reducing bacterium Desulfovibrio gigas. Biochem. Biophys. Res. Commun., 45: 452-458.

133. TRUDINGER, P. A. (1970) On the absorbance of reduced methyl viologen. Anal. Biochem., 36: 222-251.

134. TSUNODA, J. N., K. T. YASUNOBU, and H. R. WHITELEY (1968) Non-heme iron proteins. IX. The amino acid sequence of ferredoxin from Micrococcus aerogenes. J. Biol. Chem., 243: 6262-6272.

135. UMBARGER, E., and B. D. DAVIS (1962). Pathways of amino acid biosynthesis. In The bacteria, Vol. III, Gunsalus, I. C., and R. Y. Stanier, Eds., New York, Academic Press.

136. VINCOW, G. (1968). Radical ions. Kaiser, E. T., and L. Kevan, Eds., New York, Interscience Publishers, p. 151.

137. von HIPPLE, P. and T. SCHLEICH (1969). The effects of neutral salts on the structure and conformational stability of macromolecules in solution. In Structure and stability of biological macromolecules. Timasheff, S. N., and G. D. Fasman, Eds., New York, Marcel Dekker, Inc.

138. WATENPAUGH, K. D., L. C. SIEKER, L. H. JENSEN, J. Le GALL, and M. DUBOURDIEU (1972). Structure of the oxidized form of a flavodoxin at 2.5 Å

resolution: resolution of the phase ambiguity by anomalous scattering. Proc. Nat. Acad. Sci. USA, 69: 3185-3188.

139. WEBB, M. (149). The influence of magnesium on cell division. 2. The effect of magnesium on the growth and cell division of various bacterial species in complex media. J. Gen. Microbiol., 3: 410-417.

140. WHITE, A., P. HANDLER, E. L. SMITH, and de Witt STETTEN, Jr. (1959). Principles of biochemistry. New York, McGraw-Hill.

141. WINFIELD, M. E. (1965). Electron transfer within and between haemo-protein molecules. J. Mol. Biol., 12: 600-611.

142. WINFIELD, M. E.(1964). In Oxidases and related redox systems, King, T. E., H. S. Mason, and M. Morrison, Eds., New York, Wiley.

143. WUTHRICH, K. (1969). High-resolution proton nuclear magnetic resonance spectroscopy of cytochrome c. Proc. Nat. Acad. Sci. USA, 63: 1071-1078.

144. FEE, J. A., S. G. MAYHEW, and G. PALMER (1971). The oxidation-reduction potentials of parsley ferredoxin and its selenium-containing homolog. Biochim. Biophys. Acta, 245: 196-200.

145. ZO BELL, C. E., and A. B. COBET (1964). Filament formation by Escherichia coli at increased hydrostatic pressures. J. Bacteriol., 87: 710-719.

146. AMES, G. J. (1964). Uptake of amino acids by Salmonella typhimurium. J. Bacteriol., 96: 1742-1749.

147. LOWRY, O. H., N. J. ROSEBROUGH, A. L. FARR, and R. J. RANDALL (1951). Protein measurement with the Folin phenol reagent. J. Biol. Chem., 193: 265-275.

148. Encyclopedia of chemical reactions (1951). Vol. IX.

149. Industrial and Engineering Chem., 42: 9 (1950).

150. PALMER, G., W. R. DUNHAM, J. A. FEE, R. H. SANDS, T. IIGUKA, and J. YONETANI (1971). The magnetic susceptibility of spinach ferredoxin from 77-250° K: a measurement of the antiferromagnetic coupling between two iron atoms. Biochim. Biophys. Acta, 245: 201-207.

151. STERNLICHT, H., G. L. KENYON, E. L. PACKER, and J. SINCLAIR (1971). Carbon-13 nuclear magnetic resonance studies of heterogeneous systems. Amino acids bound to cationic exchange resins. J. Am. Chem. Soc., 93: 199-208.

LEGAL NOTICE

This report was prepared as an account of work sponsored by the United States Government. Neither the United States nor the United States Atomic Energy Commission, nor any of their employees, nor any of their contractors, subcontractors, or their employees, makes any warranty, express or implied, or assumes any legal liability or responsibility for the accuracy, completeness or usefulness of any information, apparatus, product or process disclosed, or represents that its use would not infringe privately owned rights.

TECHNICAL INFORMATION DIVISION
LAWRENCE BERKELEY LABORATORY
UNIVERSITY OF CALIFORNIA
BERKELEY, CALIFORNIA 94720